論文 / 著書情報
Article / Book Information

題目(和文)	中性ジアミドを配位子とする硝酸ランタノイド(III)錯体の錯形成反応及び分子構造に関する研究
Title(English)	Studies on Complex Formation and Molecular Structures of Lanthanoid(III) Nitrate Complexes with Neutral Diamide Derivatives
著者(和文)	奥村森
Author(English)	Sin Okumura
出典(和文)	学位:博士(学術), 学位授与機関:東京工業大学, 報告番号:甲第9672号, 授与年月日:2014年9月25日, 学位の種別:課程博士, 審査員:池田　泰久,竹下　健二,小澤　正基,加藤　之貴,塚原　剛彦
Citation(English)	Degree:Doctor (Academic), Conferring organization: Tokyo Institute of Technology, Report number:甲第9672号, Conferred date:2014/9/25, Degree Type:Course doctor, Examiner:,,,,
学位種別(和文)	博士論文
Type(English)	Doctoral Thesis

Doctoral Thesis, 2014

Studies on Complex Formation and Molecular Structures of Lanthanoid(III) Nitrate Complexes with Neutral Diamide Derivatives

Shin OKUMURA

Department of Nuclear Engineering

Graduate School of Science and Engineering

Tokyo Institute of Technology

To my father

Abstract

The selective complexation of trivalent actinides (An(III)) over trivalent lanthanide (Ln(III)) is the most challenging key issue for the developments of new efficient extractant because of their chemical similarities. There is extensive research to find new efficient extractants for this purpose. These attempts have been mainly based on the trial-and-error method and not focused on the molecular interpretation. Understanding fundamental properties of extracted species must be crucial for the development of more efficient extractant. However, despite some efficient extractants have been examined by solvent extraction, natures of the extracted species, i.e. metal complexes, have not been elucidated.

In this thesis, the Ln(III) nitrates and two neutral diamide derivatives, *N,N,N',N'*-tetraalkyl-diglycolamide (DGA) and *N,N,N',N'*-tetraalkyl-3,6- dioxaoctanediamide (DOODA), were chosen as model cases, the structure of their complexes and complex formation behavior were investigated by single crystal X-ray diffraction, UV-visible, infrared (IR), and multi nuclear magnetic resonance (NMR) spectroscopy techniques. This study also focused on the relationship between the molecular structures and the selectivity of hard donor extractants through the systematical investigation across the Ln(III) series.

The Ln(III) nitrate complexes (Ln=La-Lu, except for Pm) with DGA and DOODA were synthesized and characterized in crystallographically to give a thorough picture of the structural features of these complexes.

The complexations, stabilities and structures of Ln(III) nitrate complexes with DGA and DOODA in acetonitrile solutions were investigated by UV-vis and multinuclear NMR spectroscopy. There are significant differences in stabilities and structures between the light and heavy Ln(III) as corresponding to the variations of distribution ratio (*D*). The complexations and stabilities of formed complexes are strongly governed by labile kinetic properties of Ln(III) ions and lanthanide contraction. Here, a deep understanding of the interaction between Ln(III) and hard donor extractant have been provided from the view point of coordination chemistry.

Contents

Chapter 1

General Introduction

1.1 Reprocessing of Spent Nuclear Fuels

Reprocessing of spent nuclear fuel has been one of the major concerns in utilization of nuclear energy. The initial motivation of reprocessing was to isolate uranium (U) and plutonium (Pu) for military purposes, but more recently with the purpose of recovery of both U and Pu has been attracted to their re-use that also saves natural U resources. The PUREX (Plutonium URanium EXtraction, Plutonium Uranium Reduction EXtraction) process is the most common industrial method. The PUREX process is a solvent extraction method and is designed to recover > 99.9% of the incoming Pu and U from the other transuranium elements (neptunium (Np), americium (Am) and curium (Cm)) and fission products.[1,2] The fission products include every element from zinc (Zn) through the lanthanides, e.g. noble gases, halides, 15- and 16-group elements, tin, indium, second row transition metals, alkali metals, alkaline earths and about two-thirds of the lanthanide series.[3] During the PUREX process, liquid wastes containing high-level radioactive elements, high-level liquid wastes (HLLW), are produced. Although the relative amount of HLLW is small with respect to the total volume of radioactive waste produced, it contains 95% of the radioactivity. Figure 1-1 shows the relative radiotoxicity of the different components of spent nuclear fuel. The potential hazard of HLLW generated by PUREX process is exceeds 10,000 years if only U and Pu are separated. Partitioning and transmutation (P&T) is one of the key technologies for reducing the radiotoxicity and volume of long-lived minor actinides (MA). (Radiotoxicity: relative to natural uranium ore.) Therefore, it would reduce the period of radiotoxicity to 300–500 years and the final waste volume requiring disposal in deep geological repositories.[4,5]

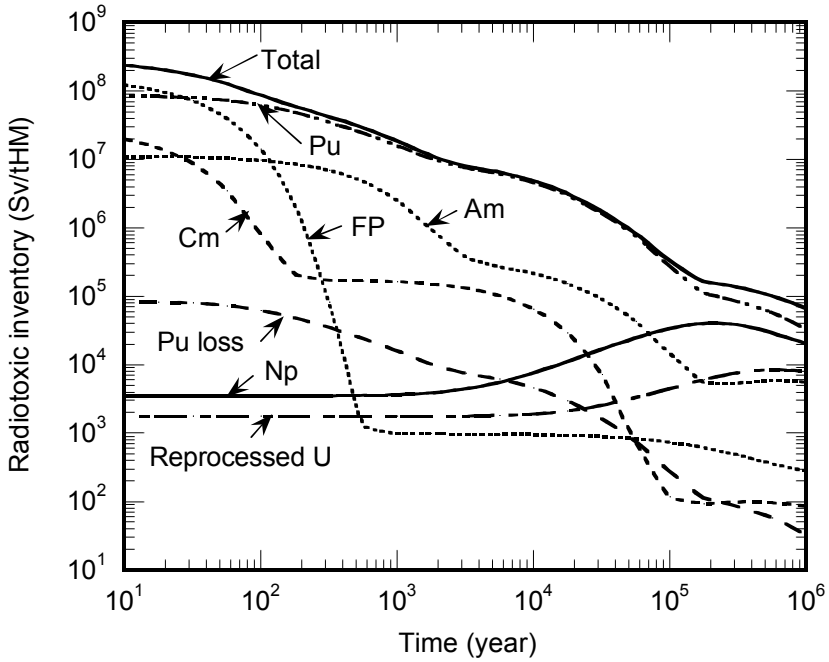

Figure 1-1 Radiotoxic inventory of UOX fuel as a function of time (3.7% 235U, 45 GWd/tHM). [4]

However, separations of MA from other fission products have been playing key role to establish the P&T technology. The difficulties arise from the similarities of oxidation states, chemical properties and ionic radii between MA and lanthanides.

1.1.1 Separations of Ln(III) and An(III) by Solvent Extraction

Although numerous separation processes exist, solvent extraction is the most facile method because the choice is wide for the chemical system. To achieve the separation of MA, it is necessary to separate them from other fission products especially for the trivalent lanthanides (Ln(III)). The Ln(III) and the trivalent MA (An(III)) possess relatively similar physical and chemical properties. Examples are follows:

- Stable in the acidic aqueous solutions with trivalent oxidation state
- Decreasing ionic radii along the series is traversed
- Accompanying 8–9 hydrated molecules in the first coordination sphere
- Possessing similar ionic radii and charge density for An(III) and Ln(III)
- Hard electron-acceptor properties according to Pearson's theory of hard and soft acids and bases
- Orientation to form hard oxygen donor atom

The separation of An(III) must be achieved by selective extraction over the Ln(III). However, properties listed above make the mutual separation of Ln(III)/An(III) difficult in a single step. Consequently, most of separation processes of Ln(III) and An(III) comprise two steps. It has been assumed that the slightly greater 5*f* orbitals can be responsible for some degree of covalency in the bonding interactions between An(III) and soft bases, such as sulfur- or nitrogen- bearing extraction reagent (extractant).[6,7] Therefore, two-step processes consist of: first, Ln(III) and An(III) co-extraction process by hard donor atom bearing extractant (hard donor extractant), and second, mutual separation process of Ln(III)/An(III) by soft donor atom bearing extractants (soft donor extractant).[8] Today, there are few processes are available that allow recovery of An(III) in a single step. However, none of the processes are available to adapt industrial processes yet.

1.1.2 Extraction Reagent (Extractant)

In order to achieve mutual separations of Ln(III) and An(III), numerous extractants have been developed. The metal ions can only be transferred from an aqueous to an organic phase as an uncharged complex with an extractant. There are two basic types of extractants, acid and neutral.[9]

Acid

The extraction mechanism of Ln(III) and An(III) ions by an acid extractant can be described by the following equilibrium, where HL symbolizes an acid extractant in the organic phase. This reaction is referred as a cation exchange process and depends on the aqueous phase acidity (or pH).

$$M^{3+}_{(aq)} + 3HL_{(org)} \overset{K_{ex}}{\rightleftharpoons} ML_{3(org)} + 3H^{+} \qquad \text{(Eq. 1)}$$

Neutral

The extraction mechanism of Ln(III) and An(III) ions by an neutral extractant can be described by the following equilibrium, where A^- symbolizes a counter anion of the aqueous phase and L is a neutral extractant of the organic phase. The extraction into an organic phase requires the co-extraction of a counter anion, often nitrate, in order to form an uncharged complex.

$$M^{3+}_{(aq)} + 3A^{-}_{(aq)} + nL_{(org)} \overset{K_{ex}}{\rightleftharpoons} MA_3L_{n(org)} \qquad \text{(Eq. 2)}$$

Logarithm expression of distribution ratio (*D*) and equilibrium constant (K_{ex}) can be derived as

follows:

$$logD = 3log[A^-] + nlog[L] + logK_{ex} \quad \text{(Eq. 3)}$$

The plots of *logD* against *log*[L] will give information about the number of extractant (*n*) participating in the extraction equilibrium.

Hard Donor Extractant

Both Ln(III) and An(III) are classified as hard ions and react with hard donors, such as oxygen. The hard donor extractants, such as CMPO, malonamides and TRPO, have been widely examined for the first step co-extraction of Ln(III) and An(III) from other fission products. For example, the octyl(phenyl)-*N,N'*-di-*iso*-butylcarbamoyl-methylphosphine oxide (OΦD(iB)CMPO) is the most popular and utilized extractant for TRUEX process. Malonamides are also widely studied extractants and *N,N'*-dimethyl-*N,N'*-dioctylhexylethoxy-malonamide (DMDOHEMA) was assigned as an extractant of the DIAMEX process. The trialkyl phosphine oxide (TRPO) process was developed in China during the 1990s for TRPO process.[1] The structures of these extractants are shown in Figure 1-2.

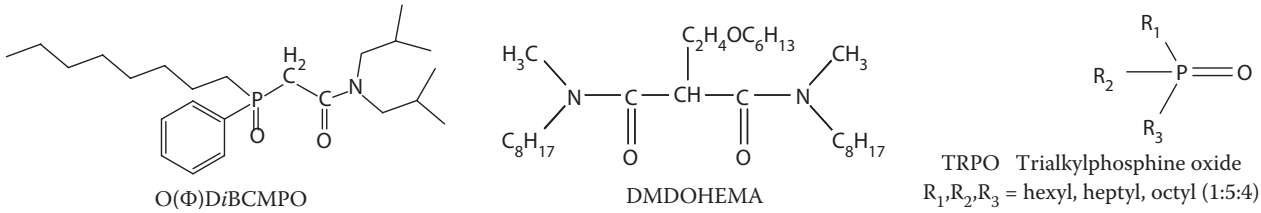

Figure 1-2 Structures of hard donor extractants used for the Ln(III)/An(III) separation processes.

Soft Donor Extractant

Most of mutual separation processes of An(III) over Ln(III) were utilized the extractant possessing soft donors with sulfur or nitrogen atoms. For example, significantly large separation factors (SF[Am/Eu]) in extraction systems of Cyanex 301. The nitrogen-bearing ligands generally used as a aqueous solution.[10] The N-donor ligands have the advantage of being completely incinerable and follow the CHON-principle (extractants that contain only C, H, O and N elements are preferred) leading to reduced secondary wastes. The 2,4,6-tri(2-pyridyl)-1,3,5-triazine (TPTZ) and bis-triazinyl-1,2,4-pyridines (BTP) derivatives have been widely investigated.[1] The structures of these extractants are shown in Figure 1-3.

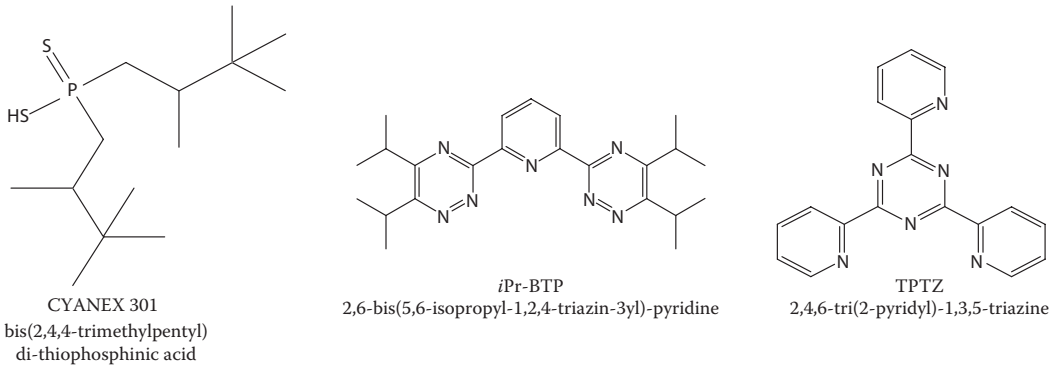

Figure 1-3 Structures of soft donor extractants used for mutual separation processes of Ln(III) and An(III).

Bitopic N, O ligands

Recently, soft (N)-hard (O) hybrid donor are in interest because N-donors of the pyridine group can discriminate between 4*f*- and 5*f*-elements and the carbonyl group can contribute to the stability in

contacting acidic solutions.[11] Picolinamides (2-pyridine carboxyamides) bear soft-hard hybrid donor atoms and it extracts An(III) from weakly acidic solution. The pyridine-2,6-dicarboxyamides (PDA) were investigated and showed higher extraction of An(III) owing to two carbonyl groups in acidic solution.[12] However, their separation abilities are rather low compared with original soft donor extractants. The structures of these extractants are shown in Figure 1-4.

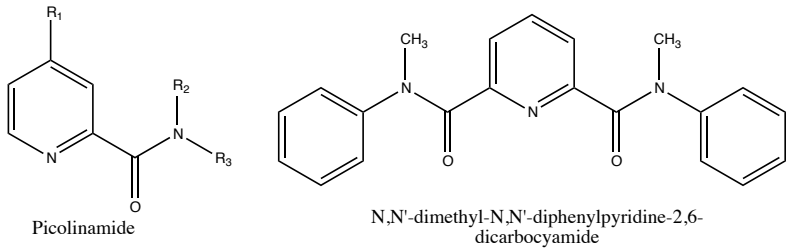

Figure 1-4 Structures of bitopic N, O extractants.

Neutral Diamide Extractant

Neutral diamide compounds are hard donor extractants and have been found to be an efficient extractant of co-extraction of Ln(III) and An(III). Malonamides are one of the most extensively investigated extractant and *N,N'*-dimethyl-*N,N'*-dioctylhexylethoxy-malonamide (DMDOHEMA) was proposed as an extractant of the DIAMEX process as explained above. Malonamides have two oxygen atoms, which are electron donors and coordinate to Ln(III) and An(III). Owing to the fact that the poor preorganization of the two carbonyl groups of malonamides, an ether oxygen was introduced between the two amide groups. *N,N,N',N'*-tetraalkyldiglycolamide (DGA) and *N,N,N',N'*-tetraalkyl-3,6-dioxaoctanediamide (DOODA) have been found to have an affinity to Ln(III) and An(III) in both organic and aqueous phase. Figure 1-5(a) shows the structures of DGA and DOODA. The lipophilic DGA derivative, *N,N,N',N'*-tetraocthyl diglycolamide (TODGA), has a strong affinity to An(III) and Ln(III) and can separate them from other fission products. The hydrophilic DGA derivative, *N,N,N',N'*-tetraethyldiglycolamide (TEDGA) can be act as the back extraction reagent or the masking agent.

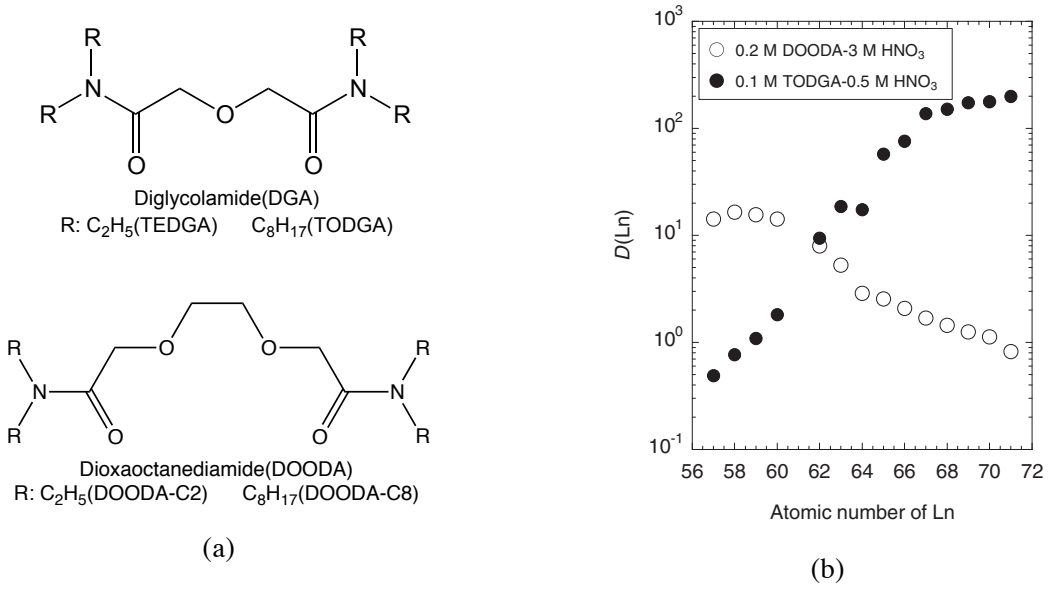

Figure 1-5 (a) Structures of DGA (top) and DOODA (bottom), (b) plots of *D*(Ln) against atomic number for DOODAC8 and TODGA extraction.[13]

As shown in Figure 1-5, TODGA shows high selectivity especially from middle to heavy Ln(III). On the other hand, the lipophilic DOODA derivative, *N,N,N',N'*-tetraocthyl-3,6-dioxaoctanediamide

(DOODCAC8), shows the opposite tendency in *D* values across the Ln(III) series.[13,14,15,16] The An(III) ions behave as light Ln(III) ions in these extraction system. Therefore, the combine use of these lipophilic and hydrophilic diamide derivatives which have high *D* value for light Ln(III) ions such as DOODA and high D value for heavy Ln(III) such as DGA is expected to display large separation factors between An(III) and Ln(III) species. Such a process has a potential to achieve one step mutual separation of Ln(III) and An(III).[17,18]

1.1.3 Development of New Extractant

The development of new extraction for the selective binding and the separation of An(III) over Ln(III) in solutions is real challenge because of the (i) similar properties of Ln(III) and An(III), and (ii) complexities of molecular interactions between metal ions and other molecules such as solvent molecules, extractants and counter anions. With regard to O-bearing hard donor extractants, the bonding nature is primarily ionic and mainly governed by charge density.[19] Therefore, hard donor extractants and nitrate ions would compete with each other in inner-sphere *vs*. outer-sphere coordination. Moreover, Ln(III) ions are stereochemically spherical and are known as being kinetically very labile with water exchange rate in the range 10^7-10^9 s^{-1}.[20]

These facts must be a problematic for development of new extractant that bears oxygen as a part of donor such as a bitopic N-,O-bearing hybrid extractant. Compared with complexation in homogeneous solutions, extraction processes are more complex because they involve a lot of chemical and physical interactions between molecular species. However, in many cases of extractants associate with Ln(III) and An(III), the chemical structures or properties of the extracted species remain unclear. There remains a need for an alternative approaches for design and development for an efficient extractant for the separation of An(III) over Ln(III).

1.2 Scope of This Thesis

The selective complexation of An(III) over Ln(III) is the most challenging key issue for the developments of extraction reagent (extractant). There is extensive research to find new efficient extractants for this purpose. These attempts have been mainly based on the trial-and-error way and not based on the molecular interpretation. Understanding fundamental properties of extracted species must be crucial for the development of more efficient extractants. However, despite some efficient extractants have been examined by solvent extraction, the natures and the structures of the extracted species, i.e. metal complexes, have not been elucidated.

In this context, coordination chemistry of Ln(III) and An(III) has potentially important implications. To clarify the molecular structure of extracted species would provide insight into both coordination chemistry of the *f* elements and the factors for affecting selectivity of extractants. Especially for hard donor extractants, it is believed that chemical bonds are ionic and the selectivity of these extractants are mainly governed by ionic radii and charge density of Ln(III) or An(III). However, the distribution ratios (*D*) do not always show linear relation with ionic radii or charge density of Ln(III) series. There should exist any relations between molecular structures and extraction efficiency other than ionic radii.

As outlined previous chapter, neutral diamide derivatives have been recognized as the promising extractant for separations of Ln(III) and An(III) from other fission products. The combine use of lipophilic or hydrophilic diamide derivatives which possess different selectivity to Ln(III) and An(III) is of interest and has high potentiality for one-step mutual separation. Despite of their high efficiency and the interesting feature, very limited information is available for the properties of extracted Ln(III) and An(III) species (complexes). In addition, the extraction into an organic phase requires the co-extraction of counter anion, often nitrate, in order to form an uncharged complex. Since both the diamide extractants and nitrate ion act as hard donor ligands which interact with Ln(III) and An(III) electrostatically not covelently, their chemical lability make experimental observations and analyses difficult in solutions.

The Ln(III) nitrates and neutral diamide derivatives (DGA and DOODA) as model cases, this study focused on the relationship between the molecular structures and the selectivity of hard donor extractants through the systematical investigation throughout the Ln(III) series in both solid and solution states. The structures of the complexes and complex formation behaviors were investigated by single crystal X-ray diffraction, UV-visible, infrared (IR), and multi nuclear magnetic resonance (NMR) spectroscopy techniques.

This thesis is composed by 7 chapters as follows:

Chapter 1 General Introduction

Chapter 2 Syntheses and Characterizations of Lanthanide(III) Nitrate Complexes with TEDGA

Chapter 3 Complexation and Structural Studies of Lanthanide(III) Nitrate Complexes with TEDGA in Acetonitrile Solutions

Chapter 4 Syntheses and Characterizations of Lanthanide(III) Nitrate Complexes with DOODAC2

Chapter 5 Complexation and Structural Studies of Lanthanide(III) Nitrate Complexes with DOODA in Acetonitrile Solutions

Chapter 6 Effect of Nitrate on Complexation of Lanthanide(III) with DGA and DOODA

Chapter 7 Summary

1.3 Chemistry of Lanthanides and Actinides

1.3.1 History

The discovery of the rare earth elements began in 1787 when Carl Axel Arrehenius, a young Swedish army officer, happened upon a new mineral at Ytterby, a small town near Stockholm, Sweden. He found a new, very dense black mineral which after he named 'ytterbite', later renamed 'gadolinite'. The first chemical analysis was carried out in 1794 by the Finnish chemist Johan Gadolin. From this mineral, he isolated ytteria - Y_2O_3. Ytteria was later revealed to be a mixture of the oxides of no fewer than ten new elements, yttrium (Y), terbium (Tb), erbium (Er), ytterbium (Yb), scandium (Sc), holmium (Ho), thulium (Tm), gadolinium (Gd), dysprosium (Dy) and lutetium (Lu).[21,22,23] In 1989, the mine was elected as the "Historical Landmark of the year" by the American Society of Metals. (Figure 1-6(a)) The names of the street in Ytterby reflected to the name of many of these elements. (Figure 1-6(b))

(a) (b)

Figure 1-6 (a) Memorial plaque of the ASM International society at the entrance of Ytterby mine near Stockholm, Sweden and (b) street plate at Ytterby in May, 2012.

Shortly after Gadolin's discovery, M.H. Klaporth in France and, independently, J.J. Berzelius and W. Hisinger in Sweden started the isolation of ceria (Ce_2O_3) in 1803. Cerite was also revealed to be a mixture of lanthanum (La), praseodymium (Pr), neodymium (Nd), samarium (Sm), gadolinium (Gd) and europium (Eu). In 1907, with the final discovery of lutetium (Lu), all of the naturally occurring rare earth had been isolated. The completion of the lanthanide series was by synthesized and characterized of the missing radioisotope element, promethium (Pm) in 1947. Figure 1-7 shows the progress in discoveries of the rare earth elements.

Thorium (Th), protoactinium (Pa), and uranium (U) are the only naturally occurring actinide elements. None of the other actinide elements occurs naturally. They must be synthesized by nuclear reactions. These 14 elements recognized as a new family in periodic table with fourth atomic primary quantum shell. Many of transuranium elements were synthesized by G.T. Seaborg as a result of the research of nuclear science. On the periodic table, 14 elements, the atomic number from 57 to 71, from 89 to 103 of rare earth (lanthanide) and actinide are listed, respectively.

Lan-thanum 57 La	Cerium 58 Ce	Praseo-dymium 59 Pr	Neo-dymium 60 Nd	Prome-thium 61 Pm	Sama-rium 62 Sm	Europ-ium 63 Eu	Gadolin-ium 64 Gd	Ter-bium 65 Tb	Dyspro-sium 66 Dy	Hol-mium 67 Ho	Erbium 68 Er	Thulium 69 Tm	Ytter-bium 70 Yb	Lute-tium 71 Lu
Actin-ium 89 Ac	Thor-ium 90 Th	Protac-tinium 91 Pa	Ura-nium 92 U	Neptu-nium 93 Np	Pluto-nium 94 Pu	Ameri-cium 95 Am	Curium 96 Cm	Berkel-ium 97 Bk	Califor-nium 98 Cf	Einstei-nium 99 Es	Fer-mium 100 Fm	Mende-levium 101 Md	Nobel-ium 102 No	Lawren-cium 103 Lr

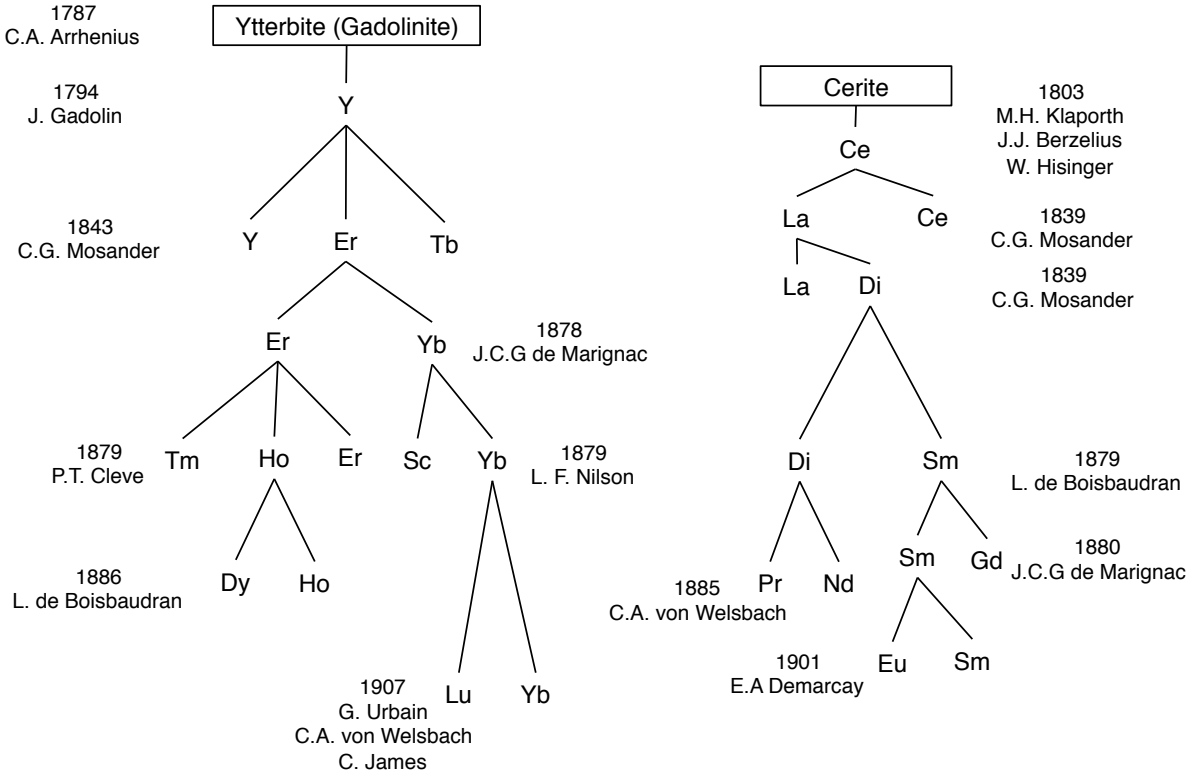

Figure 1-7 Chronology and dendrology of the isolation of rare earths. [21,23]

1.3.2 Physical and Chemical Properties

Oxidation States

In general, the +3 oxidation stat is the most stable for all the lanthanide, while +2 and +4 are known for several lanthanides in the solid state. For the early actinides (An= Ac-Np) have higher oxidation states such as +6, +5 and +4. For the later actinides (transplutonium), most of elements tend to exhibit stable oxidation state, +3, as same as lanthanide, and thus resembling the Ln(III). As shown in Table 1-1 and Table 1-2, the ionic radius of An(III) are close to that of Ln(III). The solution chemistry of the Ln(III) and An(III) are not just similar, they are known that nearly identical in aqueous solutions. Both Ln(III) and An(III) are classified as hard ions and react with hard donors bearing such as oxygen atom. On the other hand, the nature of 5*f* electrons has large relativistic effect and degree of covalency makes the An(III) ions slightly softer than Ln(III) ions.

Lanthanide and Actinide Contraction

There is a steady decrease in metallic and ionic radii of the Ln(III) as the lanthanide series is traversed from La to Lu. The ionic radii for six-, nine- and twelve-coordination of Ln(III) are listed in Table 1-1. The shrinking of the ionic radii as the 4*f* sub-shell is filled is referred as the "lanthanide contraction".[24] This occurs due to the relativistic effects.[25],26] Figure 1-8 shows the radial distribution functions of 4*f*, 5*s*, 5*p*, 5*d*, 6*s* and 6*p*. The 5*s* and 5*p* orbitals penetrate the 4*f* subshell and are not shielded. The increase in 4*f* electrons only partly shields the increase in nuclear charge.

Therefore, as the atomic number increases the effective attraction between the nucleus and the outer electrons increases, and results cause shrinkage of the ionic radius. A similar contraction can be found in the actinide series.[27] The ionic radii for six- and eight-coordination of Ln(III) are listed in Table 1-2.

Table 1-1 Electron configurations and ionic radii of the Ln(III) in six-, nine- and twelve-coordination [28]

#	Symbol	Electron Configurations	Ionic Radius(Å) CN=6	Ionic Radius(Å) CN=9	Ionic Radius(Å) CN=12
20	Ca^{3+}	[Ar]	0.99	1.18	n.a
21	Sc^{3+}	[Ar]	0.75	0.93	1.06
39	Y^{3+}	[Kr]	0.90	1.08	1.22
57	La^{3+}	[Xe]	1.03	1.22	1.36
58	Ce^{3+}	$[Xe]4f^{1}$	1.01	1.20	1.34
59	Pr^{3+}	$[Xe]4f^{2}$	0.99	1.18	1.32
60	Nd^{3+}	$[Xe]4f^{3}$	0.98	1.16	1.30
61	Pm^{3+}	$[Xe]4f^{4}$	0.97	1.14	1.28
62	Sm^{3+}	$[Xe]4f^{5}$	096	1.13	1.27
63	Eu^{3+}	$[Xe]4f^{6}$	0.95	1.12	1.25
64	Gd^{3+}	$[Xe]4f^{7}$	0.96	1.11	1.24
65	Tb^{3+}	$[Xe]4f^{8}$	0.92	1.10	1.23
66	Dy^{3+}	$[Xe]4f^{9}$	0.91	1.08	1.22
67	Ho^{3+}	$[Xe]4f^{10}$	0.90	1.07	1.21
68	Er^{3+}	$[Xe]4f^{11}$	0.89	1.06	1.19
69	Tm^{3+}	$[Xe]4f^{12}$	0.88	1.05	1.18
70	Yb^{3+}	$[Xe]4f^{13}$	0.87	1.04	1.17
71	Lu^{3+}	$[Xe]4f^{14}$	0.86	1.03	1.16

Table 1-2 Electron configurations and ionic radii of the An(III) in six- and eight-coordination [28]

#	Symbol	Electron Configurations	Ionic Radius(Å) CN=6	Ionic Radius(Å) CN=8
89	Ac^{3+}	[Rn]	1.12	1.26
90	Th^{3+}	$[Rn]4f^{1}$		
91	Pa^{3+}	$[Rn]4f^{2}$	1.05	1.2
92	U^{3+}	$[Rn]4f^{3}$	1.028	1.16
93	Np^{3+}	$[Rn]4f^{4}$	1.011	1.141
94	Pu^{3+}	$[Rn]4f^{5}$	0.995	1.123
95	Am^{3+}	$[Rn]4f^{6}$	0.98	1.106
96	Cm^{3+}	$[Rn]4f^{7}$	0.97	1.094
97	Bk^{3+}	$[Rn]4f^{8}$	0.955	1.077
98	Cf^{3+}	$[Rn]4f^{9}$	0.945	1.066
99	Es^{3+}	$[Rn]4f^{10}$	0.934	1.053
100	Fm^{3+}	$[Rn]4f^{11}$	0.922	1.04
101	Md^{3+}	$[Rn]4f^{12}$	0.912	1.028
102	No^{3+}	$[Rn]4f^{13}$	0.902	1.017
103	Lr^{3+}	$[Rn]4f^{14}$	0.896	1.01

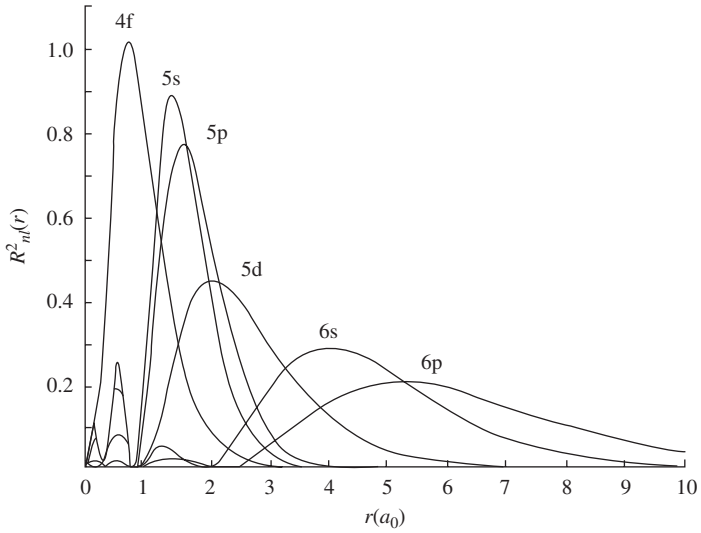

Figure 1-8 Radial distribution functions of 4*f*, 5*s*, 5*p*, 5*d*, 6*s*, and 6*p* electrons for cerium [29]

1.3.3 Structural Chemistry of Ln(III) Complexes

Many transition metals have more than one oxidation state and adopt characteristic coordination numbers for each oxidation state. The lanthanides adopt primarily the +3 oxidation state, however, the lanthanides do not have characteristic coordination number. The outer $5s^2$ and $5p^6$ sub shells shield inner 4*f* electrons from outer interactions, hence, the Ln(III) are essentially spherical like alkali and alkaline earth ions. The bonding in Ln(III) complexes will be mostly ionic in nature and the geometrical arrangement of the ligands will not be affected by bonding requirements but by steric requirements. The Ln(III) interact strongly with negatively charged groups because of the electrostatic nature of their own.

Table 1-3 The statistic number of lanthanide complexes with different coordination number [27]

CN	La	Ce	Pr	Nd	Sm	Eu	Gd	Tb	Dy	Ho	Er	Tm	Yb	Lu
3		1		1	1	2		1					1	
4	3	3			1		1	1					7	2
5	3	3	3	4			1				3		3	1
6	8	7	12	8	15	10	7		3	1	6	1	20	7
7	10	7	5	10	12	7	6	1	5	1	5	1	13	6
8	31	36	27	53	73	34	24	6	13	16	39	5	68	40
9	31	17	26	26	36	32	25	11	16	12	25	5	21	13
10	33	20	16	16	18	13	4	1	3	2	2	1	9	1
11	14	5	6	6	2	3				1			2	
12	11	7	2	2		1	1		1					
total	144	106	97	97	158	102	69	21	41	33	80	13	144	70

The Ln(III) have a wide range of coordination numbers from 3 to 12. Table 1-3 shows the number of lanthanide complexes with different coordination number. Many factors affect coordination numbers and coordination polyhedral. When small ligand like water, chloride, carbonate or nitrate bind to metal, coordination number is determined by how many ligands can wrap around the metal ion.[30] Still now, there is no certain way to know the coordination number of Ln(III) species and the structure cannot be known until the synthesis have completed. Single crystal X-ray diffraction is the only certain way to know the coordination environment around Ln(III). Here some examples of the structural chemistry of coordination number 8, 9, 10 and 12 are presented.

Coordination Number 8

Ln(III) complexes with eight-coordination are well known. The two polyhedra of coordination geometry of eight-coordination are the square anti prism (D_{4d}) and the dodecahedron with triangular faces (D_{2d}).[31,32,33,34] The idealized polyhedra are shown in Figure 1-9. The geometrical distortions required to send one structure into another are often rather small. The energy difference between these two types of polyhedral is also very small.

The square antiprism may be characterized by following two shape parameters; [31]

(1) The ratio of the length of the side of a triangular face to that of the edge of the square face (1/S) and

(2) the angle between the 8 fold axis and the vector from the central atom to one of the atom on the vertex of the square.

The most favorable values for the two parameters are l/s = 1.057 and θ = 57.3°.

The dodecahedron may be characterized by following three parameters,

(1) θ_A: the angle between the 4 fold axis and the bond vector of central atom to vertex A (M-A)

(2) θ_B: the angle between the 4 fold axis and the bond vector of central atom to vertex B (M-B)

(3) the ratios of bond length M-A/M-B

The most favorable values for the three parameters are $\theta_A = 35.2°$, $\theta_B = 73.5°$ and M-A/M-B = 1.03.

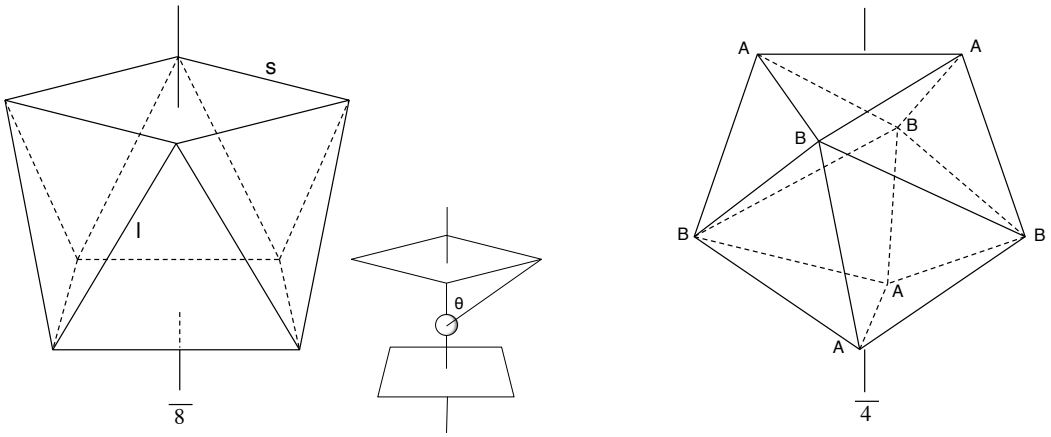

(a) (b)

Figure 1-9 Idealized octa-coordination polyhedra (a) square antiprism(D_{4d}) (b) dodecahedron with triangular faces (D_{2d}), labeled according to Hoard and Silverton.[31]

Coordination Number 9

Nine-coordinate structures are common among light Ln(III). The most common polyhedron is tricapped trigonal prism (D_{3h}). [35,36] Less favorable monocapped square antiprismatic (C_{4v}) geometry can also be found in some Ln(III) complexes. The idealized polyhedra are shown in Figure 1-10. Rearrangement in the nine-coordination polyhedral readily generated by stretching motion as shown in Figure 1-11. Guggenberger and Mutterties proposed the criteria for distinction of both geometry based on the dihedral angles along the edges of the coordination polyhedron.[37]

To examine of opposite triangular faces and measure their deviation from planarity (180° for the planar case) is most expeditious way to make symmetry distinction. The dihedral angle criteria for idealized nine-coordination structures are listed in Table 1-4.

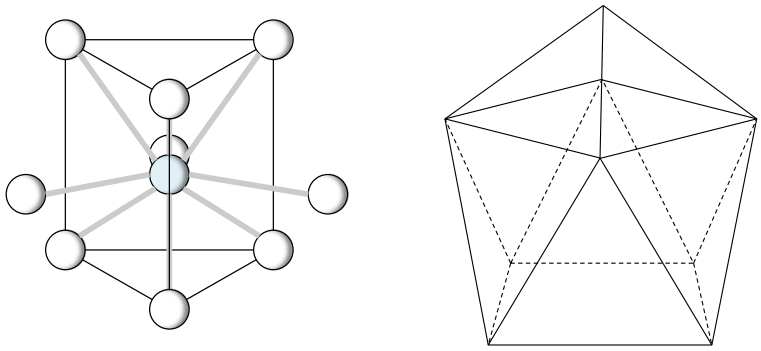

(a) (b)

Figure 1-10 Idealized nine-coordination polyhedra (a) tricapped trigonal prism (D_{3h}) (b) monocapped square antiprismatic (C_{4v}).

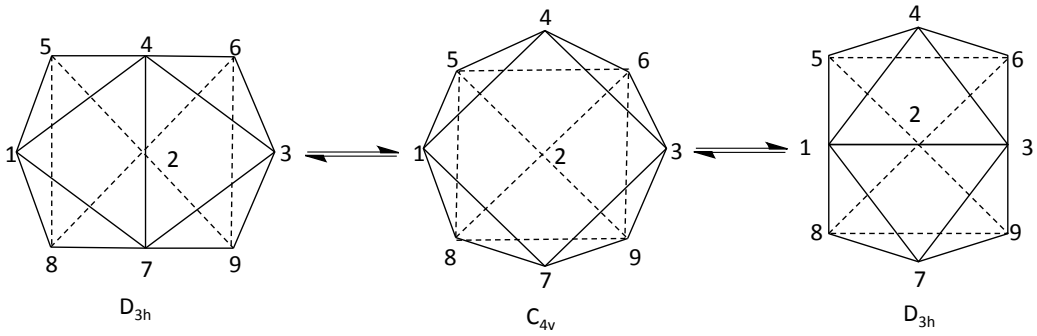

Figure 1-11 Rearrangement process from D_{3h} to C_{4v}.

Table 1-4 Dihedral angles in nine-coordination for idealized complexes. See **Figure 1-11** for plane identifications.

Symbol	Type of faces	Face 1	Face 2	Angle (°)
	Opposed(⊥)	(4,6,5)	(7,8,9)	180
D_{3h}	Opposed(‖)	(1,7,4)	(2,6,9)	3 at 146.4
	Vicinal(‖)	(1,7,4)	(3,4,7)	3 at 26.4
	Opposed	(1,5,8)	(3,6,9)	2 at 163.5
C_{4v}	Opposed	(1,4,5)	(3,7,9)	2 at 138.2
	Vicinal(⊥)	(1,3,4)	(1,7,3)	0.0

Coordination Number 10

The coordination polyhedra for ten-coordination have been reported for various Ln(III) complexes. [38, 39, 40] Three types of coordination polyhedra considered for ten-coordination are the bicapped square antiprism (D_{4d}), the bicapped dodecahedron (D_2) and the polyhedron based on a dodecahedron (C_{2v}).[41] The idealized polyhedra are shown in Figure 1-12. In each polyhedron, vertices placing at the capped position in D_{4d}, or position C in D_2 and C_{2v}, are linked to 4 other vertices and others are linked to 5 others.

The bicapped square antiprism (D_{4d}) is the most favorable geometry for ten-coordination. When all the central atom to each vertex distances are the same, then the shape of the bicapped antiprism is defined by the angle, θ, between the 4 fold axis and the bond vector of central atom to vertex A. The most favorable angular parameter for the bicapped square antiprism polyhedron (D_{4d}) is $\theta = 64.8°$. In the bicapped dodecahedron (D_2), most favorable angular parameters are $\theta_A = 32.8°$, $\theta_B = 77°$ and $\theta_c = 60°$. In the polyhedron based on a dodecahedron (C_{2v}), most favorable angular parameters are $\theta_A =$

32.8°, θ_B = 65.8° and θ_c = 63.8°.

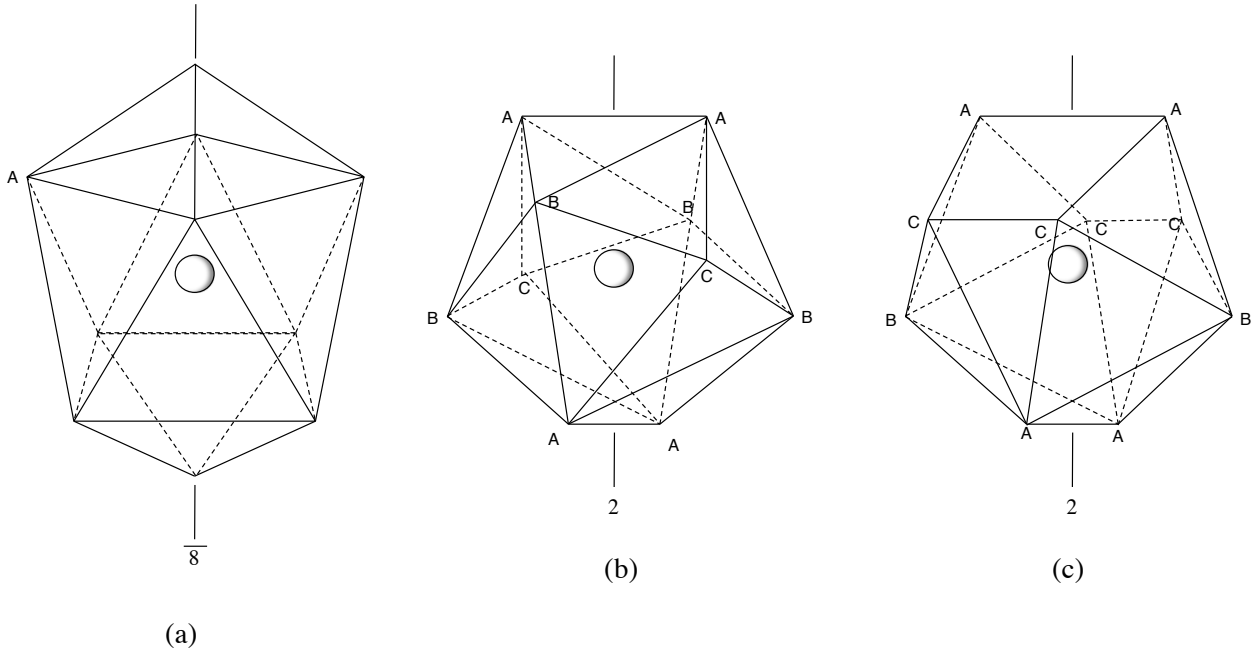

Figure 1-12 Idealized ten-coordination polyhedra (a) the bicapped square antiprism (D_{4d}), (b) the bicapped dodecahedron (D_2) and (c) the polyhedron based on a dodecahedron (C_{2v}), labeled according to Al-Karaghouli, and Wood. [41]

Based on the repulsion energies, the biccaped square antiprism is the most stable geometry for ten-coordination. Assuming that the five bidentate ligand are wrrapping around the metal ion, two arrangements, *cis* and *trans*, are possible. The two differenct arrangements are shown in Figure 1-13.

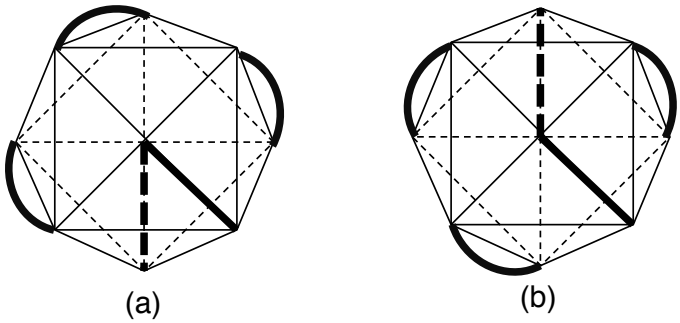

Figure 1-13 Two bicapped square antiprismatic isomers, (a) *cis* conformation and (b) *trans* conformation [35]

Coordination Number 12

Twelve-coordination can be found in the Ln(III) complexes with macrocyclic ligands such as 18-crown-6 ether. High coordination numbers can also be found when the small multidentate ligand with a small "bite angle" such as nitrate or carbonate, or in combination with other ligands.[30] The large homoleptic twelve-coordinate $[M(NO_3)_6]^{3+}$ (M=La(III)-Dy(III) and Pu(IV)) ions are known to co-crystallize with large cationic complexes.[42,43,44,45,46,47] Dy(III) is the largest metal among the Ln(III) and An(III) to form $[M(NO_3)_6]^{3+}$ type anion.[48]

The polyhedron of twelve-coordination is icosahedron. Icosahedron is a polyhedron with 20 triangular faces, 30 edges and 12 vertices as shown in Figure 1-14. A regular icosahedron would require 60° angles between the symmetry axis and the bond vector of central atom to vertex, and all 12 vertices are identical and are linked to 5 other vertices. Three structural isomers may be formed by

wrapping six bidentate ligands along the edges of an icosahedron as shown in Figure 1-15. Isomer I is the most high symmetric with the symmetry T_h compared with other isomers.

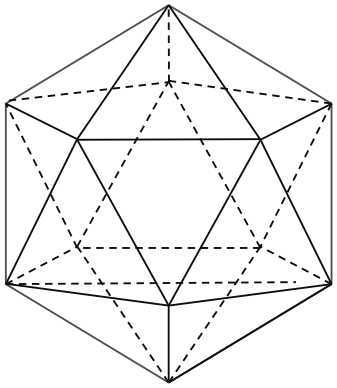

Figure 1-14 Regular icosahedron (I_h).

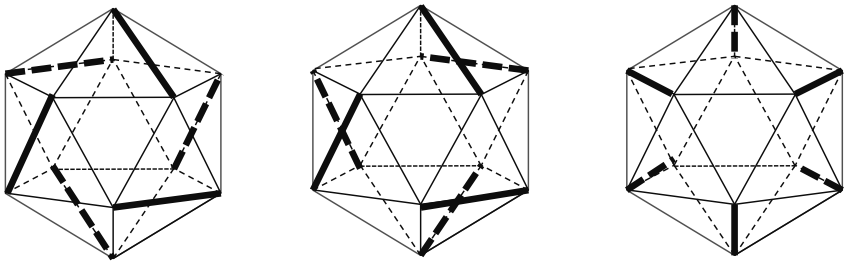

Figure 1-15 Icosahedral isomers with six bidentate ligands, $[M(bidentate)_6]$. [35]

1.3.4 Solution Chemistry of Ln(III) and An(III)

Metal Ion Solvation

Numerous studies of the solvation, solvent exchange or complex formation processes of Ln(III) and An(III) ions, particularly in aqueous solution have been reported.[49,50] Solvation properties of metal ions provide an important perspective as a reference for further studies on complexation, because generally first shell solvent molecules are replaced by the ligand upon coordination. It is therefore kinetics and mechanisms of solvent exchange have been studied to understand fundamental reaction for metal ions.[51]

Complexation of Ln(III) and An(III) in organic solvent is also important because solvent extraction is usually performed with organic solvent and Ln(III) and An(III) ions are extracted to the organic phase. Although most of the anion coordination often occurs, even in non-aqueous polar organic solvents such as dimethylsulfoxide (DMSO), alcohols or acetonitrile, where Ln(III) salts are soluble, have been received less attention. Here some historical and recent studies of solvation and complexation of the Ln(III) are briefly introduced.

Aquo Complexes (Solvation in Water)

Historically, for cations in aqueous solution, a model consisting of four structurally different zones of solvation about the cation was proposed by J. Burgess.[51] The four zones are as follows:

- Zone A is the primary solvation shell in which solvent molecules are directly bonded or interacting with the cation.
- Zone B is a secondary solvation. An additional number of water molecules are influenced by the charge field of the cation.
- Zone C is a disorderd region in which the cation-oriented waters of zone B compete with the bulk structure of D.
- Outermost zone D is a bulk solvent.

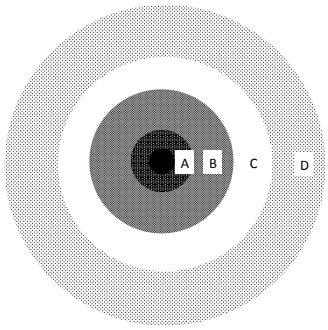

Figure 1-16 The environment of a cation in solution.

In the aqueous solutions, the most common complex is Ln(III) aquo ion, i.e, $[Ln(H_2O)_n]^{3+}$. The coordination number of Ln(III) aquo complexes is now believed to be 9 for the light lanthanides (La–Eu) and 8 for the later metals (Dy–Lu), with the intermediate metals exhibiting a mixture of species.[52] Figure 1-17 shows the calculated nona (left) and octa (right) aqua ion of Ln(III).[53] Skanthakumar *et al*. reported that the coordination environment of the hydrated Cm(III) ion probed to be nine both in the solid state and in solution. [54,55,56,57]

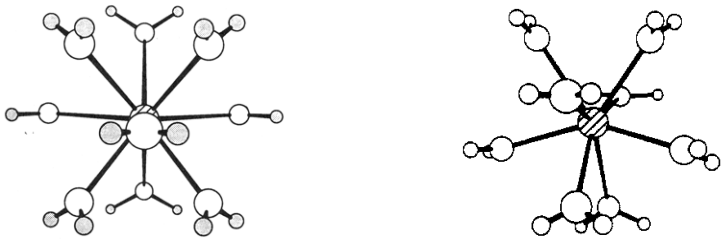

Figure 1-17 Calculated nona (left) and octa (right) aqua ion.[53]

Solvation in Organic Solvent

Most of the experimental studies have focused on water as solvent.[52] In contrast to aqueous solvation, there are limiting experimental results that report the solvation numbers (coordination numbers) and the corresponding metal to solvent distances.[58] Recently, molecular modeling simulations have contributed for understanding of Ln(III) solvation. They gave reasonable results for Ln(III)-solvate distances and corresponding coordination numbers. For example, Baaden *et al*. performed the molecular dynamics simulations for the un-complexed Ln(III) solvating in acetonitrile in the absence and presence of counter anions. In case of absence of counter anions, coordination number varies from 9.75 for La(III) to 7.95 for Yb(III).[59] These coordination numbers are almost consistent with the solid-state structure of $Ln(MeCN)_9^{3+}$ (Ln = La, Pr and Sm) and $Yb(MeCN)_8^{3+}$ reported by Deacon *et al*.[60] In other example, Bernardo *et al*. reported that the average number of metal-coordinated DMSO in acetonitrile/DMSO mixtures was estimated by FT-IR spectroscopy.[61] The coordination number changed smoothly from 7.8 for La(III) to the lowest value of 7.4 for Lu(III). Coordination numbers vary wildly with both the nature of the ligands, counter ions and the composition of the solutions, although coordination number = 9 is often found (cf. the acetonitrile

solvates).

Complex Formation with Charged Inorganic Ligands

The interactions of Ln(III) with various anions have been studied, such as perchlorate, triflates, halides and nitrates in various organic solvents. For example, interactions between nitrate ions and Ln(III)s have been studied in various solvents, e.g. aqueous and anhydrous alcohols[62], DMF[63,64], acetonitrile[65], water-acetone-Freon-22 mixtures[66,67,68,69,70,71]. Bünzli *et al*. reported from FT-IR spectral studies in acetonitrile solutions, and showed the formation of $[Ln(NO_3)_5]^{2-}$ (Ln=La, Nd, Eu, Tb and Er) with coordination number 9.9 and the coordination mode of nitrate showed approximate C_{2v} symmetry.[72] Fratiello *et al*. revealed formation of mono-, bis-, tetra-nitrato complexes from ^{15}N NMR spectroscopy for lanthanide complexation with nitrate in water-acetone-Freon-22 mixtures at –115 C°.[71] Silber *et al*. reported that $[Eu(NO_3)]^{2+}$, $[Eu(NO_3)_2]^{+}$, and $[Eu(NO_3)_3]$ species are in water-methanol mixtures, and complexation are thermodynamically different in the same conditions among Ln(III) ions (Ln= Nd, Eu and Er).[62] In addition, Choppin *et al*. suggested that the light Ln(III) (Ln = La–Sm/Gd) species form $LnNO_3^{2+}$ complexes more stably than the heavy Ln(III) (Ln = Tb–Lu) from thermodynamic data on the association reaction of Ln(III) ions with nitrate in water.[73]

Complex Formation with Neutral Organic Ligands

In general, a complex formation in aqueous solution with a neutral ligand is occurred by replacing solvated solvent to a ligand. The equilibrium and stability constants are defined as follows:

$$M + L \rightleftharpoons ML \qquad K_1 = \frac{[ML]}{[M][L]} \tag{Eq. 4}$$

$$ML + L \rightleftharpoons ML_2 \qquad K_2 = \frac{[ML_2]}{[ML][L]} \tag{Eq. 5}$$

$$ML_{n-1} + L \rightleftharpoons ML_n \qquad K_n = \frac{[ML_n]}{[ML_{n-1}][L]} \tag{Eq. 6}$$

The products of individual stability constants give overall formation constants denoted by:

$$\beta_1 = K_1 \tag{Eq. 7}$$

$$\beta_2 = K_1 \cdot K_2 = \frac{[ML_2]}{[M][L]^2} \tag{Eq. 8}$$

$$\beta_n = \prod_{i=1}^{n} K_n = \frac{[ML_n]}{[M][L]^n} \tag{Eq. 9}$$

Stability constants have been reported for both inorganic and organic ligands in aqueous and non-aqueous solutions. Many methods have been utilized to this purpose, such as luminescence, infrared vibration, nuclear magnetic resonance, electron magnetic resonance, electron paramagnetic resonance, spectrophotometry, conductometry or calorimetry etc.

Ln(III) ions are hard acids which prefer to form bonds with O-donor ligands. The interaction of Ln(III) with acidic O-donor ligands such as β-diketon in aqueous solutions, and various types of neutral organic ligand such as macrocyclic ligands in non-aqueous solutions have been well studied. For example, Ln(III) complexes with β-diketones such as $[Ln(thd)_3]$ (thd=$Bu^tC(O)CHC(O)Bu^t$) and many analogues have been prepared and used as NMR shift reagents.[23] DMSO is a strong donor solvent which dissolves the Ln(III) salts readily. Lugina *et al*. reported that the Nd(III) perchlorate forms $[Nd(DMSO)_8](ClO_4)_3$ in DMSO solution.[74] Macrocyclic ligands are define as compound with a hydrophilic cavity in which Ln(III) can be accommodated. The stability of the Ln(III) complexes

with crown ether derivatives have been extensively determined.

1.4 Experimental Methods

The objectives of this thesis is to clarify the structures of Ln(III) complexes. In order study the stabilities, dynamics and structural properties of these complexes, combine use of several experimental techniques is necessary. This chapter describes the general principles and backgrounds and methods used in this thesis.

1.4.1 Electronic Absorption Spectroscopy

The 4*f* shells of lanthanide elements are unfilled, different arrangements of 4*f* electrons generate different energy levels. A partial energy diagram is shown in Figure 1-18. The 4*f* electron transitions, between the various energy levels, could generate numerous absorption and emission spectra. However, since the 4*f* shell is efficiently shielded by the closed 5*s* and 5*p* shells, the effect of coordination of the ligand has only a weak influence on the electric environment of lanthanide ions.[75] In addition, Ln(III) coordinate with ligands through 5*d* orbital, thus the vibronic coupling, which is usually observed in a transition metal coordination compounds, is not occur at *f-f* transition.[76]

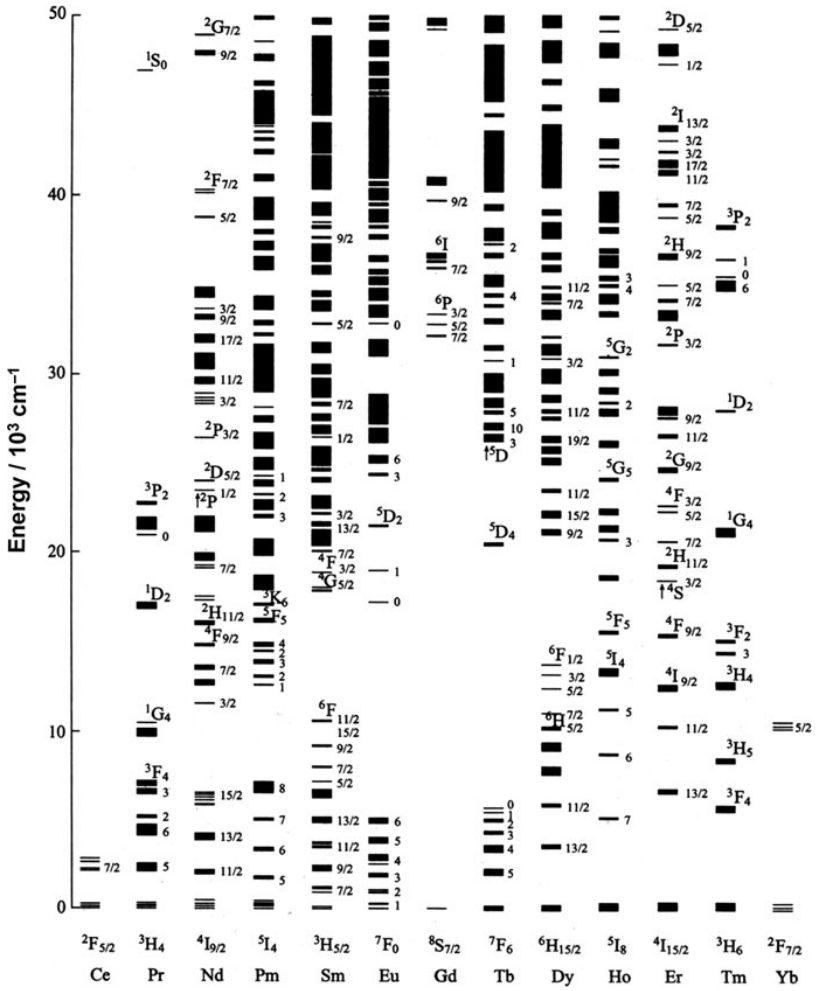

Figure 1-18 Energy level diagram for Ln(III) ions doped in a low-symmetry crystal, LaF_3.[77]

There are three transition mechanisms for lanthanide ions, namely the magnetic dipole (MD) transition, the induced electric dipole (ED) transition and the electric quadrupole (EQ) transition. The MD transitions are allowed, but only a few of them for lanthanide ions are exist and their intensity is weak. The EQ transitions are also allowed, but their intensities are much weaker than MD transitions.

The majority of the observed optical transitions in lanthanide ions are induced ED transitions. Since the 4f orbitals are odd function, *f-f* transitions are Laporte forbidden. However, when the lanthanide ion is under the influence of a ligand-filed, non-centrosymmetric interactions allow the mixing of electronic states of opposite parity into 4*f* wavefunctions, and the transition becomes partially allowed. It is the induced ED transition and some of induced ED transitions are sensitive to the changes in the environment around lanthanide ions and are called *hypersensitive transitions*. A list of the hypersensitive transitions for Ln(III) ions are given in Table 1-5.

Table 1-5 Hypersensitive transitions for trivalent lanthanide ions [78]

Ln	Transition	ν /cm^{-1}	λ /nm
Pr	$^3F_2 \leftarrow {}^3H_4$	5,200	1,920
Nd	$^4G_{5/2} \leftarrow {}^4I_{9/2}$	17,300	578
	$^2H_{9/2}, {}^4F_{5/2} \leftarrow {}^4I_{9/2}$	12,400	806
	$^4G_{7/2}, {}^3K_{13/2} \leftarrow {}^4I_{9/2}$	19,200	521
Sm	$^4F_{1/2}, {}^4F_{3/2} \leftarrow {}^6H_{5/2}$	6,400	1,560
Eu	$^5D_2 \leftarrow {}^7F_0$	21,500	465
	$^5D_1 \leftarrow {}^7F_1$	18,700	535
	$^5D_0 \leftarrow {}^7F_2$	16,300	613
Gd	$^6P_{5/2}, {}^6P_{7/2} \leftarrow {}^8S_{7/2}$	32,500	308
Dy	$^6F_{11/2} \leftarrow {}^6H_{15/2}$	7,700	1,300
	$^4G_{11/2}, {}^4I_{15/2} \leftarrow {}^6H_{15/2}$	23,400	427
Ho	$^3H_6 \leftarrow {}^5I_8$	27,700	361
	$^5G_6 \leftarrow {}^5I_8$	22,100	452
Er	$^4G_{11/2} \leftarrow {}^4I_{15/2}$	26,400	379
	$^2H_{11/2} \leftarrow {}^4I_{15/2}$	19,200	521
Tm	$^1G_4 \leftarrow {}^3H_6$	21,300	469
	$^3H_4 \leftarrow {}^3H_6$	12,700	787
	$^3F_4 \leftarrow {}^3H_6$	5,900	1,695

The intensities of hypersensitive transitions are usually small and are strongly affected by not only the coordination environment around Ln(III) ions, but also the polarity of the solvent, ionic strength, or acidity of the aqueous solution.[78] Choppin *et al*. suggested that the band shape and intensity of hypersensitive transitions can be used as a qualitative indication of the site symmetry. The higher site symmetry gives lower intensity in hypersensitive transition. This is because the lower site symmetry in the ligand field, opposite parity states such as $4f^N$-$5d^1$, is mixed into $4f^N$ states due to the presence of odd parity crystal or ligand fields. [79]

1.4.2 Infrared Spectroscopy

Infrared spectra also give useful information about structures both in solid state and in solutions. For example, the nitrate ion in D_{3h} symmetry has four fundamental vibrations, three of which are infrared active (ν_2, ν_3, ν_4). [80] The four normal mode of vibration of XY_3 molecules like nitrate ion is shown in Figure 1-19.

Upon coordination, either in monodentate or bidentate, the symmetry was reduced from D_{3h} to C_{2v} because one of the oxygen atoms in the nitrate ion would be different from the other two. The different mode of binding nitrate ion to a metal (M) is shown in Figure 1-20. For the coordinated nitrate, all six

bands of C_{2v} symmetry are infrared active.[81] The bands ν_4 and ν_1 are assigned to the N-O asymmetrical stretching vibration, the band ν_2 is composed of the N-O symmetrical stretching vibration, and the band ν_6 is the out-of-plane bending vibration.[82,83]

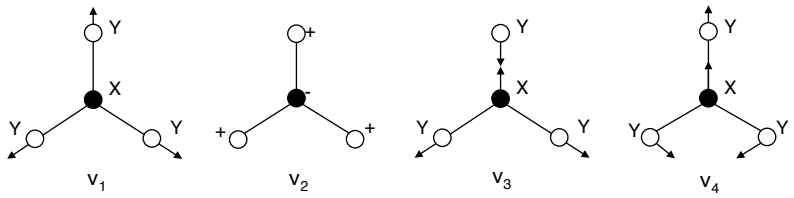

Figure 1-19 Normal modes of vibration of planar XY_3 molecules.[80]

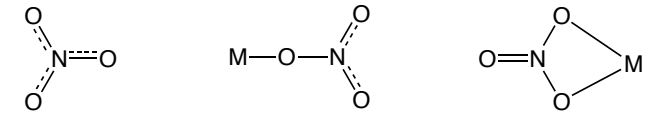

Figure 1-20 Biding mode of nitrate ion to a metal ion.

Table 1-6 Correlation of symmetry and vibration of the D_{3h} and C_{2v} nitrate

Point group	Bonding mode				
D_{3h}	ionic	ν_1	ν_2	ν_3	ν_4
		↓	↓	↓	↓
C_{2v}	bidentate	ν_2	ν_6	ν_1 ν_4	ν_3 ν_5

By comparing the separation between two highest-frequency bands, ν_1 and ν_4, used to distinguish between monodentate and bidentate of coordination mode. It is usually greater (> 180 cm^{-1}) for bidentate nitrate relative to that for monodentate nitrate (< 130 cm^{-1}).[84] The use of the combination band($\nu_1+\nu_4$) of free nitrate ion that appears in the 1800–1700 cm^{-1} region was also proposed for structural diagnosis. Upon coordination, the two ($\nu_1+\nu_4$) bands in the 1800–1700 cm^{-1} region split into two bands. The nitrate ion is bidentate if the separation is 66–20 cm^{-1}, and is unidentate if the separation is 25–5 cm^{-1}.[85]

1.4.3 Nuclear Magnetic Resonance Spectroscopy

Chemical Exchange

In case of the simple two-site exchange ($A \rightleftharpoons B$) with equal forward and backward rates in very slow exchange, two equally intense of resonance of the two sites, ν_A and ν_B, will appear. As the exchange rates constant (k) increased, the two lines first broaden, then shift towards one another, and broadening further until they merge into a single resonance. Further increase in k produces a sharp resonance at the mean frequency $1/2(\nu_A+\nu_B)$.[86] Thus, if the exchange is fast enough on NMR timescale, the difference in resonance frequencies of the two sites comes close to zero. Experimentally, these changes can be observed by increasing the temperature.

In case of the two sites have different populations, with two first-order rate constants k_A and k_B,

$$A \underset{k_B}{\overset{k_A}{\rightleftharpoons}} B$$

if the fractional populations of the two sites are p_A and p_B where $p_A + p_B = 1$, then $p_B k_A = p_B k_B$ at equilibrium. If the exchange between two sites is fast, single resonance is observed at the weighted average frequency (ν_{av}) expressed in (Eq. 10).

$$\nu_{av} = p_A\nu_A + p_B\nu_B \qquad p_A + p_B = 1 \qquad \text{(Eq. 10)}$$

Figure 1-21 shows spectra calculated for a range of exchange rates for the case where the site B has twice the population of the site A. With increasing the rate, the signal will become broadening, coalescence and subsequent narrowing in the spectra.

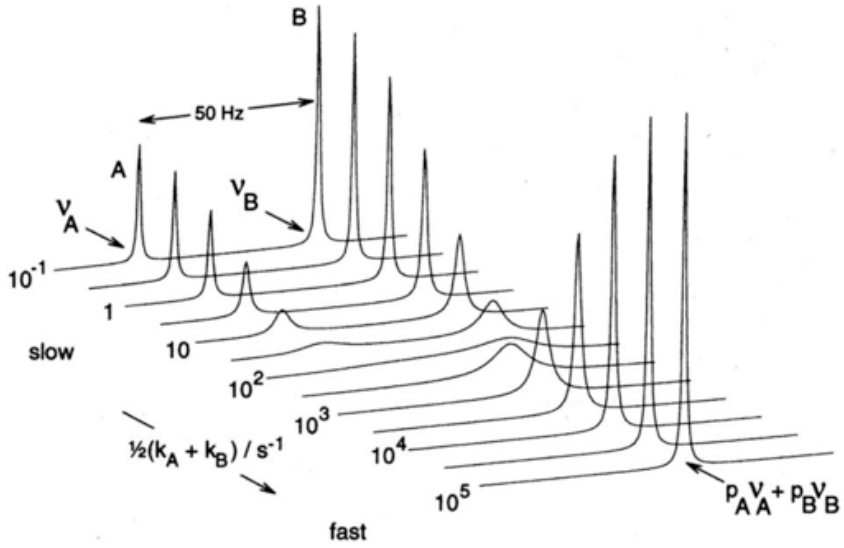

Figure 1-21 Calculated NMR spectra for exchanging between tow sites A and B with populations in the ratio p_B/p_A=2.[86]

Lanthanide Induced Shift (LIS)

Almost all of lanthanides and actinides are paramagnetic due to the presence of unpaired electron in their *f*-orbitals. The NMR spectra of paramagnetic lanthanides complexes are significantly different from those of diamagnetic analogues. This paramagnetic contribution was called lanthanide-induced shift (LIS). The experimental chemical shift (δ_{ij}^{exp}) of a nucleus i in a paramagnetic complex of a lanthanide j consist of three contributions, diamagnetic (δ_i^{dia}), contact (δ_{ij}^{c}, through-bond) and pseudo-contact (δ_{ij}^{pc}, through-space) as express in (Eq. 11).

$$\delta_{ij}^{exp} = \delta_i^{dia} + \delta_{ij}^{c} + \delta_{ij}^{pc} \qquad \text{(Eq. 11)}$$

Upon substracting the diamagnetic contribution, LIS contribution corresponding the sum of contact and pseudo-contact contribution can be easily obtained from experimental chemical shift.

$$LIS = \delta_{ij}^{para} = \delta_{ij}^{exp} - \delta_i^{dia} = \delta_{ij}^{c} + \delta_{ij}^{pc} = F_i < S_z >_j + G_i C_j \qquad \text{(Eq. 12)}$$

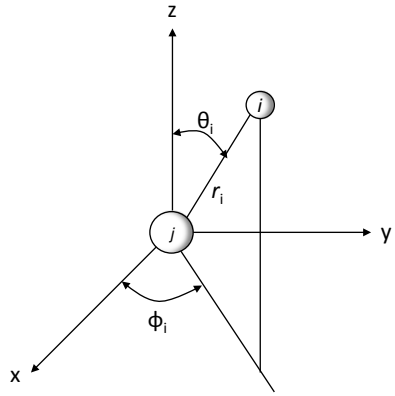

Figure 1-22 Spherical coordinates for a nucleus *i*.

where $<S_z>_j$ is the spin expectation value, C_j is lanthanide nucleus-dependent parameter. The anisotropic part of the axial magnetic susceptibility tensor of the free Ln(III) ions given in (Eq. 12). The contact term F_i reflects through-bond Fermi interactions between the paramagnetic centerr and the nucleus *i* and is given by

$$F_i = \frac{A_i}{\hbar\gamma B_0} \qquad \text{(Eq. 13)}$$

where A_i is the hyperfine interaction parameter of the nucleus *i*, γ is a gyromagnetic ratio, and B_0 is the applied magnetic induction. The pseudo-contact term G_i depends on the teometric position of the nucleus *i* and is given by(Eq. 14).

$$G_i = \frac{a}{T^2}\frac{1-3cos^2\theta_i}{r_i^3} \qquad \text{(Eq. 14)}$$

where r_i and θ_i are the internal axial coordinates of the nucleus *i* with respect to the ligand field axes, *a* is a ligand field constant, and *T* is a given temperature. [87]

The separation of contact (δ_{ij}^{c}) and pseudo-contact (δ_{ij}^{pc}) contributions to the observed LIS values for the series of lanthanides complexes allows gain further structural information. Eq x can be rearranged into the linear forms given by (Eq. 15) and (Eq. 16). Multi-linear regression for at least two different paramagnetic Ln(III) are expected to be linear for isostructural series. (Eq. 15) is particularly suited for the lanthanide complexes where the dipolar contribution is prevalent.

$$\frac{\delta_{ij}^{para}}{< S_z >_j} = F_i + G_i\frac{C_j}{< S_z >_j} \qquad \text{(Eq. 15)}$$

$$\frac{\delta_{ij}^{para}}{C_j} = F_i\frac{< S_z >_j}{C_j} + G_i \qquad \text{(Eq. 16)}$$

There is very little covalent contribution in the metal-ligand bond for lanthanides complexes and thus the mechanism of interaction between ligand and unpaired *f*-electron is almost through-space.[88,89, 90]

Table 1-7 Spin expectation values <S_z> and Bleany's factor C for free lanthanide ions at 300 K

Ln^{3+}	<S_z>	C_j
Ce^{3+}	–0.98	–6.3
Pr^{3+}	–2.97	–11.0
Nd^{3+}	–4.49	–4.2
Pm^{3+}	–4.01	2.0
Sm^{3+}	0.06	–0.7
Eu^{3+}	10.68	4.0
Gd^{3+}	31.50	0.0
Tb^{3+}	31.82	–86
Dy^{3+}	28.55	–100
Ho^{3+}	22.63	–39
Er^{3+}	15.37	33
Tm^{3+}	8.21	53
Yb^{3+}	2.59	22

Solomon-Bloembergen Equation

When the contact contribution of the Ln(III) induced relaxation rate enhancements is negligible, the longitudinal relaxation time for the paramagnetic Ln(III) complexes are depends on the inverse of the sixth power of the metal to nucleus distance (*r*) according to following equation: [91,92]

$$\frac{1}{T_{1p}} = \frac{1}{T_{1exp}} - \frac{1}{T_{1dia}} = \frac{4}{3}\left(\frac{\mu_0}{4\pi}\right)\left(\frac{{\mu_{eff}}^2\gamma^2\beta^2T_{1e}}{r^6}\right) \qquad \text{(Eq. 17)}$$

Here $\mu_0/4\pi$ is the magnetic permeability under the vacum, μ_{eff} is the effective Bohr magneton, γ is the gyromagnetic ratio of the observed nucleus, β is the Bohr magneton, T_{1e} is the electron spin relaxation time, T_{1exp} is the longitudinal relaxation time of the nucleus in the complex and T_{1dia} is that of the diamagnetic complexes.

References

1 Tachimori, S; Morita, Y. "Overview of Solvent Extraction Chemistry for Reprocessing." *Ion Exchange and Solvent Extraction: A Series of Advances*, **2009**, 19, 1-64.

2 Baisden, P. A., and C. E. Atkins-Duffin. "Radioactive waste management." *Handbook of Nuclear Chemistry*, **2011**. 2797-2835.

3 Nash, Kenneth L.; LUMETTA, Gregg J. (ed.). "Advanced separation techniques for nuclear fuel reprocessing and radioactive waste treatment." *Elsevier*, **2011**.

4 International Atomic Energy Agency, "Assessment of Partitioning Processes for Transmutation of Actinides." *IAEA-TECDOC-1648*, **2010**.

5 Nuclear Energy Agency of the OECD, Actinide and Fission Product Partitioning and Transmutation, Status and Assessment Report, OECD/NEA, **1999**.

6 Kaltsoyannis, N. "Does covalency increase or decrease across the actinide series? Implications for minor actinide partitioning." *Inorganic Chemistry*, **2012**, 52.7: 3407-3413.

7 Jensen, M.; Bond, A. "Comparison of Covalency in the Complexes of Trivalent Actinide and Lanthanide Cations." *Journal of the American Chemical Society,* **2002**,*124*.

8 Hill, C. "Overview of Recent Advances in An (III)/Ln (III) Separation by Solvent Extraction." *Ion Exchange and Solvent Extraction, A Series of Advances,* **2009**, 19, 119-193.

9 Nash, K. L. "Separation Chemistry for Lanthanides and Trivalent Actinides.", *Handbook on the Physics and Chemistry of Rare Earths*, **1994**, 18, 121.

10 KOLARIK, Zdenek. "Complexation and separation of lanthanides (III) and actinides (III) by heterocyclic N-donors in solutions."*Chem. Rev*, **2008**, 108.10: 4208-4252.

11 Marie, C.; Miguirditchian, M.; Guillaumont, D.; Tosseng, A.; Berthon, C.; Guilbaud, P.; Duvail, M.; Bisson, J.; Guillaneux, D.; Pipelier, M.; Dubreuil, D. "Complexation of Lanthanides(III), Americium(III), and Uranium(VI) with Bitopic N,O Ligands: an Experimental and Theoretical Study." *Inorganic Chemistry*, **2011**, *50*.

12 Shimada, A.; Yaita, T.; Narita, H.; Tachimori, S.; Okuno, K. "Extraction studies of lanthanide(III) ions with *N,N*'-dimethyl-*N,N'*-diphenylpyridine-2,6-dicarboxyamide (DMDPhPDA) from nitric acid solutions. " *Solvent Extraction and Ion Exchange*. ,**2004**, 22 ,147–161.

13 Sasaki Y.; Choppin, G. R. "Solvent extraction of Eu, Th, U, Np and Am with *N, N'*-dimethyl-*N, N*'-dihexyl-3-oxapentanediamide and its analogous compounds." *Analytical Sciences*, **1996**, 12, 225-230.

14 Narita, H.; Yaita, T.; Tamura, K.; Tachimori, S. "Solvent extraction of trivalent lanthanoid ions with *N,N'*-dimethyl-*N, N*'-diphenyl-3-oxapentanediamide." *Radiochimica Acta* **1998**, *81*, 223–226.

15 Sasaki, Y.; Rapold, P.; Arisaka, M.; Hirata, M.; Kimura, T.; Hill, C.; Cote, G. "An Additional Insight into the Correlation between the Distribution Ratios and the Aqueous Acidity of the TODGA System." *Solvent Extraction and Ion Exchange,* **2007**, 25, 187-204.

16 Narita, H.; Yaita, T.; Tamura, K.; Tachimori, S. "Study on the extraction of trivalent lanthanide ions with N,N′-dimethyl-N,N′-diphenyl-malonamide and diglycolamide." *Journal of Radioanalytical and Nuclear Chemistry,* **1999**, 239, 381-384.

17 Sasaki, Y.; Sugo, Y.; Kitatsuji, Y.; Kirishima, A.; Kimura T. "Complexation and back extraction of various metals by water-soluble diglycolamide." *Analytical Sciences*, **2007**, 23.

18 Sasaki, Y.; Morita, Y.; Kitatsuji, Y.; Kimura, T. "Mutual Separation of Actinides from Middle Lanthanides by the Combination of Two Neutral Donors, *N,N,N′,N′*-Tetraoctyl-3,6-dioxaoctanediamide and *N,N,N′,N′*-Tetraethyldiglycolamide." *Chemistry Letters,* **2010**, *39*,

898-899.

19 Nash, K. "A REVIEW OF THE BASIC CHEMISTRY AND RECENT DEVELOPMENTS IN TRIVALENT f-ELEMENTS SEPARATIONS." *Solvent Extraction and Ion Exchange*, **1993**, 11, 729.

20 Eigen, M. "Fast elementary steps in chemical reaction mechanisms." *Pure and Applied Chemistry*, **1963**, 6, 97-116

21 Anwander, R. "Episodes from the History of the Rare Earth Elements." *Herausgegeben von CH Evans. Kluwer Academic Publishers, Dordrecht*, **1996**. 240

22 Kaltsoyannis, N.; Scott, P. "The f elements." *Oxford University Press*, **1999**.

23 Aspinall, Helen C. "*Chemistry of the f-Block Elements*." Vol. 5. CRC Press, **2001**.

24 Karraker, D." Coordination of trivalent lanthanide ions." *Journal of Chemical Education,* **1970**, 424.

25 Laerdahl, J.; Fægri, K.; Visscher, L.; Saue, T. "A fully relativistic Dirac–Hartree–Fock and second-order Moller–Plesset study of the lanthanide and actinide contraction." *The Journal of Chemical Physics,* **1998**, 109, 10806-10817.

26 Pitzer, K. "Relativistic effects on chemical properties." *Accounts of Chemical Research,* **1979**, 271.

27 Huang, C.-H. "Rare earth coordination chemistry: Fundamentals and applications." John Wiley & Sons, **2010**.

28 Shannon, R. "Revised Effective Ionic Radii and Systematic Studies of Interatomic Distances in Halides and Chalcogenides." *Acta Crystallographica Section A: Crystal Physics, Diffraction, Theoretical and General Crystallography,* **1976**, *32*, 751–767.

29 Goldschmitd, Z.B. "*Atomic Properties (Free Atom)", Handbook on the Physics and Chemistry of Rare Earths,* **1980**, Vol. 1**,** Ch 1 pp. 1–171.

30 Cotton, S. "Coordination Chemistry of the Lanthanides", in Lanthanide and Actinide Chemistry, *John Wiley & Sons, Ltd, Chichester, UK*.

31 Hoard, J.; Silverton, J. "Stereochemistry of Discrete Eight-Coördination. I. Basic Analysis." *Inorganic Chemistry,* **1963**, 235.

32 Lippard, S. J. "Eight-Coordination Chemistry." *Progress in Inorganic Chemistry,* **1967**, *8*, 109–193.

33 Burdett, J.; Hoffmann, R.; Fay, R. "Eight-Coordination." *Inorganic Chemistry*, **1978**, 2533.

34 Kepert, DL, "Aspects of the Stereochemistry of Eight-Coordination." *Progress in Inorganic Chemistry,* **1978**, *24*, 179.

35 Favas, MC; Kepert, DL "Aspects of the Stereochemistry of Nine-Coordination, Ten-Coordination, and Twelve-Coordination." *Progress in Inorganic Chemistry,* **1981**, *28*, 239–308.

36 Robertson, B. "Coordination Polyhedra with Nine and Ten Atoms." *Inorganic Chemistry,* **1977**, 2735.

37 Guggenberger, L.; Muetterties, E. "Reaction path analysis. 2. The nine-atom family." *Journal of the American Chemical Society,* **1976**. 98.

38 Lind, M., Lee, B. & Hoard, J. "Structure and Bonding in a Ten-Coordinate Lanthanum(III) Chelate of Ethylenediaminetetraacetic Acid." *Journal of the American Chemical Society,* **1965**, 1611.

39 Moss, D.; Sinha, S. "The Crystal Structure of Decacoordinated Terbium(III)-Bis-(2,2′-bipyridyl)-Tris-Nitrate: Tb $(NC_5H_4{\cdot}C_5H_4N)_2(NO_3)_3$." *Zeitschrift für Physikalische Chemie,* **1969**, *63*.

40 Bhandary, K.; Manohar, H. "Crystal and molecular structure of a dimethyl sulphoxide complex

with lanthanum nitrate, $La(NO_3)_3.4(CH_3)_2SO$." *Acta Crystallographica Section B Structural Crystallography and Crystal Chemistry,* **1973**, *29*.

41 Al-Karaghouli, A.; Wood, J. "Crystal and Molecular Structure of trinitratobis(bipyridyl) lanthanum(III)." *Inorganic Chemistry*, **1972**, *11, 2293*.

42 Bünzli, J. C. G., Klein, B., Wessner, D., J Schenk, K., Chapuis, G., Bombieri, G., De Paoli, G. "Crystal and molecular structure of the 4: 3 complex of 18-crown-6 ether with neodymium nitrate." *Inorganica Chimica Acta,* **1981**, 54, L43-L46.

43 Hart, F.; Hursthouse, M.; Malik, K.; Moorhouse, S. "X-Ray crystal structure of a cryptate complex of lanthanum nitrate." *Journal of the Chemical Society, Chemical Communications*, **1978**, 549-550**.**

44 Matonic, J. H., Neu, M. P., Enriquez, A. E., Paine, R. T., & Scott, B. L. (2002). "Synthesis and crystal structure of a ten-coordinate plutonium (IV) ion complexed by 2-[(diphenylphosphino) methyl] pyridine N,P-dioxide:$[Pu(NO_3)_3\{2\text{-}[(C_6H5)2P(O)CH_2]C_5H_4NO\}_2][Pu(NO_3)_6]_{0.5}$." *Journal of the Chemical Society, Dalton Transactions*, (11), 2328-2332.

45 Kannan, S.; Moody, M. A.; Barnes, C. L.; Duval, P. B. "Lanthanum(III) and uranyl(VI) Diglycolamide Complexes: Synthetic Precursors and Structural Studies Involving Nitrate complexation." *Inorganic Chemistry,* **2008**,*47*, 4691–4695.

46 Kawasaki, T.; Okumura, S.; Sasaki, Y.; Ikeda, Y. "Crystal Structures of Ln(III) (Ln = La, Pr, Nd, Sm, Eu, and Gd) Complexes with *N,N,N',N'*-Tetraethyldiglycolamide Associated with Homoleptic $[Ln(NO_3)_6]^{3-}$" *Bulletin of the Chemical Society of Japan,* **2014**, *87*, 294-300.

47 Matloka, K., Gelis, A., Regalbuto, M., Vandegrift, G., & Scott, M. J. "Highly efficient binding of trivalent f-elements from acidic media with a C3-symmetric tripodal ligand containing diglycolamide arms." *Dalton Transactions*, **2005**, (23), 3719-3721.

48 Chekhlov, A. N. "Synthesis and crystal structure of hexa(nitrato-O,O′)dysprosium(III)Bis [4,7,13,16,21,24-hexaoxa-1,10-diazoniabicyclo[8.8.8]hexacosane] nitrate dihydrate." *Russian Journal of Inorganic Chemistry*, **2007,** 52, 1741-1745.

49 Choppin, G.R. and Rizkalla, E.N., "Solution chemistry of actinides and lanthanides." *Handbook on the Physics and Chemistry of Rare Earths*, **1994**, 18, Ch 128, pp. 559-590.

50 Choppin, G. R. "Structure and thermodynamics of lanthanide and actinide complexes in solution." *Pure and Applied Chemistry*, **1971**, *27*, 23–42.

51 Burgess, J. "Ions in solution: basic principles of chemical interactions." *Elsevier*, **1999**.

52 Rizkalla, E.N. and Choppin, G.R., "*Lanthanides and actinides hydration and hydrolysis*", *Handbook on the Physics and Chemistry of Rare Earths*, **1994**, 18, Ch 127, pp. 529-558.

53 Hay, B. "Extension of molecular mechanics to high-coordinate metal complexes. Calculation of the structures of aqua and nitrato complexes of lanthanide(III) metal ions." *Inorganic Chemistry,* **1991**, 30, 2876-2884.

54 Skanthakumar, S.; Antonio, M.; Wilson, R.; Soderholm, L. "The Curium Aqua Ion." *Inorganic Chemistry* **2007**, *46*. 3485-3491.

55 Lindqvist-Reis, P.; Klenze, R.; Schubert, G.; Fanghänel, T. "Hydration of Cm 3+ in Aqueous Solution from 20 to 200 °C. A Time-Resolved Laser Fluorescence Spectroscopy Study." *The Journal of Physical Chemistry B*, **2005**, *109*.

56 Atta-Fynn, R.; Bylaska, E.; Schenter, G.; Jong, W. "Hydration Shell Structure and Dynamics of Curium(III) in Aqueous Solution: First Principles and Empirical Studies." *The Journal of Physical Chemistry A*, **2011**, *115*.

57 Wiebke, J.; Moritz, A.; Cao, X.; Dolg, M. "Approaching actinide(+III) hydration from first principles." *Physical Chemistry Chemical Physics,* **2007**, *9*.

58 Ishiguro, S.; Umebayashi, Y.; Komiya, M. "Thermodynamic and structural aspects on the

solvation steric effect of lanthanide (III)—dependence on the ionic size." *Coordination Chemistry Reviews*, **2002**, 226.1: 103-111.

59 Baaden, M.; Berny, F.; Madic…, C. "M^{3+} lanthanide cation solvation by acetonitrile: The role of cation size, counterions, and polarization effects investigated by molecular dynamics and quantum mechanical simulations." *The Journal of Physical Chemistry A*, **2000**, 104.32: 7659-7671.

60 Deacon, G.; Görtler, B.; Junk, P.; Lork, E.; Mews, R.; Petersen, J.; Zemva, B. "Syntheses and structures of some homoleptic acetonitrile lanthanoid (III) complexes." *Journal of the Chemical Society, Dalton Transactions*, **1998**, 22: 3887-3892.

61 Bernardo, P.; Zanonato, P.; Melchior, A.; Portanova, R.; Tolazzi, M.; Choppin, G.; Wang, Z. "Thermodynamic and Spectroscopic Studies of Lanthanides(III) Complexation with Polyamines in Dimethyl Sulfoxide." *Inorganic Chemistry,* **2008**, *47*.

62 Silber, H.; Bakhshandehfar, R.; Contreras, L.; Gaizer, F.; Gonsalves, M.; Ismail, S. "Equilibrium studies of lanthanide nitrate complexation in aqueous methanol." *Inorganic Chemistry,* **1990**, 29, 4473-4475.

63 Krishnamurthy, S.; Soundararajan, S. "Dimethyl formamide complexes of rare-earth nitrates." *Journal of Inorganic and Nuclear Chemistry*, **1966**, 28.8: 1689-1692.

64 Bünzli, J.-C.; Vuckovic, M. "Spectroscopic properties of anhydrous and aqueous solutions of terbium perchlorate and nitrate: Coordination numbers of the Tb(III) ion." *Inorganica Chimica Acta,* **1983**, *73*.

65 Bünzli, J.-C.; Vuckovic, M. "Solvation of neodymium(III) perchlorate and nitrate in organic solvents as determined by spectroscopic measurements." *Inorganica Chimica Acta*, **1984**, *95*.

66 Fratiello, A.; Kubo-Anderson, V.; Azimi, S.; Flores, T.; Marinez, E.; Matejka, D.; Perrigan, R.; Vigil, M. "A hydrogen-1, nitrogen-15, and chlorine-35 NMR coordination study of Lu(ClO4)3 and Lu(NO3)3 in aqueous solvent mixtures." *Journal of Solution Chemistry,* **1990**, *19*, 811-829

67 Fratiello, A; Kubo-Anderson, V; Azimi, S; Marinez, E; Matejka, D; Perrigan, R; Yao, B "A direct15N NMR study of erbium (III)-nitrate complexation in aqueous solvent mixtures." *Journal of Solution Chemistry,* **1991**, *20*, 893–903.

68 Fratiello, A; Kubo-Anderson, V; Azimi, S; Laghaei, F; Perrigan, RD; Reyes, F "A direct nitrogen-15 NMR study of neodymium (III)-nitrate complex formation in aqueous solvent mixtures." *Journal of Solution Chemistry,* **1992**, *21*, 1015–1033

69 Fratiello, A.; Kubo-Anderson, V.; Azimi, S.; Marinez, E.; Matejka, D.; Perrigan, R.; Yao, B. "A direct nitrogen-15 NMR study of cerium(III)-nitrate complexes in aqueous solvent mixtures." *Journal of Solution Chemistry***1992**, 21, 651-666.

70 Fratiello, A; Kubo-Anderson, V; Azimi, S; Chavez, O; Laghaei, F; Perrigan, RD "A direct nitrogen-15 NMR study of praseodymium (III)-nitrate complex formation in aqueous solvent mixtures." *Journal of Solution Chemistry,* **1993**, *22*, 519–538.

71 Fratiello, A.; Kubo-Anderson, V.; Lee, R.; Patrick, M.; Perrigan, R.; Porras, T.; Sharma, S.; Stoll, S. "Direct 1H, 13C, and 15N NMR Study of Lanthanum (III), Thulium (III), and Ytterbium (III) Complex Formation with Nitrate and Isothiocyanate." *Journal of Solution Chemistry,* **2002**.

72 Bünzli, J. C. G.; Milicic-Tang, A.; Mabillard, C. "Lanthanide−nitrate interaction in anhydrous acetonitrile and coordination numbers of the lanthanide ions: FT−IR study." *Helvetica chimica acta*, **1993**, 1292-1304.

73 Choppin, G.; Strazik, W. "Complexes of Trivalent Lanthanide and Actinide Ions. I. Outer-Sphere Ion Pairs." *Inorganic Chemistry* **1965**, *4*. b) C. Bonal, J. P. Morel, N Morel-Desrosies, *Journal of the Chemical Society, Faraday Transactions*, **1998**, *94*, 1431.

74 Bünzli, J. C. G.; Milicic-Tang, A."*Solvation and anion interaction in organic solvents", Handbook on the Physics and Chemistry of Rare Earths*, **1995**, Vol. 21**,** Ch 145, pp. 305-365.

75 Bünzli, J.-C. G.; Eliseeva, S. V.. "Basics of lanthanide photophysics." in Lanthanide Luminescence. *Springer Berlin Heidelberg,* **2011**. 1-45.

76 山内清吾・野崎浩一 編著 「配位化合物の電子状態と光物理- 複合系の光機能研究会選書」（三共出版）

77 Carnall, W.; Goodman, G.; Rajnak, K.; Rana, R. "A systematic analysis of the spectra of the lanthanides doped into single crystal LaF3." *The Journal of Chemical Physics,* **1989**, 90, 3443**.**

78 Görller-Walrand, C.; Binnemans, K. "Spectral intensities of f-f transitions." *Handbook on the physics and chemistry of rare earths*, **1998**, vol 25. 221.

79 Choppin, G.; Henrie, D.; Buijs, K. "Environmental Effects on f-f Transitions. I. Neodymium(III)." *Inorganic Chemistry,* **1966**, 1743.

80 Nakamoto, K. "Infrared and Raman Spectra of Inorganic and Coordination Compounds: Part A: Theory and Applications in Inorganic Chemistry, Sixth Edition", *John Wiley & Sons, Inc*.: New York, **2004**.

81 Bullock J. I. “Infrared spectra of some uranyl nitrate complexes.” *Journal of Inorganic and Nuclear Chemistry*, **1967**, 29.9: 2257-2264.

82 Brooker, M.H.; Irish, D.E. “Crystalline-field effects on the infrared and Raman spectra of powdered alkali-metal, silver, and thallous nitrates.” *Canadian Journal of Chemistry,* **1970**, *48*, 1183–1197.

83 Ferraro, J.; Walker, A. “Comparison of the Infrared Spectra (4000–70 cm−1) of Several Hydrated and Anhydrous Salts of Transition Metals.” *The Journal of Chemical Physics,* **1965**, 42, 1278.

84 Sathyanarayana, D. N. “Vibrational spectroscopy: theory and applications.” New Age International, 2007.

85 Lever, A. B.; Mantovan, E.; Ramswamy, B.S. "Infrared combination frequencies in coordination complexes containing nitrate groups in various coordination environments. A probe for the metal-nitrate interaction.”, *Canadian Journal of Chemistry*, **1971,** 49, 1957

86 P. J. Hore "Nuclear Magnetic Resonance." *Oxford Chemistry Primers No. 32 Oxford Science Publications, Oxford University Press, Oxford*, 1995

87 Renaud, F.; Piguet, C.; Bernardinelli, G.; Bünzli, J.-C.; Hopfgartner, G. “In Search for Mononuclear Helical Lanthanide Building Blocks with Predetermined Properties: Triple-stranded Helical Complexes with *N,N,N',N'*-tetraethylpyridine-2,6-dicarboxamide.” *Chemistry - A European Journal* **1997**, 10, 1646.

88 Piguet, C.; Geraldes, C.; "Paramagnetic NMR lanthanide induced shifts for extracting solution structures." *Handbook on the Physics and Chemistry of Rare Earths*, **2003**, vol 33, 353-463.

89 Bertini, I.; Luchinat, C.; Parigi, G. “Solution NMR of paramagnetic molecules: applications to metallobiomolecules and models.” *Elsevier*, **2001**.

90 Pintacuda, G.; John, M.; Su, X.-C.; Otting, G. “NMR Structure Determination of Protein−Ligand Complexes by Lanthanide Labeling.” *Accounts of Chemical Research,* **2007**, 40, 206-212.

91 Sano, Y.; Karino, J.; Koyama, T.; Funasaka, H. "NMR study of lanthanide (III) nitrate complexes in CMPO/TBP systems." *Journal of Alloys and Compounds,* **2000**, *303-304*, 151156.

92 Bertini, I.; Luchinat, C.; and Parigi, G. "Paramagnetic Molecules, in NMR of Biomolecules: Towards Mechanistic Systems Biology" Wiley-VCH Verlag GmbH & Co. KGaA, Weinheim, Germany, **2012**.

Chapter 2

Syntheses and Characterizations of Lanthanide(III) Nitrate Complexes with TEDGA

2.1 Introduction

As described in Chapter 1, despite of their high efficiency in extraction experiments, limited information is available for the structural properties of Ln(III) and An(III) complexes with the diamide derivatives. Crystal structures of Ln(III) with DGA derivatives were first reported by Kannan *et al*. and the La(III) complex with DGA possesses $[La(DGA)_3]^{3+}$ cation associated with a homoleptic $[La(NO_3)_3]^{3+}$ counter anion.[1] Matloka *et al*. also reported that the crystal structure of Ce(III) complex with a C3 symmetric tripodal ligand (L) containing DGA arms exhibits a similar structure to La(III) complex reported by Kannan *et al*. The crystal structure of Yb(III) complex with the same tripodal ligand was also reported and its chemical formula is $[YbL](NO_3)_3$.[2] Hirata *et al*. performed the molecular dynamics simulation of Ln(III)-DGA complex, and reported that the interaction energy between Ln(III) and DGA decreases in the order Lu(III)>Eu(III)>La(III).[3] These structural and molecular dynamics simulation studies have suggested that the heavy Ln(III) tend to form outer-sphere complex with nitrate and make enhances in stability of extracted complexes. However, these studies have provided information separately, and no studies have focused on the structural differences in the solid state and in the solution throughout the Ln(III) series.

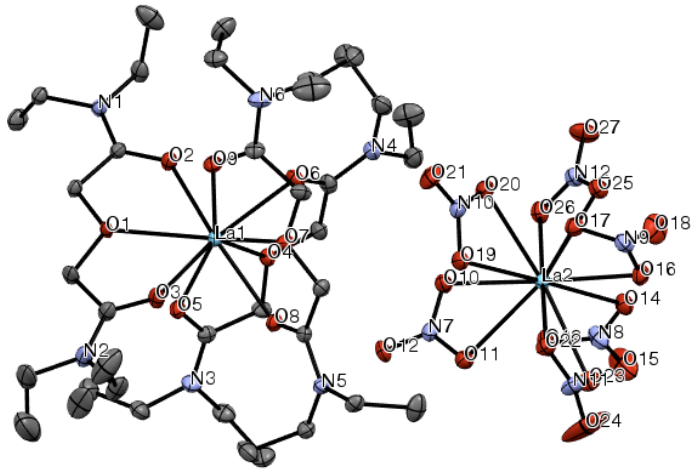

Figure 2-1 ORTEP representation of Type 1 Complex; $[La(TEDGA)_3][La(NO_3)_6]$. Ellipsoids displayed at 30% probability. Hydrogen atoms are omitted for clarity.[4]

In our laboratory, Kawasaki *et al*. have already reported the crystal structure of Ln(III) nitrate complexes with *N,N,N',N'*-tetraethyl-diglygolamide (TEDGA) for light Ln(III) (Ln = La–Gd, except for Pm).[4] These complexes all exist in the space group *P*1 (#2) and are constructed by the packing of $[Ln(TEDGA)_3]^{3+}$ cations and $[Ln(NO_3)_6]^{3-}$ anions. A representative example of this type of La(III) complex, $[La(TEDGA)_3][La(NO_3)_6]$, is shown in Figure 2-1.

The Ln(III) ions are quite similar but they sometimes display an apparent difference between light and heavy Ln(III). From the view point of coordination chemistry, there remains a need for elucidation of structures of the Ln(III)-DGA complexes throughout the Ln(III) series to understand the selectivity between the DGA types of extractant and Ln(III). In this chapter, a systematic investigation of the structural differences among the all Ln(III) nitrate complexes with DGA were examined in solid state. The heavy Ln(III) nitrate complexes with TEDGA (Ln = Tb–Yb) were synthesized and characterized by single crystal X-ray diffraction and IR spectra.

2.2 Experimental

2.2.1 Materials

Anhydrous diethyl ether, methanol, ethyl acetate and acetonitrile were purchased from KANTO chemical co ltd., and used without further purification. Ln(III) nitrates used in this study were purchased from Kanto Chemical Co., Inc. for Ln = Tb, Dy and Lu, from Sigma-Aldrich Co. LLC. for Ln = Ho, Er, Yb, and from Stream Chemicals, Inc. for Ln = Tm, and used as received. TEDGA were provided by JAEA (Japan Atomic Energy Agency) and used as received, however, TEDGA can be synthesized by simple procedure as follows; the triethylamine and *N*-methylaniline dissolved in chloroform. Diglycollic acid chloride in chloroform was added slowly, and the mixture was heated at reflux for 2 hours. The resulting solution was washed with water, with 3.5% hydrochloric acid, with 5% sodium carbonate and finally with water. The solvent was removed at reduced pressure. The crystalline residue was recrystallized from toluene and hexane.[1] The structure of DGA is shown in Figure 2-2.

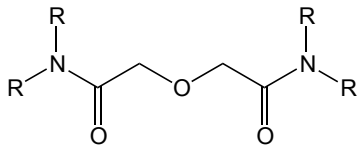

Figure 2-2 Schematic structures of *N,N,N',N'*-tetraalkyl diglygolamide (DGA).

2.2.2 Synthesis

*Preparation of [Tb(TEDGA)$_3$](NO$_3$)$_3$·4H$_2$O (**8**)*: $Tb(NO_3)_3 \cdot 6H_2O$ 0.259 g (0.572 mmol) and TEDGA 0.408 g (1.67 mmol) (Ln : TEDGA ≈ 1 : 3) were dissolved in 2 ml of water. The crystals suitable for X-ray diffraction were obtained by the concentration with heating and cooling. Yield: 21.5 %, Elemental analysis, Found: C 37.72, H 6.77, N 10.95 %; Calculated for $C_{36}H_{80}N_9O_{22}Tb$: C 37.60, H 7.01, N 10.96 %

*Preparation of [Dy(TEDGA)$_3$](NO$_3$)$_3$·4H$_2$O (**9**)*: This and other heavy Ln(III) complexes were synthesized in a similar manner to the method in $[Tb(TEDGA)_3](NO_3)_3 \cdot 4H_2O$. The synthesis conditions are as follows: $Dy(NO_3)_3 \cdot 5H_2O$ 0.256 g (0.584 mmol), TEDGA 0.428 g (1.75 mmol). Yield: 42.3 %, Elemental analysis, Found: C 37.61, H 6.94, N 10.88 %; Calculated for $C_{36}H_{80}N_9O_{22}Dy$: C 37.48, H 6.99, N 10.93 %.

*Preparation of [Ho(TEDGA)$_3$](NO$_3$)$_3$·4H$_2$O (**10**):* The synthesis conditions are as follows: $Ho(NO_3)_3 \cdot 5H_2O$ 0.205 g (0.465 mmol), TEDGA 0.348 g (1.42 mmol). Yield: 17.9 %, Elemental analysis, Found: C 37.58, H 6.98, N 10.89 %; Calculated for $C_{36}H_{80}N_9O_{22}Ho$: C 37.40, H 6.98, N 10.90 %.

*Preparation of [Er(TEDGA)$_3$](NO$_3$)$_3$·4H$_2$O (**11**):* The synthesis conditions are as follows: $Er(NO_3)_3 \cdot 5H_2O$ 0.236 g (0.531 mmol), TEDGA 0.394 g (1.61 mmol). Yield: 21.9 %, Elemental analysis, Found: C 37.51, H 6.97, N 10.86 %; Calculated for $C_{36}H_{80}N_9O_{22}Er$: C 37.33, H 6.96, N 10.88 %.

*Preparation of [Tm(TEDGA)$_3$](NO$_3$)$_3$·4H$_2$O (**12**):* The synthesis conditions are as follows: $Tm(NO_3)_3 \cdot 6H_2O$ 0.254 g (0.549 mmol), TEDGA 0.395 g (1.62 mmol). Yield: 16.8 %, Elemental analysis, Found: C 37.32, H 6.93, N 10.87 %; Calculated for $C_{36}H_{80}N_9O_{22}Tm$: C 37.27, H 6.95, N

10.87 %.

*Preparation of [Yb(TEDGA)$_3$](NO$_3$)$_3$·4H$_2$O (**13**):* The synthesis conditions are as follows: Yb(NO$_3$)$_3$·5H$_2$O 0.233 g (0.519 mmol), TEDGA 0.379 g (1.55 mmol). Yield: 24.5 %, Elemental analysis, Found: C 37.26, H 6.93, N 10.81 %; Calculated for $C_{36}H_{80}N_9O_{22}Yb$: C 37.14, H 6.93, N 10.83 %.

*Preparation of [Lu(TEDGA)$_3$](NO$_3$)$_3$·4H$_2$O (**14**):* The synthesis conditions are as follows: Lu(NO$_3$)$_3$·4H$_2$O 0.239 g (0.552 mmol), TEDGA 0.405 g (1.66 mmol). Yield: 34.7 %, Elemental analysis, Found: C 37.30, H 6.94, N 10.78 %; Calculated for $C_{36}H_{80}N_9O_{22}Lu$: C 37.08, H 6.92, N 10.81 %.

2.2.3 Instruments and General Procedures

Crystal structures were determined by using a Rigaku RAXIS RAPID imaging plate area detector system with Mo K_α radiation from a graphite monochromator (λ = 0.71075 Å) under cold N_2 gas flow. Crystal data collection and final refinement parameters are summarized in Table 7-1. A numerical absorption correction was applied, which resulted in transmission factors described in the crystallographic information file of each complex. The empirical absorption correction was performed using intensity measurement.[5] The structures were solved by direct methods (SHELXS-97),[6] and expanded using Fourier techniques. The non-hydrogen atoms were refined using anisotropic temperature factors by SHELXL-97.[6] Hydrogen atoms were introduced at calculated positions using the riding model. [6] All calculations were performed using the Crystal Structure crystallographic software package.[7] IR spectra (KBr pellet) of complexes **1**-**7** were measured by the diffuse reflection method using a Shimadzu FT-IR-8400S spectrometer at room temperature.

2.3 Results and Discussion

2.3.1 Crystal Structures

In this study, heavy Ln(III) complexes could not be crystallized as same way as light Ln(III), water was thus used as a solvent. [4] The method of syntheses and crystallization were heated and cooled the of water dissolving hydrated Ln(III) nitrate and TEDGA. Then, the structures of the heavy Ln(III) complexes were determined by single crystal X-ray diffraction.

Heavy Ln(III)-TEDGA Complexes

The structures of heavy Ln(III) nitrates with TEDGA were revealed to be [Ln(TEDGA)$_3$](NO$_3$)$_6$ (Ln = Tb-Lu), whereas the light Ln(III) form [Ln(TEDGA)$_3$][Ln(NO$_3$)$_6$] (Ln = La-Gd, except for Pm) complexes.[4] The heavy Ln(III) complexes exists in the space group P_n or P_c. Their crystal structures are constructed by the packing of $[Ln(TEDGA)_3]^{3+}$ cations, three nitrate ions as counter anions, and four water of crystallization, i.e., [Ln(TEDGA)$_3$](NO$_3$)$_3$·4H$_2$O. A representative example of this type of complex for Tb(III), [Tb(TEDGA)$_3$](NO$_3$)$_3$, is shown in Figure 2-3. Crystallographic data and structures of other [Ln(TEDGA)$_3$](NO$_3$)$_3$ complexes are shown in Appendix A. The average values of selected bond lengths and angles are listed in Table 2-1.

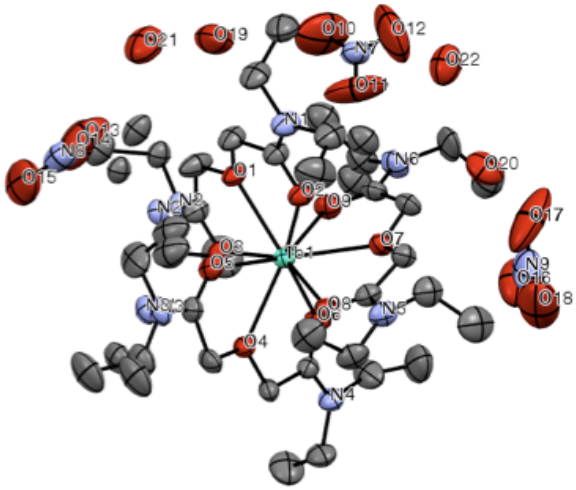

Figure 2-3 ORTEP representation of $[Tb(TEDGA)_3](NO_3)_3 \cdot 4H_2O$. Ellipsoids are displayed at 30% probability. Hydrogen atoms are omitted for clarity.

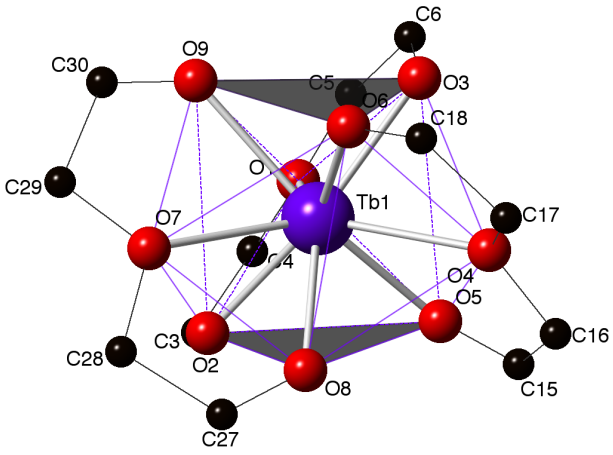

Figure 2-4 Tricapped trigonal prismatic view of the $[Tb(TEDGA)_3]^{3+}$ cation in which the TEDGA molecule has triple-helical arrangement.

In comparison with Ln-O bond lengths in $[Ln(TEDGA)_3]^{3+}$ cations across the lanthanide series, the bond lengths from carbonyl oxygen atom to Ln(III) ($Ln\text{-}O_{carbo}$) are significantly shorter than that of ether oxygen atom to Ln(III) ($Ln\text{-}O_{ether}$). The difference in bond length indicates that $Ln\text{-}O_{carbo}$ is stronger than $Ln\text{-}O_{ether}$. The bond angles across amide nitrogen are all approximately 120°. This suggests that the amide nitrogen is sp^2 hybridized and the lone pair in complexes is conjugated on the amide bonds.

Table 2-1 Selected bond length and angles for heavy Ln(III) complexes

	Tb	Dy	Ho	Er	Tm	Yb	Lu
$Ln\text{-}O_{ether}$ /Å	2.478 (0.016)	2.469 (0.019)	2.454 (0.014)	2.442 (0.023)	2.445 (0.005)	2.427 (0.012)	2.429 (0.015)
$Ln\text{-}O_{carbo}$ /Å	2.365 (0.022)	2.356 (0.023)	2.342 (0.028)	2.332 (0.021)	2.326 (0.020)	2.309 (0.018)	2.306 (0.025)
O-C /Å	1.425 (0.008)	1.426 (0.010)	1.427 (0.005)	1.429 (0.009)	1.427 (0.005)	1.419 (0.010)	1.430 (0.007)
O=C /Å	1.242 (0.010)	1.247 (0.005)	1.244 (0.007)	1.245 (0.007)	1.252 (0.004)	1.247 (0.018)	1.247 (0.009)
C-C /Å	1.510 (0.010)	1.509 (0.008)	1.507 (0.012)	1.505 (0.017)	1.511 (0.006)	1.505 (0.011)	1.514 (0.009)
$O_{ether}\text{-}Ln\text{-}O_{carbo}$ / °	63.20 (0.49)	63.58 (0.41)	63.72 (0.31)	63.98 (0.49)	64.30 (0.44)	64.36 (0.51)	64.63 (0.51)
C-O-C / °	113.3 (0.6)	112.8 (1.0)	112.4 (1.2)	112.4 (1.2)	112.3 (0.5)	113.4 (0.4)	112.0 (1.2)
O-C-C / °	106.7 (0.6)	106.1 (0.5)	106.1 (0.5)	105.9 (0.4)	106.0 (0.5)	106.1 (0.5)	105.5 (0.4)
O=C-C / °	118.8 (0.4)	119.6 (0.4)	119.2 (0.5)	119.4 (0.6)	119.3 (0.5)	119.0 (0.8)	119.3 (0.3)

Coordination geometries of these complexes were analyzed by the dihedral angles for the nine-coordination described in the Chapter 1.3.1. The dihedral angles for $[Ln(TEDGA)_3]^{3+}$ cations were calculated and the results are summarized in Table 2-2. Kawasaki *et al.* have reported $[Ln(TEDGA)_3]^{3+}$ (Ln = La-Gd, except for Pm) cations exhibit the distorted tricapped trigonal prismatic geometry and three TEDGA molecules are in the triple-helical arrangement around Ln(III).[4] As seen

from this table, $[Ln(TEDGA)_3]^{3+}$ cation for heavy Ln(III) can also be described as distorted tricapped trigonal prismatic (D_{3h}) geometry. A representative example of tricapped trigonal prismatic view of the $[Tb(TEDGA)_3]^{3+}$ cations is shown in Figure 2-4.

Table 2-2 Dihedral angles for Ln(III) TEDGA complexes together with the values of light Ln(III) complexes (Ln = La-Gd) reported by Kawasaki *et al*. [4]

	tricapped trigonal prism (D_{3h})			monocapped square antiprismatic (C_{4v})		
Complex	Opposed(⊥)	Average of 3 at Opposed(‖)	Average of 3 at Vicinal(‖)	Opposed	Opposed	Vicinal(⊥)
Idealized	180.0	146.4	26.4	163.5	138.2	0.0
La	177.1	142.4	23.1	165.0	142.3	11.6
Ce	177.4	142.3	22.9	164.6	138.9	14.6
Pr	177.3	142.8	23.4	160.1	138.0	29.0
Nd	177.5	143.0	23.5	156.3	136.5	48.2
Sm	179.4	143.3	23.7	159.6	136.6	36.4
Eu	179.5	137.0	24.0	163.8	138.3	21.4
Gd	179.6	143.7	24.1	163.9	138.1	21.7
Tb	173.7	148.9	29.2	163.1	139.6	16.6
Dy	173.1	144.3	24.6	139.2	144.6	6.86
Ho	173.9	144.6	26.5	133.8	145.4	7.93
Er	174.1	145.3	23.4	140.4	144.9	7.61
Tm	173.2	143.1	24.8	138.1	145.2	6.98
Yb	174.8	143.7	24.6	138.5	146.3	7.88
Lu	173.3	144.4	24.1	137.6	147.5	9.01

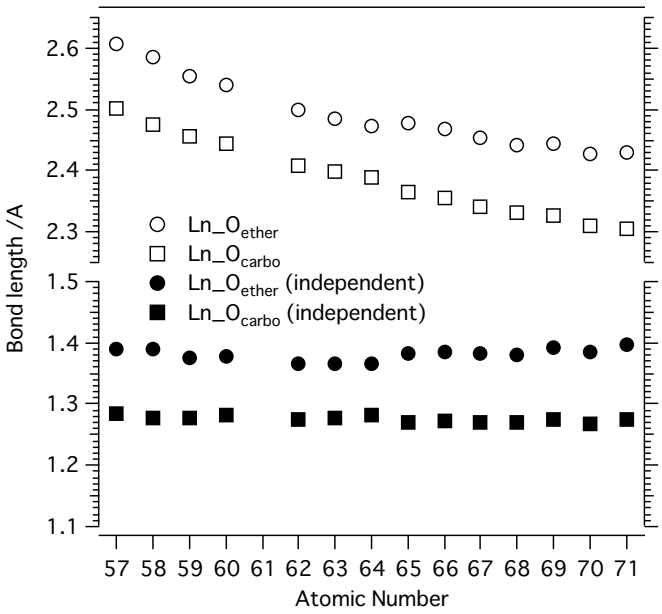

Figure 2-5 Plots of average bond lengths of Ln-O and the residual values of Ln-O against Ln(III) atomic number, together with the values of light Ln(III) complexes (Ln = La-Gd) reported by Kawasaki *et al*.[4]

The bond length of Ln-O regularly decreases as the Ln(III) atomic number increases. By subtraction of the ionic radii of nine-coordination from Ln-O, the residual values are nearly constant. Figure 2-5 shows plots of bond lengths and the residual values of these complexes together with the light Ln(III) complexes.[4] The decrease in bond lengths could be related to the changes of ionic radii due to the lanthanide contraction.[8,9,10]

The decrease in Ln-O bond lengths was further analyzed as evidence for the lanthanide contraction.

The decrease can be best described by a second-order polynomial.[11,12] The sum of Ln-O and O-O bond lengths shows in Figure 2-6 and Figure 2-7, respectively. The sum of either the Ln-O bond lengths or the O-O distances shows an almost perfect quadratic decrease in $[Ln(TEDGA)_3]^{3+}$ cation complexes. This decrease is modeled by Slater's model for calculating ionic radii and thus the decrease in Ln-O bond lengths can be attributed to the lanthanide contraction. [12]

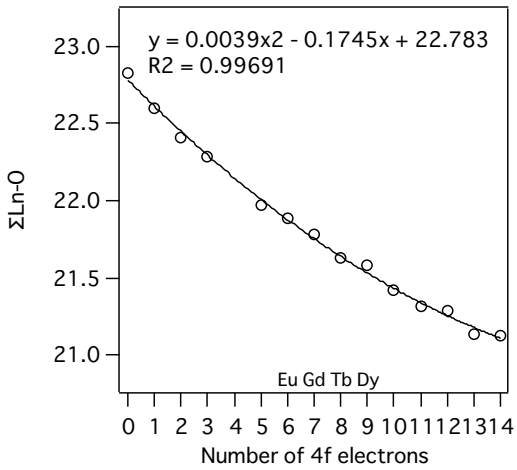

Figure 2-6 The sum of the Ln-O bond lengths against the number of f electrons with quadratic fit.

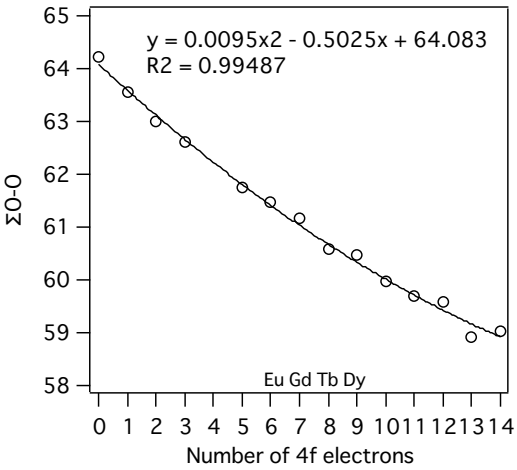

Figure 2-7 The sum of the O-O bond lengths against the number of f electrons with quadratic fit.

The structural difference between two forms of light and heavy Ln(III) complexes could be attributed to following factors: (i) lanthanide contraction, (ii) crystal-packing stability and (iii) bonding affinity of the nitrate ion. For the (i) lanthanide contraction factor, the shrinkage of ionic radii makes it difficult to form the nitrate complexes with high coordination number, e.g. $[Ln(NO_3)_6]^{3-}$, in heavy Ln(III). In fact, the Ln(III) complexes having large coordination number are often found in the multidentate ligands with a small "bite-angle" such as nitrate ion. The $[Ln(NO_3)_6]^{3-}$ ions in crystalline salts have been reported only in the light Ln(III).[13,14] As far as we know, Dy(III) is the heavies Ln(III) element that forms such high-coordination anionic complexes, i.e. $[Dy(NO_3)_6]^{3-}$.[15,16]

The influence of (ii) crystal-packing would also be important, because it will affect the lattice energy and determine which complex species crystallize first. The packing coefficient (K) can be express by $K=ZV_{mol}/V$, where Z is the number of molecules in the unit cell, V is the volume of the unit cell, and the V_{mol} is the molecular volume. The packing coefficient of common molecular crystal (0.72 ± 0.05) should be close to the value of hexagonal close-packed (0.74).[17] The parameters for La(III) and Lu(III) crystals are summarized in Table 2-3. The K values show well agreement with the common molecular crystal and the difference between La(III) and Lu(III) crystals are small. This means the crystal-packing can be considered same.

Table 2-3 Packing parameters of the La(III) and Lu(III) complexes. V_{mol} were calculated by Winmostar v4.015.[18]

	La		Lu	
	$[La(TEDGA)_3][La(NO_3)_6]$	$[La(TEDGA)_3]^{3+}$	$[Lu(TEDGA)_3](NO_3)_3$	$[Lu(TEDGA)_3]^{3+}$
V	2915.00		2714.09	
V_{mol}	1005.79	749.52	926.98	738.57
Z	2		2	
K	0.69		0.68	

The influence of (iii) the bonding affinity of Ln(III) to nitrate ions can be more pronounced for formations of these complexes. As introduced in Chapter 1.3.4, the thermodynamic data of the association reaction between Ln(III) and nitrate in water indicate that the light Ln(III) (Ln = La–Sm/Gd) species form $LnNO_3^{2+}$ complex more stably than the heavy Ln(III) (Ln = Tb–Lu).[19,20] Therefore, it can be concluded by qualitatively that the bonding affinity in light Ln(III) is TEDGA ≥ NO_3^-, whereas in heavy Ln(III) is clearly TEDGA > NO_3^-.

2.3.1 Infrared Spectra

Infrared spectra of heavy Ln(III) nitrate complexes TEDGA and free TEDGA were measured. The spectra are shown in Figure 2-9. In general, the O–H stretching vibration in water is observed in the 3500–2500 cm^{-1} range. The complexes showed significant strength of broad bands around 3500 cm^{-1}. This band thus can be corresponding to the four water of crystallization. Figure 2-8 shows the IR spectra for free TEDGA, reported La(III) and Lu(III) complexes as representative examples of the features in IR bands for comparison of light and heavy Ln(III) complexes, respectively.[4] The sharp band was observed at 1645 cm^{-1} that can be assigned to $\nu_{(C=O)}$ of free TEDGA. This $\nu_{(C=O)}$ band shifted to 1615–1623 cm^{-1} in both La(III) and Lu(III) complexes. Relatively narrow band was observed at 1120 cm^{-1} that can be assigned to $\nu_{(C\text{-}O\text{-}C)}$ for free TEDGA, and the band showed small red shift for La(III) complex and blue shift for Lu(III) complex. Other assignments for the IR bands of the complexes are summarized in Table 2-4.

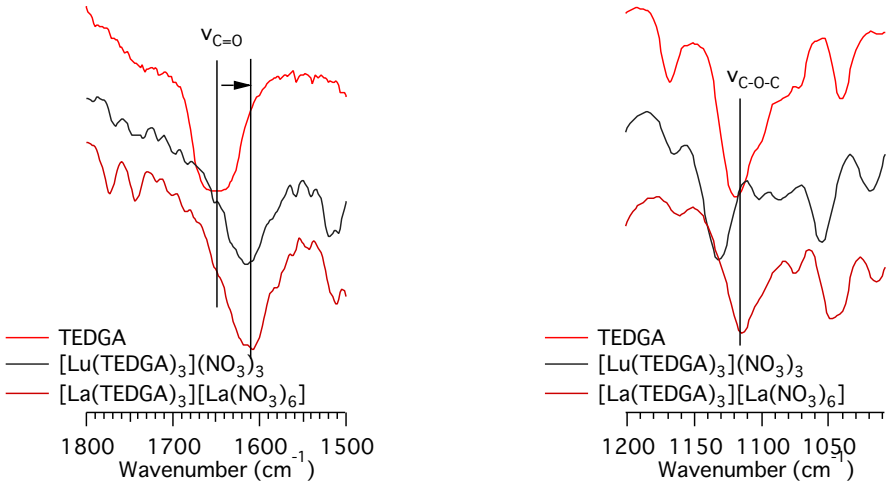

(a) (b)

Figure 2-8 Representative examples of IR spectra for TEDGA, (a) La- and (b) Lu-complexes.

The characteristic bands for nitrate were also observed. In light Ln(III) complexes, C_{2v} symmetric N-O stretching modes ν_1, ν_4, and ν_2, along with the bending mode ν_6 and ν_3 were observed with the corresponding peaks at ν = 1508–1514, 1326–1334, 1045–1049, 819, and 734–740 cm^{-1}, respectively. In addition, no obvious absorbance band at 1385 cm^{-1} corresponding to the ionic nitrate of D_{3h} symmetry was observed.[4] These IR bands suggest that the nitrate ions coordinate to the Ln(III) in bidentate manner as depicted in the light Ln(III) complexes.[4] The combination frequency band (ν_1+ν_4) also suggest that the nitrate ions coordinate to the Ln(III) by bidentate fashion, because the differences between two band ($\Delta_{conbination}$) around 1700–1800 cm^{-1} are 32 cm^{-1}. (see Chapter 1.4.2 for details.)

In contrast to the light Ln(III) complexes, the bands assigned to C_{2v} symmetric nitrate were not observed in heavy Ln(III) complexes. The bands observed at about ν= 1053, 831, and 774 cm^{-1} are correspond to the ν_1, ν_2, and ν_4 vibration mode of the D_{3h} symmetric nitrate. D_{3h} symmetry is resulting from when the nitrate ion is ionic. Frequently observed ν_3 band around 1384 cm^{-1} were not observed clearly, however, broad bands appeared at around this region. Existence of such broad bands indicates that the nitrate ions in the heavy Ln(III) complexes are ionic. Only one band at the 1700–1800 cm^{-1} region also suggests that the nitrate ions are in ionic. These IR bands are consistent with the features of crystal structures As a result, it may be reasonable to assume that the strong affinity with TEDGA and outer-sphere complex formations with nitrate ions contribute to the high selectivity in solvent extraction.

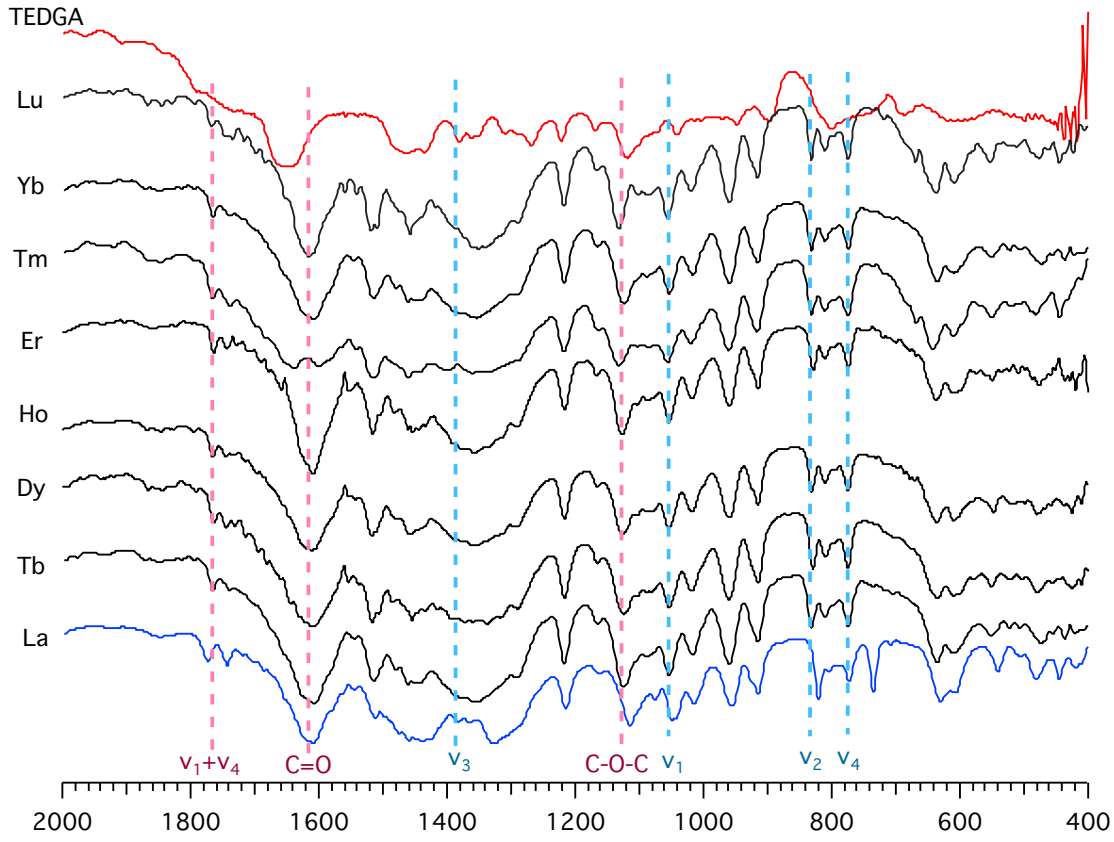

Figure 2-9 IR spectra of Ln-TEDGA complexes, together with the La(III)-TEDGA complex as a representative example for light Ln(III) form the reported data by Kawasaki *et al.*[4] (KBr pellet, room temp)

Table 2-4 Observed IR bands of Ln(III)-TEDGA complexes (Ln=Tb-Lu)

	water	C=O	C-O-C	D_{3h}				Combination frequencies $\nu_1+\nu_4$	$\Delta_{conbination}$
				ν_3	ν_1	ν_2	ν_4		
TEDGA		1645	1120						
Tb	3500	1610	1126	1384(br)	1053	831	774	1764	-
Dy	3500	1610	1126	1384(br)	1053	831	774	1762	-
Ho	3500	1611	1126	1384(br)	1055	831	774	1765	-
Er	3500	1609	1125	1384(br)	1052	827	774	1763	-
Tm	3500	1604	1132	1384(br)	1055	831	774	1764	-
Yb	3500	1610	1124	1384(br)	1053	831	774	1764	-
Lu	3500	1612	1132	1384(br)	1053	831	774	1734	-

2.4 Conclusion

$[Ln(TEDGA)_3](NO_3)_3$ (Ln = Tb–Lu) were synthesized and characterized in crystallographically and the coordination modes of TEDGA and nitrate ions were confirmed by IR spectroscopy. Together with the previous report by Kawasaki *et al*., the systematical investigations across the Ln(III) series in the solid state were completed and found that there are difference in the structure.[4] The heavy Ln(III) (Ln = Tb–Lu) complexes exist in the space group P_n or P_c. Their crystal structures are constructed by the packing of $[Ln(TEDGA)_3]^{3+}$ cations, three nitrate as counter anions, and four water of crystallization, i.e., $[Ln(TEDGA)_3](NO_3)_3{\cdot}4H_2O$.

In comparison with the light Ln(III) complexes reported by Kawasaki *et al*., the structures of Ln(III) nitrate complexes with TEDGA are split into two groups. The first half light Ln(III) (Ln = La–Gd, except for Pm) are constructed by the packing of $[Ln(TEDGA)_3]^{3+}$ cations and $[Ln(NO_3)_6]^{3-}$ anions.[4] The $[Ln(TEDGA)_3]^{3+}$ cations exhibit distorted tricapped trigonal prismatic geometry, in which Ln(III) ions are coordinated by nine oxygen atoms from three tridentate TEDGA ligands. The heavy half group (Ln = Tb–Lu) in this study are constructed by $[Ln(TEDGA)_3]^{3+}$ cation, the three nitrate ions exist as counter anions, and four hydrates as water of crystallization. The $[Ln(TEDGA)_3]^{3+}$ cations exhibit distorted tricapped trigonal prismatic coordination geometry in both groups.

The structural differences between light and heavy complexes in the crystal structures can be attributed to the following factors: (i) lanthanide contraction, (ii) crystal-packing stability and (iii) bonding affinity of the nitrate ion. The decrease in the Ln-O bond lengths can be attributed to the lanthanide contraction by the evaluation of quadratic decay of the sum of Ln-O and O-O bond lengths. According to the lanthanide contraction, the shrinkage of ionic radii makes it difficult to form the nitrate complexes with high coordination number for heavy Ln(III). The packing coefficient of light and heavy Ln(III) are approximately same. Therefore, in case of this study, (i) and (iii) are the possible effects of the causes of the structural difference in the solid state.

References

1 Kannan, S.; Moody, M. A.; Barnes, C. L.; Duval, P. B. "Lanthanum(III) and uranyl(VI) diglycolamide complexes: synthetic precursors and structural studies involving nitrate complexation ." *Inorganic Chemistry,* **2008**, *47*, 4691-4695.

2 Matloka, K.; Gelis, A.; Regalbuto, M.; Vandegrift, G.; Scott, M. J. "Highly efficient binding of trivalent f-elements from acidic media with a C3-symmetric tripodal ligand containing diglycolamide arms." *Dalton Transactions,* **2005**, 3719–3721.

3 Hirata, M.; Guilbaud, P.; Dobler, M.; Tachimori, S. "Molecular Dynamics Simulations for the Complexation of Ln^{3+} and UO_2^{2+} Ions with Tridentate Ligand Diglycolamide (DGA)." *Physical Chemistry Chemical Physics,* **2003**.

4 Kawasaki, T.; Okumura, S.; Sasaki, Y.; Ikeda, Y. "Crystal Structures of Ln(III) (Ln = La, Pr, Nd, Sm, Eu, and Gd) Complexes with *N,N,N',N'*-Tetraethyldiglycolamide Associated with Homoleptic $[Ln(NO_3)_6]^{3-}$." *Bulletin of the Chemical Society of Japan,* **2014**, 87, 294-300.

5 T. HIGASHI, "*Abscor* - Empirical Absorption Correction based on Fourier Series Approximation." Rigaku Corporation, Tokyo, Japan, **1995**.

6 Sheldrick, G. "A short history of SHELX." *Acta crystallographica. Section A, Foundations of crystallography*, **2008**, A64, 112-122.

7 *CrystalStructure 3.8*: Crystal Structure Analysis Package, Rigaku and Rigaku/MSC (2000-2006). 9009 New Trails Dr. The Woodlands TX 77381 USA.

8 Yaita, T.; Narita, H.; Suzuki, S.; Tachimori, S.; Motohashi, H.; Shiwaku, H. "Structural study of lanthanides (III) in aqueous nitrate and chloride solutions by EXAFS." *Journal of Radioanalytical and Nuclear Chemistry*, **1999**, 239, 371–375.

9 Bowden, A.; Horton, P.; Platt, A. "Lanthanide nitrate complexes of tri-isobutylphosphine oxide: solid state and CD_2Cl_2 solution structures." *Inorganic Chemistry*, **2011**, 50, 2553–2561.

10 Bowden, A.; Coles, S.; Pitak, M.; Platt, A. "Complexes of lanthanide nitrates with tri tert butylphosphine oxide." *Inorganic Chemistry,* **2012,** 51, 4379−4389.

11 Quadrelli, E. "Lanthanide Contraction over the 4f Series Follows a Quadratic Decay." *Inorganic Chemistry,* **2002**, 41, 167-169.

12 Seitz, M.; Oliver, A.; Raymond, K. "The Lanthanide Contraction Revisited." *Journal of the American Chemical Society*, **2007**, 129.

13 Zhu, Y.; Liu, W.; Tan, M.; Jiao, T.; Tan, G. "X-Ray Crystal Structure of the 1:1 Complex between Lanthanum Nitrate and N,N,N',N'-Tetraphenyl-3,6-Dioxaoctanedioic Diamide." *Polyhedron,* **1993**, 12.

14 Palewska, K.; Chojnacki, H. "A Possible Mechanism of Reversible Photocyclization of [5]-Helicene in Shpol'skii-Type Matrices at 4.2K." *Journal of Molecular Structure*, **2002**, 611.

15 Chekhlov, A. N. "Synthesis and crystal structure of hexa(nitrato-O,O′)dysprosium(III)Bis [4,7,13,16,21,24-hexaoxa-1,10-diazoniabicyclo[8.8.8]hexacosane] nitrate dihydrate." *Russian Journal of Inorganic Chemistry*, **2007,** 52, 1741-1745.

16 Hursthouse, M.; Short, R.; Kelly, P.; Woollins, J. "Metal Complexes of Sulfur–nitrogen Ligands: The Structure of Amino(triphenyl)phosphonium[di(thiazane)-3-Eno](thiosulfato) (triphenylphosphine)platinate." *Acta Crystallographica Section C Crystal Structure Communications*, **1988**, 44.

17 小林 啓二, 林 直人 著, 「固体有機化学」 化学同人

18 Tanaka, S.; Ono, Y.; Uuda, Y. "Extension of the CNDO/S method to the calculation of aromatic

and heterocyclic compounds containing Si, P, S and Cl." *Chemical and Pharmaceutical Bulletin*, **1985**, 33, 3077.

19 Choppin, G.; Strazik, W. "Complexes of Trivalent Lanthanide and Actinide Ions. I. Outer-Sphere Ion Pairs." *Inorganic Chemistry*, **1965**, *4*.

20 Bonal, C.; Morel, J.-P.; Morel-Desrosiers, N. "Interactions between lanthanide cations and nitrate anions in water. Part 1.Effect of the ionic strength on the Gibbs energy, enthalpy and entropy of complexation of the neodymium cation." *Journal of the Chemical Society, Faraday Transactions*, **1996**, *92*.

Chapter 3

Complexation and Structural Studies of Lanthanide(III) Nitrate Complexes with TEDGA in Acetonitrile Solutions

3.1 Introduction

In Chapter 2, crystal structures of Ln(III)-TEDGA complexes and the structural difference between light and heavy Ln(III) in the solid state were studied and discussed. In addition to the previous chapter, complexations and the structures in organic solutions are of interest to know the circumstances of the extracted species existing in the organic phase after an extraction. According to our knowledge, there are only three studies are available concerning the complexation and the structural study between Ln(III) or An(III) with DGA derivatives in the organic solution.

Narita *et al*. characterized the extracted Ln(III)-DGA (Ln=Ho and Lu) complexes by FT-IR and UV-vis spectroscopy. The UV-vis spectrum of extracted Ho(III)-DGA complex showed characteristic band shape that indicates the symmetry around Ho(III) ion. The peak shift of $\nu_{C=O}$ band in IR spectrum of Lu(III)-DGA complex indicated that the complex has a strong bond between carbonyl oxygen and Lu(III).1] They further investigated the Er(III) complexes extracted from HNO_3 and HCl by the extended X-ray absorption fine structure (EXAFS) spectroscopy. The local structures of $Er(NO_3)_3$-DGA and $ErCl_3$-DGA complexes were quite similar. This similarity in the local structure around Er(III) suggested that the formation of inner-sphere complex with DGA and outer-sphere complex with nitrate ions during the extraction.[2] Pathank *et al*. have conducted the complexation study of Eu(III) with TODGA by a time resolved luminescence spectroscopy (TRFS) in water-methanol mixture. The formations of 1:1, 1:2 and 1:3 species have been confirmed and the stability constants ($\log\beta_n$) for n=1, 2, and 3 have been calculated as 6.1 ± 0.5, 10.8 ± 0.7, and 14.3 ± 0.6, respectively.[3] As described above, although this kind of approach is useful to understand the natures of extracted species, few researchers have addressed in the viewpoint of such coordination chemistry based approaches. UV-vis, luminescence, NMR and IR spectroscopy, or calorimetry and conductometry, etc. are frequently applied method for this purpose.

The objective of this chapter is the systematic investigations of the differences in comlexations and structures throughout the Ln(III) nitrate complexes with DGA in the solution. Since hypersensitive transitions are sensitive to the changed in the environment around Ln(III) ions, and chemical shifts of the ligand are also directly affected by the variations in their magnetic environment. In this chapter, systematic investigations of the Ln(III) nitrate complexes with DGA were examined by spectrophotometric titrations, NMR structural analyses and NMR titrations were carried.

3.2 Experimental

3.2.1 Syntheses

The Ln(III) nitrate complexes with TEGDA (Ln = La, Nd, Ho and Lu) were synthesized by the procedure described in Chapter 2.

3.2.2 Instruments and General Procedures

Ultraviolet・Visible Absorption Spectroscopy

Spectrophotometric titrations of TEDGA complex were conducted on SHIMADZU UV-3150 spectrophotometer equipped with sample holders of temperature controller. The metal ion must have

at least one hypersensitive transition and molar absorptivity of suitable wavelength in the UV-vis region. The Ln(III) ions in this study, Nd(III), Ho(III) and Er(III) can be met for these requirements. The absorption band at 581 nm for Nd(III), 452 nm for Ho(III) and 379 nm for Er(III) are attributed to the hypersensitive transitions of $^4G_{5/2} \leftarrow {}^4I_{9/2}$, $^5G_6 \leftarrow {}^5I_8$ and $^4G_{11/2} \leftarrow {}^4I_{15/2}$, respectively. Absorption spectra of 1×10^{-2} M of Nd(III) (650–500 nm, 0.05 nm interval), Ho (700–390 nm, 0.05 nm interval) and Er (570–350 nm, 0.05 nm interval) were collected at 298 ± 0.1 K. The samples with a constant concentration of Ln(III) were used and the [TEDGA]/[Ln] ratios were varied in the range 0 < [TEDGA]/[Ln] < 10. The mixture was then stirred for 1 minute. The spectra were analyzed by HypSpec computer program to estimate the conditional stability constant.[4] The data processing ranges were selected around hypersensitive peaks as follows: Nd(III), 560–580 nm; Ho(III), 445–460 nm; and Er(III), 377–379 nm.

Nuclear Magnetic Resonance (NMR) Study

All NMR spectra were recorded on JEOL ECX-400P (400 MHz) spectrometer at 298 K in acetonitrile-d_3 solutions. Chemical shifts were referenced with respect to the following standards: for ^{1}H: solvent residual signals at 1.94 ppm and for ^{13}C: methyl signal at 1.32 ppm. All of the ^{1}H and ^{13}C signals were assigned by using ^{1}H-^{1}H COSY, DEPT, HMQC and EXSY techniques. TEDGA was used for NMR measurement mainly because of the spectrum simplification. Various molar ratios of acetonitrile sample solutions dissolving TEDGA and hydrated Ln(III) (Ln = La–Lu, except for Pm and Gd) nitrate were prepared. The compositions of sample solutions are given in Table 3-1.

Table 3-1 Acetonitrile-d_3 solutions used in the NMR experiments

Sample solutions	[Ln] /mM	[TEDGA] /mM	[Ln]:[TEDGA]
A	0	10	0:1
B	10	10	1:1
C	10	20	1:2
D	10	30	1:3
E	10	40	1:4
F	$[La(TEDGA)_3][La(NO_3)_6]$		
G	$[Lu(TEDGA)_3](NO_3)_3$		

3.3 Results and Discussion

3.3.1 Spectrophotometric Titration

Complex formations of Ln(III) (Ln=Nd, Ho and Er) with TEDGA were investigated by spectrophotometric titrations. Neodymium(III) was used as a representative of light Ln(III), and Ho(III) and Er(III) were used as that of heavy Ln(III) ions.

Nd(III) System

The UV-vis absorption spectra of acetonitrile solutions dissolving 10 mM of the hexa-hydrated Nd(III) nitrate ,i.e. $Nd(NO_3)_3{\cdot}6H_2O$, and $[Nd(TEDGA)_3][Nd(NO_3)_6]$ crystal were measured and resulting spectra are shown in Figure 3-1. The absorption spectrum of acetonitrile solution dissolving the hexa-hydrated $Nd(NO_3)_3$ was quite similar to that of acetonitrile solution dissolving anhydrous $Nd(NO_3)_3$ reported by Bünzli *et al.*[5] According to the previous reports by Bünzli *et al.*, conductometric measurements of Nd(III), Eu(III), or Tb(III) nitrates indicated that no dissociation of

nitrate occurs in acetonitrile solution.[6,7] Bunzli *et al*. have also reported the coordination number of Ln(III) tri-nitrate species, i.e. $Ln(NO_3)_3$, in acetonitrile solution are 9.0, 9.1, 8.3, and 8.2 for Nd, Eu, Tb, and Er, respectively.[8] Hence, the coordination environment around Nd(III) seems to be similar even in the hydrated water molecules exist in the solution, that is, nitrate ions do not dissociate from Nd(III) and coordination number of Nd(III) can be considered as nine.

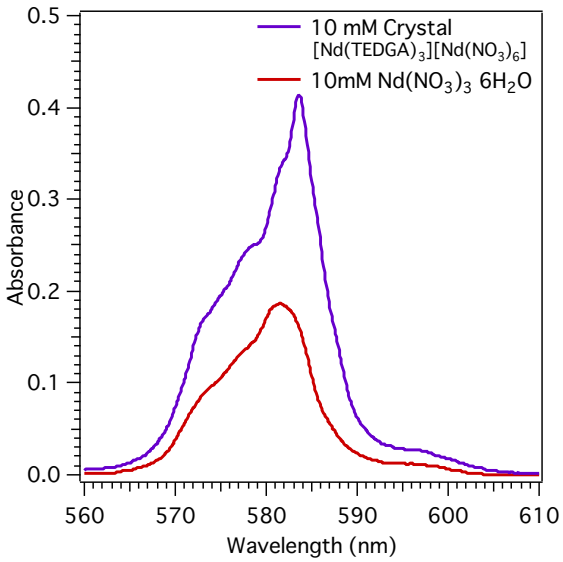

Figure 3-1 Absorption of 10 mM of $[Nd(TEDGA)_3][Nd(NO_3)_6]$ crystal and 10 mM of hydrated $Nd(NO_3)_3$.

The absorption spectrum of acetonitrile solution dissolving 10 mM of $[Nd(TEDGA)_3][Nd(NO_3)_6]$ crystal showed approximately twice intense compared to 10 mM of hexa-hydrated $Nd(NO_3)_3$, and the shape of the absorption band slightly changed. Twice intense in spectra is due to 10 mM of $[Nd(TEDGA)_3][Nd(NO_3)_6]$ crystal contains twice molar of Nd(III) ions.

In order to confirm the complex formation and to evaluate the variations of coordination environment around Nd(III), spectrophotometric titration of Nd(III) nitrate with TEDGA was performed and the resulting UV-vis spectra are shown in Figure 3-2. As can be seen from this figure, the Nd(III) absorption spectra changed not only intensity but also its shape with the titration of TEDGA. At the beginning, the absorption band of Nd(III) at 581 nm shifted to 583.8 nm and increased its intensity with addition of TEDGA until the metal to ligand ratio ([Nd]:[TEDGA]) reached 1:1. The absorption intensity at 583.8 nm then drastically decreased with the addition of TEDGA up to [Nd]:[TEDGA]=1:3. Further additions of TEDGA also lead to a subtle decrease in the absorption intensity for most of the spectral ranges. At the end, the absorption band split into three and the change in the intensity became small at [Nd]:[TEDGA]=1:6.

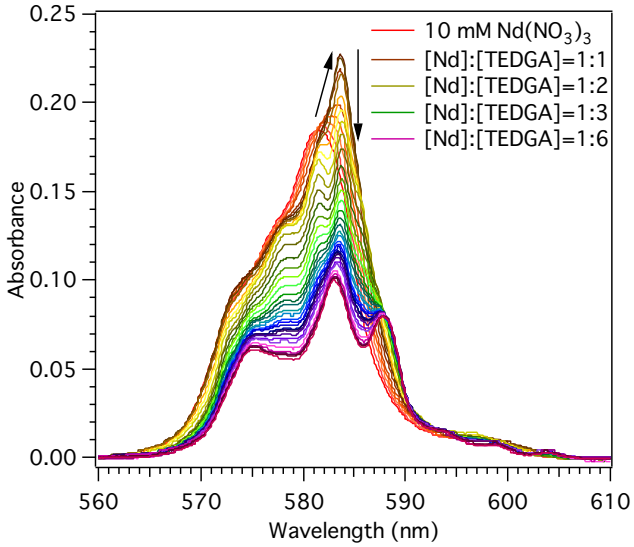

Figure 3-2 Spectrophotometric titration of 10 mM Nd(III) with TEGDA in acetonitrile at 298 K.

Figure 3-3 shows the plots of concentration dependence of the spectra intensity at 583.6 and 582.0 nm as examples. Two linear regression trend lines cross at [Nd]:[TEDGA]=1:1, and 1:3, indicating that the formations of 1:1 and 1:3 Nd-TEDGA complexes.

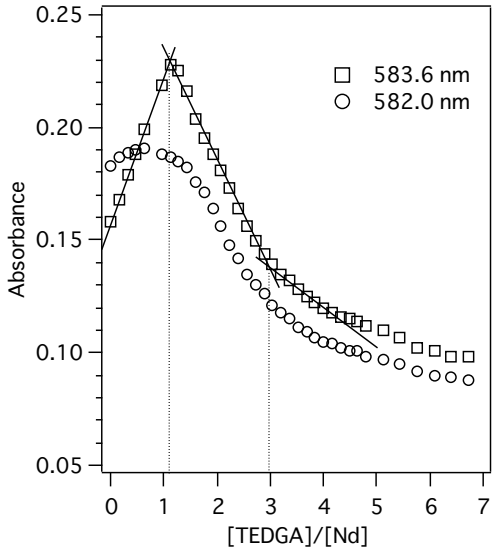

Figure 3-3 Mole ratio plot of the Nd(III)-TEDGA titration. Regression trend lines cross at approximately 1 and 3.

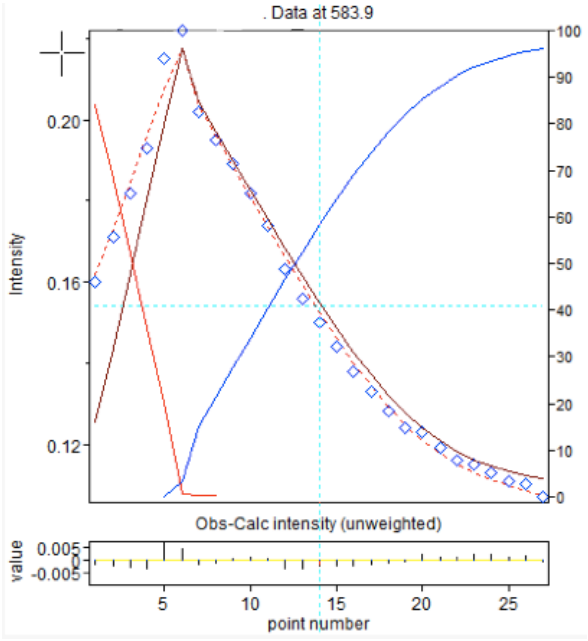

Figure 3-4 Fitting result for the spectrophotometric titration of Nd(III)-TEDGA system. Blue square symbols represent experimental data; dashed red curve represents the model fit; red, brown and blue curve represents the speciation of $Nd(NO_3)_3$, $[Nd(TEDGA)]^{3+}$ and $[Nd(TEDGA)_3]^{3+}$, respectively.

To evaluate the conditional overall stability constant (stability constant) in this system, the spectra were analyzed by HypSpec program.[4] The best fit was obtained when 1:1 and 1:3 complexes were refined. Although Panthak *et al*. have reported three formation constants, $\log\beta_1$, $\log\beta_2$ and $\log\beta_3$, (6.1 ± 0.5, 10.8 ± 0.7, and 14.3 ± 0.6) corresponding to 1:1, 1:2: and 1:3 complex formation of Eu(III)-TODGA system in ethanol/water mixture by TRFS measurements[3], only 1:1 and 1:3 complex formations were observed in this study. Figure 3-4 shows the titration curve and distribution diagram of chemical species of Nd(III)-nitrate-TEDGA system. The following reactions can be

proposed to the complexations for this system:

$$Ln(III) + TEDGA \rightleftharpoons [Ln(III)TEDGA] \quad \text{(Eq. 18)}$$

$$Ln(III) + 3TEDGA \rightleftharpoons [Ln(III)(TEDGA)_3] \quad \text{(Eq. 19)}$$

The stability constants $\log\beta_{ij}$ where j=1 and 3 were calculated as 5.4 ± 0.3, 10.4 ± 0.3, respectively. The $\log\beta_{11}$ is approximately same and $\log\beta_{13}$ is slightly lower compared to that of reported by Panthak *et al*.[3] This result suggests that the $\log\beta_{13}$ reflects the instability of 1:3 complex for light Ln(III).

Theoretically, the oscillator strength of hypersensitive transition is enhanced as the symmetry of the ligand field is reduced (see Chapter 1.4.1 for details.). Therefore, increase in absorption intensity indicates that low symmetric complexes compared with Nd(III) nitrate were formed at [Nd]:[TEDGA]=1:1. On the other hand, the absorption intensity at [Nd]:[TEDGA]=1:3 was approximately 30% lower than that of Nd(III) nitrate. The decrease in absorption intensity at this condition, therefore, indicates that the high symmetric 1:3 complex was formed. According to the $\log\beta_{13}$, the distribution of 1:3 complex is 85% in the [Nd]:[TEDGA]=1:3 solution. Therefore, the continuous gradual changes in absorption can be attributed to the gradual increase of 1:3 complex. In addition, the relatively low $\log\beta_{13}$ for Nd(III) may be due to the additional complexation with nitrate ions at the vacant site of large Nd(III).

The comparison of the spectra obtained in this study provides further information. The spectra of the [Ln]:[TEDGA]=1:n (n=0, 1, 1.5, 3 and 6) solutions are shown together with the spectra of solutions dissolving crystals in Figure 3-5. The similarity in absorption shapes and twice higher intensity between [Nd]:[TEDGA]=1:1.5 solution and $[Nd(TEDGA)_3][Nd(NO_3)_6]$ crystal indicate that the dissociation of homoleptic ion pair complex in the acetonitrile solution.

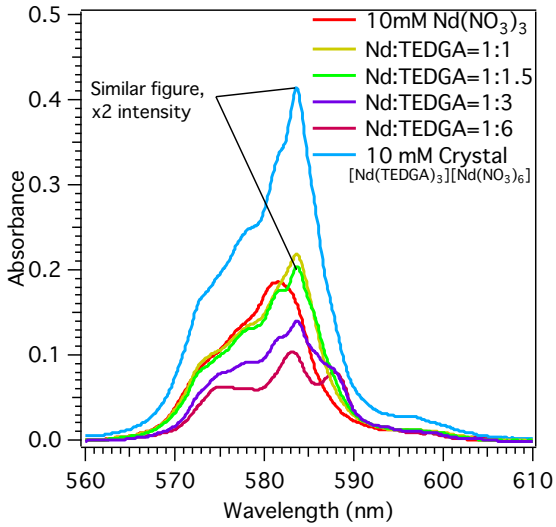

Figure 3-5 UV-vis spectra of acetonitrile solutions of 10 mM $Ln(NO_3)_3$ in red, [Ln]:[TEDGA]=1:1 in yellow, 1:3 in purple, and dissolving crystal in blue for Nd(III).

Ho(III) and Er(III) System

The UV-vis absorption spectra of acetonitrile solutions dissolving the penta-hydrated Ln(III) nitrate $Ln(NO_3)_3{\cdot}5H_2O$, and $[Ln(TEDGA)_3](NO_3)_3$ crystals of Ho(III) and Er(III) were observed and resulting spectra are shown in Figure 3-6 (a) and (b), respectively. In contrast to Nd(III) system, the shapes and intensity of absorption bands in both Ho(III) and Er(III) showed significant differences. These differences indicate that there are large difference in symmetry (i.e. coordination environment) around Ln(III) ions.

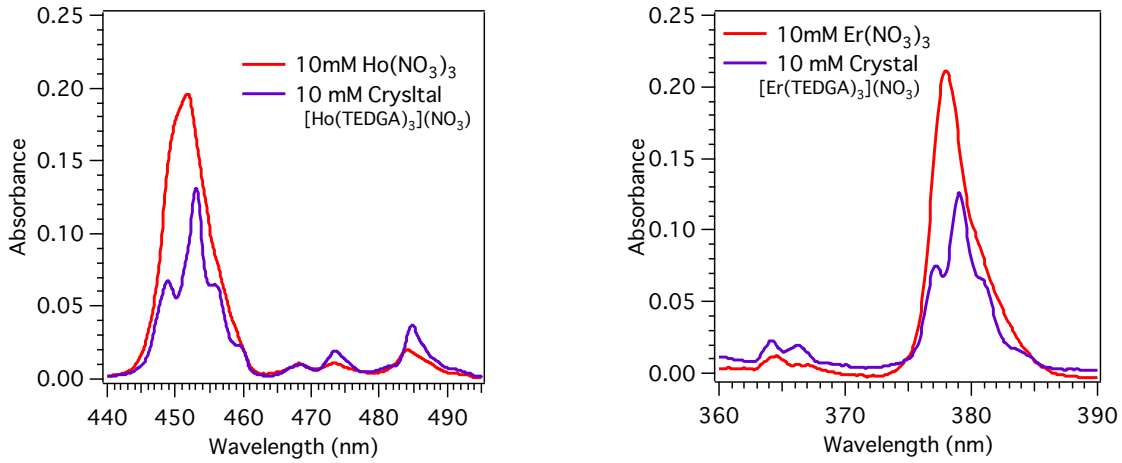

(a) (b)

Figure 3-6 Absorption of 10 mM of $[Ln(TEDGA)_3(NO_3)_3]$ crystal and 10 mM of hydrated $Ln(NO_3)_3$. (Ln= (a) Ho(III) and (b) Er(III).

Spectrophotometric titrations of Ho(III) and Er(III) with TEDGA were also performed and the resulting spectra are shown in Figure 3-7. The absorption of Ho(III) at 451 nm and Er(III) at 378 nm during the TEDGA titration changed similar to Nd(III) system. However, the changes in the intensity and the shape clearly terminated when the titration reached [Ln]:[TEDGA]=1:3.

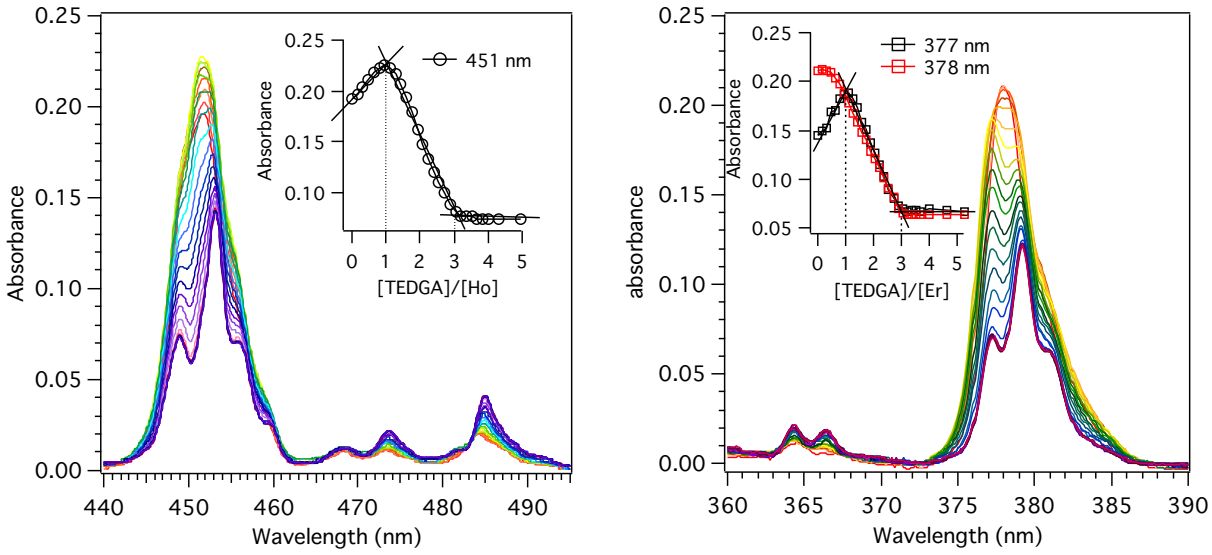

(a) (b)

Figure 3-7 Spectrophotometric titration of 10 mM (a) Ho(III) and (b) Er(III) with TEGDA in acetonitrile at 298 K.

The linear regression lines on the concentration dependence of the spectral intensity clearly suggests that the formation of 1:1 and 1:3 complexes. The increase in intensity by [Ln]:[TEDGA]=1:1 indicates the formation of low symmetric 1:1 complex compared with Ln(III) nitrate, and the steep decrease in intensity up to [Ln]:[TEDGA]=1:3 indicates the formation of high symmetric 1:3 complex. Excess of TEDGA did not cause further spectral change in both Ho(III) and Er(III) cases, indicating that no further structural change happen around Ln(III) after 1:3 complex formation. Therefore, 1:3 complexes of heavy Ln(III) are stable and rigid in the acetonitrile solution. Figure 3-8 shows the

representative best-fitted titration curves and the distribution curves of each chemical species. The overall stability constant $\log\beta_{ij}$ where j=1 and 3 for (Eq. 18) and (Eq. 19) were calculated as 6.2 ± 0.1 and 14.1 ± 0.1 for Ho(III), and 5.9 ± 1.7, 16.2 ± 0.5 for Er(III), respectively.

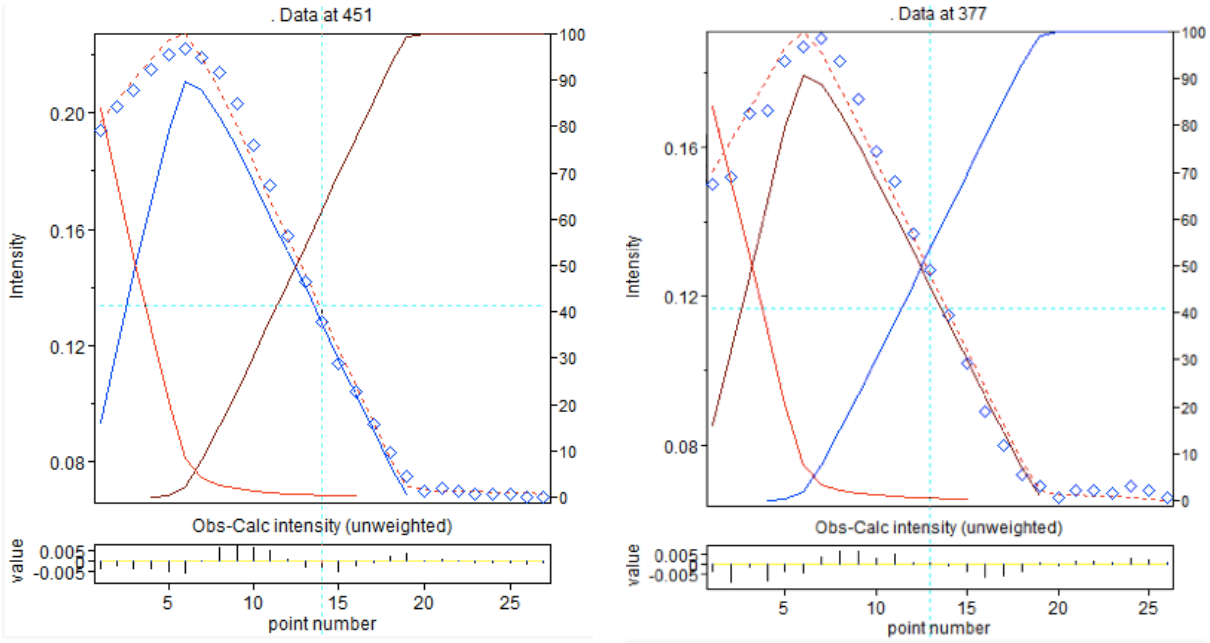

(a) (b)

Figure 3-8 Speciation diagram of (a) Ho(III) and (b) Er(III).

In contrast to Nd(III) system, the identical absorption spectra between [Ln]:[TEDGA]=1:3 (Ln= Ho and Er) solution and the solution dissolving $[Ln(TEDGA)_3](NO_3)_3$ crystal were obtained. Figure 3-9 shows the spectra of the [Ln]:[TEDGA]=1:n (n=0, 1 and 3) solutions together with the spectra of solutions dissolving crystals ($[Ln(TEDGA)_3](NO_3)_3$, Ln = Er and Ho). From these results, it can be assumed that the structures of these 1:3 complexes are quite similar to the crystal structures, $[Ln(TEDGA)_3](NO_3)_3$. Narita *et al*. suggested that Er(III) form inner-sphere 1:3 complex with DGA and outer-sphere complex with nitrate from EXAFS measurements.[2] These results also support that the reported 1:3 complexes and outer-sphere complexation with nitrate.[2,9] These results strongly suggest that the outer-sphere coordination of nitrate ions in both solid and solution for heavy Ln(III).

Moreover, these changes in absorption spectra were almost same when TODGA was introduced instead of TEDGA, meaning that the complexation ability is not affected by the hydrophilic or lipophilic property of the DGA in acetonitrile solutions.

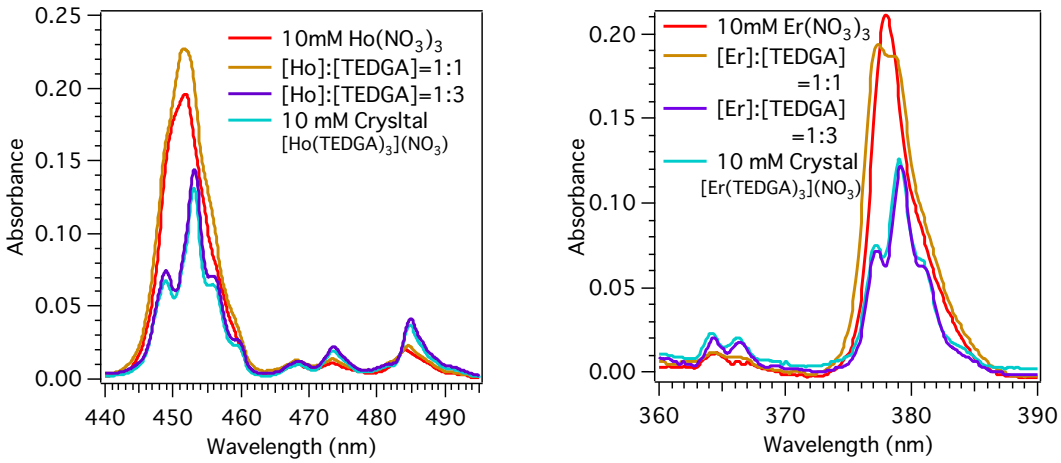

(a) (b)

Figure 3-9 UV-vis spectra of acetonitrile solutions of 10 mM $Ln(NO_3)_3$ in red, [Ln]:[TEDGA]=1:1 in yellow, 1:3 in purple, and dissolving crystal in blue for (a) Ho(III) and (b) Er(III).

Figure 3-10 shows the plots of the stability constants for Ln(III)-nitrate-TEDGA systems (Ln= Nd, Ho and Er) obtained in this study together with the Eu(III)-TODGA data reported by Panthak *et al*.[3] The $\log\beta_{11}$ for Ln(III) are approximately constant through the Ln(III) series, whereas $\log\beta_{13}$ increase with an increase in the atomic number. Increase in $\log\beta_{13}$ is well accordance with the qualitative discussion in Chapter 2 that the heavy Ln(III) ions prefer to form $[Ln(TEDGA)_3](NO_3)_3$ type complexes. This tendency on the stability constans are also consitent with the extraction behaviour of DGA in which the distribution ratio (D) of the heavy Ln(III) are larger than that of light Ln(III).

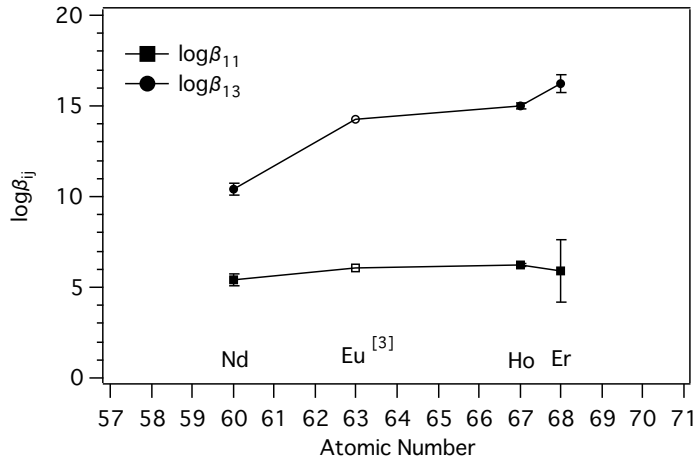

Figure 3-10 Plots of overall stability constants with error bars determined for Ln(III)-TEDGA from spectrophotometric titration in acetonitrile solutions at 298 K, together with Eu(III)-TODGA data reported by Panthak *et al*. [3]

3.3.2 NMR Structural Analysis

To assess the structures of complexes in the solution, Ln(III) nitrate complexes with TEDGA (Ln = La and Lu) in the acetonitrile-d_3 solutions were studied. First, Ln(III)-nitrate-TEDGA complexes, $[La(TEDGA)_3][La(NO_3)_6]$ and $[Lu(TEDGA)_3](NO_3)_3$, in acetonitrile solutions were investigated. Both complexes are readily soluble in acetonitrile-d_3, but the $[La(TEDGA)_3][La(NO_3)_6]$ complex is slightly soluble in chloroform-d.

To investigate the structures of complexes in the solution, ^{1}H NMR spectra of the acetonitrile-d_3

solutions dissolving free TEDGA (sample solutions **A**), crystals of diamagnetic Ln(III) complexes, i.e. $[La(TEDGA)_3][La(NO_3)_6]$ (sample solutions **G**), and $[Lu(TEDGA)_3](NO_3)_3$ (sample solutions **F)**, were recorded. The results for these spectra are shown in Figure 3-11 for comparison.

^{1}H NMR spectra of free TEDGA (sample solution **A**, on the top of Figure 3-11) shows five signals. The peaks observed at 1.2, 3.3 and 4.2 ppm were assigned to H(3), H(2) and H(1), respectively. One signal from methylene proton (CO-C*H*$_2$-O, H(1)) and a set of two signals of the ethyl chain on the amide group (N-C*H*$_2$C*H*$_3$, dq: H(2,2'), dt: H(3,3')) indicate that the existence of axial symmetry (C_{2v}) in the molecule and the rotation about N-CH_2CH_3 bond.

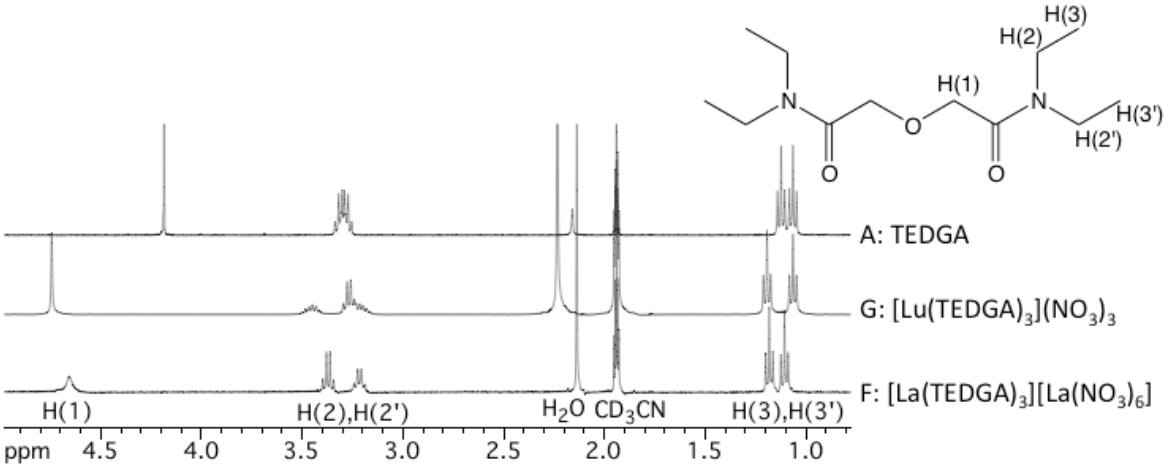

Figure 3-11. ^{1}H-NMR spectra of the acetonitrile solutions, **A** (free TEDGA on the top), **G** ($[Lu(TEDGA)_3](NO_3)_3$ on the middle) and **F** ($[La(TEDGA)_3][La(NO_3)_6]$ on the bottom) at 298 K.

^{1}H NMR spectra of sample solutions **G** and **F** also showed similar patterns of signals. The chemical shift differences between H(2) and H(2'), and between H(3) and H(3') are widened in both sample solution **G** and **F**. These expanses in the chemical shifts arise from the restricted rotation about the N-CH_2CH_3 bond.

On the spectra of sample solutions **F**, methylene signal of H(1) broadened and shifted approximately 0.5 ppm to downfield compared to sample solution **A**. The number of the signals remains the same as free TEDGA, indicating that the axial symmetry of TEDGA upon coordination to La(III) does not change. The broadening at the signal H(1) indicate that there is a dynamics in the system such as ligand exchange reaction.

On the spectra of sample solutions **G**, the methylene signal of H(1) was relatively sharp and shifted approximately 0.6 ppm to the downfield compared with sample solution **A**. The N-CH_2 signal, H(2), of sample solution **G** exhibited complex spin-spin coupling. The coupling pattern was simulated on the assumption that the existence of *geminal* proton coupling with ABX spin system with coupling constants of $^2J_{AB}$=13.8 Hz. The result is shown in Figure 3-12. The coupling probably results from the frozen of rotation about the N-C bond in one configuration upon coordination to Lu(III).

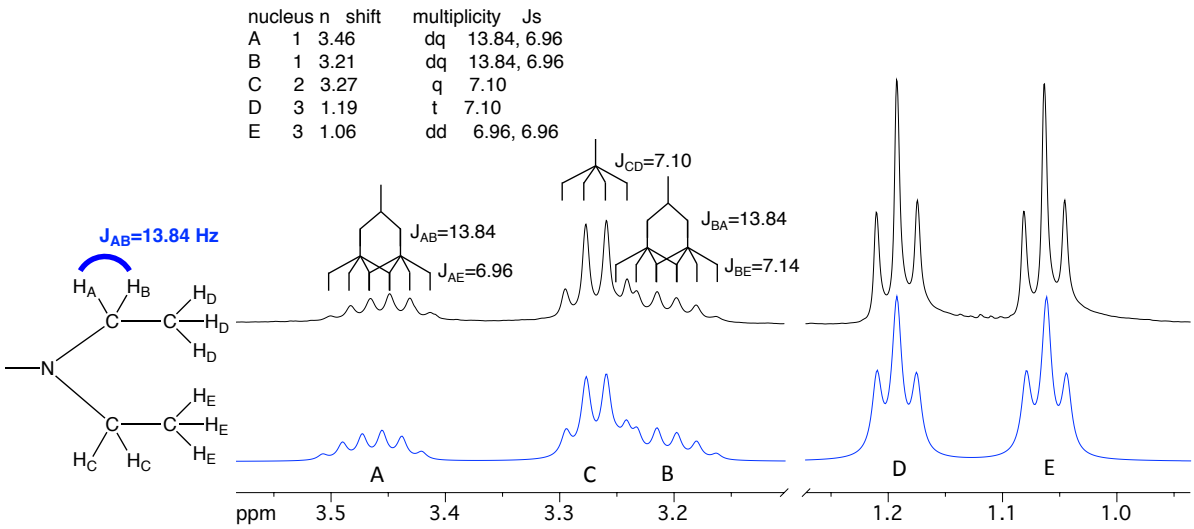

Figure 3-12 Coupling pattern analysis of sample solution G ($[Lu(TEDGA)_3](NO_3)_3$ on the top) and simulated spectrum on the bottom.

The cause of the coupling was further analyzed by the two-dimentional Nuclear Overhauser Effect SpectroscopY (NOESY) method. Figure 3-13 shows the NOESY spectrum of the sample solution **G**. Two intense crosspeaks between H(1) and H(2), and H(2) and H(3) were observed. The correlation peak on the NOESY spectrum provides information that there are spatially closes each other. The intense crosspeak between H(1) and H(2) is thus attribute to the frozen of rotation about the N-C bond described above.

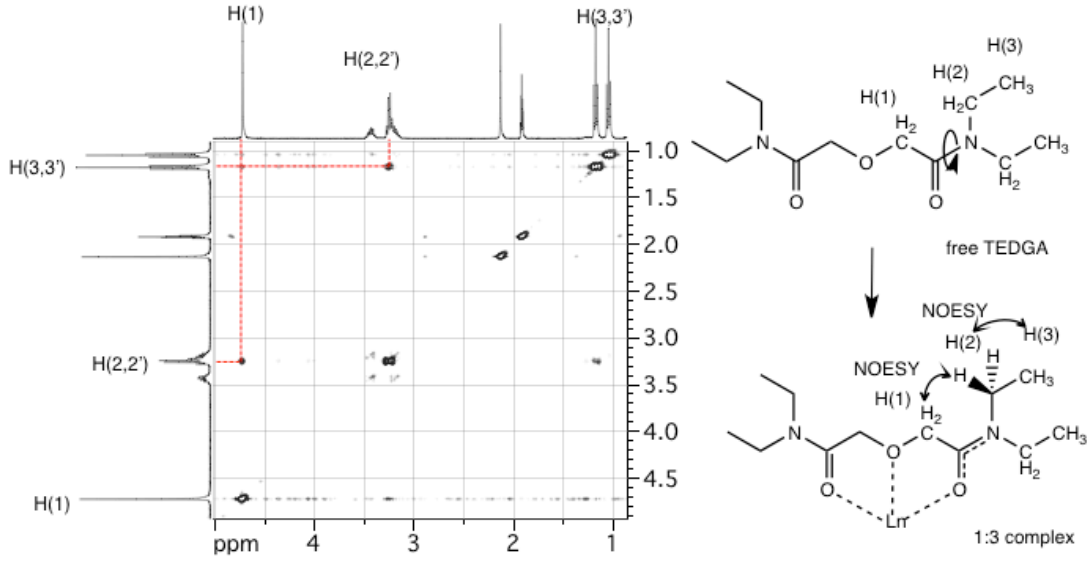

Figure 3-13 NOESY spectrum of $[Lu(TEDGA)_3](NO_3)_3$ in acetonitirle-d_3 solution.

3.3.3 NMR Titration Studies

The complex formation of Ln(III) were studied to gain further structural information on each complexation steps. Various molar ratios of acetonitrile solutions dissolving free TEDGA and hydrated Ln(III) (Ln = La–Lu, except for Pm and Gd) nitrate were prepared and ^{1}H NMR spectra were measured. The compositions of sample solutions are given in Table 3-1 in Chapter 3.2.2.

La(III) System

Figure 3-14 shows ^{1}H NMR spectra of sample solution **A**, **B**, **C**, **D** and **E** for La(III) system. In sample solution **B** ([La]:[TEDGA]=1:1), the methylene signal H(1) showed downfield shift by 0.5 ppm, and the chemical shift difference between two methylene signal H(2) and H(2') was widened compared to that of sample solution **A**. Since the system contains water from hydrated Ln(III) nitrate in a starting material, a signal of water was observed at 0.3 ppm downfield compared to bulk water typically observed in acetonitrile-d_3. The downfield shift in water signal indicate that the water molecules exist around Ln(III) ions. Although the attempt was made to obtain the number of coordinated water in this system, the signal from water cannot give a separate signal even in lowest temperature of acetonitrile.

For sample solution **C** ([La]:[TEDGA]=1:2), the signals from TEDGA are almost same as that of sample solution **B**, indicating that no significant conformational change under this condition from the viewpoint from TEDGA. Only upfield shift on the signal of water was observed, and its chemical shift agreed with bulk water typically observed in acetonitrile-d_3, that is, the displacement of water by reaction with TEDGA was completed when metal to ligand ratio is above [La]:[TEDGA]=1:2.

For sample solution **D** ([La]:[TEDGA]=1:3), the chemical shift of H(1) showed upfield shift compared to that of sample solution **B**. The large upfield shift of H(1) indicate that the TEDGA exhibits different conformation compared to 1:1 complex. Hence, the 1H NMR spectra of sample solution **D** indicates that the formation of 1:3 complex, and TEDGA still maintains same axial symmetry in 1:3 complex.

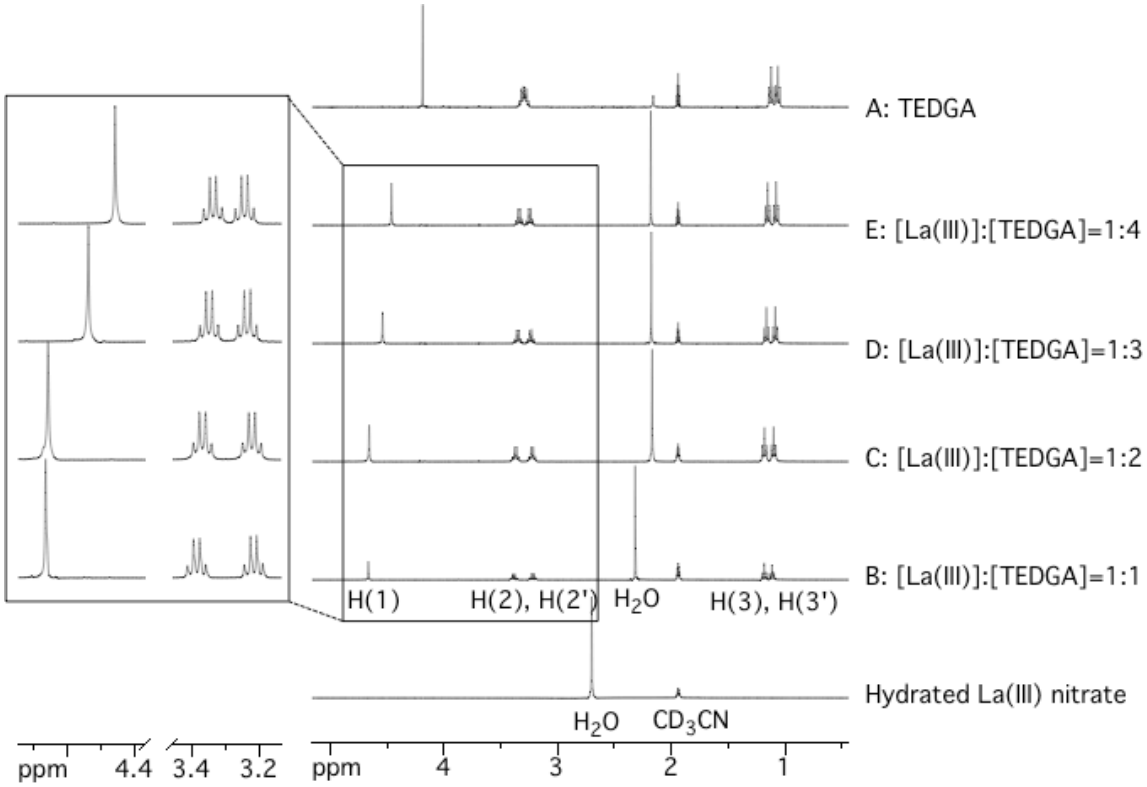

Figure 3-14 ^{1}H NMR spectra of TEDGA in acetonitrile-d_3 for different molar ratios of sample solution (A, B, C, D and E) for La(III) systems.

According to the spectrophotometric titration of Nd(III) in Chapter 3.3.1, the complexes with 1:1 and 1:3 metal to ligand ratio are formed. The distributions of 1:1 and 1:3 complexes were calculated using the stability constants of Nd(III) and are listed in the Table 3-2. The stability constants of Nd(III)

complexes indicate that 1:1 complex is dominant in the solution **B**. However, sample solutions **C** and **D** contain considerable amount of 1:1 and 1:3 complexes. Therefore, the no separate signals observed on both sample solutions **C** and **D** could be linked to the fast exchange reaction between 1:1 and 1:3 complexes.

Table 3-2 Speciation of the sample solutions

Sample solutions	Nd	
([Ln]:[TEDGA])	1:1 complex (%)	1:3 complex (%)
B (1:1)	79.8	0.00
C (1:2)	41.6	58.3
D (1:3)	14.6	85.3
E (1:4)	5.3	94.6

Furthermore, the excess of TEDGA to La(III) does not provide separate signals for the free and coordinated TEDGA, and cannot distinguish additional complexes, or 1:1 and 1:3 complexes even at low temperatures (< 238 K). Above [La]:[TEDGA] > 1:4, during the titration of TEDGA, all of the observed signals of TEDGA approached toward the chemical shift of sample solution **A**. Only one set of signals assigned to TEDGA indicates that the excess of TEDGA in the system causes a fast exchange on the NMR timescale. According to the stability constants of Nd(III) complexes, 1:3 complex is a dominant species in sample solution **E**. (see Table 3-2) Therefore, the fast exchange reaction in this condition can be associated between the free TEDGA and the coordinated TEDGA molecules in 1:3 complex.

It should be noted that nitrate ion also could participate in the exchange reaction. The presence of a dynamic behavior between free and coordinated TEDGA in 1:3 complexes would be related to the large ionic radii of light Ln(III). The large ionic radii in the light Ln(III) may provide some vacant sites that makes nitrate ions possible to be in the inner-sphere of the Ln(III), although the Ln(III) is wrapped around by three TEDGA molecules. As the result of the nitrate ion coordination, TEDGA forced to compete with them and change its position very fast.

By taking into account both results of UV-vis and ^{1}H NMR spectra, following can be concluded. (i) At the beginning, below the metal to ligand ratio [La]:[TEDGA]=1:1, 1:1 complex is formed with some hydrated water in its inner-sphere. (ii) Under the [La]:[TEDGA]=1:2 condition, all of the water molecules are replaced and out from the inner-sphere by complexation with TEDGA, and 1:1 and 1:3 complexes are exists and they exchange each other. (iii) Under [La]:[TEDGA]=1:3 condition, 1:3 complex become dominant, but still displays a fast exchange with 1:1 complex. (vi) Finally under [La]:[TEDGA]=1:4 condition, the amount of 1:1 complex become negligible. However, excess of TEDGA causes the fast exchange between the free TEDGA and the coordinated TEDGA in the 1:3 complexes. Figure 3-15 shows the reaction scheme estimated from the spectrophotometric and ^{1}H NMR titration result for light Ln(III).

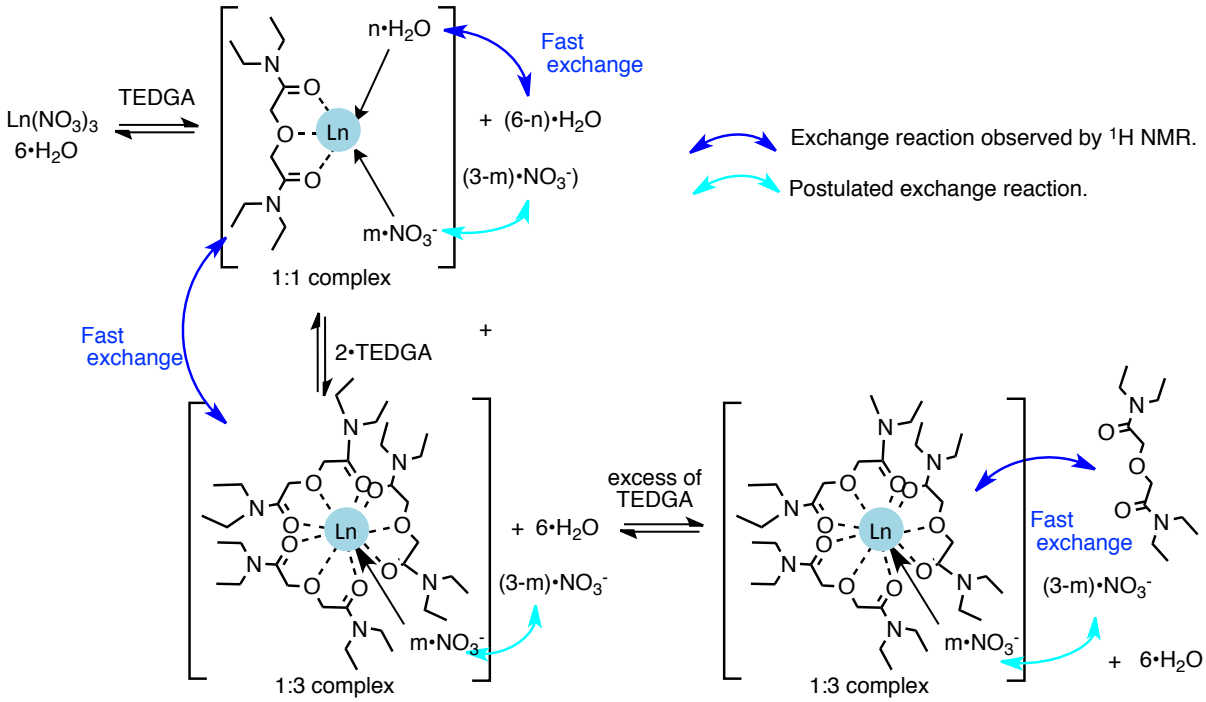

Figure 3-15 Scheme of complex formations for La(III) (light Ln(III)) with TEDGA estimated from NMR titration.

Additionally, the observed ^{1}H spectra of sample solution **F** was able to reproduced by [La]:[TEDGA]=1.15 sample solution, indicating the dissociation of homoleptic ion pair complex ($[La(TEDGA)_3][La(NO_3)_6]$). The idea of dissociation and re-formation was also introduced in previous chapter by spectrophotometric titration result and the UV-vis spectrum of $[Nd(TEDGA)_3][Nd(NO_3)_6]$.

Nd(III) and Eu(III) Systems

In order to evaluate the systematic investigations of the structural or complexation differences among the all Ln(III) nitrates with DGA in the solution, same procedure was applied to the paramagnetic Ln(III) (Ln = Ce–Yb, except for Pm and Gd). Gd(III). In general, a paramagnetism makes NMR spectra analysis difficult because the paramagnetism gives rise to pronounced changes in chemical shifts of the nucleus located nearby the Ln(III) ions. Although this difficulty, NMR spectra obtained from paramagnetic Ln(III) are valuable. Recently, Szabó *et al*. have successfully demonstrated that the stoichiometry, the structure and the ligand exchange dynamics in the paramagnetic Ln(III) ion complex, Y(III)/Eu(III)-tris[4,4,4-trifluoro-1-(2-thienyl)-1,3-butanedione] (TTA), by NMR spectroscopy.[10] They prepared test solutions with various concentration ratios of metals and ligands. The same kind of method was applied to this system.

Sample solutions **B**, **C**, **D**, and **E** were prepared and observed for paramagnetic Ln(III) was excluded because of its very long relaxation time. Here, Nd(III) and Eu(III) are shown as representative examples for light Ln(III) ions.

Figure 3-16 shows the spectra of solution **B**, **C**, **D**, and **E** of Nd(III) system. The spectrum of sample solution **B** showed at least ten signals except for the signals from solvent and water, that can be assigned to the two H(1) and four set of a N-CH_2CH_3 chain. These nine signals were attributed to the one TEDGA molecule coordinated to the Nd(III) ion.

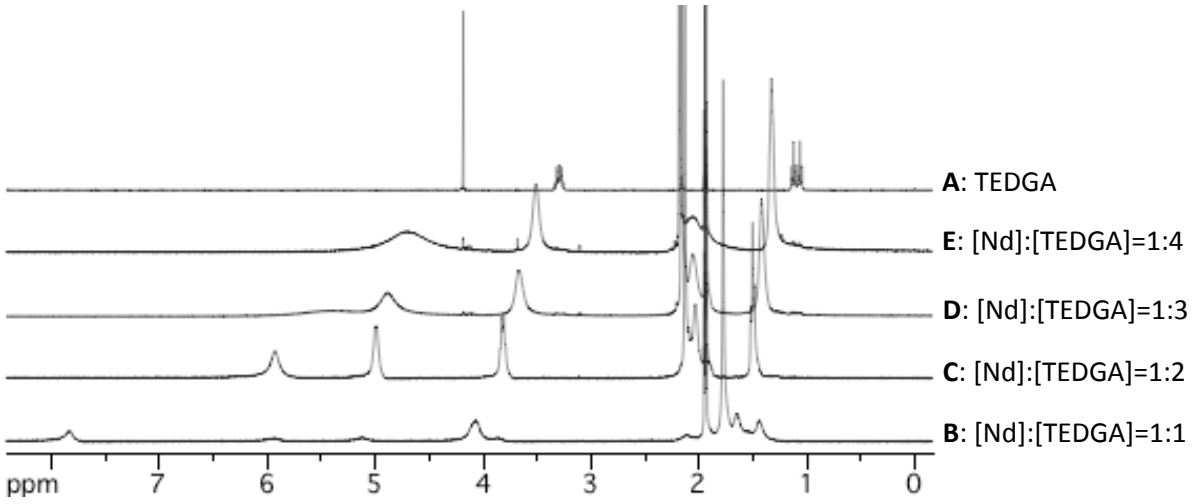

Figure 3-16 ^{1}H NMR spectra of TEDGA in acetonitrile-d_3 for different molar ratios of sample solution (A, B, C, D and E) for Nd(III) system.

With increasing the TEDGA concentration, the observed signals became broad and shifted, and finally coalesced into four signals at sample solution **E**. The spectral change in the spectra of solutions **B**, **C**, **D**, and **E** of Nd(III) system are reasonably in accordance with the results obtained in both spectrophotometric titration of Nd(III) and NMR titration of La(III). As descried above and listed the speciation in Table 3-2, in the sample solution **B**, 1:1 complex is the dominant species. In sample solution **C**, both 1:1 and 1:3 complexes are formed and exchange each other. In sample solution **D**, the 1:3 complex is dominant but still significant amount of 1:1 complex is exist. In sample solution **E**, 1:3 complex is formed and starts exchange with the free TEDGA. The fast exchange of TEDGA also observed in other light to middle Ln(III) (Ln = Ce to Eu, except for Pm) systems as well. Since the differences in the chemical shift between coordinated and free TEDGA are pronouncedly large in paramagnetic Ln(III) system, signal were coalescence when the fast exchange between free and coordinated TEDGA exists. The elements at the boundary of fast exchange reaction is Eu, and the spectra Eu(III) system are shown in Figure 3-17.

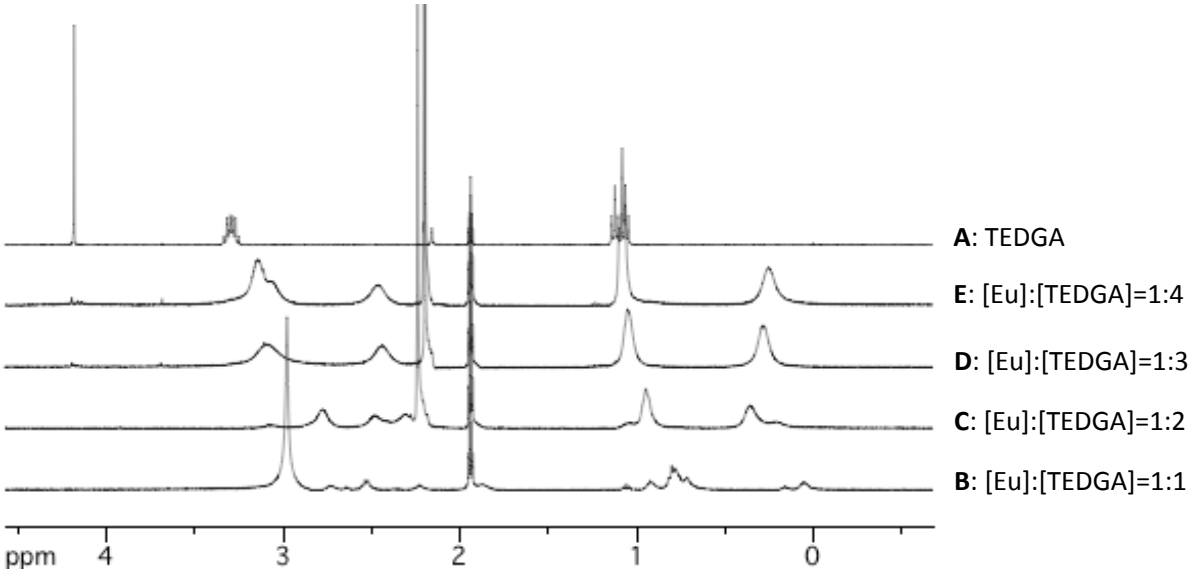

Figure 3-17 ^{1}H NMR spectra of TEDGA in acetonitrile-d_3 for different molar ratios of sample solution (A, B, C, D and E) for Eu(III) system.

Lu(III) System

The difference of complexation with TEDGA between light and heavy Ln(III) were investigated by NMR titration method by using Lu(III). The sample solutions were prepared as described in La(III) system and ^{1}H NMR spectra were measured for each samples. The resulting spectra of sample solution **A**, **B**, **C**, **D** and **E** for Lu(III) system are shown Figure 3-18.

For sample solution **B**, at least four inequivalent H(1) signals and broadened water signal were observed, indicating TEDGA forms 1:1 complex with more than one conformation and exchanging water. For sample solution **C**, one component become predominantly, and finally for sample solution **D**, only one component was observed. H(1) gave only one sharp signal, but complex spin-spin coupling was observed at H(2) and H(2'). The spectrum of sample solution **D** is completely identical to sample solution **G** that mentioned at previous section and the coupling system is completely same as well. Therefore, in contrast to the La(III) system, ^{1}H NMR of Lu(III) system clearly indicates the formation of 1:3 complex.

Even though there are excess of TEDGA, the exchange reaction in the Lu(III) system is slow enough on the NMR time scale. Sample solution **E** showed additional signals at the same position as that of sample solution **A.** These signals thus can be assigned to free TEDGA. The integral ratio of between coordinated and free is 3:1, thus this observation clearly indicates the formation of 1:3 complex in Lu(III) system. This result is in accordance with the results of UV-vis. In addition, three TEDGA molecules in the 1:3 complex coordinate to the Lu(III) by tetradentate fashion and are magnetically equivalent. Therefore, The structure of the 1:3 complex can be considered to be the same structure as solid state.

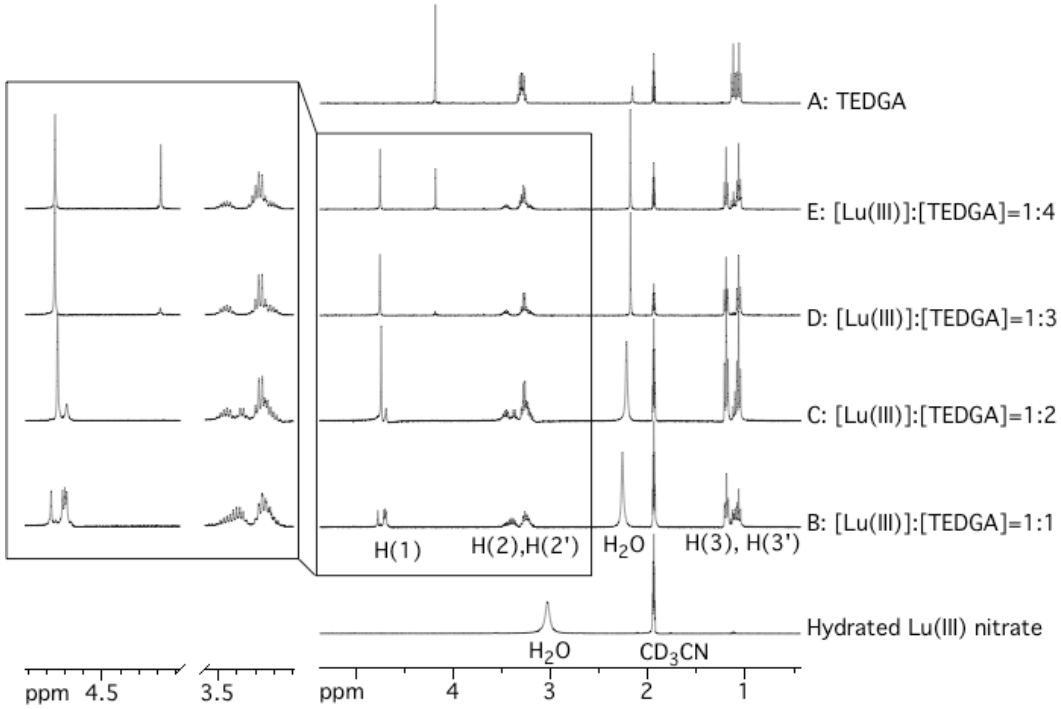

Figure 3-18 ^{1}H NMR spectra of TEDGA in acetonitrile-d_3 for different molar ratios of sample solution (A, B, C, D and E) for Lu(III) (right) systems.

According to the spectrophotometric titration of Ho(III) and Er(III) in Chapter 3.3.1, the complexes with 1:1 and 1:3 metal to ligand ratio are formed. The stability constants of Ho(III) and Er(III) complexes indicate that 1:1 and 1:3 complex is dominant in the solution **B** and **D**, respectively. The distribution of 1:1 and 1:3 complexes were calculated according to the stability constants, and are

listed in the Table 3-3.

Table 3-3 Distributions of the species in sample solutions

Sample solutions	Ho		Er	
	1:1 complex (%)	1:3complex (%)	1:1 complex (%)	1:3complex (%)
B 1:1	89.7	2.1	59.3	6.8
C 1:2	53.0	46.2	56.9	37.3
D 1:3	0.6	99.3	0.0	99.9
E 1:4	0.0	99.9	0.0	100.0

By taking into account both UV-vis and ^{1}H NMR spectra, following can be concluded. (i) At the beginning, under the [Lu]:[TEDGA]=1:1 conditions, 1:1 complex is dominant but small amount of 1:3 complex already exists. (ii) Under [Lu]:[TEDGA]=1:3 condition, 1:3 complex is completely dominant. (iii) Excess of TEDGA do not causes the fast exchange. Figure 3-19 illustrates the reaction scheme estimated from the spectrophotometric and NMR titration result for light Ln(III). The evaluations of the complexation behavior of heavy Ln(III) with TEDGA clearly demonstrate the contribution of the structure of complex for the stability.

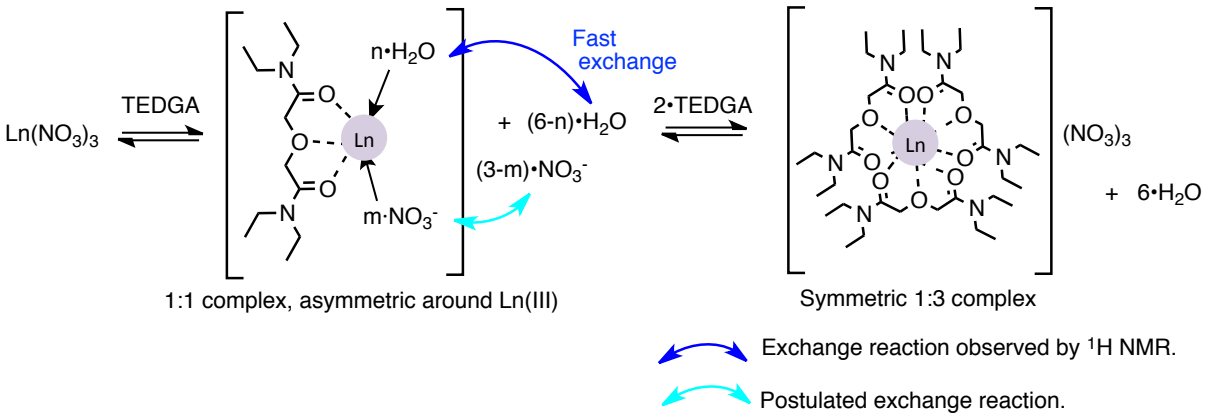

Figure 3-19 Scheme of complex formations for Lu(III) (heavy Ln(III)) with TEDGA estimated from NMR titration.

Tb(III) and Ho(III) Systems

Figure 3-20 shows the spectra of solutions **B**, **C**, **D**, and **E** of Ho(III) system. In contrast to the Nd(III) system, Ho(III) system showed the same feature as observed at NMR titration of Lu(III). In sample solution **B**, at least 14 signals were observed. Even though the all of signal cannot be assigned precisely in sample solution **B**, **C** and **D**, however, clear indication of 1:3 complex formation can be found. In sample solution **E**, four new signals appeared at the same chemical shift of sample solution **A**. These four signals can be thus assigned to free TEDGA, and can be concluded that the exchange dynamics in Ho(III) system is slow enough on the NMR time scale. The slow exchange was observed in other heavy Ln(III) (Ln = Tb to Yb) systems as well. The elements at the boundary of slow exchange reaction is Tb and the spectra of that of Yb(III) system are shown in Figure 3-21.

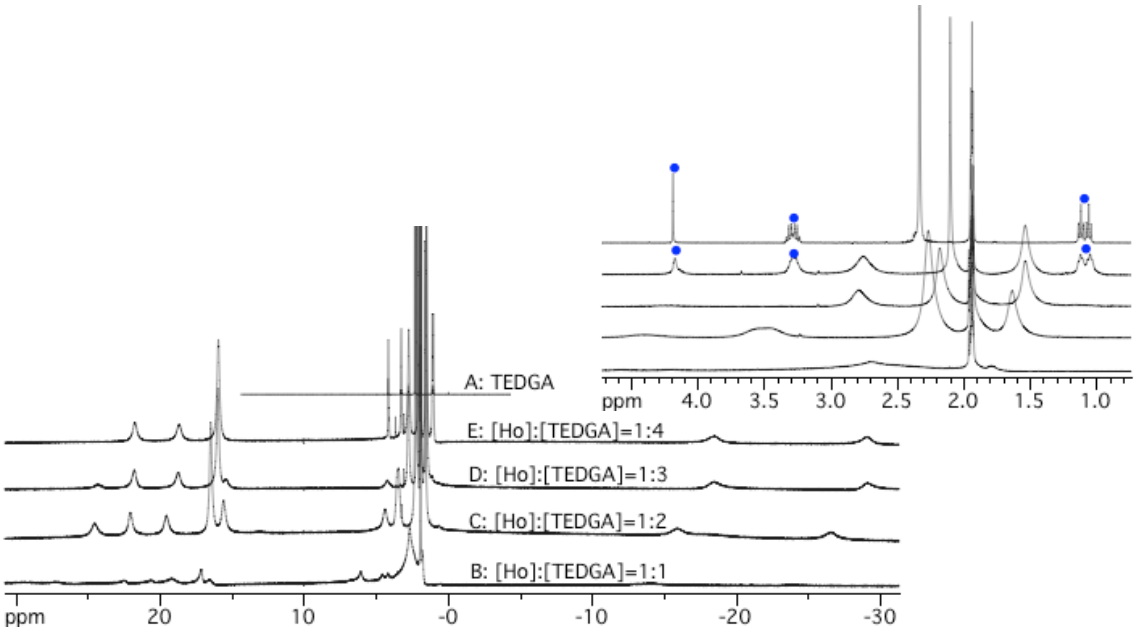

Figure 3-20 ^{1}H NMR spectra of TEDGA in acetonitrile-d_3 for different molar ratios of sample solution (A, B, C, D and E) for Ho(III) system. The signals marked by (●) are assigned to the free TEDGA ligand.

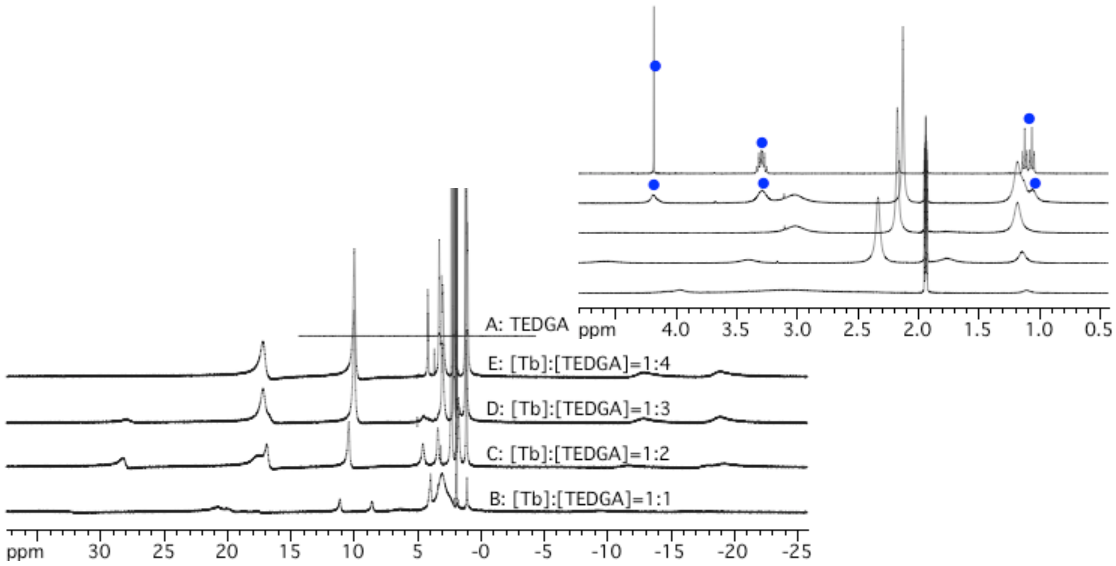

Figure 3-21 ^{1}H NMR spectra of TEDGA in acetonitrile-d_3 for different molar ratios of sample solution (A, B, C, D and E) for Tb(III) system. The signals marked by (●) are assigned to the free TEDGA ligand.

3.4 Conclusion

The differences in complex formation and structures among the Ln(III) series with DGA ligand in acetonitrile solutions were demonstrated by UV-vis and NMR spectroscopy.

Hypersensitive peaks are good indicators of ligand binding events. In this study, Nd(III), Ho(III) and Er(III) were selected. Intensity changes in UV-vis spectra by addition of TEDGA clearly showed that the 1:1 and 1:3 metal to ligand ratio complexes were formed. Sharp decrease in the absorption intensity of Ln(III) indicates that the 1:3 complexes are highly symmetric around Ln(III) ions. However, the stability of complexes of light and heavy Ln(III) are somewhat different. Combined with the UV-vis and NMR results, following can be concluded:

(i) Light Ln(III) ions form 1:1 and 1:3 complexes. 1:3 complexes are unstable because of the fast exchange between 1:1 complex, free TEDGA and nitrate ions. The fast exchange dynamics arise from the large ionic radii, preference of large coordination number and higher affinity to nitrate ions compared to heavy Ln(III). These factors make nitrate ions possible to be in the inner-sphere.

(ii) Heavy Ln(III) ions form 1:1 and 1:3 complexes, however, 1:3 complexes are highly symmetric compared with corresponding nitrate and are more favorable as the stability constants indicated. Once 1:3 complexes have formed, the 1:3 complexes for heavy Ln(III) are highly stable in the acetonitrile solutions.

(iii) The fast exchange reactions were detected between 1:1 and 1:3 complexes, and between 1:3 and free TEDGA for the light Ln(III). The boundary of the existence of fast exchange reactions in these systems is between Eu and Tb.

The systematical investigation across the Ln(III) series in the acetonitrile solution provided the information about the difference in structures and fast exchange reactions. The observations in this chapter successfully explain why the heavy Ln(III) ions are extracted by DGA derivatives with highly D values. In addition, the coordination of nitrate ions will be further investigated in Chapter 6.

References

1 Narita, H.; Yaita, T.; Tamura, K.; Tachimori, S. "Study on the extraction of trivalent lanthanide ions with N,N′-dimethyl-N,N′-diphenyl-malonamide and diglycolamide." *Journal of Radioanalytical and Nuclear Chemistry*, **1999**, *239*.

2 H. Narita, T. Yaita, S. Tachimori, " Extraction Behavior for Trivalent Lanthanides with Amides and EXAFS Study of Their Complexes." *Proceedings of the International Solvent Extraction Conference, ISEC'99*, **2001**, 693.

3 Pathak, P. N.; Ansari, S. A.; Godbole, S. V.; Dhobale, A. R.; Manchanda, V. K. "Interaction of Eu^{3+} with *N,N,N',N'*-tetraoctyl diglycolamide: a time resolved luminescence spectroscopy study." *Spectrochimica Scta. Part A, Molecular and biomolecular spectroscopy* **2009**, *73*, 348–52.

4 Gans, P.; Sabatini, A.; Vacca, "A. Investigation of equilibria in solution. Determination of equilibrium constants with the HYPERQUAD suite of programs." **1996**, 43, 1739-1753.

5 Karraker, D. G. "Hypersensitive transitions of six-, seven-, and eight-coordinate neodymium, holmium, and erbium chelates." *Inorganic Chemistry*, **1967,** 6, 1863–1868.

6 Bünzli, J.-C. G.; Vuckovic, M. M. "Solvation of neodymium (iii) perchlorate and nitrate in organic solvents as determined by spectroscopic measurements." *Inorganica Chimica Acta*, **1984**, *95*, 105–112.

7 Bünzli, J. G.; Mabillard, C.; Yersin, J. "FT IR and fluorometric investigation of rare-earth and metallic ion solvation. 2. Europium perchlorate and nitrate in anhydrous solutions containing dimethyl sulfoxide." *Inorganic Chemistry*, **1982**, *21*, 4214–4218.

8 Bünzli, J.-C.; Milicic-Tang, A.; Mabillard, C. "Lanthanide-nitrate interaction in anhydrous acetonitrile and coordination numbers of the lanthanide ions: FT-IR study." *Helvetica Chimica Acta*, **1993**, *76*.

9 Matloka, K.; Gelis, A.; Regalbuto, M.; Vandegrift, G.; Scott, M. J. "Highly efficient binding of trivalent f-elements from acidic media with a C3-symmetric tripodal ligand containing diglycolamide arms." *Dalton Transactions,* **2005**, 3719–3721.

10 Szabó, Z.; Vallet, V.; Grenthe, I. "Structure and dynamics of binary and ternary lanthanide(iii) and actinide(iii) tris[4,4,4-trifluoro-1-(2-thienyl)-1,3-butanedione] (TTA) complexes. Part 2, the structure and dynamics of binary and ternary complexes in the Y(iii)/Eu(iii) –TTA – tributylphosphate (TBP) system in chloroform as studied by NMR spectroscopy." *Dalton Transactions*, **2010**, 39, 10944–10952.

Chapter 4

Syntheses and Characterizations of Lanthanide(III) Nitrate Complexes with DOODAC2

4.1 Introduction

In Chapter 2 and 3, the crystal structures of Ln(III)-nitrate-TEDGA complexes and complex formation behavior of Ln(III) nitrate with TEDGA were demonstrated and have provided reasonable evidences that the structures of complexes are strongly related to their stability. In this chapter, the same approach was adopted to the tetradentate neutral diamide extractand, DOODA derivatives.

As outlined in the Chapter 1, maloneamide have been known to shown the relatively weak affinity to Ln(III) and poor preorganization of the two carbonyl groups formed upon complexes with Ln(III) and An(III) ions. In this reason, the extraction process requires a higher concentration of malonamide. By introducing of ether oxygen between the two amide groups of malonamide, diglycolamide (DGA) has three oxygen atoms to bind Ln(III) and An(III).[1] Consequently, DGA derivatives have been found to have surprisingly high selectivity with binding to tridentate fashion to Ln(III) and An(III). Recently, the extractant that possesses one other ether oxygen atom, *N,N,N',N'*-tetraalkyl-dioxaoctanediamide (DOODA) have been developed and examined. DOODA involves two ether oxygen and two carbonyl oxygen atoms. Figure 4-1 shows the structure of DOODA.

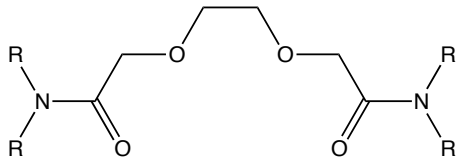

Figure 4-1 Schematic structures of *N,N,N',N'*-tetraalkyl dioxaoctanediamide (DOODA).

DOODA have a coordination ability to metal ions as tetradentate fassion and have expected to be more efficiently extract Ln(III) and An(III).[2] In contrast to the DGA derivatives, Sasaki *et al* have reported that the *D* values decrease gradually with an increase in the Ln(III) atomic number.[3,4,5] According to the stoichiometry during Ln(III) extraction by *N,N,N',N'*-tetraoctyl-dioxaoctanediamide (DOODA-C8), approximately two DOODAC8 molecules were involved in the extracted species.[3] The lipophilic/hydrophilic DOODA can be controlled by changing the alkyl chain length on the amide group. The An(III) ions behave as light Ln(III) in this extraction system. Therefore, the combined use of hydrophilic DOODA and lipophilic DGA is expected to lead large separation factors between MA(III) and Ln(III) species. Despite such very interesting separation approaches, no information is available concerning related to the structures of extracted complexes.

In this chapter, in order to find differences in structures of Ln(III) nitrates complexes with DOODA, the systematical investigation across the Ln(III) series in the solid state were carried out. The Ln(III) nitrates complexes with DOODA were synthesized and characterized by single crystal X-ray diffraction and IR spectra.

4.2 Experimental

4.2.1 Materials

Anhydrouns ethyl acetate and acetonitrile were purchased from KANTO chemical co ltd., and used without further purification. Other chemicals used in this experiment are as same as described in the Chapter 2. DOODAC2 and C8 were provided by JAEA (Japan Atomic Energy Agency) and used as received. However, DOODA can be synthesized by simple procedure as follows; the 3,6-dioxaoctanedioic chloride was synthesized from the reaction between 3,6-dioxaoctanedioic acid and thionyl chloride. The chloride product was then reacted with the secondary amine such as *N*,*N*-dioctylamin in an ice bath.[3]

4.2.2 Synthesis

*Preparation of [La(DOODA)$_3$(MeOH)$_2$][La(NO$_3$)$_6$] (**1**)*: $La(NO_3)_3 \cdot 6H_2O$ 0.216 g (0.499 mmol) in 10 ml of ethyl acetate was slowly added to a solution of DOODAC2 0.433 g (1.50 mmol) in 10ml of ethyl acetate. (Ln:DOODAC2 ≈ 1:3) The mixture was stirred at room temperature for 1 h and then the solvent was decanted off. The products were washed with hot ethyl acetate and dried in vacuo over P_2O_5 for 1 week, yielding colorless solid. Crystals suitable for X-ray diffraction were obtained by vapor diffusion with diethyl ether over a period of 1 week. Yield: 44.8 %, Elemental analysis, Found: C 25.58, H 4.40, N 10.73 %; Calculated for $C_{31}H_{68}N_{10}O_{29}La_2$: C 28.15, H 5.18, N 10.59 %. The large error from accurate values in elemental analysis was due to the hygroscopic property of the complex.

*Preparation of [Ce(DOODA)$_3$(MeOH)$_2$][Ce(NO$_3$)$_6$] (**2**)*: This and other complexes were synthesized in a similar matter to the method mentioned above. The synthesis conditions are as follows: $Ce(NO_3)_3 \cdot 6H_2O$ 0.217 g (0.50 mmol), DOODAC2 0.433 g (1.50 mmol). Yield: 53.6 %, Elemental analysis, Found: C xx, H xx, N xx %; Calculated for $C_{31}H_{68}N_{10}O_{29}Ce_2$: C xx, H xx, N xx %.

*Preparation of [Nd(DOODA)(NO$_3$)$_3$] (**2**)*: This and other complexes were synthesized in a similar matter to the method mentioned above. The synthesis conditions are as follows: $Nd(NO_3)_3 \cdot 6H_2O$ 0.219 g (0.50 mmol), DOODAC2 0.433 g (1.50 mmol). Yield: 44.8%, Elemental analysis, Found: C xx, H xx, N xx %; Calculated for $C_{14}H_{30}N_5O_{14}Nd$: C xx, H xx, N xx %.

*Preparation of [Sm(DOODA)(NO$_3$)$_3$] (**3**)*: This and other complexes were synthesized in a similar matter to the method mentioned above. The synthesis conditions are as follows: $Sm(NO_3)_3 \cdot 6H_2O$ 0.109 g (0.25 mmol), DOODAC2 0.144 g (0.50 mmol). Yield: 44.8%, Elemental analysis, Found: C 26.18, H 4.51, N 10.98 %; Calculated for $C_{14}H_{30}N_5O_{14}Sm$: C 26.16, H 4.70, N 10.90 %.

*Preparation of [Eu(DOODA)(NO$_3$)$_3$] (**4**)*: This and other complexes were synthesized in a similar matter to the method mentioned above. The synthesis conditions are as follows: $Eu(NO_3)_3 \cdot 6H_2O$ 0.22 g (0.50 mmol), DOODAC2 0.288 g (1.00 mmol). Yield: 63.5%, Elemental analysis, Found: C 26.10, H 4.69, N 10.87 %; Calculated for $C_{14}H_{30}N_5O_{14}Eu$: C 26.16, H 4.70, N 10.90 %.

*Preparation of [Gd(DOODA)(NO$_3$)$_3$] (**5**)*: This and other complexes were synthesized in a similar matter to the method mentioned above. The synthesis conditions are as follows: $Gd(NO_3)_3 \cdot 6H_2O$ 0.23 g (0.50 mmol), DOODAC2 0.433 g (1.50 mmol). Yield: 45.6%, Elemental analysis, Found: C 25.61, H 4.35, N 10.72 %; Calculated for $C_{14}H_{30}N_5O_{14}Gd$: C 25.58 H 4.65, N 10.65 %.

*Preparation of [Tb(DOODA)(NO$_3$)$_3$] (**6**)*: This and other complexes were synthesized in a similar matter to the method mentioned above. The synthesis conditions are as follows: $Tb(NO_3)_3 \cdot 6H_2O$ 0.23 g (0.50 mmol), DOODAC2 0.433 g (1.50 mmol). Yield: 45.6%, Elemental analysis, Found: C 26.55, H 4.46, N 10.83 %; Calculated for $C_{14}H_{30}N_5O_{14}Tb$: C 25.81 H 4.41, N 10.83 %.

*Preparation of [Dy(DOODA)(NO$_3$)$_3$] (**7**)*: This and other complexes were synthesized in a similar matter to the method mentioned above. The synthesis conditions are as follows: Tb(NO$_3$)$_3$·6H$_2$O 0.23 g (0.50 mmol), DOODAC2 0.433 g (1.50 mmol). Yield: 45.6%, Elemental analysis, Found: C 26.55, H 4.46, N 10.83 %; Calculated for $C_{14}H_{30}N_5O_{14}Tb$: C 25.81 H 4.41, N 10.83 %.

*Preparation of [Ho(DOODA)(NO$_3$)$_3$] (**8**)*: This and other complexes were synthesized in a similar matter to the method mentioned above. The synthesis conditions are as follows: Ho(NO$_3$)$_3$·6H$_2$O 0.23 g (0.50 mmol), DOODAC2 0.433 g (1.50 mmol). Yield: 45.6%, Elemental analysis, Found: C 26.55, H 4.46, N 10.83 %; Calculated for $C_{14}H_{30}N_5O_{14}Tb$: C 25.81 H 4.41, N 10.83 %.

*Preparation of [Er(DOODA)(NO$_3$)$_3$] (**9**)*: This and other complexes were synthesized in a similar matter to the method mentioned above. The synthesis conditions are as follows: Er(NO$_3$)$_3$·6H$_2$O 0.23 g (0.50 mmol), DOODAC2 0.433 g (1.50 mmol). Yield: 45.6%, Elemental analysis, Found: C 26.55, H 4.46, N 10.83 %; Calculated for $C_{14}H_{30}N_5O_{14}Tb$: C 25.81 H 4.41, N 10.83 %.

*Preparation of [Tm(DOODA)(NO$_3$)$_3$] (**10**)*: This and other complexes were synthesized in a similar matter to the method mentioned above. The synthesis conditions are as follows: Tm(NO$_3$)$_3$·6H$_2$O 0.23 g (0.50 mmol), DOODAC2 0.433 g (1.50 mmol). Yield: 45.6%, Elemental analysis, Found: C 25.84, H 4.23, N 10.81 %; Calculated for $C_{14}H_{28}N_5O_{13}Tm$: C 26.14 H 4.39, N 10.89 %.

*Preparation of [Yb(DOODA)(NO$_3$)$_3$] (**11**)*: This and other complexes were synthesized in a similar matter to the method mentioned above. The synthesis conditions are as follows: Yb(NO$_3$)$_3$·5H$_2$O 0.23 g (0.50 mmol), DOODAC2 0.433 g (1.50 mmol). Yield: 45.6%, Elemental analysis, Found: C 25.65, H 4.21, N 10.75 %; Calculated for $C_{14}H_{28}N_5O_{13}Tb$: C 25.97 H 4.36, N 10.82 %.

*Preparation of [Lu(DOODA)(NO$_3$)$_3$] (**12**)*: This and other complexes were synthesized in a similar matter to the method mentioned above. The synthesis conditions are as follows: Lu(NO$_3$)$_3$·4H$_2$O 0.23 g (0.50 mmol), DOODAC2 0.433 g (1.50 mmol). Yield: 45.6%, Elemental analysis, Found: C 26.55, H 4.46, N 10.83 %; Calculated for $C_{14}H_{30}N_5O_{14}Tb$: C 25.81 H 4.41, N 10.83 %.

4.2.3 Instruments and General Procedures

Crystal structures were determined using a Rigaku RAXIS RAPID and IR spectra were measured by the diffuse reflection method using a Shimadzu FT-IR-8400S spectrometer. Details of instruments and analytical method used in this experiments are as same as described in Chapter 2.

4.3 Results and Discussion

4.3.1 Crystal Structures

The structures of the complexes of Ln(III) (Ln=La–Lu, except for Pr and Pm) nitrate with DOODAC2 were determined. Their structures are classified into three groups. The first two light Ln(III) form [Ln(DOODAC2)$_2$(EtOH)$_2$][Ln(NO$_3$)$_6$] (Ln = La–Ce) complexes, the next ten light to middle Ln(III) form [Ln(DOODAC2)(NO$_3$)$_3$] (Ln = Nd–Yb) complexes, and final one Ln(III), i.e. Lu, forms [Lu(DOODAC2)(NO$_3$)$_2$](NO$_3$) complex. Several attempts were made to crystalize the Pr complex with DOODAC2. However, no attempts were succeeded and oily products were obtained.

The First Group

The first two light Ln(III) (Ln= La and Ce) complexes exist in the P-1 (#2) space group and are constructed by the packing of $[Ln(DOODA)_3(EtOH)_2]^{3+}$ cations and $[Ln(NO_3)_6]^{3-}$ anions. The

representative example of the first group complex $[La(DOODAC2)_2(EtOH)_2][La(NO_3)_6]$ is shown in Figure 4-2. The structure of $[Ce(DOODAC2)_2(EtOH)_2][Ce(NO_3)_6]$ complex is shown in Appendix B.

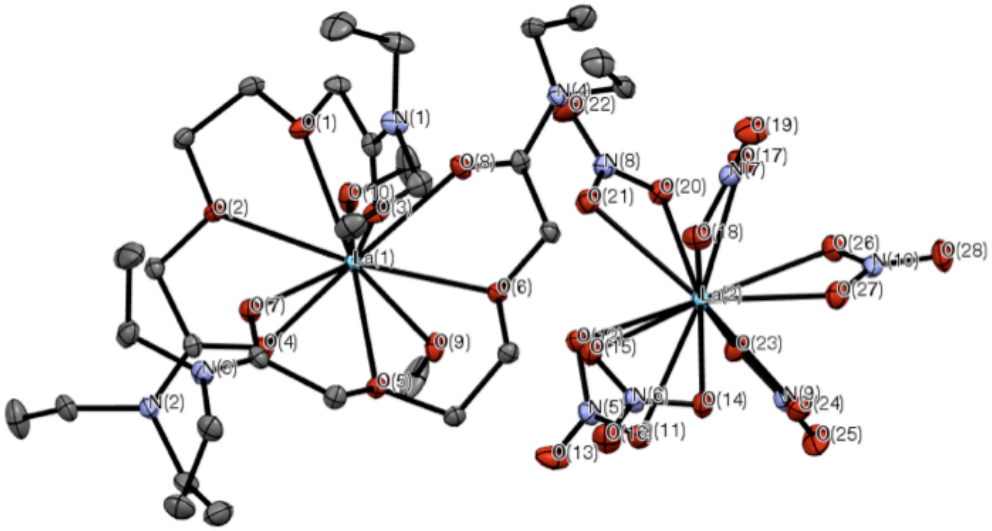

Figure 4-2 ORTEP representation of the $[La(DOODA)_3][La(NO_3)_6]$. Ellipsoids are displayed at 30% probability. Hydrogen atoms are omitted for clarity.

The $[Ln(DOODAC2)_2(EtOH)_2]^{3+}$ cations exhibit ten-coordination, where the Ln(III) ions are coordinated by the ten oxygen atoms from the two chelating tridentate DOODAC2 molecules and two ethanol molecules. As described in the Chapter 1.3.1, common polyhedra for the ten-coordination geometry are bicapped square antiprism (D_{4d}), the bicapped dodecahedron (D_2) and the polyhedron based on a dodecahedron (C_{2v}). The angular parameters for these cations are listed in Table 4-1. The average values of the angular parameters are close to that of bicapped dodecahedron (D_2). Long bond length from the ether oxygen of DOODAC2 (O2, O6) placing at the position C makes it difficult to maintain the polyhedron to be bicapped square antiprism (D_{4d}). The resulting coordination polyhedron of $[Ln(DOODAC2)_2(EtOH)_2]^{3+}$ (Ln = La and Ce) cation thus can be described as a distorted bicapped dodecahedron (D_2). Bicapped dodecahedral view of $[Ln(DOODAC2)_2(EtOH)_2]^{3+}$ is shown in Figure 4-3.

Table 4-1 The angular parameters for the La(III) and Ce(III) complexes

	bicapped square antiprism (D_{4d})	bicapped dodecahedron (D_2)		
Complex	θ	θ_A	θ_B	θ_C
Idealized	64.8	32.8	77.0	60.0
La	62.8	36.2	76.5	
Ce	62.8	36.0	76.8	

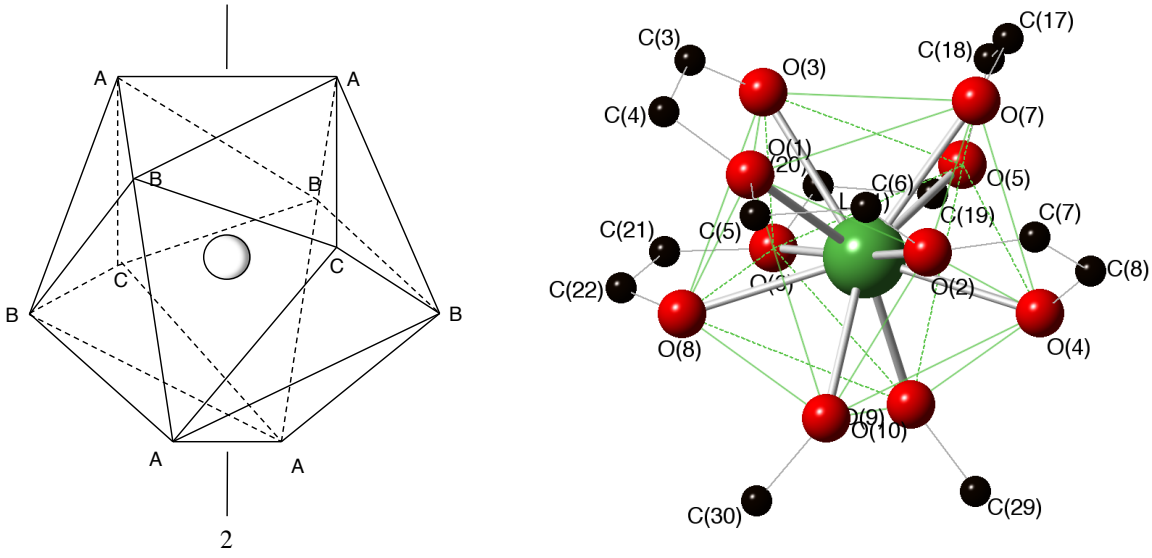

(a) (b)

Figure 4-3 (a) Bicapped dodecahedon(D_2) and (b) $[Ln(DOODAC2)_2(EtOH)_2]^{3+}$ion in Ln(III)-DOODAC2 complex.

The $[Ln(NO_3)_6]^{3-}$ anions exhibit twelve-coordination, where the Ln(III) ions are coordinated by twelve oxygen atoms from the six chelating nitrate. Such as structure is quite similar to the analogs anionic complexes, $[Nd(NO_3)_6]^{3-}$, reported by Bünzli *et al*. Figure 4-4 shows the $[Nd(NO_3)_6]^{3-}$ anion reported by Bünzli *et al*. and the $[La(NO_3)_6]^{3-}$ anion in this study. From a comparison with these structures, it is apparent that the $[La(NO_3)_6]^{3-}$ anion in this study have low symmetry than the $[Nd(NO_3)_6]^{3-}$ anion reported by Bünzli *et al*. As discussed in Chapter 1.3.1, there are three structural isomers in the icosahedoral geometry and the geometry has three types of isomer, I II and III. The reported $[Nd(NO_3)_6]^{3-}$ anion is isomer-I that has the symmetry I_h, and this type of isomer can find elsewhere. [6,7,8,9,10] On the other hand, $[Ln(NO_3)_6]^{3-}$ anion of the first group complexes were found to be the isomer III with D_{3d} symmetry, and not likely to that of $[Ln(NO_3)_6]^{3-}$ anions in Ln(III)-TEDGA complexes which are all isomer II.[11] In Figure 4-5, the geometrical position of isomer II for $[M(bidentate)_6]$ [12] and the geometrical view of $[La(NO_3)_6]^{3-}$ ion in La(III)-DOODAC2 complex are shown for comparison.

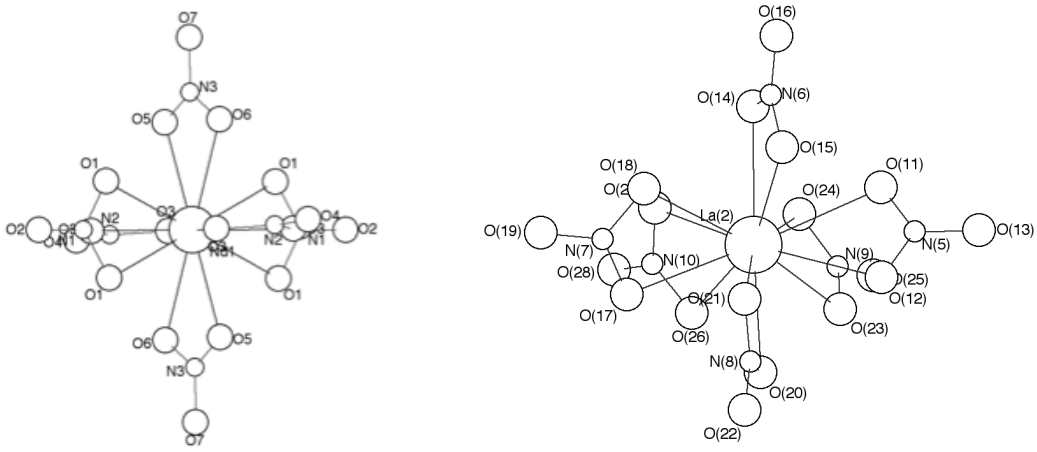

(a) (b)

Figure 4-4 (a) $[Ln(NO_3)_6]^{3-}$ ion reported by Bünzli *et al*. [6] and (b) $[Ln(NO_3)_6]^{3-}$ ion in La(III)-TEDGA complex (right).

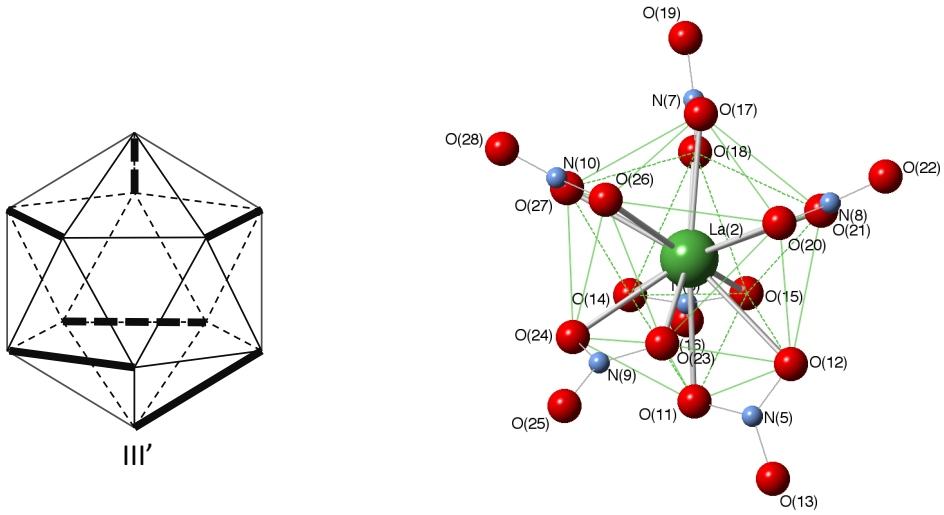

(a) (b)

Figure 4-5 Icosahedron isomer II of [M(bidentate)$_6$] defined in the literature (left) [12] and the same geometrical view of [La(NO$_3$)$_6$]$^{3-}$ ion in La(III)-TEDGA complex as isomer II(right).

The Second Group

The second ten Ln(III) (Ln = Nd–Yb) complexes exist in the P21/c or P21/a (#14) space group. Their crystal structures are constructed by Ln(III) with ten-coordination wrapped around by one DOODAC2 and three nitrate ions with chemical formula [Ln(DOODAC2)(NO$_3$)$_3$]. A representative example of this type of complex [Eu(DOODAC2)(NO$_3$)$_3$] is shown in Figure 4-6. All other [Ln(DOODAC2)(NO$_3$)$_3$] complexes are shown in Appendix B.

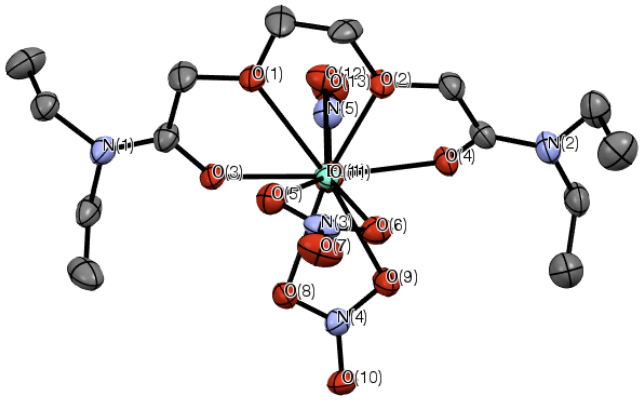

Figure 4-6 ORTEP representation of [Eu(DOODAC2)(NO$_3$)$_3$]. Ellipsoids are displayed at 30% probability. Hydrogen atoms and solvent molecule are omitted for clarity.

The angular parameters of these complexes are listed in Table 4-2. The average values of the angular parameters are close to that of bicapped square antiprism (D_{4d}). Therefore, the coordination polyhedra of all [Ln(DOODAC2)(NO$_3$)$_3$] complexes in the second group thus can be described as a distorted bicapped square antiprism (D_{4d}). Bicapped square antiprism (D_{4d}) views of [Ln(DOODAC2)(NO$_3$)$_3$] (Ln= Eu and Yb) are shown in Figure 4-7.

Assuming that each O-CH$_2$-CH$_2$-C=O fragment of DOODAC2 is considered to be pseudo-bidentate ligand, five bidentate ligands wrap around Ln(III) ions. Five bidentate ligands can be arranged in two different ways called *cis* and *trans* isomers.[12] Two bidentate ligands with atoms at the capping position have their other ends on two adjacent vertices of the square antiprism. Thus, all complexes

belonging to the second group are described as a distorted bicapped square antiprism with *cis* conformation. It is interesting to note that one of the capping atoms is always O_{ether} (O(1)) of DOODAC2 molecule which could be involved in the longest Ln-O distance in the complexes.

Table 4-2 The angular parameters for the Nd–Yb complexes

	bicapped square antiprism (D_{4d})	bicapped dodecahedron (D_2)	
Complex	θ	θ_A	θ_B
Idealized	64.8	32.8	77.0
Nd	65.5	24.9	75.9
Sm	65.0	25.3	76.9
Eu	64.9	25.5	76.8
Gd	64.9	25.7	76.5
Tb	65.0	25.3	76.4
Dy	65.4	25.7	75.1
Ho	64.8	26.0	76.2
Er	65.4	26.5	74.4
Tm	65.5	25.7	76.0
Yb	65.6	26.2	74.9

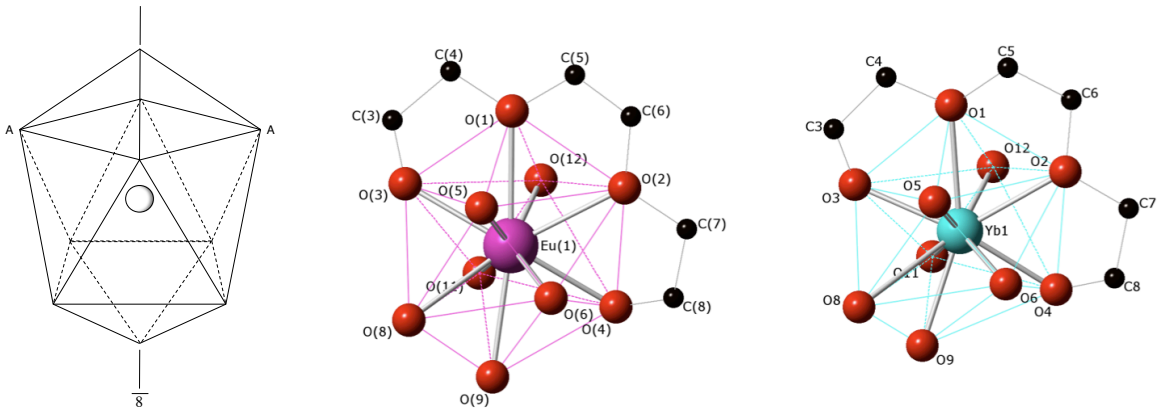

Figure 4-7 Coordination polyhedron of bicapped square antiprism (left) and [Ln(DOODA)$(NO_3)_3$] (Ln = Eu (middle) and Yb(right))

The Third Group

The final Ln(III) elements, Lu(III), exist in the P212121 (#19) with chemical formula [Lu(DOODA)$(NO_3)_2$](NO_3). This has a disordered one nitrate anion in the outer sphere.

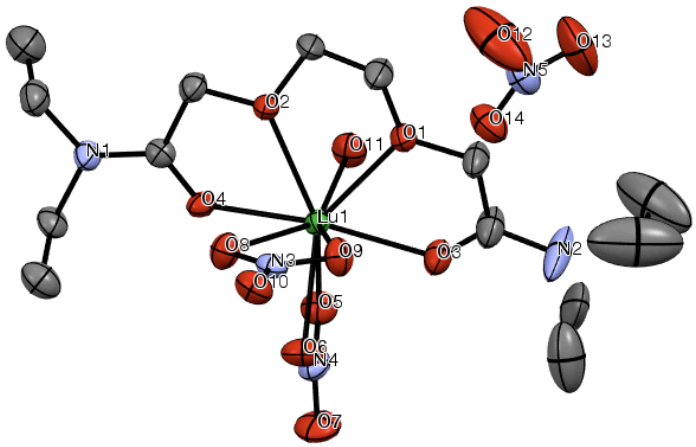

Figure 4-8 ORTEP representation of Type3; Lu-DOODA complex. Ellipsoids are displayed at 30% probability. Hydrogen atoms and solvent molecule are omitted for clarity.

In this complex, Lu(III) is nine-coordination. As outlined in 1.3.1, favorable arrangements of nine-coordination are the tricapped trigonal prism (D_{3h}) and the monocapped square antiprism (C_{4v}). The polyhedron of this complex was analyzed by using method of Guggenberger and Mutterties based on the dihedral angles along the edges of the coordination polyhedron.[13] The dihedral angles of $[Lu(DOODA)(NO_3)_2](NO_3)$ are summarized in Table 4-3. As seen from this table, the dihedral angles of this complex are close to that of monocapped square antiprism (C_{4v}). Therefore, the polyhedron of $[Lu(DOODA)(NO_3)_2]^{2+}$ cation can be described as distorted monocapped square antiprism (C_{4v}). Monocapped square antiprism view of coordination polyhedron of $[Lu(DOODA)(NO_3)_2]^{2+}$ cation is shown in Figure 4-9.

Table 4-3 Dihedral angles for $[Lu(DOODA)(NO_3)_2](NO_3)$ complexes

	tricapped trigonal prism (D_{3h})			monocapped square antiprism (C_{4v})		
Complex	Opposed(⊥)	Average of 3 at Opposed(‖)	Average of 3 at Vicinal(‖)	Opposed	Opposed	Vicinal(⊥)
Idealized	180.0	146.4	26.4	163.5	138.2	0.0
Lu	171.8	148.1	13.4	163.7	137.5	13.37

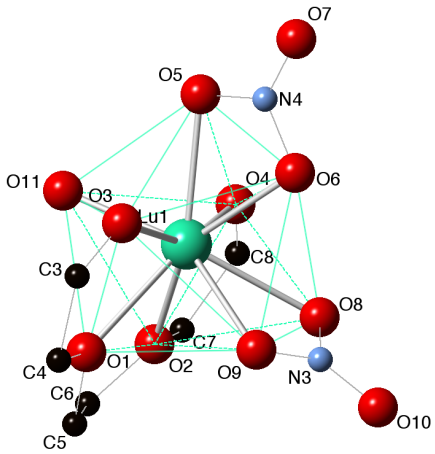

Figure 4-9 Monocapped square antiprism view of coordination polyhedron of $[Lu(DOODA)(NO_3)_2]^{2+}$ cation.

Table 4-4 Selected bond lengths and angles for light Ln(III) complexes

	La	Ce	Nd	Sm	Eu	Gd
$Ln\text{-}O_{ether}$ / Å	2.68	2.67	2.56	2.54	2.53	2.53
$Ln\text{-}O_{carbo}$ / Å	2.52	2.50	2.40	2.39	2.37	2.37
$Ln\text{-}O_{nitrate}$ / Å	2.67	2.66	2.55	2.53	2.51	2.50
O-C /Å	1.44	1.43	1.43	1.41	1.41	1.40
O=C /Å	1.25	1.25	1.25	1.25	1.25	1.25
C-C /Å	1.51	1.51	1.51	1.48	1.48	1.48
$O_{ether}\text{-}Ln\text{-}O_{carbo}$ / °	58.8	59.2	61.1	62.3	62.7	62.9
$O_{ether}\text{-}Ln\text{-}O_{ether}$ / °	59.7	59.9	62.6	61.6	61.8	62.0
C-O-C / °	113.1	112.5	112.8	116.3	116.2	116.1
O-C-C / °	107.5	107.4	107.8	113.5	114.3	114.2
O=C-C / °	120.1	120.0	118.7	118.7	119.2	118.4

Table 4-5 Selected bond lengths and angles for heavy Ln(III) complexes

	Tb	Dy	Ho	Er	Tm	Yb	Lu
Ln-O_{ether} / Å	2.52	2.50	2.51	2.52	2.47	2.46	2.39
Ln-O_{carbo} / Å	2.35	2.33	2.33	2.33	2.30	2.27	2.28
Ln-$O_{nitrate}$ / Å	2.49	2.49	2.47	2.44	2.47	2.48	2.40
O-C /Å	1.42	1.44	1.41	1.43	1.42	1.43	1.42
O=C /Å	1.26	1.25	1.24	1.25	1.26	1.25	1.26
C-C /Å	1.51	1.51	1.48	1.51	1.49	1.52	1.43
O_{ether}-Ln-O_{carbo} / °	62.6	65.3	63.6	61.4	65.4	66.4	67.4
O_{ether}-Ln-O_{ether} / °	62.3	63.3	62.0	61.8	63.3	63.7	65.0
C-O-C / °	115.3	112.7	115.8	113.9	114.4	113.7	114.9
O-C-C / °	113.0	107.4	113.3	106.3	109.8	107.2	110.4
O=C-C / °	118.6	118.8	118.9	117.9	118.7	118.2	119.8

The average values of selected bond lengths and angles of the complexes are listed in Table 4-4 and

Table 4-5. In comparison of each Ln-O bond lengths in Ln-DOODAC2 moiety, the bond lengths of carbonyl oxygen atom to Ln(III) (Ln-O_{carbo}) are significantly shorter than that of ether oxygen atom to Ln(III) (Ln-O_{ether}). The difference in bond length between Ln-O_{carbo} and Ln-O_{ether} indicates that the Ln-O_{carbo} bond is the stronger than Ln-O_{ether} bond as same as in TEDGA complexes.

The Ln-O bond lengths regularly decreases as the Ln(III) atomic number increases. The decrease in bond length is correlated with the change of ionic radii.[14,15,16] By subtracting of the ionic radius of corresponding coordination number, the residual values are independent from lanthanide contraction. Figure 4-10 shows plots of Ln-O bond lengths and the residual values of Ln-O bonds. The residual values were further examined by standard deviation values in statistically and confirmed that the Ln-O lengths are approximately constant in entirely Ln(III) series, except for the Ln-$O_{nitrate}$ in the first group complexes. This may reflect the strong affinity of Ln(III) to the nitrate ions.

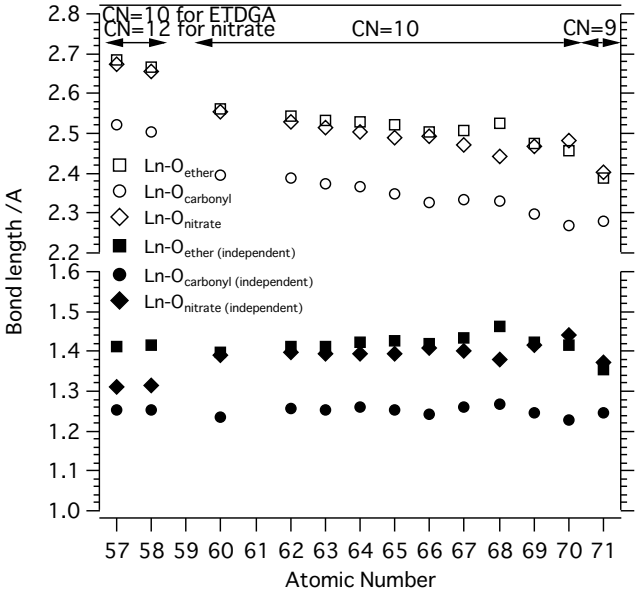

Figure 4-10 Plots of average bond distance and ionic radii independent distances against Ln(III) atomic number.

4.3.2 Infrared Spectra

Infrared spectra of all Ln(III)-DOODAC2 complexes and free TEDGA were measured. The resulting spectra are shown in Figure 4-11. Assignments for the IR bands for all groups of complexes are summarized in Table 4-6.

The sharp peak at 1645 cm^{-1} and the broad peak at 1110 cm^{-1} are assigned to $\nu_{C=O}$ and ν_{C-O-C} of TEDGA, respectively. IR spectra of the range 1800–1500 cm^{-1} and 1200-1000 cm^{-1} for free TEDGA, La(III), Nd(III), Yb(III) and Lu(III) complexes are shown in Figure 4-12 as representative examples. In all group of the complexes of Ln(III)-DOODA-C2, $\nu_{C=O}$ and ν_{C-O-C} shifted to 1614–1623 cm^{-1} and 1083–1090 cm^{-1}, respectively. Band shifts on $\nu_{C=O}$ and ν_{C-O-C} indicate that the of the carbonyl and ether oxygen atoms take part in coordination to the Ln(III) ion. The larger shifts of $\nu_{C=O}$ in the spectra of the complexes suggests that the Ln-$O_{calbonyl}$ bond is stronger than Ln-O_{ether}.

Table 4-6 Observed IR Bands of Ln(III)-DOODAC2 Complexes

	C=O	C-O-C	ν_4	ν_1	ν_2	ν_6	ν_3	$\Delta_{highest\text{-}frequency}$	Combination frequencies $\nu_1+\nu_4$		$\Delta_{conbination}$
DOODAC2	1645	1110									
La(1st group)	1615	1083	1303	1511	1036	819	735	208		1771	1740	31
Ce(1st group)	1619	1085	1281	1511	1041	819	735	230		1780	1745	35
Pr	1620	1084	1281	1511	1040	819	735	230		1778	1747	31
Nd(2nd group)	1612	1088	1283	1508	1032	819	735	225		1766	1730	36
Sm(2nd group)	1614	1090	1287	1503	1033	818	740	216		1770	1733	37
Eu(2nd group)	1616	1083	1283	1510	1036	825	742	227		1762	1732	30
Gd(2nd group)	1618	1087	1285	1509	1032	818	742	224		1764	1730	34
Tb(2nd group)	1619	1089	1288	1505	1029	818	744	217		1767	1730	37
Dy(2nd group)	1620	1088	1289	1508	1027	818	748	219		1766	1732	34
Ho(2nd group)	1621	1089	1291	1506	1029	818	748	215	(1780)	1765	1730	35
Er(2nd group)	1620	1089	1292	1506	1029	818	750	214	(1784)	1765	1730	35
Tm(2nd group)	1622	1089	1294	1506	1029	818	752	212	(1786)	1765	1730	35
Yb(2nd group)	1622	1090	1296	1508	1030	818	752	212	(1787)	1765	1732	33
Lu(3rd group)	1623	1090	1297	1509	1031	818	754	212	(1787)	1763	1732	31

The N-O stretching modes ν_1, ν_4, and ν_2, along with the bending modes ν_6 and ν_3 are observed at about ν = 1505–1511, 1288–1303, 1027–1041, 818–825, and 753–750 cm^{-1}, respectively. These IR bands suggest that the nitrate ions coordinate to the Ln(III) by bidentate manner as depicted in the crystal structures and they are not ionic.[17] The nitrate ions coordinate to the Ln(III) by bidentate fashion, because the differences of combination frequency band ($\nu_1+\nu_4$) around 1700–1800 cm^{-1} are 31–37 cm^{-1} across the Ln(III) series.[18,19] Although the crystal structure of Lu(III) complex has one nitrate ion in the outer-sphere, no other band were observed for ionic nitrate.

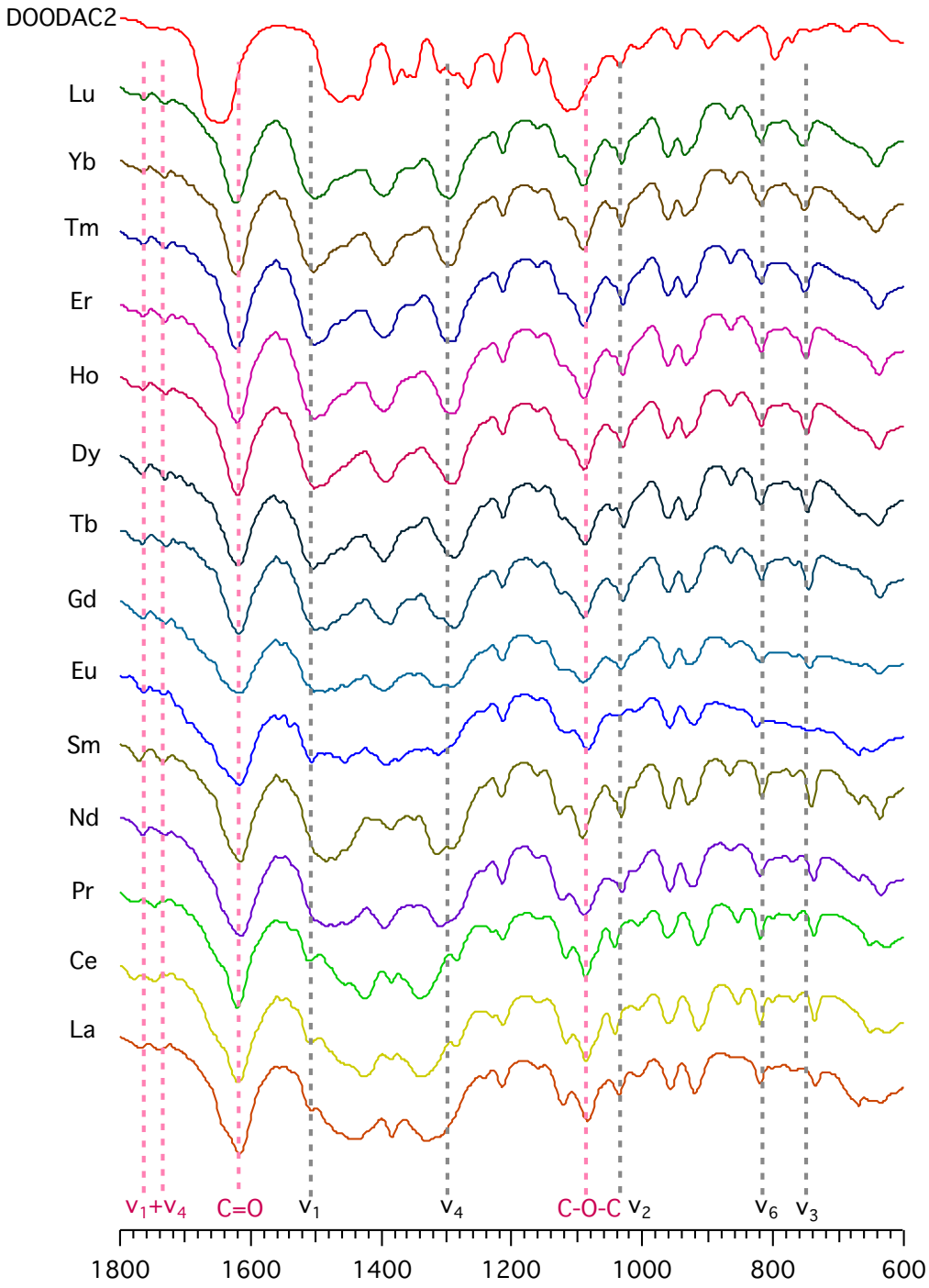

Figure 4-11 IR spectra of Ln-DOODAC2 complexes.

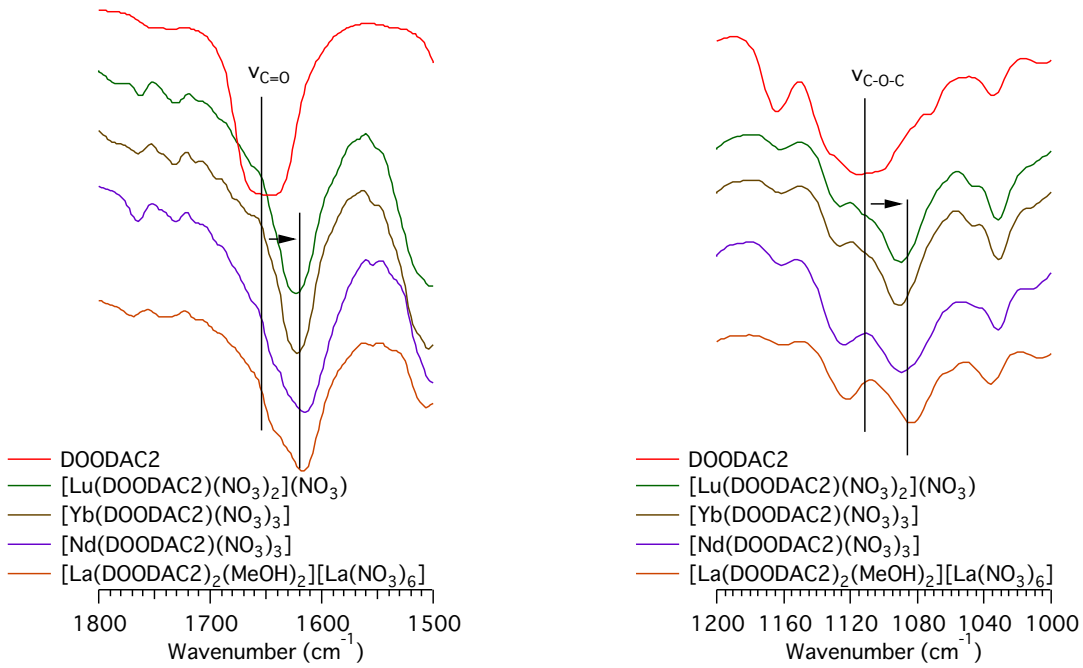

Figure 4-12 Representative examples of IR spectra of Ln-DOODA complexes.

4.4 Conclusion

The Ln(III) nitrate complexes with DOODAC2 were synthesized and characterized in crystallographically. The coordination modes of DOODA and nitrate ions were confirmed by infrared spectroscopy. Although the synthesis procedures are same through the Ln(III) series, differences were appeared among the structures of complexes. The structures of complexes are classified into three groups, the first group, $[Ln(DOODAC2)_2(EtOH)_2][Ln(NO_3)_6]$ (Ln = La and Ce); the second group, $[Ln(DOODAC2)(NO_3)_3]$ (Ln = Nd–Yb except for Pm); and the third group, $[Ln(DOODAC2)(NO_3)_3]$ (Ln = Lu). The coordination polyhedra of these complexes were determined.

As discussed in Chapter 2.3.1, the structural differences in these complexes can be attributed to the following factors: (i) lanthanide contraction, (ii) crystal-packing stability and (iii) bonding affinity of the nitrate ion. In case of this study, (i) and (iii) are the likely effects for the causes of the differences as well as TEDGA system.

References

1 Tachimori, S; Morita, Y. "Overview of Solvent Extraction Chemistry for Reprocessing." *Ion Exchange and Solvent Extraction: A Series of Advances*, **2009**, 19: 1.

2 Narita, H.; Yaita, T.; Tachimori, S. "Extraction of lanthanides with N, N dimethyl N, N diphenyl malonamide and 3, 6 dioxaoctanediamide." *Solvent Extraction and Ion Exchange,* **2004**, 22, 135–145.

3 Sasaki, Y.; Morita, Y.; Kitatsuji, Y.; Kimura, T. "Extraction of Actinides and Fission Products by the New Ligand, N, N, N', N'-Tetraoctyl-3, 6-dioxaoctanediamide." *Chemistry Letters*, **2009**, 38, 630-631.

4 Sasaki, Y.; Morita, Y.; Kitatsuji, Y.; Kimura, T. "Extraction Behavior of Actinides and Metal Ions by the Promising Extractant,*N,N,N′,N′*-Tetraoctyl-3,6-dioxaoctanediamide (DOODA)." *Solvent Extraction and Ion Exchange*, **2010**, *28*, 335-349.

5 Sasaki, Y.; Tsubata, Y.; Kitatsuji, Y.; Sugo, Y.; Shirasu, N.; Morita, Y.; Kimura, T. "Extraction Behavior of Metal Ions by TODGA, DOODA, MIDOA, and NTAamide Extractants from HNO3ton-Dodecane." *Solvent Extraction and Ion Exchange,* **2013**, 31, 401-415.

6 Bünzli, J. C. G., Klein, B., Wessner, D., J Schenk, K., Chapuis, G., Bombieri, G., & De Paoli, G. "Crystal and molecular structure of the 4: 3 complex of 18-crown-6 ether with neodymium nitrate." *Inorganica Chimica Acta,* **1981**, 54, L43-L46.

7 Hart, F.; Hursthouse, M.; Malik, K.; Moorhouse, S. "X-Ray crystal structure of a cryptate complex of lanthanum nitrate." *Journal of the Chemical Society, Chemical Communications*, **1978**, 549-550**.**

8 Matonic, J. H., Neu, M. P., Enriquez, A. E., Paine, R. T., & Scott, B. L. "Synthesis and crystal structure of a ten-coordinate plutonium (IV) ion complexed by 2-[(diphenylphosphino) methyl] pyridine N,P-dioxide:$[Pu(NO_3)_3\{2\text{-}[(C_6H5)2P(O)CH_2]C_5H_4NO\}_2][Pu(NO_3)_6]_{0.5}$." *Journal of the Chemical Society, Dalton Transactions, **2002**,*(11), 2328-2332.

9 Kannan, S.; Moody, M. A.; Barnes, C. L.; Duval, P. B. "Lanthanum(III) and uranyl(VI) Diglycolamide Complexes: Synthetic Precursors and Structural Studies Involving Nitrate Complexation ." *Inorganic Chemistry,* **2008**,*47*, 4691–4695.

10 Matloka, K., Gelis, A., Regalbuto, M., Vandegrift, G., & Scott, M. J. (2005). "Highly efficient binding of trivalent f-elements from acidic media with a C3-symmetric tripodal ligand containing diglycolamide arms." *Dalton Transactions*, (23), 3719-3721.

11 Kawasaki, T.; Okumura, S.; Sasaki, Y.; Ikeda, Y. "Crystal Structures of Ln(III) (Ln = La, Pr, Nd, Sm, Eu, and Gd) Complexes with *N,N,N',N'*-Tetraethyldiglycolamide Associated with Homoleptic $[Ln(NO_3)_6]^{3-}$." *Bulletin of the Chemical Society of Japan,* **2014**, *87*, 294-300.

12 Favas, MC; Kepert, DL "Aspects of the Stereochemistry of Nine-Coordination, Ten-Coordination, and Twelve-Coordination." *Progress in Inorganic Chemistry,* **1981**, *28*, 239–308.

13 L. J. Guggenberger and E. L. Muetterties, "Reaction path analysis. 2. The nine-atom family." *Journal of the American Chemical Society*, **1976**, 98.

14 Yaita, T.; Narita, H.; Suzuki, S.; Tachimori, S.; Motohashi, H.; Shiwaku, H. "Structural study of lanthanides (III) in aqueous nitrate and chloride solutions by EXAFS." *Journal of Radioanalytical and Nuclear Chemistry,* **1999**, 239, 371–375.

15 Bowden, A.; Horton, P.; Platt, A. "Lanthanide nitrate complexes of tri-isobutylphosphine oxide: solid state and CD2Cl2 solution structures." *Inorganic Chemistry,* **2011**, 50, 2553–2561.

16 Bowden, A.; Coles, S.; Pitak, M.; Platt, A. "Complexes of lanthanide nitrates with tri tert butylphosphine oxide." *Inorganic Chemistry* **2012,** 51, 4379−4389.

17 Bullock, J. "Infrared Spectra of Some Uranyl Nitrate Complexes" *Journal of Inorganic and*

Nuclear Chemistry, **1967**, 29, 2257.

18 Nakamoto, K. "Infrared and Raman Spectra of Inorganic and Coordination Compounds: Part A: Theory and Applications in Inorganic Chemistry, Sixth Edition", *John Wiley & Sons, Inc.*: New York, **2004**.

19 Curtis, N. F.; Curtis, Y. M. "Some Nitrato-Amine Nickel(II) Compounds with Monodentate and Bidentate Nitrate Ions." *Inorganic Chemistry* **1965**, 4.

Chapter 5

Complexation and Structural Studies of Lanthanide(III) Nitrate Complexes with DOODA in Acetonitrile Solutions

5.1 Introduction

In Chapter 2 and 3, the crystal structures and complexation of Ln(III) nitrate with TEDGA in acetonitrile solution were examined and the difference between light and heavy Ln(III) were discussed. The structures of complexes in both solid state and solution, and stability constants showed good relation to the reported variations of distribution ratios (*D*) (i.e. selectivity) in solvent extraction.[1,2,3,4]

As outlined in the introduction of Chapter 4, tetradentate DOODA derivatives have also been examined as a efficient extractant for Ln(III) and An(III). DOODA derivatives have a selectivity for mostly light Ln(III) whereas the TEDGA have a selectivity for heavy Ln(III).[5,6,7] The difference between DGA and DOODA derivatives is the number of oxygen atoms participating in the bond to Ln(III) and An(III). In Chapter 4, it was revealed that the crystal structures of Ln(III) nitrate complexes displayed three types of complexes with coordination number 12, 10, and 9. The Ln(III) nitrate with DOODAC2 system in solution is also of interest because the differences in coordination structures of Ln(III) with DOODAC2 must be found.

The objective of this chapter is the systematic investigation of the structural or complexation differences among the all Ln(III) nitrate complexes with DOODA in the solution. In this chapter, the same approaches were utilized as explained in Chapter 3. The complexation behaviors and structures of complexes in each complexation steps were investigated by UV-vis and NMR spectra in the acetonitrile solutions.

5.2 Experimental

5.2.1 Instruments and General Procedures

Spectrophotometric Titrations

Spectrophotometric titrations of DOODAC2 complex were conducted on SHIMADZU UV-3150 spectrophotometer equipped with sample holders of temperature controller at 298 K. Other details were same as those described in Chapter 3.2.2.

Nuclear Magnetic Resonance Study

The ^{1}H NMR spectra were recorded on JEOL ECX-400P. Various molar ratios of acetonitrile sample solution dissolving DOODAC2 and hydrated Ln(III) (Ln= La–Lu, except for Pm and Gd) nitrate were prepared. The compositions of sample solutions are given in Table 5-1. ^{1}H longitudinal relaxation times (T_1) were determined by using the inversion recovery method with a 180°–t–90°pulse sequence. The diamagnetic contributions of T_1 values were corrected by using the T_1 value for the La(III). All inversion recovery measurements were performed after the sample was degassed by Ar gas. Other details were same as those described in Chapter 3.2.2.

Table 5-1 Acetonitrile-d_3 solutions used in the NMR experiments

Sample solutions	[Ln] /mM (Ln= La-Nd, Eu-Lu)	[DOODAC2] /mM	[Ln]:[DOODAC2]
A	0	10	0:1
B	10	10	1:1
C	10	20	1:2
D	10	30	1:3
E	10	40	1:4
F	$[La(DOODAC2)_2(MeOH)_2][La(NO_3)_6]$		
G	$[Lu(DOODAC2)(NO_3)_2](NO_3)$		

5.3 Results and Discussion

5.3.1 Spectrophotometric Titration

Nd(III) System

To evaluate the complex formation of Nd(III) nitrate with DOODAC2 and to analyze the coordination structure around Nd(III), spectrophotometric titration of Nd(III) nitrate with DOODAC2 was performed. The resulting absorption spectra with the titration range [Nd]:[DOODAC2] = 1:0–1:5 are shown in Figure 5-1 (a). As seen from the spectra, the absorption band of Nd(III) at 581 nm shifts to 583.8 nm and its intensity increased with addition of DOODAC2 until the metal to ligand ratio reached [Nd]:[DOODAC2]=1:1. The absorption intensity at 583.8 nm then drastically decreased with the addition of DOODA. Two linear regression lines cross at [Nd]:[DOODA]=1:1, and 1:2, indicating the formation of 1:1 and 1:2 Nd-DOODA complexes. The stability constants in this system were calculated and the best fit was obtained when 1:1 and 1:2 complexes were refined. The overall stability constant $\log\beta_{ij}$ where j=1 and 2 were calculated as 8.4 ± 1.0 and 12.3 ± 1.0, respectively. Relatively large standard deviations were due to the small change in the spectra intensity. The following reactions can be proposed to the complexations for this system:

$$Ln(III) + DOODAC2 \rightleftharpoons [Ln(DOODAC2)] \quad \text{(Eq. 20)}$$

$$Ln(III) + 2\cdot DOODAC2 \rightleftharpoons [Ln(DOODAC2)_2] \quad \text{(Eq. 21)}$$

The spectra of the titration range [Nd]:[DOODAC2] = 1:0–1:1 are shown for clarity in Figure 5-1(b). As seen from this figure, the absorption band at [Nd]:[DOODAC2]=1:1 showed characteristic shape possessing flat area within the wavelength range 570–580 nm and intense sharp band around 583.8 nm. This characteristic shape is similar to that of reported ten-coordinated Nd(III) spectrum of $Nd(NO_3)_5^{2-}$ species. The complex formed on this condition possess ten-coordination as similar coordination environment around Nd(III) ion, that is, the complex with formula $[Nd(DOODAC2)(NO_3)_3]$ (CN=10). In Chapter 4, the crystal structures of Ln(III) nitrate complexes with DOODAC2 have been reported. Nd(III) involved in the second group complexes with chemical formula $[Nd(DOODAC2)(NO_3)_3]$. Therefore, it appears that the 1:1 complex in acetonitrile solution can be assumed to be same structure as in its crystal structure.

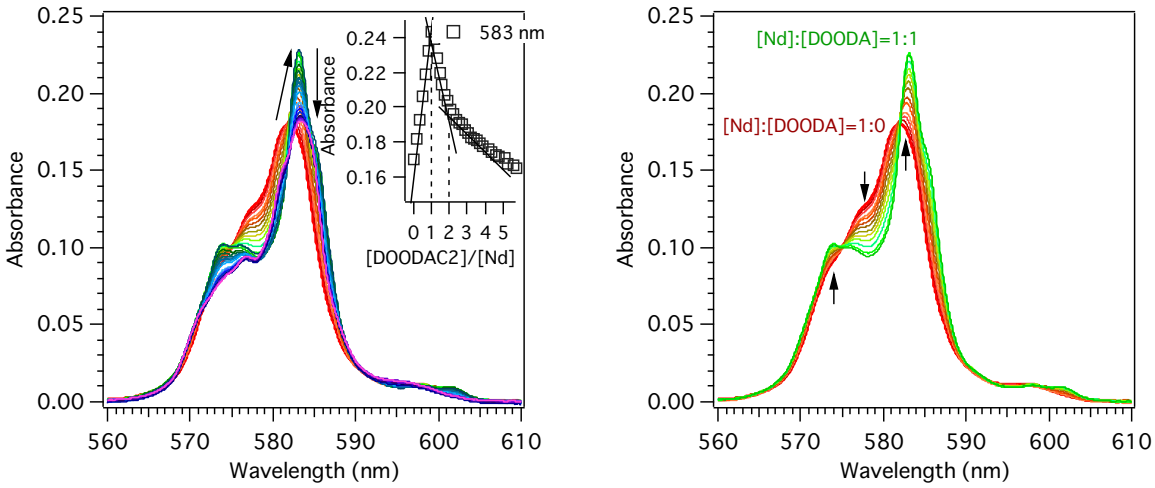

Figure 5-1 Spectrohotometric titration of 10 mM Nd(III) with DOODAC2 in acetonitrile at 298 K, (a) [Nd]:[DOODAC2] = 1:0–1:5 and (b) [Nd]:[DOODAC2] = 1:0–1:1.

The drastic decrease in intensity like observed in TEDGA system did not observed in this system. The small decrease in the absorption intensity by further adding DOODAC2 also indicate that the changes in symmetry around Nd(III) ion is small. The small change in absorption bands reflects that the coordination environment around Nd(III) is similar to that of hydrated Nd(III) nitrate.

Ho(III) System

Spectrophotometric titration of Ho(III) with DOODAC2 was also performed. The obtained spectra are shown in Figure 5-2. From these spectra, stability constants were calculated. The best fit was obtained when 1:1 and 1:2 complexes were refined. The overall stability constant $\log\beta_{ij}$ where j=1 and 2 were calculated as 6.2 ± 0.2, 8.6 ± 0.2, respectively. In Ho(III) system, spectral difference between the formed species are quite small. The small differences in the absorption band indicate that the environment around Ho(III) ions are similar to that of Ho(III) nitrate.

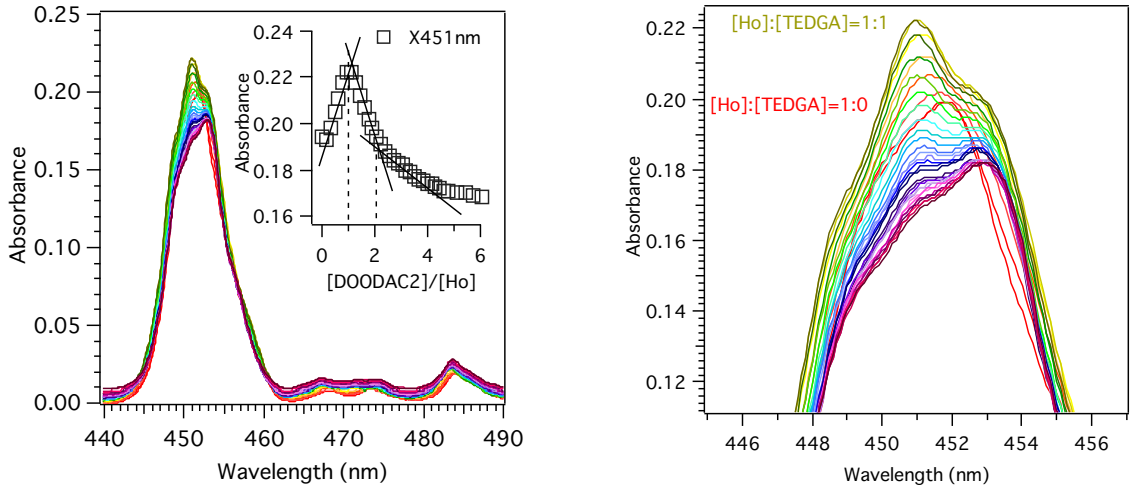

Figure 5-2 Spectrophotometric titration of (a) 10 mM Ho(III) with DOODAC2 in acetonitrile at 298 K and (b) expansion of the wavelength range 445–456 nm.

Figure 5-3 shows the plots of the stability constants for complexes of Ln(III) nitrate with TEDGA system obtained in this study. As seen from this figure, Nd(III) has large stability constants compared to Ho(III). As mentioned above, DOODA are known to have high selectivity to light Ln(III) compared

to that of DGA. Hence, higher stability constants for light Ln(III) are consistent with the affinity in extraction experiments.[5]

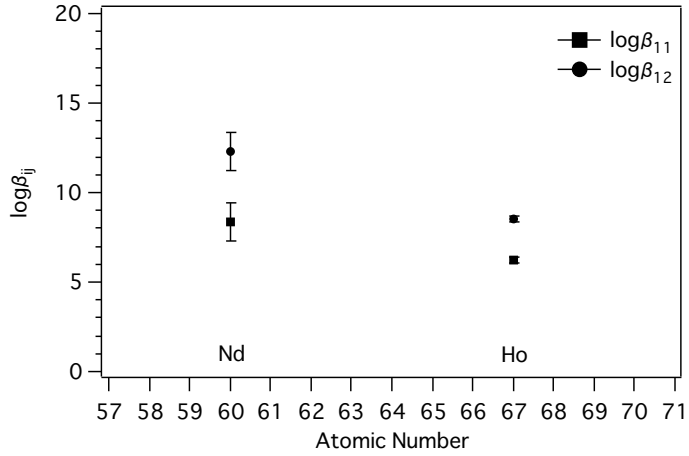

Figure 5-3 Stability constants with error bars determined for Ln(III)-DOODAC2 from spectrophotometric titration experiments in acetonitrile solutions at 298 K.

5.3.2 NMR Structural Analysis

To investigate the structures of Ln(III) nitrate complexes with DOODA (Ln = La and Lu), ^{1}H NMR spectra of the acetonitrile-d_3 solutions dissolving free DOODA (sample solutions **A**), crystals of Ln(III) complexes, i.e. $[La(DOODAC2)_2(MeOH)_2][La(NO_3)_6]$ (sample solutions **G**), and $[Lu(DOODAC2)(NO_3)_2](NO_3)$ (sample solution **F**), were measured. The resulting spectra are shown in Figure 5-4.

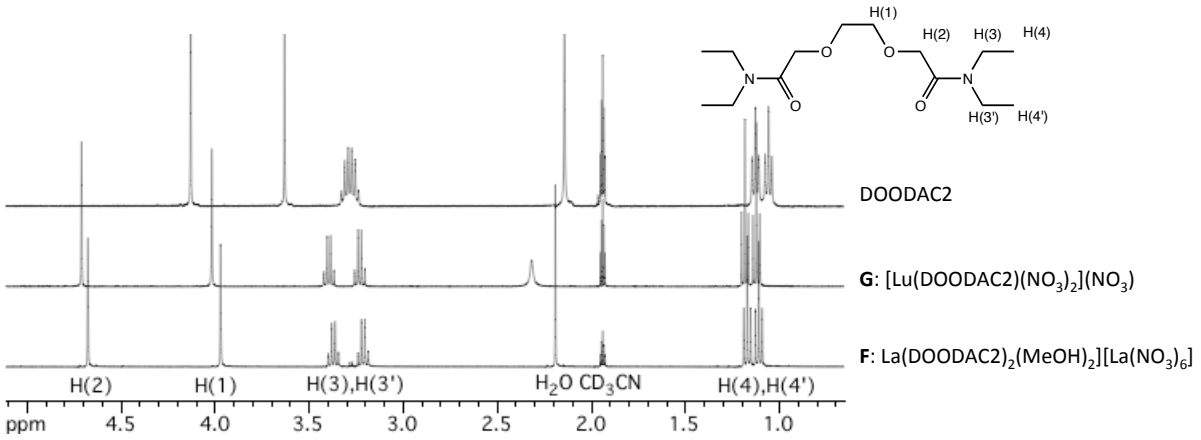

Figure 5-4 ^{1}H-NMR spectra of the acetonitrile-d_3 solutions, **A** (free TEDGA on the top), **G** ($[Lu(DOODAC2)(NO_3)_2](NO_3)$ on the middle) and **F** ($[La(DOODAC2)_2(MeOH)_2][La(NO_3)_6]$ on the bottom) at 298 K.

^{1}H NMR spectrum of free DOODAC2 (sample solution **A**, on the top of Figure 5-4) showed six resonances and similar features as observed on sample solution **A** of TEDGA system. The peaks observed double triplet at 1.2, double quartet at 3.3, singlet at 3.7 and singlet at 4.1 ppm were assigned to H(4), H(3) and H(1), and H(2), respectively. The spectrum indicates that the existence of axial symmetry (C_{2v}) and rotation about N-CH_2CH_3 in the DOODAC2 molecule.

The spectra of sample solutions **G** and **F** also showed similar features. As observed at TEDGA system (see Chapter 3.3.2 for details.), the free rotation around N-CH_2CH_3 was restricted upon coordination. On the spectra of sample solutions **F**, methylene signal of H(2) and H(1) shifted to

downfield compared to sample solution **A**. This indicates that the DOODA coordinates to La(III) symmetrically by both ether and carbonyl oxygen atoms.

Lanthanide Induced Shift (LIS) Analysis of 1:1 Complexes

It was assumed that the 1:1 complexes of Ln(III) nitrate with DOODAC2 are stable throughout the Ln(III) series. Observed chemical shifts of sample solution **B** (Ln = La–Lu, except for Gd) are listed in Table 5-2 and all ^{1}H NMR spectra are shown in Appendix C.

Table 5-2 ^{1}H-NMR chemical shifts (with respect to solvent residual peak) of sample solution **B** in CD_3CN at 298 K

	H(1)	H(2)	H(3)	H(3')	H(4)	H(4')
DOODAC2	3.98	4.66	3.38	3.22	1.18	1.12
$[La(DOODAC2)]^{3+}$	–4.86	6.43	8.69	5.85	4.50	2.99
$[Ce(DOODAC2)]^{3+}$	–13.01	9.95	15.62	9.48	8.75	5.46
$[Pr(DOODAC2)]^{3+}$	–1.88	9.06	9.76	6.62	4.98	3.45
$[Nd(DOODAC2)]^{3+}$	2.09	4.84	4.30	3.76	1.69	1.51
$[Sm(DOODAC2)]^{3+}$	11.72	0.00	0.05	–2.04	–0.96	–2.34
$[Eu(DOODAC2)]^{3+}$	3.98	4.66	3.38	3.22	1.18	1.12
$[Tb(DOODAC2)]^{3+}$	–187.41	21.33	103.72	54.82	61.48	37.03
$[Dy(DOODAC2)]^{3+}$	–217.62	46.57	–138.66	75.65	81.59	50.72
$[Ho(DOODAC2)]^{3+}$	–89.72	33.71	73.46	41.65	42.01	26.88
$[Er(DOODAC2)]^{3+}$	108.95	13.14	–10.09	–22.16	–9.55	–16.03
$[Tm(DOODAC2)]^{3+}$	150.00	–4.23	–51.79	–28.28	–33.48	–21.76
$[Yb(DOODAC2)]^{3+}$	72.75	–2.40	–24.97	–13.43	–16.54	–10.82
$[Lu(DOODAC2)]^{3+}$	4.02	4.72	3.3955	3.231	1.183	1.121

The paramagnetic Ln(III) complexes allow the separation of contact (δ^c) and pseudo-contact (δ^{pc}) contributions to the isotropic NMR paramagnetic shifts (δ^{iso}). Theory and method used in this section are described detail in Chapter 1.4.3. The diamagnetic correction (δ^{dia}) in (Eq. 11) is taken from the chemical shifts measured for the isostructural diamagnetic Ln(III) complexes. In this cases, La(III) was used for Ln = Ce–Dy, and Lu(III) was used for Ln = Tb–Yb. The series of isostuructural can be checked from plots of (Eq. 15) and (Eq. 16), which are expected to be linear for if these complexes are isostructural. Figure 5-5 and Figure 5-6 show the plots according to (Eq. 15) and (Eq. 16) for H(1) and H(2) as representative examples, respectively. These plots according to (Eq. 15) gave two straight lines. Two straight lines according to (Eq. 15) associate with two different isostructural groups involving light/middle Ln(III) (Ln = Ce–Ho) and heavy Ln(III) (Ln = Er–Yb). This means that there is a structural break between Ho and Er in acetonitrile solutions, and light/middle and heavy Ln(III) are not isostructural, but the difference between two isostrucural series would be small because the slope of (Eq. 15) directory relates to the structural information.

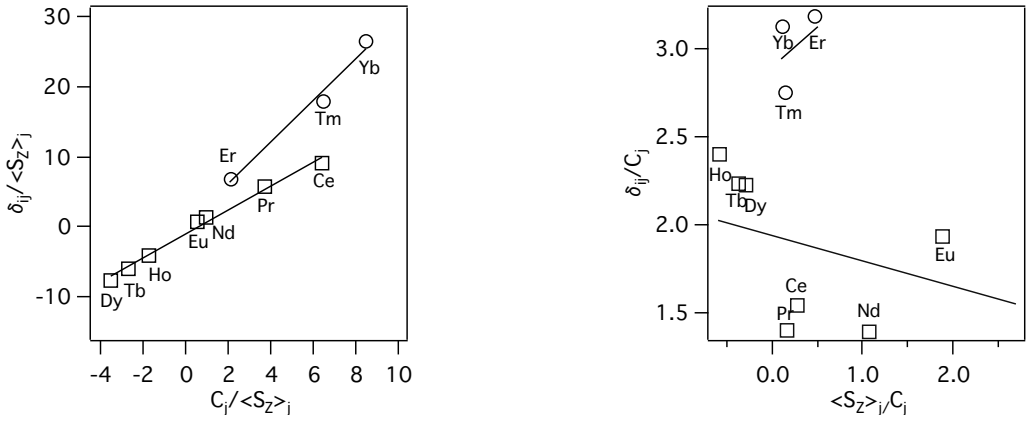

(a) (b)

Figure 5-5 Plots for H(1) in $[Ln(DOODAC2)]^{3+}$ (a) $\delta^{iso}_{ij}/<Sz>_j$ v $C_j/<Sz>_j$ and (b) δ^{iso}_{ij}/C_j v $<Sz>_j/C_j$.

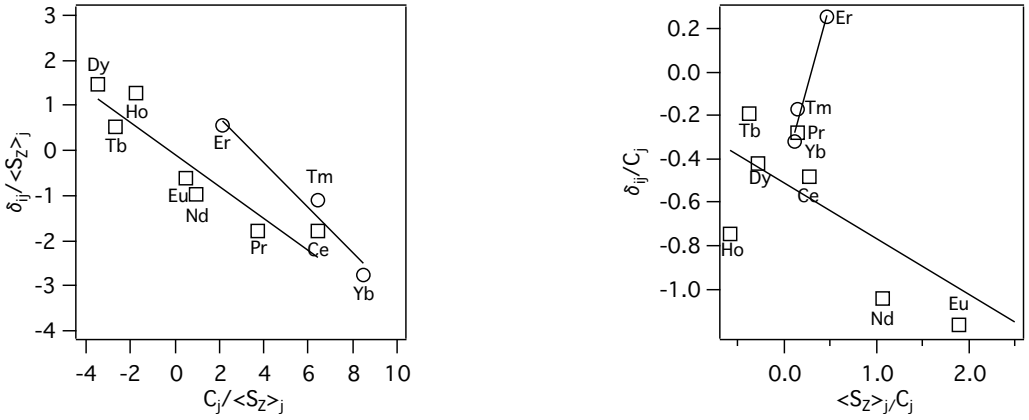

(a) (b)

Figure 5-6 Plots for H(2) in $[Ln(DOODAC2)]^{3+}$ (a) $\delta^{iso}_{ij}/<Sz>_j$ v $C_j/<Sz>_j$ and (b) δ^{iso}_{ij}/C_j v $<Sz>_j/C_j$.

As displayed in Chapter 4, complexes of Ln(III) nitrate with DOODAC2 took three types across the Ln(III) series. The last elements, Lu(III), hardly take ten-coordination as shown in Chapter 1.3.3, and the fact that the complex with DOODAC2 exhibit nine-coordination with one nitrate ion in the outer-sphere. Take into account these facts, the coordination mode change of nitrate ions such as bidentate to monodentate in 1:1 complexes of heavy Ln(III) (Ln = Er–Yb and Lu also).

Distance Estimation from T_1 and Solomon-Bloembergen Equation

The distance estimation from the relaxation time measurement was carried out for some paramagnetic Ln(III). When center of the complexes are paramagnetic Ln(III) ions, the ^{1}H NMR relaxation time can be related to its structure by the reduced Solomon-Bloembergen equation. (see Chapter 1.4.3 for details.) The equation (Eq. 17) means the paramagnetic relaxation enhancement is related to the reciprocal value of the distance between paramagnetic Ln(II) center and observed nucleus. Some of the paramagnetic Ln(III) exhibited too short relaxation time (ns order) and large error. In this system, Ce(III), Nd(III), Ho(III) and Yb(III) showed ms order of relaxation time.

The ^{1}H observed longitudinal relaxation time (T_1), the distances estimated from (Eq. 17), and the distances in the crystal structures are summarized in Table 5-3. Since the H nucleus cannot be assigned the certain position by X-ray diffraction, this discussion contains uncertainty. However, they show well agreement especially for light Ln(III). This results indicates that the DOODAC2 do not

dissociate from Ln(III), and observed 'break' of the LIS plots could be attributed to the changes in coordination mode of nitrate ion.

Table 5-3 Observed longitudinal relaxation times(T_1) of H(1) and H(2) in the some 1:1 complexes

	T_1		r (Å)$_{calc}$		Crystal Strucuture(Å)	
	H(1)	H(2)	H(1)	H(2)	H(1)	H(2)
La(dia)	0.812s	0.855s				
Ce	0.119s	0.120s	3.94	3.94	3.66–4.51	3.66–4.41
Nd	33.0ms	33.0ms	3.66	3.66	3.71–4.36	3.94–4.29
Ho	1.42ms	1.28ms	3.36	3.30	3.94–4.26	3.89–4.16
Yb	7.53ms	1.11ms	3.16	3.37	3.62–4.26	3.84–4.19

5.3.3 NMR Titration

La(III) and Lu(III) system

As demonstrated in Chapter 3, NMR titration method is useful to investigate the complex formation and to obtain the structural information. The spectrophotometric titration of Nd(III) and Ho(III) showed the formations of 1:1 and 1:2 metal to ligand ratio complexes with DOODAC2. The complex formation of Ln(III) were studied to gain further structural information on each complexation steps. Various molar ratios of acetonitrile solutions dissolving free DOODAC2 and Ln(III) (Ln = La–Lu, except for Pm and Gd) nitrate were prepared and ^{1}H NMR spectra were measured. The compositions of sample solutions are given in Table 5-1.

Figure 5-7 and Figure 5-8 shows the spectra of sample solutions **A**, **B**, **C**, **D** and **E** for La(III) and Lu(III) system, respectively. In both La(III) and Lu(III) system, the methylene signals H(1) and H(2) shifted to downfield and showed relatively sharp signals in sample solution **B**. In the La(III) system (Figure 5-7), the methylene signal H(2) shifted to upfield and broadened in sample solution **C** ([La]:[DOODAC2] = 1:2). Then, both H(1) and H(2) shifted to upfield in sample solution **D** ([La]:[DOODAC2] = 1:3), and the signal broadenings and upfield shifts continued with increasing TEDGA concentration. In the Lu system (Figure 5-8), both H(1) and H(2) shifted to upfield and broadened with increasing TEDGA concentration.

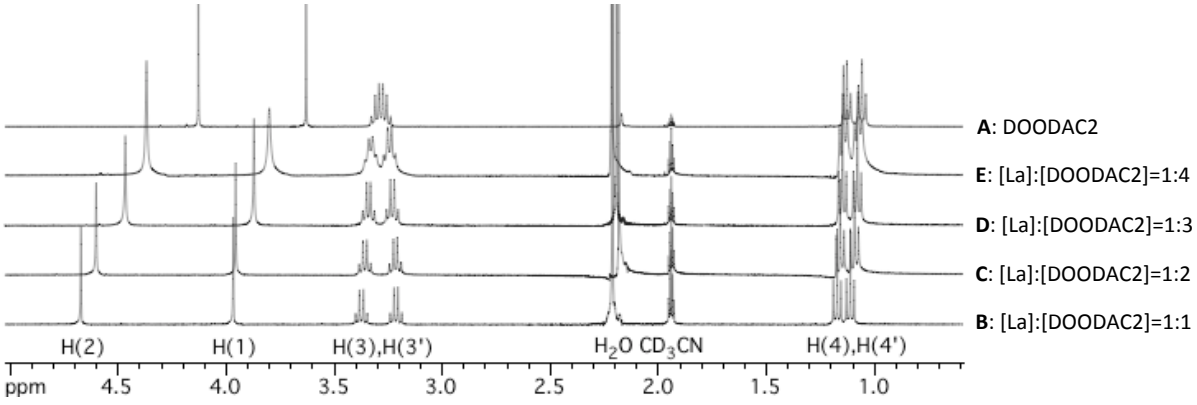

Figure 5-7 ^{1}H NMR spectra of DOODAC2 in acetonitrile-d_3 for different molar ratios of sample solution (A, B, C, D and E) for La(III) systems, measured at 298 K.

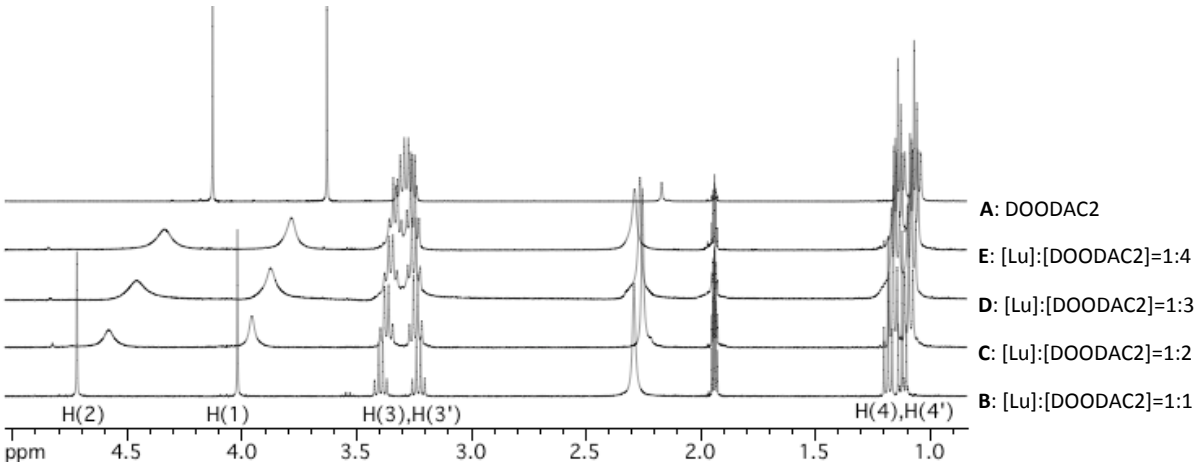

Figure 5-8 ^{1}H NMR spectra of DOODAC2 in acetonitrile-d_3 for different molar ratios of sample solutions (A, B, C, D and E) for Lu(III) systems, measured at 298 K.

These shifts and broadenings can be attributed to the fast exchange on the NMR timescale. Assuming that the Nd(III) and Ho(III) are the analogues of La(III) and Lu(III), respectively, the ratios of 1:1 and 1:2 complexes in sample solutions **B**, **C**, **D** and **E** were calculated by using stability constants and are summarized in Table 5-4.

Table 5-4 Distributions of the species in sample solutions.

Sample solutions	Nd		Ho	
([Ln]:[DOODAC2])	1:1 complex (%)	1:2 complex (%)	1:1 complex (%)	1:2 complex (%)
B (1:1)	95.8	0.1	95.4	0.2
C (1:2)	2.9	97.1	47.8	52.1
D (1:3)	0.8	99.2	28.2	71.8
E (1:4)	0.0	99.9	19.3	80.7

As can be seen from this table and the ^{1}H NMR spectra, the species of sample solutions **B** and **C** of La(III) system can be attributed to the 1:1 and 1:2 complexes, respectively, because they are dominant species under these conditions. On the other hand, sample solutions **C**, **D** and **E** of Lu(III) system contains both 1:1 and 1:2 complexes. Such mixed states cause the fast exchange between two complexes. From these results, following can be concluded: (i) Both light and heavy Ln(III) form relatively rigid 1:1 complexes with DOODAC2 as illustrated in Figure 5-9 and their structures are similar to the second group crystal structures (see Chapter 4.3.1) in ten-coordination, (ii) however, there is small structural difference between two isostructural group for light/middle Ln(III) (Ln = La–Ho) and heavy Ln(III) (Ln = Er–Lu) groups, and (iii) fast exchange reactions are caused when the excess of DOODAC2 (above [Ln]:[DOODAC2]=1:1) exist in the system.

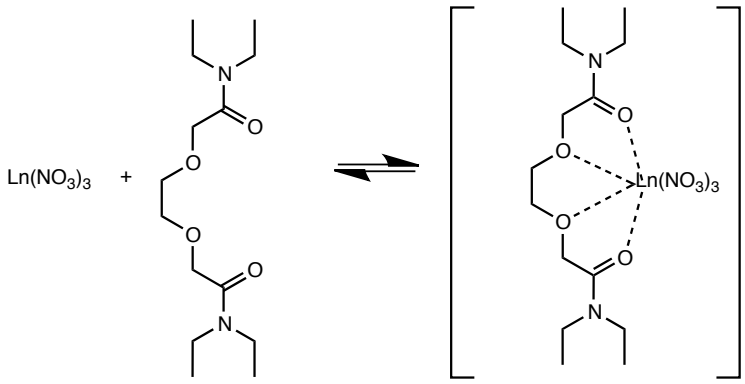

Figure 5-9 Scheme of 1:1 complex formations for Ln(III) nitrate with DOODA estimated from NMR titration.

In addition, the observed ^{1}H spectra of sample solution **F** ([La(DOODAC2)$_2$(MeOH)$_2$][La(NO$_3$)$_6$]) of La(III) system was able to reproduced by sample solution **B** ([La]:[DOODAC2]=1:1), indicating the dissociation of homoleptic ion pair complex and the reformation of 1:1 complex in the acetonitrile solution.

Eu(III) System

With increasing DOODAC2 concentration, the signals were extensively broadened and almost disappeared into the baseline in every paramagnetic Ln(III) system because of the existence of the fast exchange reactions. Europium(III) were selected as a representative example for further investigation of the structures of [Ln]:[DOODAC2]=1:2 complexes. By cooling down the sample to 238K, the exchange reaction became slow and the signals became relatively sharp. Figure 5-10 shows the concentration dependency of ^{1}H NMR spectra of Eu(III) nitrate with DOODAC2 measured at 238K. With increasing the DOODAC2 concentration, from [Ln]:[DOODAC2]=1:1 to 1:2, the signals changed drastically. In the [Eu]:[DOODAC2]=1:1 system, six signals observed and can be assigned to coordinated DOODAC2.

In the [Eu]:[DOODAC2]=1:2 system, H(1) and H(2) broadened and disappeared into baseline, and four other signals appeared from 0 ppm to 5 ppm, which can be assigned to free (or partially dissociated) DOODAC2. The coordinated signals have total integral for less than two DOODAC2 molecules. The ratios of total integrals of free and coordinated signals are non-stoichiometric composition, [free]:[coordinated] = 2.4:1.6. This indicates that one or two DOODAC2 molecules are not symmetrically coordinated (i.e., only by two or three oxygen atoms) probably due to weak coordination ability of ether oxygen and the competition with the nitrate ions. Therefore, two DOODAC2 molecules are coordinated asymmetrically in the symmetric position in the 1:2 complex.

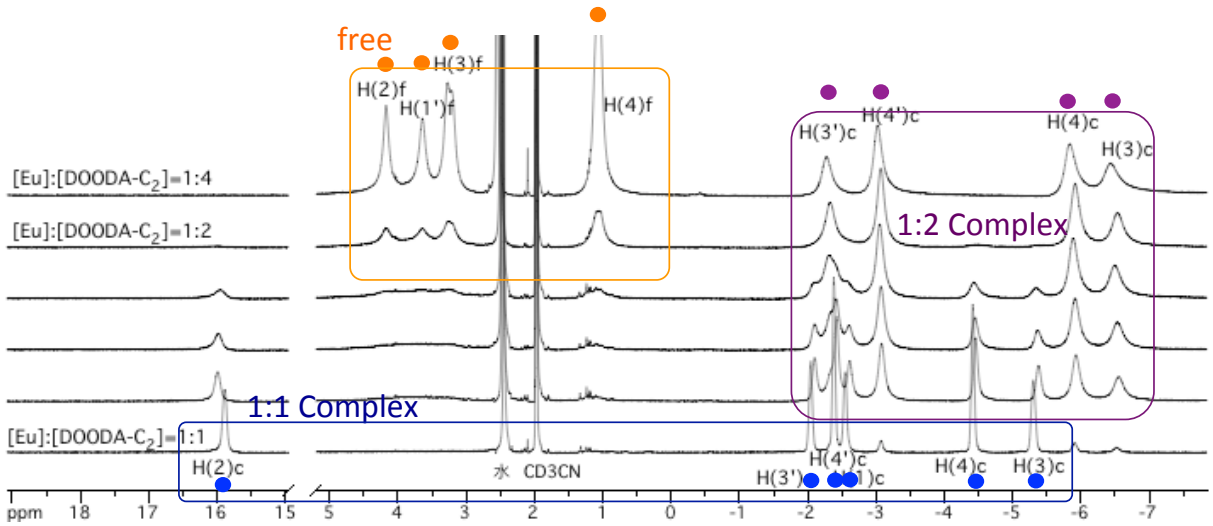

Figure 5-10 DOODAC2 concentration dependent ^{1}H NMR spectra measured at 238K in CD$_3$CN. The ratios [Eu]:[DOODAC2]=1:1—1:4 from bottom to top.

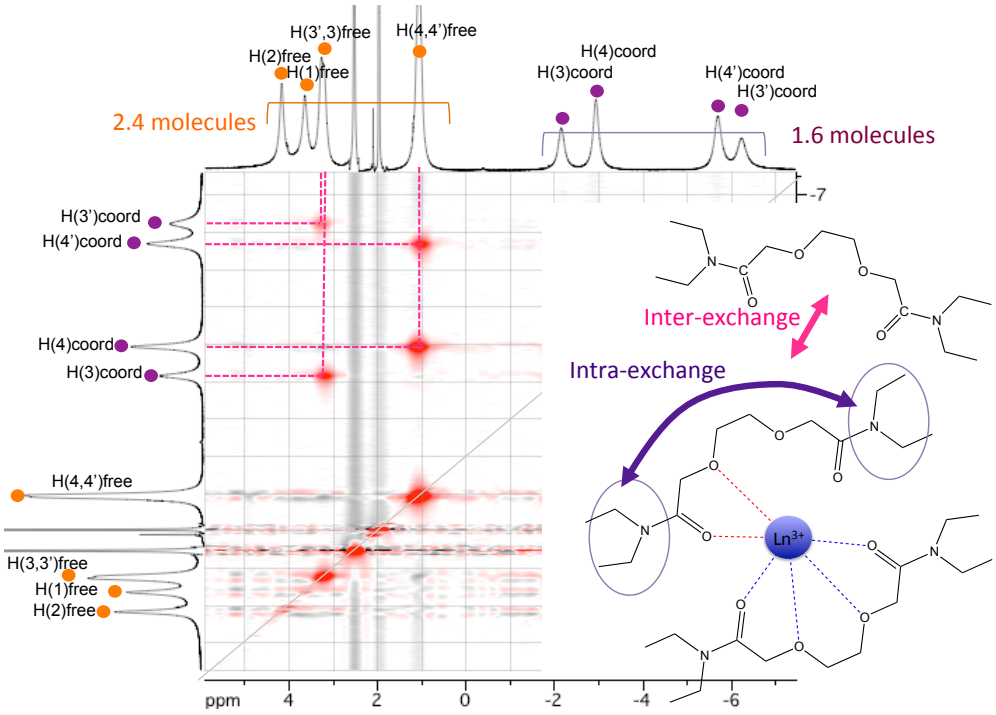

Figure 5-11 EXSY spectrum of [Eu]:[DOODAC2] = 1:4 measured in CD_3CN at 238K.

Further increase of DOODAC2 concentration, the signals of coordinated H(1) and H(2) were disappeared. In the conditions above [Eu]:[DOODAC2] = 1:2, the integrals of coordinated signals did not change, whereas that of free signals increased by increasing DOODAC2 concentrations. Thus, it is clear that 1:2 complex was formed in twice excess of DOODGAC2, i.e. above [Eu]:[DOODAC2] = 1:2.

The exchanging reaction was further analysed by EXSY spectrum. Figure 5-11 shows the EXSY spectra of the [Eu]:[DOODAC2] = 1:4 system measured at 238 K. The EXSY spectrum showed the correlation peak at ethyl chains between free and coordinated DOODAC2. This indicates that the existence of the exchange reaction between free and coordinated DOODAC2. The exchange reaction is possibility of inter-molecular exchange between free (*) and coordinated DOODAC2 represented as following equation.

$$[Ln(NO_3)_3(DOODAC2)_2] + DOODAC2^* \rightleftharpoons [Ln(NO_3)_3(DOODAC2)(DOODAC2^*)] + DOODAC2$$

However, there is possibility of intra-molecular exchange between partially dissociated and coordinated DOODAC2, or both inter- and intra-molecular exchange are occurring at the conditions above [Ln]:[DOODA] = 1:2. Unfortunately, in the temperature range of this study, the exchange system and pathway could not be clarified.

To explain the structure of 1:2 complex, it is necessary to consider the coordination mode of DOODAC2 by bidentate or tridentate. Three possible partial coordination modes of DOODAC2 were considered. (Figure 5-12) In case 1, DOODAC2 associates with Ln(III) by two carbonyl oxygen to make an eleven-membered ring (bidentate). In case 2, DOODAC2 associates with Ln(III) by one carbonyl oxygen and one ether oxygen to make a one five-membered ring (bidentate). In case 3, it associates by carbonyl oxygen and two ether oxygen atoms (tridentate) to form two five-membered rings. While the eleven-membered ring is not stable, the case 2 or 3 are likely species.

The ratios of total integrals of free and coordinated, [free]:[coordinated] = 2.4:1.6, can be well explained if one DOODAC2 coordinates to Ln(III) by tetradentate mode and one other DOODAC2

coordinates to Ln(III) by bidentate mode (Case2). This result suggests that the -CH_2-O-CH_2-CH_2-O-CH_2- fragment in DOODAC2 molecule is too flexible to form stable complexes with Ln(III) and causes very fast inner- and/or inter-exchange reaction.

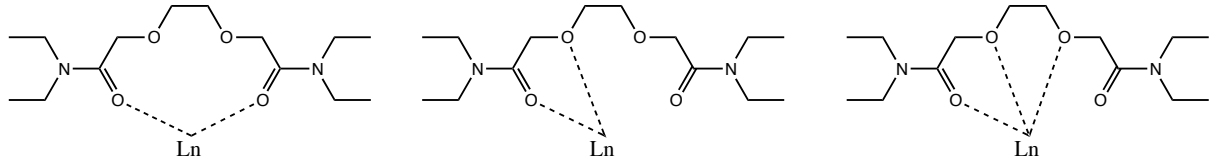

Figure 5-12 Possible partial coordination mode of DOODAC2.

In addition, in cases of Nd(III) and Ho(III) system, the signals from free DOODAC2 could not be observed even at 238 K. The reason why the free DOODAC2 signal could not be observed were because of the very fast exchange reaction in case of Nd(III) system, and because of the large difference in signal frequency between free and coordinated state in case of Ho(III) system.

Figure 5-13 and Figure 5-14 show the reaction schemes estimated from spectrophotometric and NMR titration results for light/middle and heavy Ln(III), respectively. Unfortunately, unlike TEDGA system, it could not determine the boundary of these two reaction scheme due to the very fast exchange throughout the Ln(III) series when the excess of DOODAC2 exist in the system (above [Ln]:[DOODAC2] = 1:1).

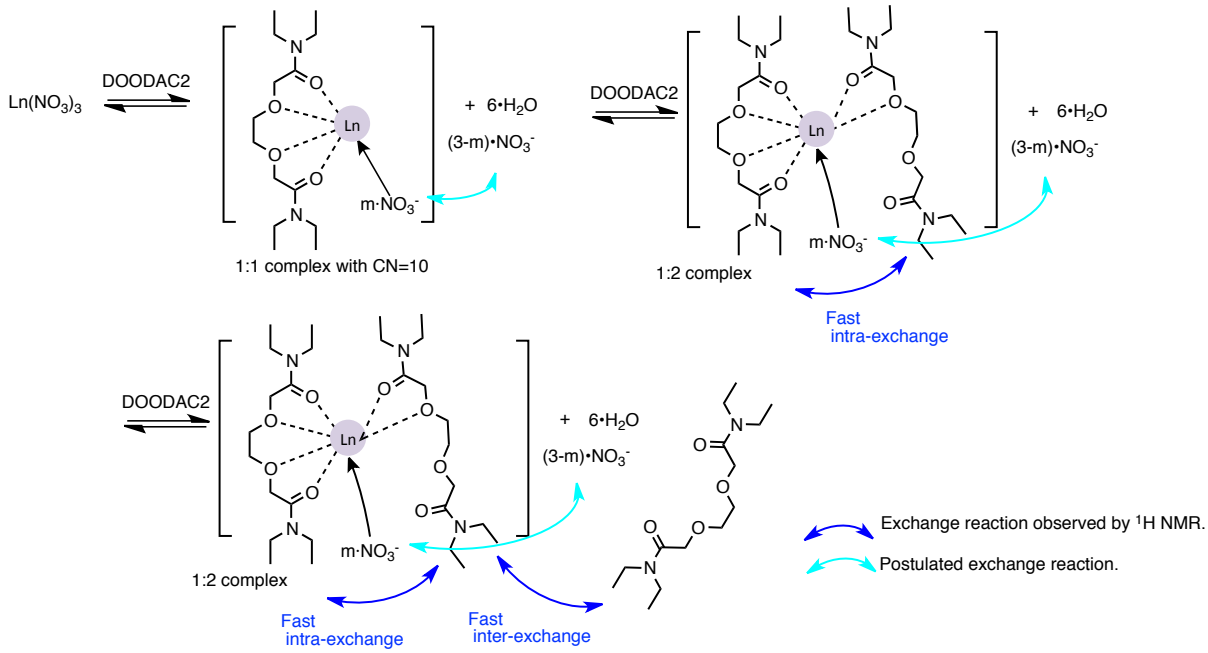

Figure 5-13 Scheme of complex formations for light/middle Ln(III) with DOODAC2 estimated from spectrophotometric and NMR titration.

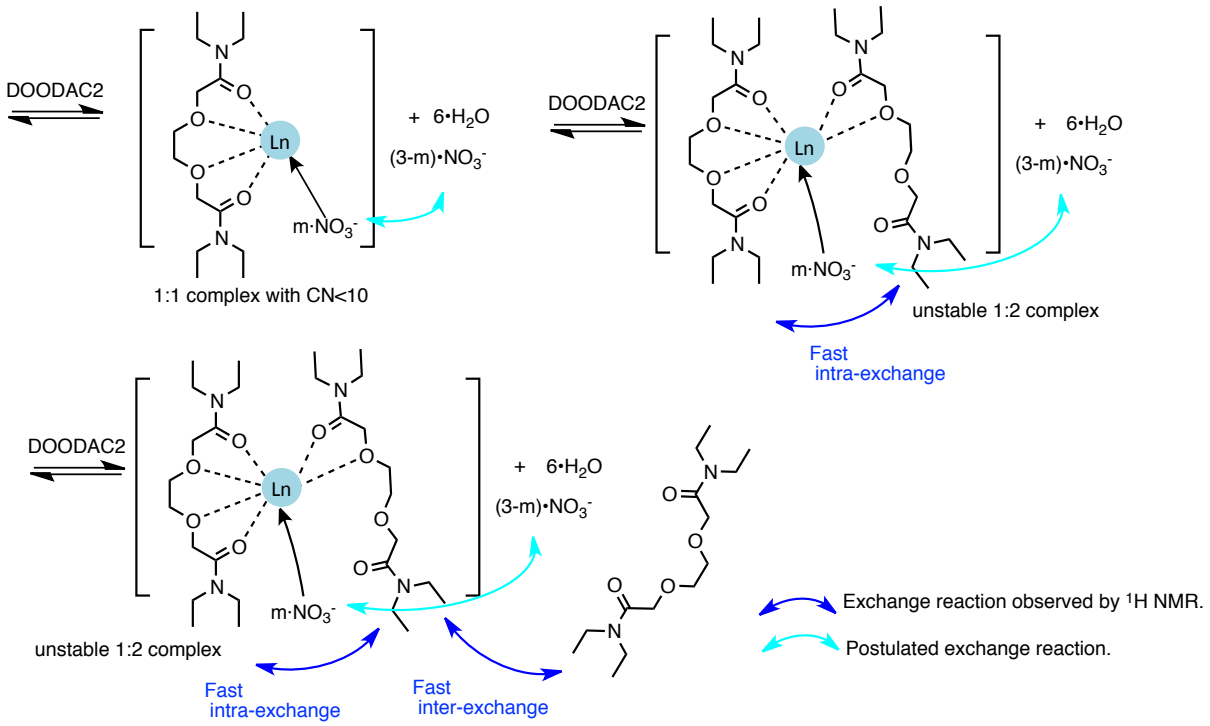

Figure 5-14 Scheme of complex formations for heavy Ln(III) with DOODAC2 estimated from spectrophotometric and NMR titration.

5.4 Conclusion

The complex formations of light and heavy Ln(III) nitrate with DOODA were examined using UV-vis and NMR spectroscopy. It was revealed that both light/middle and heavy Ln(III) nitrates form 1:1 and 1:2 complexes with DOODA in acetonitrile solutions. The stability constants for these complexes evidenced that the 1:1 complexes are stable for Ln(III) series whereas 1:2 complexes are less stable for heavy Ln(III). Combined with the UV-vis and NMR results, following can be concluded:

(i) Both light/middle and heavy Ln(III) form 1:1 and 1:2 complexes.

(ii) Hypersensitive peak for Nd(III) provided information that the coordination number of 1:1 complex can be assumed to ten-coordination as displayed in the second group of crystal structure ([Ln(DOODAC2)$(NO_3)_3$]).

(iii) The lanthanide induced shift (LIS) plots of 1:1 complexes indicate that there are two isostructural groups with small variation in their structures, and the heavy Ln(III) (Ln = Er–Yb and also Lu) would have smaller coordination number compared with light/middle Ln(III) (Ln = La–Ho) with rearrangement of nitrate ion.

(iv) Very fast inter- and/or intra-exchange reactions are caused when the excess of DOODAC2 (above [Ln]:[DOODAC2] = 1:1) exist in the system. The -CH2-O-CH2-CH2-O-CH2- fragment in DOODAC2 molecule is too flexible to form stable complexes with Ln(III) and this is the reason of the very fast exchange.

Although the structures of 1:2 complexes could not been elucidated, these results in this chapter can explain the differences in *D* values across the Ln(III) series by the structure and stability of complexes in the acetonitrile solution.

References

1 Sasaki Y.; Choppin, G. R. "Solvent extraction of Eu, Th, U, Np and Am with *N, N'*-dimethyl-*N, N*'-dihexyl-3-oxapentanediamide and its analogous compounds." *Analytical Sciences*, **1996**, 12, 225

2 Narita, H.; Yaita, T.; Tamura, K.; Tachimori, S. "Solvent extraction of trivalent lanthanoid ions with *N,N'*-dimethyl-*N, N*'-diphenyl-3-oxapentanediamide." *Radiochimica Acta,* **1998**, *81*, 223–226.

3 Sasaki, Y.; Rapold, P.; Arisaka, M.; Hirata, M.; Kimura, T.; Hill, C.; Cote, G. "An Additional Insight into the Correlation between the Distribution Ratios and the Aqueous Acidity of the TODGA System." *Solvent Extraction and Ion Exchange,* **2007**, 25, 187-204.

4 Narita, H.; Yaita, T.; Tamura, K.; Tachimori, S. "Study on the extraction of trivalent lanthanide ions with N,N′-dimethyl-N,N′-diphenyl-malonamide and diglycolamide." *Journal of Radioanalytical and Nuclear Chemistry*, **1999**, *239*.

5 Sasaki, Y.; Morita, Y.; Kitatsuji, Y.; Kimura, T. "Extraction Behavior of Actinides and Metal Ions by the Promising Extractant,N,N,N′ ,N′ -Tetraoctyl-3,6-dioxaoctanediamide (DOODA)." *Solvent Extraction and Ion Exchange*, **2010**, 28, 335-349.

6 Sasaki, Y.; Sugo, Y.; Kitatsuji, Y.; Kirishima, A.; Kimura T. "Complexation and back extraction of various metals by water-soluble diglycolamide." *Analytical Sciences*, **2007**, 23.

7 Sasaki, Y.; Morita, Y.; Kitatsuji, Y.; Kimura, T. "Mutual Separation of Actinides from Middle Lanthanides by the Combination of Two Neutral Donors, *N,N,N′,N′*-Tetraoctyl-3,6-dioxaoctanediamide and *N,N,N′,N′*-Tetraethyldiglycolamide." *Chemistry Letters,* **2010**, *39*, 898-899.

Chapter 6

Effect of Nitrate on Complexation of Lanthanide(III) with DGA and DOODA

6.1 Introduction

As described in Chapter 1.3.4, interactions with ionic salts in organic solvents are essentially to understand Ln(III) complex formation, because they work as a counter ions in to form uncharged complexes. In this point of view, interactions of perchlorate, trifrate, halide and nitrate with Ln(III) have been widely studied.[1] The interaction between Ln(III) and nitrate in the aqueous solutions also have been still in one of the topic. Recently, these interactions have been studied by modern techniques such as Extended X-ray Absorption Fine Structure (EXAFS) measurements, molecular dynamics simulations, quantum mechanical or quantum chemical calculations.[2,3,4] For instance, Dobler *et al*. have performed the quantum mechanical calculations in gas phase to investigate the structural, electronic and energetic features of nitrate coordination to Ln(III).[5] They have revealed that the CN ranges from 9 (3 monodentate nitrates and 6 water) to 10 (3 bidentate nitrates and 4 water) or 11 (3 bidentate nitrates and 5 water) are isoenergetic for $La(NO_3)_3(H_2O)_m$ species. However, the coordination mode of nitrate in the complexes of the Ln(III) nitrate with neutral hard donor extractant have not been well studied because of the difficulties of their labile properties.

Narita *et al*. have reported the coordination environment of Er(III) nitrate with a DGA derivatives. However, EXAFS cannot give the information about the outer-sphere coordinated nitrate ions in general.[6] Although Hirata *et al*. have also addressed the molecular dynamics simulations of the Ln(III) nitrate with DGA ligand system, interaction energy differenced between Ln(III) ions has been carried out without nitrate ions take into account.[7] Gannaz *et al*. have proposed the Ln(III) and An(III) complexes formed upon solvent extraction with malonamide and nitrate by EXAFS and IR study, but the proposal was a speculate based on several experimental result.[8]

Since one of the goals in this study is to clarify the coordination environment around Ln(III) complexes including counter ions, investigations of the interaction and the coordination mode of the nitrate ions to Ln(III) is important. Therefore, this chapter focuses on the coordination state and coordination mode of nitrate with Ln(III) upon coordination with neutral diamide ligands by using spectrophotometric titration, ^{15}N NMR and IR spectroscopy.

6.2 Experimental Details

6.2.1 Materials

98% ^{15}N enriched sodium nitrate ($Na^{15}NO_3$) was purchased from Isotec Inc. and used as received. The tetrabutylammonium nitrate ($TBANO_3$) were purchased from Sigma-Aldrich Co. LLC. and used as received.

6.2.2 Syntheses

The TEGDA complexes for Ln = La, Nd, Ho and Lu were synthesized by the procedure described in Chapter 2. The ^{15}N enriched Ln(III) nitrate complexes with TEDGA (Ln = La and Lu) were also synthesized by following procedures: The ^{15}N enriched HNO_3 was obtained by cation exchange (AG-50W-X2) of $Na^{15}NO_3$. Hydrated Ln(III) nitrate were prepared by the procedure reported everywhere by using $H^{15}NO_3$.[9]

6.2.3 Instruments and General Procedures

Spectrophotometric Titrations

Spectrophotometric titrations were performed for Nd(III), Ho(III) and Er(III) with $TBANO_3$, TEDGA and DOODAC2. The absorption spectra were recorded on SHIMADZU UV-3150 spectrophotometer at 298 K. Other details were same as those described in Chapter 3.2.2.

Nuclear Magnetic Resonance Study

All NMR spectra were recorded on JEOL ECX-400P (400 MHz) spectrometer at 298 K in acetonitrile-d_3 solutions. ^{15}N chemical shifts were referenced with respect to the solvent peak at 240 ppm. The acetonitrile solutions dissolving TEDGA and hydrated Ln(III) (Ln=La and Lu) nitrate were prepared and ^{15}N NMR spectrum were recorded. Other details were same as those described in Chapter 3.2.2.

Infrared Spectroscopy

IR spectra (CaF_2 window, 4000–900 cm^{-1}) of acetonitrile solutions dissolving ligand and Ln(III) nitrate were r various molar ratios were recorded on Shimadzu FT-IR-8400S spectrometer at room temperature.

6.3 Results and Discussion

6.3.1 Spectrophotometric Titration

Nd(III) System

To evaluate the effect of nitrate concentration on complexation with DGA/DOODA derivatives, spectrophotometric titration of Nd(III) nitrate ($Nd(NO_3)_3$) with tetrabutylammonium nitrate ($TBANO_3$) was carried out. The resulting absorption spectra were shown in Figure 6-1. The absorption band at 581 nm showed bathochromic shift to 583.5 nm and intensity enhancement with increasing nitrate concentration.

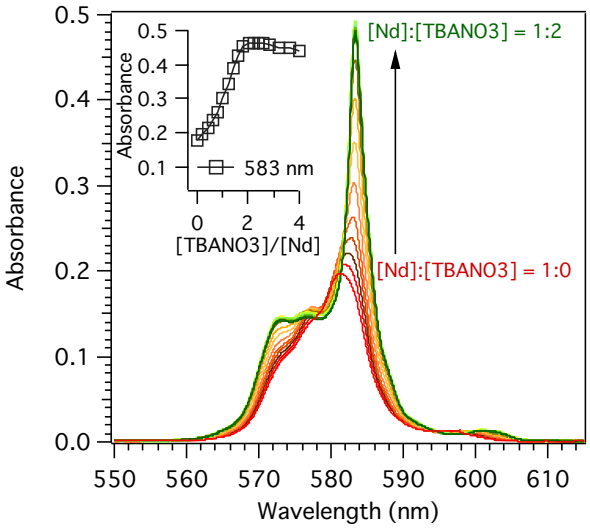

Figure 6-1 Spectrophotometric titration of Nd(III) by $TBANO_3$ in acetonitrile solutions at 298 K.

As mentioned in Chapter 3.3.1, the spectrum of acetonitrile solution dissolving hydrated Nd(III) nitrate is quite similar to that of reported by Bünzli, *et al.*[10] Thus, the coordination environment

around Nd(III) in acetonitrile solution dissolving hexa-hydrated Nd(III) nitrate ($Nd(NO_3)_3 \cdot 6H_2O$) seems to be quite similar even in the hydrated water is exist in the system. By comparison of reported spectra and Figure 6-1, the figure of Nd(III) absorption band of $[Nd(NO_3)_3]$:$[TBANO_3]$ = 1:2 condition showed excellent agreement with reported spectra of R=$[NO_3^-]$/[Nd]=5 in acetonitrile solution.[10] This result implies that the formations of $Nd(NO_3)_5^{2-}$ species. Bünzli, *et al*. have conducted the further investigation of coordination mode of nitrate ions in $Nd(NO_3)_5^{2-}$ by FT-IR spectra. In the anionic $Nd(NO_3)_5^{2-}$ complex has CN=10.2 and the all nitrate ions are coordinated to Nd(III) by bidentate fashion. Therefore, the spectrum of $[Nd(NO_3)_3]$:$[TBANO_3]$ = 1:2 in this study may reflect the CN=10 around Nd(III) ion.

In order to evaluate the competition between nitrate and DGA/DOODA derivatives, the complexation of Nd(III) with diamide ligands (TEDGA and DOODAC2) were performed under the condition of $[Nd(NO_3)_3]$:$[TBANO_3]$ = 1:2, i.e. $Nd(NO_3)_5^{2-}$ is already formed. The resulting absorption spectra for TEDGA and DOODA titrations were shown in Figure 6-2. The changes in the Nd(III) absorption spectra by adding TEDGA or DOODAC2 became small when the titration reached to the $[Nd(NO_3)_3]$:$[TBANO_3]$:[TEDGA]=1:2:3 and $[Nd(NO_3)_3]$:$[TBANO_3]$:[DOODA]=1:2:1, respectively. As demonstrated in Chapter 3.3.1, Nd(III) forms 1:3 complex with TEDGA. The changes in absorption spectra illustrated in Figure 6-2(a) indicate that the Nd(III) form 1:1 and 1:3 inner-sphere complexes with TEDGA step-by-step and the nitrate ions replaced to the outer-sphere. However, in case of DOODAC2 titration, the absorption spectrum of $[Nd(NO_3)_3]$:$[TBANO_3]$:[DOODA] = 1:2:1.6 in Figure 6-2(b) implies that the DOODAC2 forms 1:1 complex and do not form 1:2 complex even though the excess of DOODAC2 exist in the system. Unfortunately, in the spectrophotometric titrations by $TBANO_3$ did not allow the calculation of the stability constants for these complexations as well as the case of DOODAC2 in Chapter 4. However, these results provide qualitative insights that the strength in coordination affinity of TEDGA is larger than that of DOODA, and DOODAC2 has a similar strength compared with nitrate.

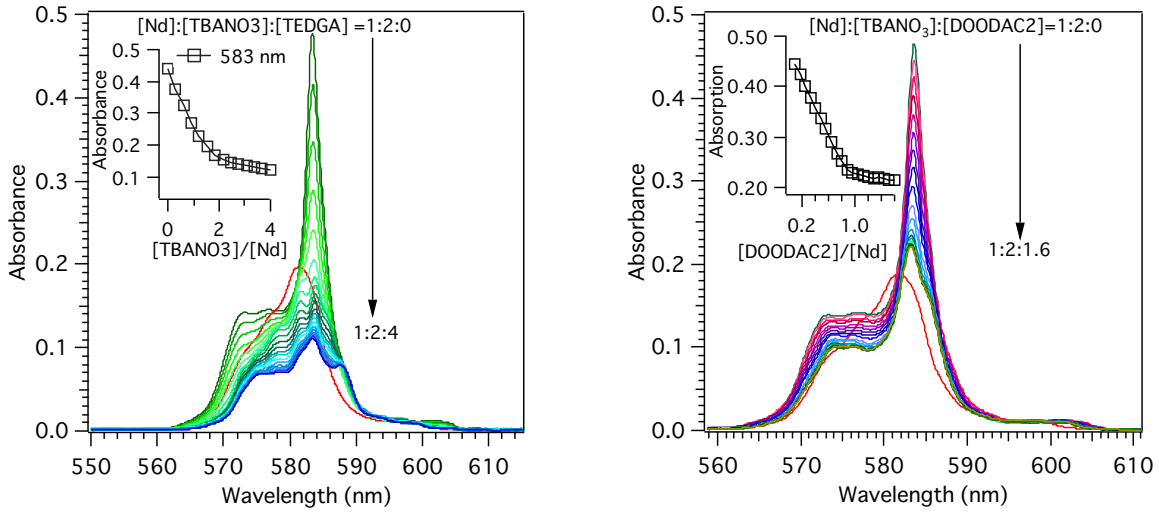

(a) (b)

Figure 6-2 Spectrophotometric titration of (a) Nd(III) by TEDGA (left) and (b) DOODAC2 (right) under the condition of $[Nd(NO_3)_3]$:$[TBANO_3]$ = 1:2 in acetonitrile solutions at 298 K.

Ho(III) and Er(III) System

To confirm the differences in complex formations between light and heavy Ln(III), firstly, the spectrophotometric titrations of Ho(III) and Er(III) with $TBANO_3$ were performed. The resulting absorption spectra are shown in Figure 6-3. The absorption bands of Ho(III) and Er(III) showed the intensity enhancement with increasing nitrate concentration by the additions of $TBANO_3$. Bünzli *et al.* have reported that the CN of $Er(NO_3)_5^{2-}$ is 9.9 and the all nitrate ions are coordinated to Er(III) by bidentate mode by FT-IR investigations in acetonitrile solution.[10] According to their report, there are not significant difference between light and heavy Ln(III) in terms of the complexation with nitrate in the acetonitrile solution. Therefore, the observed change in the absorption spectra of Ho(III) and Er(III) can be considered as the formation of $Ln(NO_3)_5^{2-}$ anionic complexes.

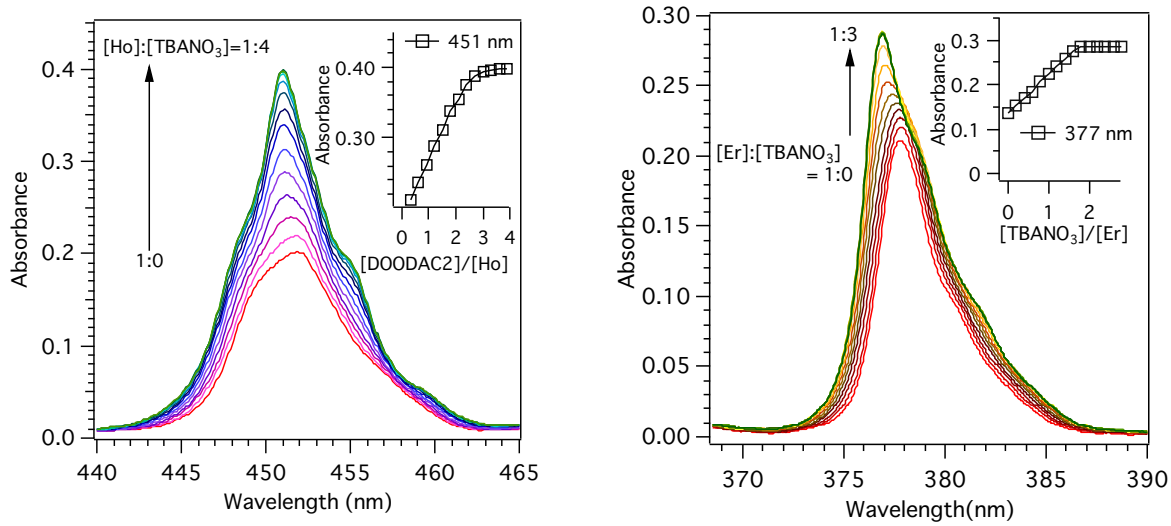

(a) (b)

Figure 6-3 Spectrophotometric titration of (a) Ho(III) (left) and (b) Er(III) (right) by $TBANO_3$ in acetonitrile solutions at 298 K.

The complexation of Ho(III) and Er(III) with diamide ligands, TEDGA and DOODAC2, were performed under the condition of $[Ln(NO_3)_3]$:$[TBANO_3]$ = 1:2 (Ln= Ho and Er) as well as Nd(III) system. The resulting spectra for Er(III)-TEDGA system and Ho(III)-DOODAC2 system are shown in Figure 6-4 as representative examples. As a result, the absorption spectra in both case decreased with increasing the diamide ligand concentration. These changes in absorption spectra can be lead the same conclusion as Nd(III) system, i.e. the formation of 1:3 complex with TEDGA and 1:1 complex with DOODAC2, under the conditions which contain excess of nitrate ions.

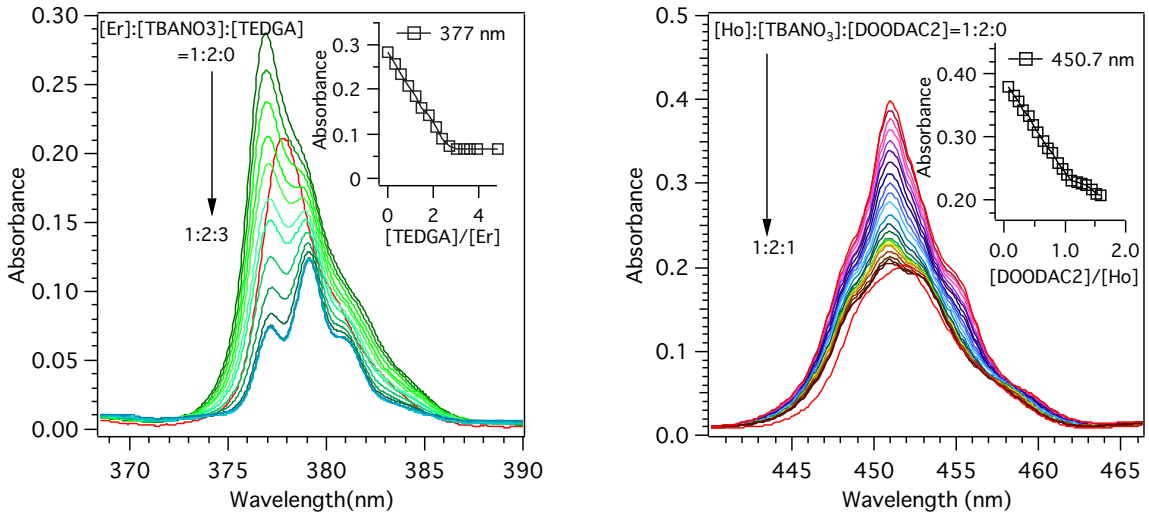

(a) (b)

Figure 6-4 Spectrophotometric titration of (a) Er(III)-TEDGA (left) and (b) Ho(III)-DOODA (right) under the condition of $[Ln(NO_3)_3]$:$[TBANO_3]$ = 1:2 in acetonitrile solutions at 298 K.

6.3.2 NMR Structural Analysis

To determine the number of nitrate ions coordinated to Ln(III), ^{15}N enriched hydrated Ln(III) nitrate (Ln = La and Lu) and $TBANO_3$ were synthesized and its ^{15}N NMR spectra were measured. The ^{15}N NMR spectra of these ^{15}N-enriched salts are shown in Figure 6-5. Only one signal appears at 375, 370 and 368 ppm for $TBA^{15}NO_3$, $La(^{15}NO_3)_3$ and $Lu(^{15}NO_3)_3$ salt, respectively. These signals can be assigned to nitrate ions. The upfield shifts in $La(^{15}NO_3)_3$ and $Lu(^{15}NO_3)_3$ salts compared with $TBA^{15}NO_3$ may due to coordination to the Ln(III) ions.

The ^{15}N NMR of nitrate ions interacting with Ln(III) ions have been studied by Fratiello *et al*. They have detected three coordinated NO_3^- signals in water-acetone-Freon-22 mixtures at −125 °C for La(III),[11] and two coordinated NO_3^- signals in water-acetone-Froen-12 mixtures at −115 °C for Lu(III).[12] In both cases, even in low temperature, the differences in observed chemical shifts assigned to different species are quite small (less than 1 ppm). Therefore, it would be expected that it is difficult to detect different coordination mode of NO_3^- species at the temperature range of acetonitrile-d_3.

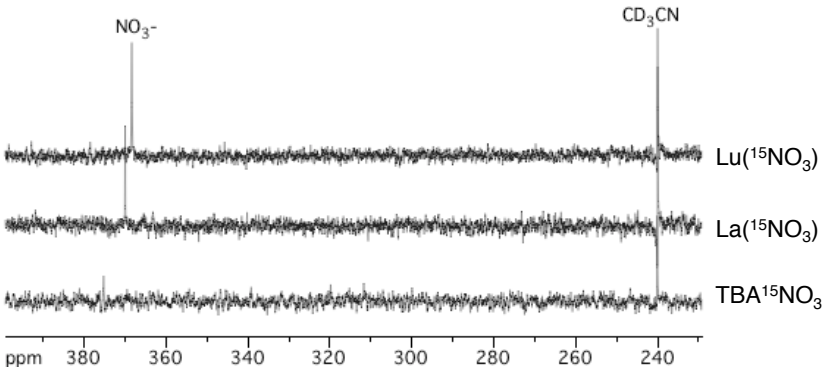

Figure 6-5 ^{15}N NMR spectra of ^{5}N enriched Ln(III) nitrate (Ln = La and Lu) and $TBANO_3$.

6.3.3 NMR Titration

DGA System

In order to investigate the number of coordinated nitrate in the Ln(III) complexes formed with neutral diamide extractant in solution, titrations of ligands (TODGA and TEDGA) to Ln(III) (Ln = La and Lu) were performed and ^{15}N NMR spectra were recorded. In Figure 6-6, the observed ^{15}N NMR chemical shifts are plotted against the ligand to metal ratio. ([Ln]:[diamide] = 1:0–1:5) Only one signal assigned to nitrate ions was observed in every titration steps. The signals shifted to the downfield with an increasing in ligand concentrations.

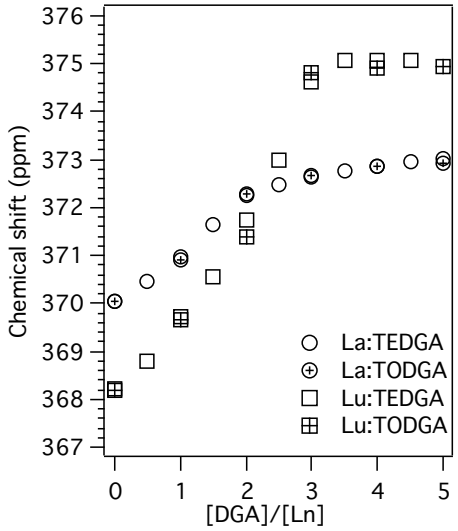

Figure 6-6 Chemical shift variations on ^{15}N NMR signals of nitrate in DGA system in acetonitrile-d_3 at 298 K.

Since the signal of nitrate ions is always one in all conditions, analyses of number of coordinate nitrate cannot be performed straightforwardly. For example, under the conditions of [Ln]:[TEDGA] = 1:2, coordinated nitrate in 1:1 and 1:3 complexes and free nitrate would exchange between each sites. However, even if there are some numbers of coordinated species in the system, their chemical shift must be close in few Hz and they are not able to observed separately at 298 K. In fact, the chemical shift differences of coordinated NO_3^- species are 0.1–0.9 ppm in low temperature such as –115 C°.[11,12] Therefore, suppose that the chemical shift in coordinate states are all same, nitrate ions can be assumed to be in a two-site exchange reaction between free and coordinated nitrate ions. In the fast exchange region on the NMR timescale, a single resonance is observed and its chemical shift appears at the weight average of two individual sites as expressed in (Eq. 10) where δ_{obs}, δ_A and δ_B are observed chemical shifts, P_A and P_B are the population of free and coordinate states, respectively. (see Chapter 1.4.3 for detail.) Three nitrate ions are initially postulated to be in a coordinated state.

The number of coordinated nitrate ions (P_B) were calculated by (Eq. 10) and summarized in Table 6-1. As can be seen from the table, the number of coordinated nitrate ion decreased with increasing of DGA concentration. The clear difference can be seen at [Ln]:[DGA]=1:3 ratio between La(III) and Lu(III) system. At least one nitrate ion remains around La(III) in coordinated state, while there is no nitrate ions in the coordinated state around Lu(III). These results are consistent with the crystal structure reported in Chapter 2 and the results concluded by spectrophotometric titrations in Chapter 3 as well.

Table 6-1 Population analysis of coordinated nitrate ions in Ln-DGA system according to **(Eq. 10)**

[Ln]:[DGA]	La-DGA (P_B)	Lu-DGA (P_B)
1:0	3.0	3.0
1:1	2.5	2.4
1:2	1.7	1.5
1:3	1.5	0.2
1:4	1.3	0.0

Structures of ^{15}N Enriched Nitrate Complexes with TEDGA

The complexes for Ln(III) (Ln = La and Lu) with ^{15}N enriched nitrate with TEDGA were synthesized and characterized by single crystal X-ray diffraction and ^{1}H NMR spectroscopy. The ORTEP views of these complexes and crystallographic parameters are shown in Figure 6-7 and summarized in Table 7-3, respectively. The structural features of these crystal structures were confirmed to be identical to the complex with normal nitrate ions reported by Kawasaki *et al* and described in Chapter 2.[13] The La(III) complex was constructed by $[La(TEDGA)_3]^{3+}$ cation and $[La(^{15}NO_3)_6]^{3-}$ anions. The Lu(III) complex was constructed by $[Lu(TEDGA)_3]^{3+}$ cation and three $^{15}NO_3^-$ ions exists as counter anions.

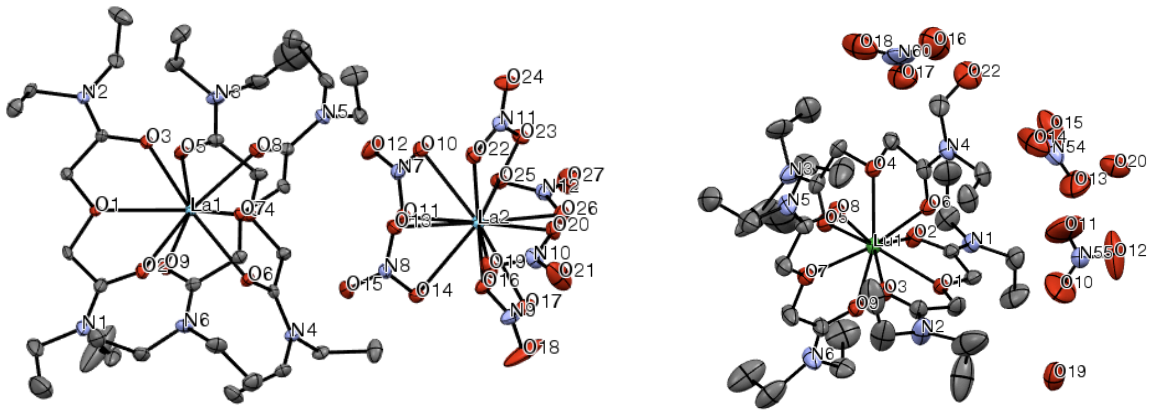

(a) (b)

Figure 6-7 ORTEP view of (a) $[La(TEDGA)_3][La(^{15}NO_3)_6]$ (left) and (b) $[Lu(TEDGA)_3](^{15}NO_3)_3$. (right).

^{1}H NMR spectra of these crystals are shown in Figure 6-8 together with the ^{1}H NMR spectra of normal nitrate complexes already shown in Chapter 3. By comparison of ^{1}H NMR spectra, the normal and ^{15}N enriched complexes seems to be identical on the ^{1}H NMR spectra.

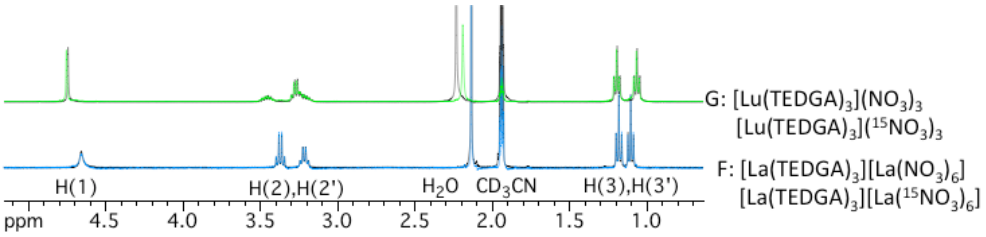

Figure 6-8 ^{1}H NMR spectra of normal and ^{15}N enriched nitrate complexes. (a) $[La(TEDGA)_3][La(NO_3)_6]$ (on the bottom) and (b) $[Lu(TEDGA)_3](NO_3)_3$ (on the top) measured in acetonitirle-d_3 at 298 K.

To confirm the validation of the assumptions about the coordination state of nitrate ions in TEDGA complex which made in previous and this chapters, ^{15}N NMR of the acetonitrile solutions dissolving complexes Ln(III) (Ln = La and Lu) with ^{15}N enriched nitrate with TEDGA were measured. The

resulting spectra are shown in Figure 6-9. The ^{15}N NMR chemical shift of $[La(TEDGA)_3][La(^{15}NO_3)_6]$ was in accordance with that of [La]:[TEDGA] = 1:1.5, indicating the dissociation of homoleptic complex and in the acetonitrile solution. In contrast, the ^{15}N NMR chemical shift of $[Lu(TEDGA)_3](^{15}NO_3)_3$ showed excellent agreement with that of [Lu]:[TEDGA] = 1:3. These results strongly support that the results of Chapter 3 made by UV-vis and ^{1}H NMR spectral evidences.

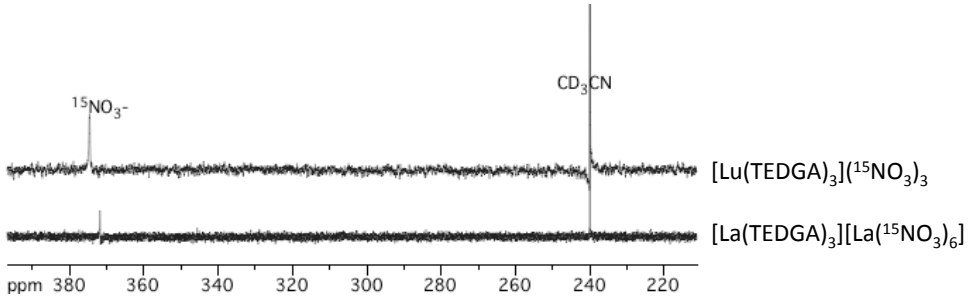

Figure 6-9 ^{15}N NMR spectra of ^{15}N enriched nitrate complexes (a) $[La(TEDGA)_3][La(^{15}NO_3)_6]$ (on the bottom) and (b) $[Lu(TEDGA)_3](^{15}NO_3)_3$ (on the top) measured in acetonitirle-d_3 at 298 K.

Integrate all the results for light Ln(III)-TEDGA system into the complex formation scheme in acetonitrile solution, the schematic representation can be illustrated as in Figure 6-10. For light Ln(III) system, they form 1:1 complexes, and also 1:3 complexes with nitrate ions in outer-sphere when the three times excess of TEDGA exist in the system. However, the large ionic radii of the light Ln(III) may provide some vacant sites that make at least one nitrate ion possible to exist in the inner-sphere of Ln(III), although the Ln(III) is wrapped around by three TEDGA molecules. As the result of the nitrate ion coordination, TEDGA are forced to compete with them and change its position very fast.

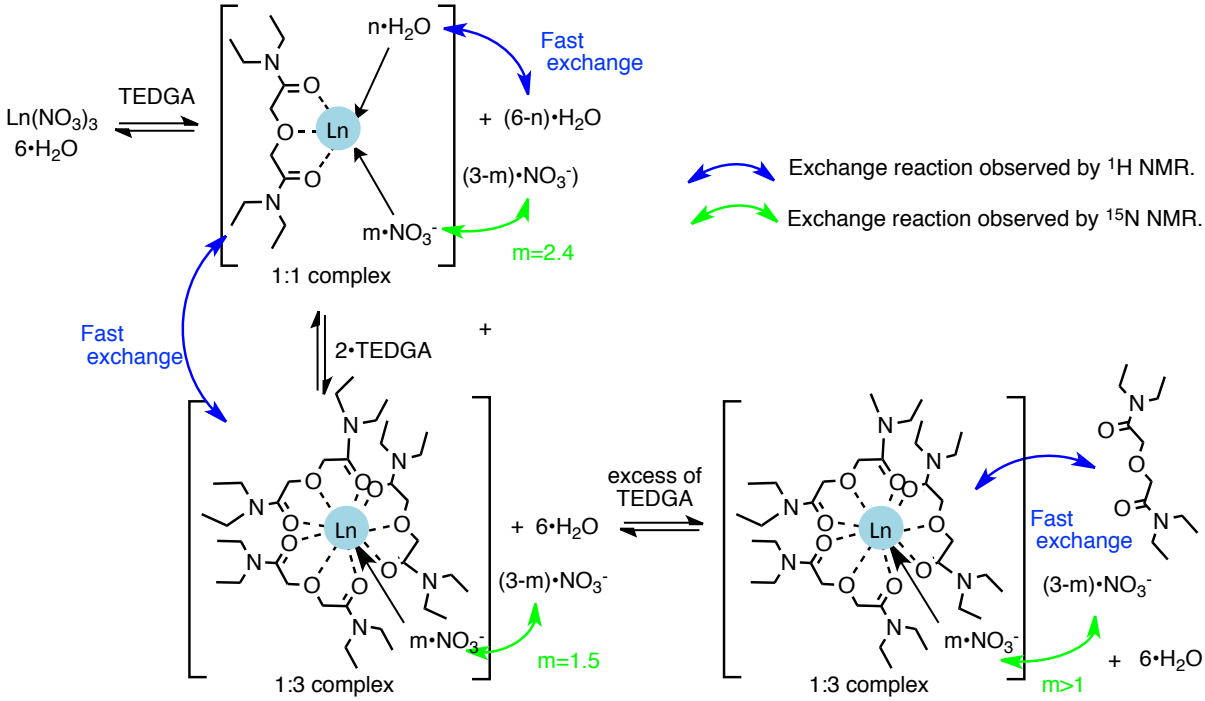

Figure 6-10 Schematic representation of light Ln(III) complexation with TEDGA.

For heavy Ln(III) system, as predicted by previous reports[4,6,7] and various kinds of measurements in this study, heavy Ln(III) form outer-sphere complexes with nitrate ions when the three times the concentration of TEDGA exists in the system. Figure 6-9 shows the reaction scheme estimated from all experimental results for heavy Ln(III). These complexation and structural features

is the main contribution of the high selectivity to heavy Ln(III) on the solvent extraction.

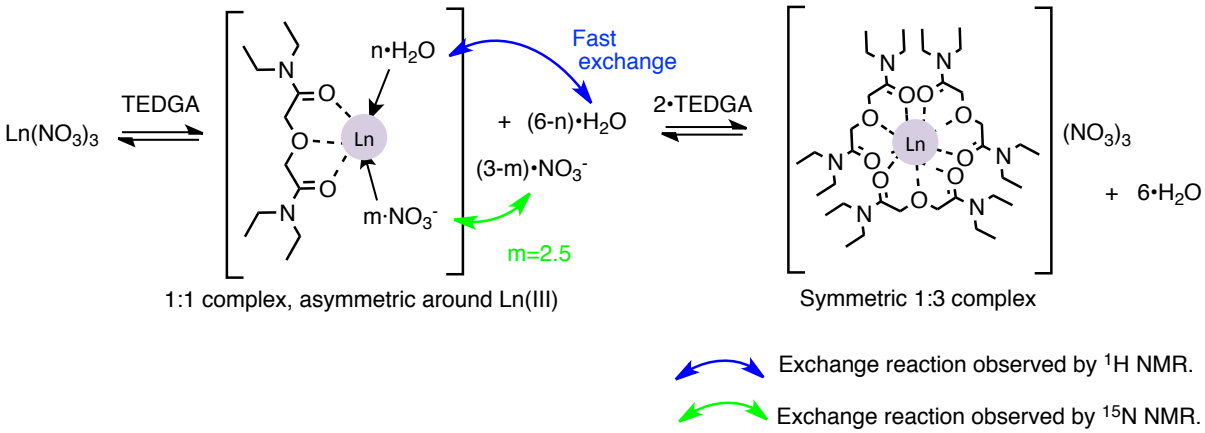

Figure 6-11 Schematic representation of heavy Ln(III) complexation with TEDGA.

DOODAC2 System

To investigate the number of coordinated nitrate in DOODA complexes, same observations and analyses were performed for DOODA system. The observed ^{15}N NMR chemical shifts plotted against the ligand to metal ratio are shown in Figure 6-12. The signals shifted to the downfield with an increasing of DOODA concentration. In both La(III) and Lu(III) systems, chemical shifts of ^{15}N NMR spectra showed gradual increase. These observations are in accordance with the results of spectrophotometric titrations in Chapter 5. Therefore, the chemical shifts observed at [Ln]:[DOODAC2] = 1:1 and [Ln]:[DOODAC2] = 1:2 are correspond to 1:1 complex and 1:2 complex with exchange reactions of DOODA, respectively.

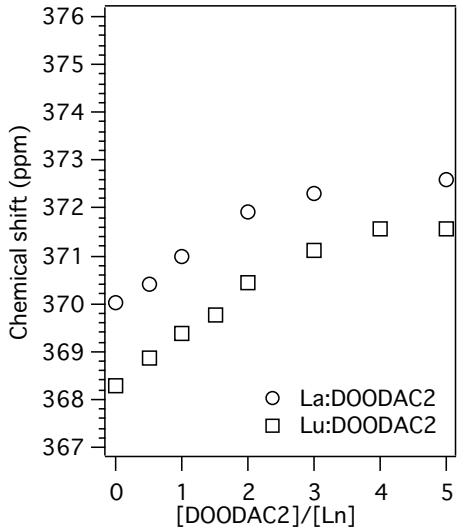

Figure 6-12 Chemical shift variations on ^{15}N NMR signals of nitrate in DOODAC2 system in acetonitrile-d_3 at 298 K.

The number of coordinated nitrate ion in DOODAC2 system was calculated by (Eq. 10) and summarized in Table 6-2. As can be seen from this table, the number of coordinated nitrate ion decreased with increasing of DOODAC2 concentration. There are no noticeable difference between La(III) and Lu(III) system. At least one nitrate ion remains around Ln(III) in coordinated state. These results are consistent with the results concluded by spectrophotometric and NMR titrations.

Table 6-2 Population analysis of coordinated nitrate ions in Ln-DOODAC2 system according to **(Eq. 10)**

[Ln]:[DOODAC2]	La-DOODAC2 (P_Δ)	Lu-DOODAC2 (P_Δ)
1:0	3.0	3.0
1:1	2.4	2.5
1:2	1.9	2.1
1:3	1.7	1.8
1:4	--	1.6
1:5	1.5	1.6
1:6	1.5	1.4

Integrate all the results for light Ln(III)-TEDGA system into the complex formation scheme in acetonitrile solution, the schematic representation can be depicted as in Figure 6-13 and Figure 6-14 for light/middle and heavy Ln(III), respectively. As can be seen from these figures, there is no big difference between them. This result is in accordance with the differences in distribution ratios (*D*). (see Figure 1-5.) The *D* values gradually decrease with atomic number increases in DOODA system. The difference between first and last elements (i.e. La(III) and Lu(III)) is tenfold, while the difference in DGA system is over hundredfold. Therefore, the difference in *D* values across the Ln(III) series is governed by the stability of 1:2 complexes, that is, Ln(III) ions possessing larger ionic radii can form relatively stable 1:2 complexes compared with heavy ones.

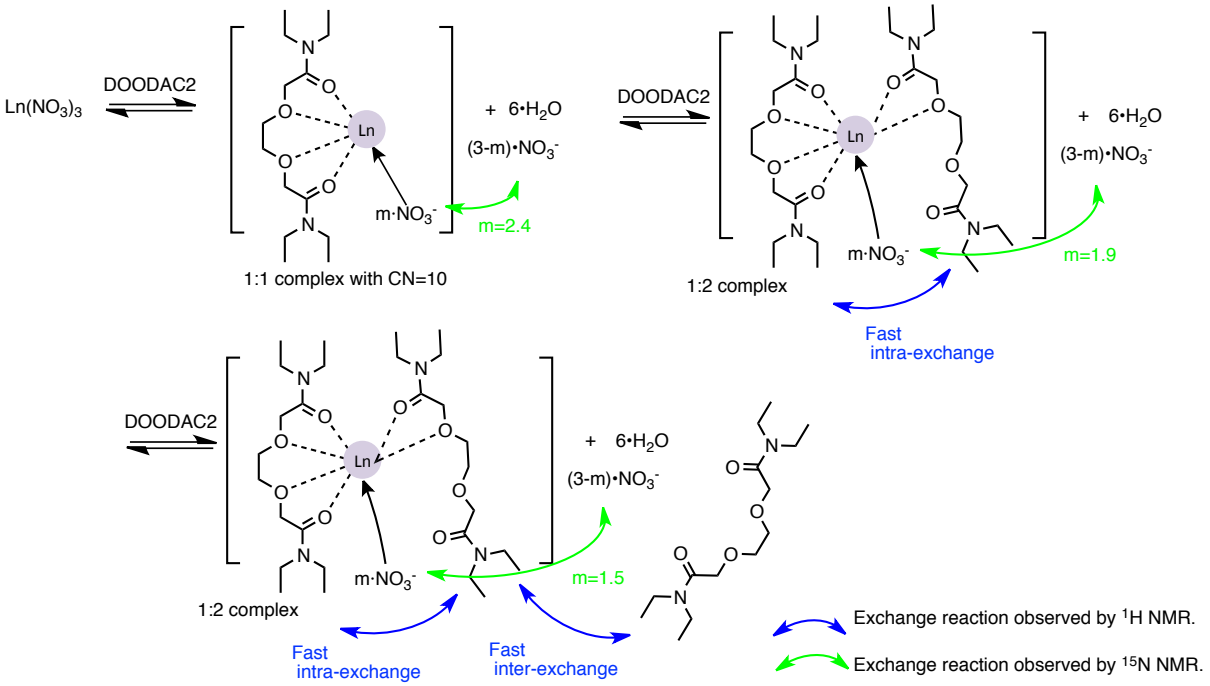

Figure 6-13 Schematic representation of light Ln(III) complexation with DOODAC2.

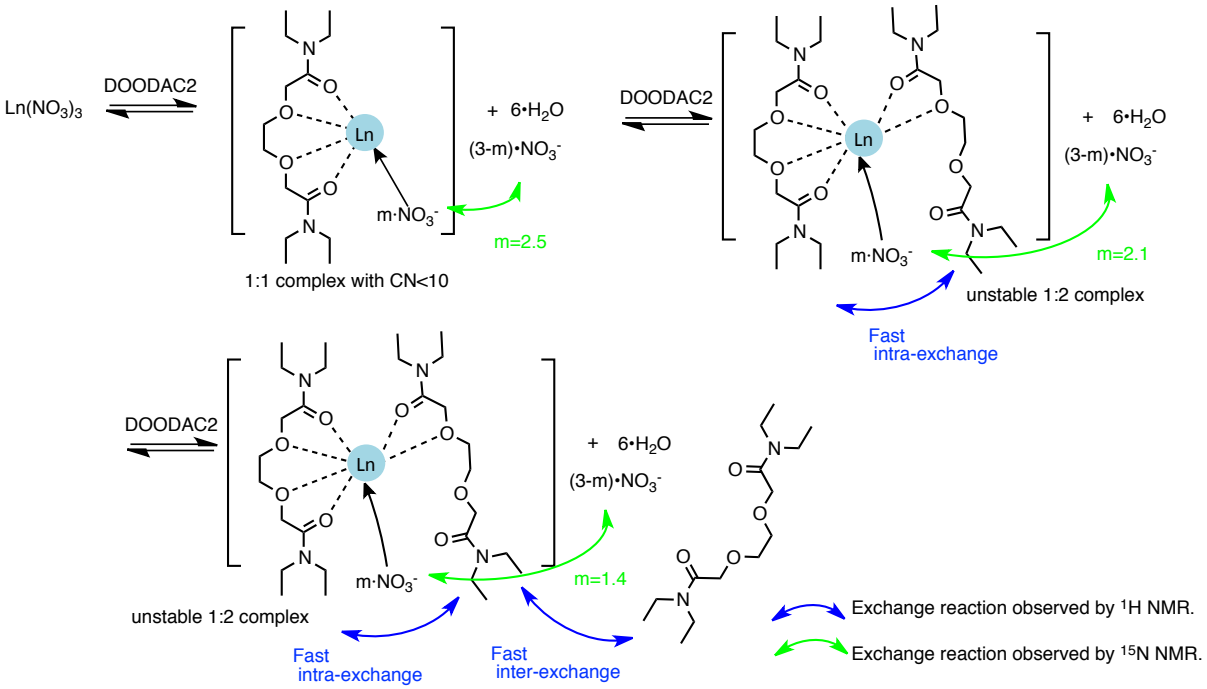

Figure 6-14 Schematic representation of heavy Ln(III) complexation with DOODAC2.

6.3.4 Infrared Spectra

As demonstrated in Chapter 2 and 4, nitrate ion possesses characteristic peaks on IR spectra. The ionic nitrate in D_{3h} symmetry shows three characteristic IR bands ν_2, ν_3, and ν_4, with corresponding peaks typically observed at around ν = 830, 1384, and 774 cm^{-1}. ν_1 is normally inactive, but sometimes becomes weakly active through crystal interactions.[14] The symmetry fall into C_{2v} symmetry by coordination either in a monodentate or bidentate nitrate complex, and then all six of the normal modes of vibration become IR active.[15] (see Chapter 1.4.2 for details.) In the acetonitrile solution, some of these bands were overrapped by vibration of acetonitrile. Fortunately, ν_1 and ν_4 vibration modes of C_{2v} nitrate were able to observed.

DGA System

The IR spectra of various [Ln]:[TEDGA] (Ln = La and Lu) ratios of acetonitrile solutions were recorded and shown in Figure 6-15. The characteristic peaks were observed at 1303 and 1490–1510 cm^{-1}, which were assigned to the ν_1 and ν_4 of C_{2v} nitrate ions. These bands were weakened and finnaly disappeared with increasing of TEDGA concentration in both La(III) and Lu(III) system. The depressions in these two bands should be corresponding to the outer-sphere complex formation with nitrate ions, that is, nitrate ions move to outer-sphere of Ln(III) ions. This result agreed with the result of ^{15}N NMR study.

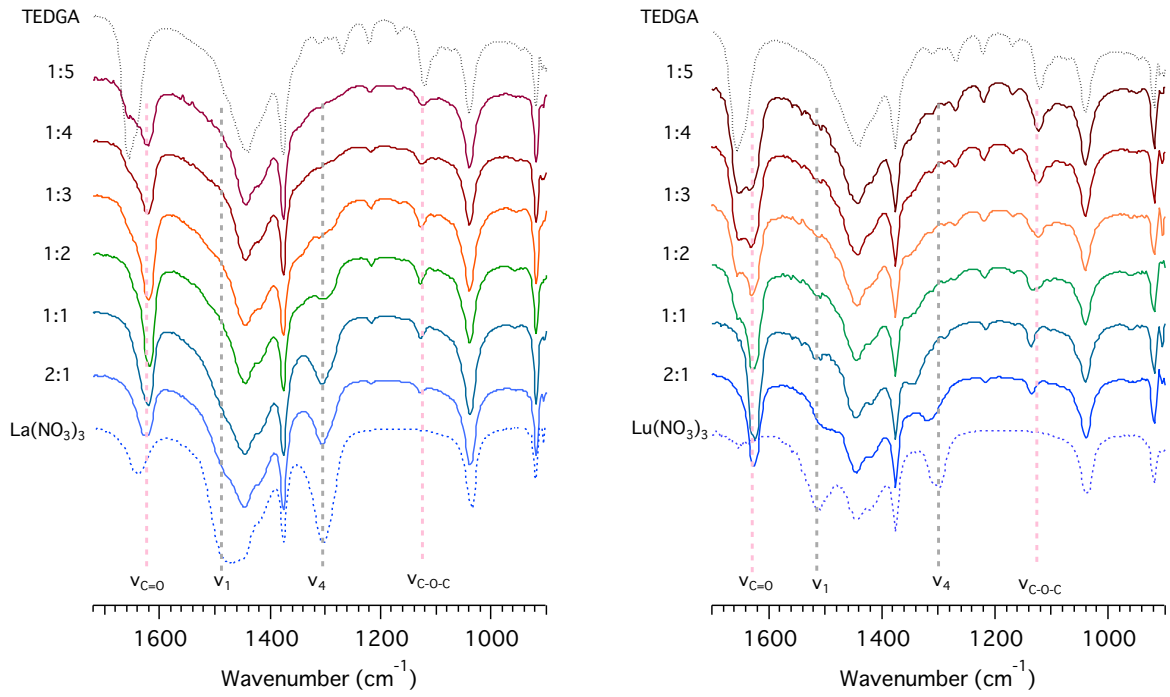

(a) (b)

Figure 6-15 IR spectra of acetonitrile solution with various [Ln]:[TEDGA] (Ln = (a) La and (b) Lu) ratios measured at room temperature.

DOODAC2 System

The various [Ln]:[DOODAC2] (Ln = La and Lu) ratios of acetonitrile solutions also prepared and their IR spectra were recorded. Figure 6-16 shows some of these spectra as representative examples. The similar changes were observed in DOODA system as well as TEDGA system. However, even in [Ln]:[DOODAC2]=1:3 system, there remains small intense in both ν_1 and ν_4 bands. Hence, the depressions in these two bands also correspond to the replacement of nitrate ions to the outer-sphere but not all of them.

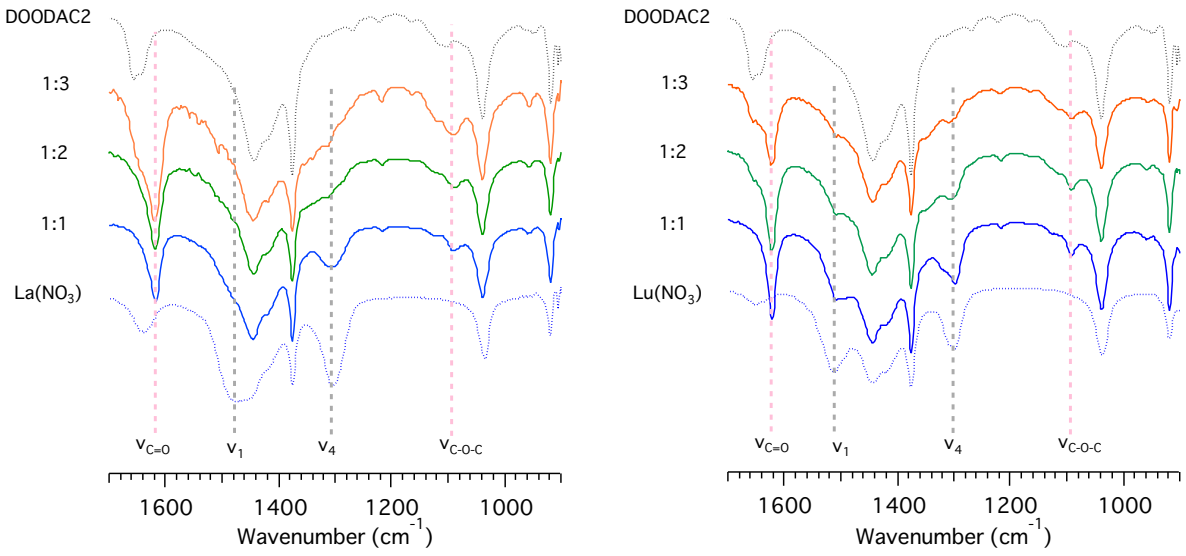

(a) (b)

Figure 6-16 IR spectra of acetonitrile solution with various [Ln]:[DOODAC2] (Ln = (a) La and (b) Lu)ratios measured at room temperature.

6.4 Conclusion

The nitrate ions form pentakis species with Ln(III) ,i.e. $[Ln(NO_3)_5]^{2-}$, in the acetonitrile solutions with both light and heavy Ln(III). The strengths of interaction of nitrate to Ln(III) are somehow weaker than that of DGA but similar to DOODA derivatives.

The ^{15}N NMR spectra provide useful information even though they showed a fast exchange on the NMR timescale. The number of nitrate ion coordinated to Ln(III) was calculated for each complexation steps. For example, for [Ln]:[DGA]=1:3 system (Ln = La and Lu), it was revealed that at least one nitrate ion exist in the inner-sphere of light Ln(III) complexes whereas all nitrate ions replace to the outer-sphere in heavy Ln(III) complexes. These results were excellent accordance with the results obtained in Chapters 2 and 3. Therefore, it is apparent that the nitrate ions in outer-sphere coordination should be one of the responsible factors contributed to the stabilities of the complexes (i.e. selectivity).

For [Ln]:[DOODAC2]=1:2 system, both light and heavy Ln(III) have at least one nitrate ion in its structures. These results indicate that inner- and outer-sphere nitrate would exchange each other. DOODAC2 also exchange among 1:1, 1:2 complexes and free TEDGA. Although fast exchange reactions are exist in the system, light Ln(III) are able to accommodate two DOODAC2 molecules and two nitrate in its ten-coordination structure, whereas heavy Ln(III) are not able to accommodate them. As the result, differences in selectivity appears between light and heavy Ln(III).

References

1 Bünzli, J. C. G.; Milicic-Tang, A."*Solvation and anion interaction in organic solvents*", *Handbook on the Physics and Chemistry of Rare Earths*, **1995**, Vol. 21**,** Ch 145, pp. 305-365.

2 Rao, L.; Tian, G. "Complexation of lanthanides with nitrate at variable temperatures: thermodynamics and coordination modes." *InorganicCchemistry,* **2009**, *48*, 964–70.

3 Duvail, M.; Ruas, A.; Venault, L.; Moisy, P.; Guilbaud, P. "Molecular dynamics studies of concentrated binary aqueous solutions of lanthanide salts: structures and exchange dynamics." *Inorganic Chemistry,* **2009**, *49*, 519–530.

4 Yaita, T.; Narita, H.; Suzuki, S.; Tachimori. S. "Structural study of lanthanides (III) in aqueous nitrate and chloride solutions by EXAFS." *Journal of Radioanalytical and Nuclear Chemistry*, **1999**, 239, 371-375.

5 Dobler, M.; Guilbaud, P.; Dedieu, A.; Wipff, G. "Interaction of trivalent lanthanide cations with nitrate anions: a quantum chemical investigation of monodentate/bidentate binding modes." *New Journal of Chemistry,* **2001**, *25*.

6 H. Narita, T. Yaita, S. Tachimori, " Extraction Behavior for Trivalent Lanthanides with Amides and EXAFS Study of Their Complexes." *Proceedings of the International Solvent Extraction Conference, ISEC'99*, **2001**, 693.

7 Hirata, M.; Guilbaud, P.; Dobler, M.; Tachimori, S. "Molecular Dynamics Simulations for the Complexation of Ln^{3+} and UO_2^{2+} Ions with Tridentate Ligand Diglycolamide (DGA)." *Physical Chemistry Chemical Physics,* **2003,** 5, 691-695.

8 Gannaz, B.; Antonio, M.; Chiarizia, R.; Hill, C.; Cote, G. "Structural study of trivalent lanthanide and actinide complexes formed upon solvent extraction." *Dalton Transactions*, **2006**, 38: 4553-4562.

9 Sastri VR, Bűnzli J-C, Ramachandra R, Rayudu GVS, Perumareddi JR. "Modern Aspects of Rare Earths and their Complexes." *Elsevier:* Amsterdam, **2003**.

10 Bünzli, J.-C. G.; Vuckovic, M. M. "Solvation of neodymium (iii) perchlorate and nitrate in organic solvents as determined by spectroscopic measurements." *Inorganica chimica acta*, **1984,** *95,* 105–112.

11 Fratiello, A.; Kubo-Anderson, V.; Lee, R.; Patrick, M.; Perrigan, R.; Porras, T.; Sharma, S.; Stoll, S. "Direct ^{1}H, ^{13}C, and ^{15}N NMR Study of Lanthanum(III), Thulium(III), and Ytterbium(III) Complex Formation with Nitrate and Isothiocyanate." *Journal of Solution Chemistry*, **2002**, 31, 681-702.

12 Fratiello, A.; Kubo-Anderson, V.; Azimi, S.; Flores, T.; Marinez, E.; Matejka, D.; Perrigan, R.; Vigil, M. "A hydrogen-1, nitrogen-15, and chlorine-35 NMR coordination study of $Lu(ClO_4)_3$ and $Lu(NO_3)_3$ in aqueous solvent mixtures." *Journal of Solution Chemistry* **1990**,*19*, 811-829.

13 Kawasaki, T.; Okumura, S.; Sasaki, Y.; Ikeda, Y. "Crystal Structures of Ln(III) (Ln = La, Pr, Nd, Sm, Eu, and Gd) Complexes with *N,N,N',N'*-Tetraethyldiglycolamide Associated with Homoleptic $[Ln(NO_3)_6]^{3-}$." *Bulletin of the Chemical Society of Japan,* **2014**, *87*, 294-300.

14 Curtis, N.; Curtis, Y. "Some Nitrato-Amine Nickel(II) Compounds with Monodentate and Bidentate Nitrate Ions." *Inorganic Chemistry,* **1965**, 4, 804-809.

15 Bullock, J. I. "Infrared spectra of some uranyl nitrate complexes." *Journal of Inorganic and Nuclear Chemistry* **1967**, *29*.

Chapter 7

Summary

The molecular structures and complex formation of Ln(III) nitrates with DGA and DOODA derivatives were studied in order to find the relationship between the molecular structures and the selectivity of hard donor extractants by the systematical investigation throughout the Ln(III) series in both solid and solution state. Based on my knowledge, it is important to evaluate the difference by using Ln(III) elements as much as possible.

Chapter 1. As the background of this thesis, the potential importance of coordination chemistry of these elements in the reprocessing of spent nuclear fuels process was described. The oxygen bearing hard donor extractants are in interest because of less of knowledge of the factors for affecting selectivity for Ln(III) and An(III). From this point, objective of this thesis was described.

Chapter 2. The Ln(III) nitrate complexes with TEDGA, $[Ln(TEDGA)_3](NO_3)_3$ (Ln = Tb-Lu) were synthesized and characterized in crystallographically and also confirmed by IR spectra.

Chapter 3. The differences in complexations, stabilities and structures of Ln(III) nitrate complexes with DGA in acetonitrile solutions were investigated by UV-vis and NMR spectroscopy. It was reveled that the 1:1 and 1:3 metal to ligand ratio complexes were formed. There are significant differences in stabilities and structures between the light and heavy Ln(III). The 1:3 complexes for heavy Ln(III) are highly stable than that of light Ln(III) in the acetonitrile solutions.

Chapter 4. The Ln(III) nitrate complexes with DOODAC2 were synthesized and characterized in crystallographically. The complexes are classified into three groups. The first two light Ln(III) form $[Ln(DOODAC2)_2(EtOH)_2][Ln(NO_3)_6]$ (Ln = La–Ce) complexes, the next ten light to middle Ln(III) form $[Ln(DOODAC2)(NO_3)_3]$ (Ln = Nd–Yb) complexes, and final one Ln(III), i.e. Lu, forms $[Lu(DOODAC2)(NO_3)_2](NO_3)$ complex. The coordination modes of DOODA and nitrate ions were confirmed by infrared spectroscopy.

Chapter 5. The differences in complexations, stabilities and structures of the Ln(III) complexes with DOODAC2 in acetonitrile solutions were examined by UV-vis and NMR spectroscopy. It was reveled that the complexes with 1:1 and 1:2 metal to ligand ratio were formed. The isostructural series of 1:1 complex were examined by LIS plots. There are small differences in stabilities and structures between the light/middle and heavy Ln(III). The 1:2 complexes are relatively unstable especially for heavy Ln(III).

Chapter 6. The effects of the existence of nitrate ion on complexation of DGA and DOODA were investigated by UV-vis spectroscopy. According to the qualitative discussion of this result, the

strength for interaction to Ln(III) ions are in the order of DGA > DOODA ≥ nitrate ion. The number of nitrate ion coordinated to the Ln(III) was calculated by the chemical shift variations of ^{15}N NMR spectra. The number of coordinated nitrate ion strongly supported that the reaction schemes obtained by UV-vis, ^{1}H NMR and IR spectra, and successfully demonstrated the formation of inner- and outer-sphere complexes with nitrate ions.

These results are in excellent agreement with the variations of distribution ratios (*D*) shown in the solvent extraction. The relationship between the molecular structures and the selectivity of hard donor extractants through the systematical investigation across the Ln(III) series have provided valuable insight into both the coordination chemistry of Ln(III) and the knowledge of the fundamental interaction properties between Ln(III) and hard donor extractants.

Appendix A Crystallographic data and Crystal Structures of Ln(III) nitrate complexes with TEDGA

Table 7-1 Crystallographic data of Ln(III)-TEDGA Complexes (Ln= Tb-Lu)

	Tb	Dy	Ho	Er	Tm	Yb	Lu
Empirical Formula	$C_{36}H_{80}N_9O_{22}Tb$	$C_{36}H_{80}N_9O_{22}Dy$	$C_{36}H_{80}N_9O_{22}Ho$	$C_{36}H_{80}N_9O_{22}Er$	$C_{36}H_{80}N_9O_{22}Tm$	$C_{36}H_{80}N_9O_{22}Yb$	$C_{36}H_{80}N_9O_{22}Lu$
Formula weight	1150.01	1153.59	1156.02	1158.35	1160.02	1164.13	1166.06
Crystal System	Monoclinic	Monoclinic	Monoclinic	Monoclinic	Monoclinic	Monoclinic	Monoclinic
Space Group	Pn	Pc	Pn	Pn	Pn	Pn	Pn
a / Å	11.9118 (4)	21.2105 (5)	11.8816 (8)	11.8682 (4)	11.9632 (6)	11.7745 (5)	11.9193 (4)
b / Å	12.3490 (4)	12.3768 (2)	12.3248 (8)	12.3032 (4)	12.1278 (5)	12.4181 (5)	12.1417 (4)
c / Å	18.6553 (7)	22.7595 (4)	18.6184 (13)	18.6219 (8)	18.8529 (10)	18.6262 (7)	18.8173 (7)
α/°							
β/°	94.454 (1)	114.756 (1)	94.630 (2)	94.593 (1)	94.704 (1)	93.876 (1)	94.702 (1)
γ/°							
Volume ($Å^3$)	2735.88 (16)	5425.69 (18)	2717.6 (3)	2710.38 (17)	2726.1 (2)	2717.24 (19)	2714.09 (16)
Z	2	4	2	2	2	2	2
d / g cm	1.396	1.412	1.413	1.419	1.413	1.423	1.427
R^1(I>2.00σ(I))	0.042	0.038	0.064	0.047	0.030	0.045	0.029
wR^2(All data)	0.100	0.092	0.155	0.101	0.074	0.103	0.075
GOF	1.02	1.02	1.06	1.03	1.06	1.06	1.07
Max Shift/Error							

All crystal structures are ellipsoids displayed at 30% probability, and hydrogen atoms are omitted for clarity.

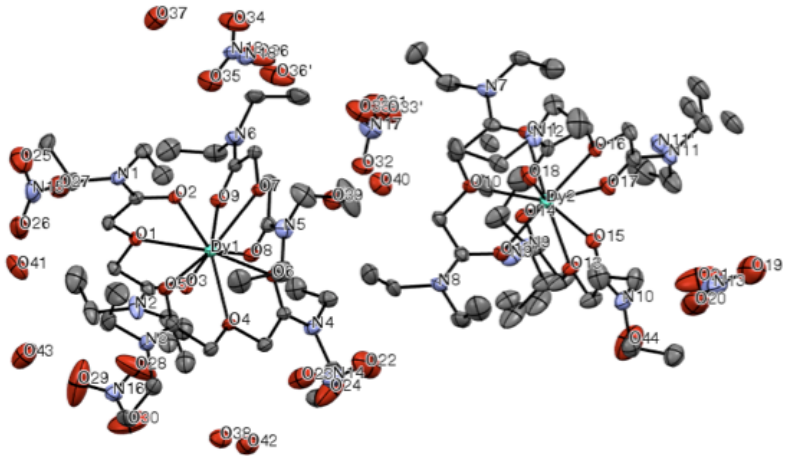

Figure 7-1 ORTEP representation of $[Dy(TEDGA)_3](NO_3)_3$ complex.

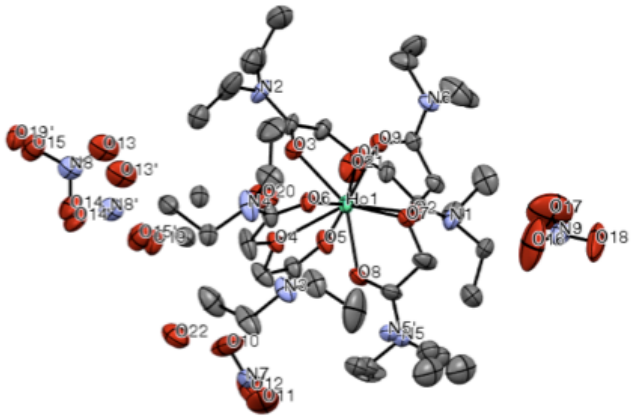

Figure 7-2 ORTEP representation of $[Ho(TEDGA)_3](NO_3)_3$ complex.

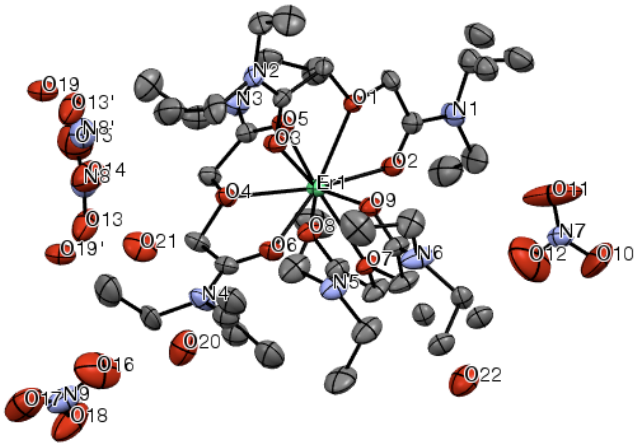

Figure 7-3 ORTEP representation of $[Er(TEDGA)_3](NO_3)_3$ complex.

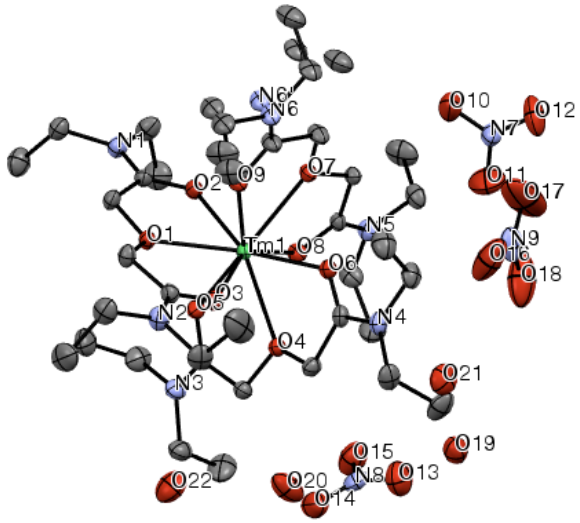

Figure 7-4 ORTEP representation of $[Tm(TEDGA)_3](NO_3)_3$ complex.

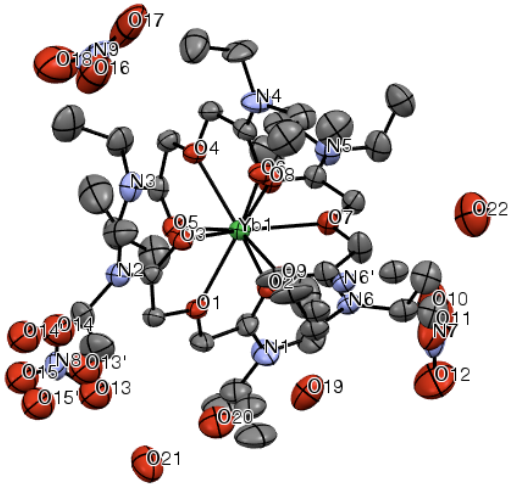

Figure 7-5 ORTEP representation of $[Tb(TEDGA)_3](NO_3)_3$complex.

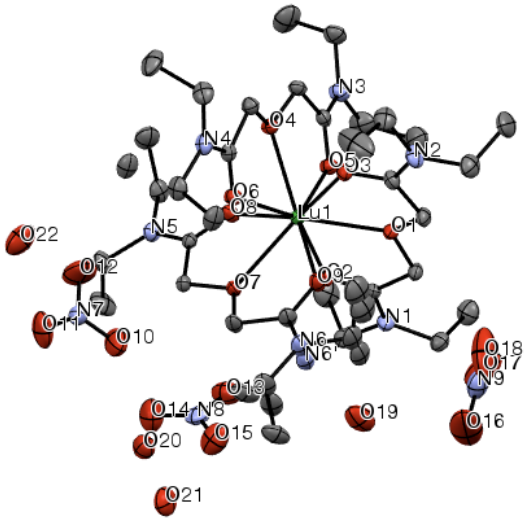

Figure 7-6 ORTEP representation of $[Lu(TEDGA)_3](NO_3)_3$ complex.

Appendix B Crystallographic data and Crystal Structures of Ln(III) nitrate complexes with DOODAC2

Table 7-2 Crystallographic data of Ln(III)-DOODA Complexes (Ln= La-Lu, except Pr and Pm)

	La(Type1)	Ce(Type1)	Nd(Type2)	Sm(Type2)	Eu(Type2)	Gd(Type2)	Tb(Type2)
Empirical Formula	$C_{31}H_{68}N_{10}O_{29}La_2$	$C_{31}H_{68}Ce_2N_{10}O_{29}$	$C_{14}H_{28}N_5O_{13}Nd$	$C_{14}H_{30}O_{14}N_5Sm$	$C_{14}H_{30}O_{14}N_5Eu$	$C_{14}H_{30}O_{14}N_5Gd$	$C_{14}H_{28}N_5O_{13}Tb$
Formula weight	1322.74	1325.17	618.64	642.82	644.38	649.67	633.33
Crystal System	triclinic	triclinic	monoclinic	monoclinic	monoclinic	monoclinic	monoclinic
Space Group	P-1 (#2)	P-1 (#2)	$P2_1/c$ (#14)	$P2_1/c$ (#14)	$P2_1/c$ (#14)	$P2_1/c$ (#14)	$P2_1/c$ (#14)
a / Å	12.6343(6)	12.6652(6)	20.3299(5)	10.7596(4)	10.768(8)	10.7676(4)	10.7677(5)
b / Å	14.7809(8)	14.7514(8)	7.7405(2)	16.4292(5)	16.316(13)	16.3145(5)	16.3603(7)
c / Å	15.3798(7)	15.3541(7)	15.5067(4)	14.5764(5)	14.578(9)	14.5764(4)	14.5775(7)
α/°	75.393(14)	75.451(2)					
β/°	77.014(12)	77.070(1)	103.550(7)	104.713(11)	104.350(18)	104.250(8)	104.301(2)
γ/°	83.5101(14)	83.583(2)					
Volume (Å^3)	2703.4(2)	2701.5(3)	2372.28(11)	2492.21(15)	2481.2(3)	2481.82(14)	2488.4(2)
Z	2	2	4	4	4	4	4
d / g cm^{-3}	1.625	1.629	1.732	1.713	1.725	1.739	1.690
R^1(I>2.00σ(I))	0.0435	0.0589	0.0285	0.0434	0.0488	0.0549	0.0673
wR^2(All data)	0.1068	0.1737	0.0604	0.0909	0.1216	0.1462	0.2098
GOF	1.088	1.082	1.050	1.044	1.111	1.14	1.084
Max Shift/Error	0.001	0.000	0.003	0.001	0.000	0.002	0.001

	Dy(Type2)	Ho(Type2)	Er(Type2)	Tm(Type2)	Yb(Type2)	Lu(Type3)
Empirical Formula	$C_{14}H_{28}N_5O_{13}Dy$	$C_{14}H_{30}N_5O_{14}Ho$	$C_{14}H_{28}N_5O_{13}Er$	$C_{14}H_{28}N_5O_{13}Tm$	$C_{14}H_{28}N_5O_{13}Yb$	$C_{14}H_{28}LuN_5O_{14}$
Formula weight	636.90	657.35	641.66	643.34	647.44	665.37
Crystal System	monoclinic	monoclinic	monoclinic	monoclinic	monoclinic	orthorhombic
Space Group	$P2_1/c$ (#14)	$P2_1/c$ (#14)	$P2_1/a$ (#14)	$P2_1/c$ (#14)	$P2_1/c$ (#14)	$P2_12_12_1$ (#19)
a / Å	20.2333(6)	10.7577(4)	14.9018(6)	20.4132(8)	20.097(2)	8.7557(2)
b / Å	7.7323(2)	16.3383(6)	15.5877(5)	7.7419(3)	7.7566(5)	13.4955(3)
c / Å	15.4305(5)	14.5259(5)	15.1497(5)	15.4694(7)	15.332(1)	21.4311(6)
β/°	103.859(1)	104.159(1)	44.3547(7)	103.537(1)	104.060(1)	
Volume (Å^3)	2343.8(2)	2475.5(2)	2460.16(15)	2376.8(2)	2318.4(3)	2532.4(1)
Z	4	4	4	4	4	4
d / g cm^{-3}	1.805	1.764	1.732	1.798	1.855	1.745
R^1(I>2.00σ(I))	0.0187	0.0483	0.0209	0.029	0.088	0.0368
wR^2(All data)	0.0485	0.1017	0.052	0.0586	0.205	0.0726
GOF	1.142	1.119	1.098	1.074	1.114	1.048
Max Shift/Error	0.002	0.002	0.002	0.002	0.000	0.003

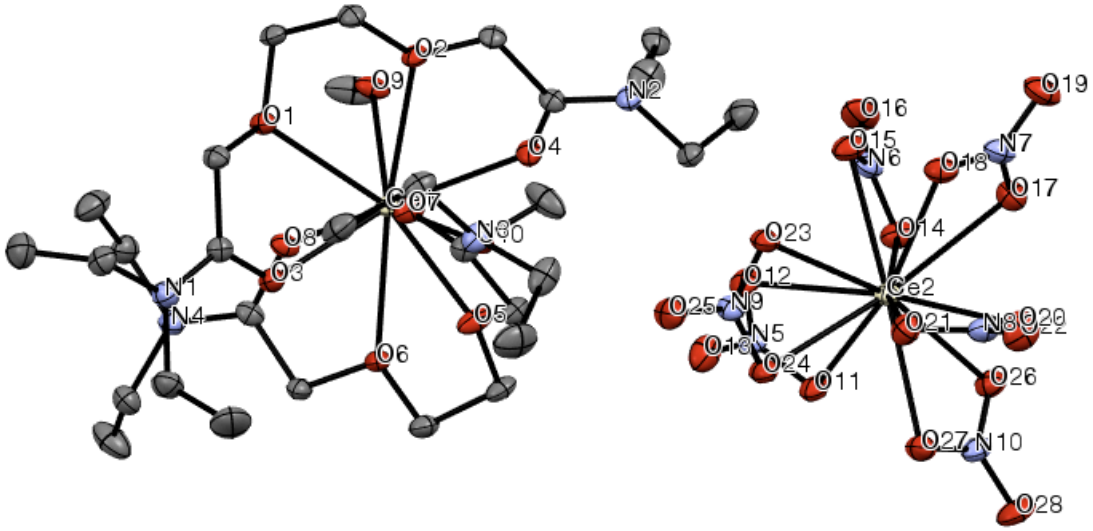

Figure 7-7 ORTEP representation of $[Ce(DOODAC2)_2(MeOH)_2][Ce(NO_3)_6]$ complex. Ellipsoids are displayed at 30% probability. Hydrogen atoms and solvent molecule are omitted for clarity.

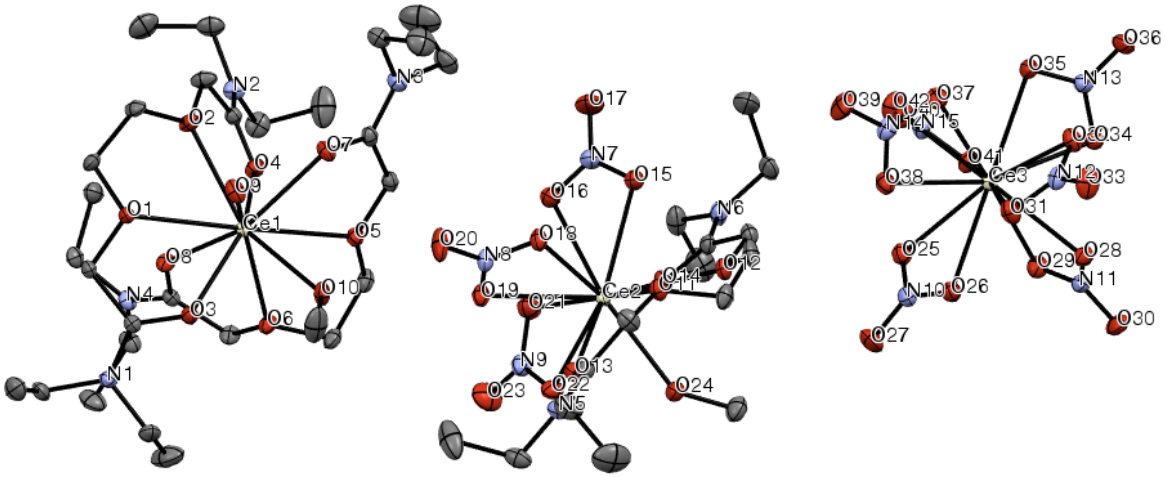

Figure 7-8 ORTEP representation of $[Ce(DOODAC2)_2(MeOH)_2][Ce(DOODAC2)(NO_3)_3][Ce(NO_3)_6]$ complex. Ellipsoids are displayed at 30% probability. Hydrogen atoms and solvent molecule are omitted for clarity.

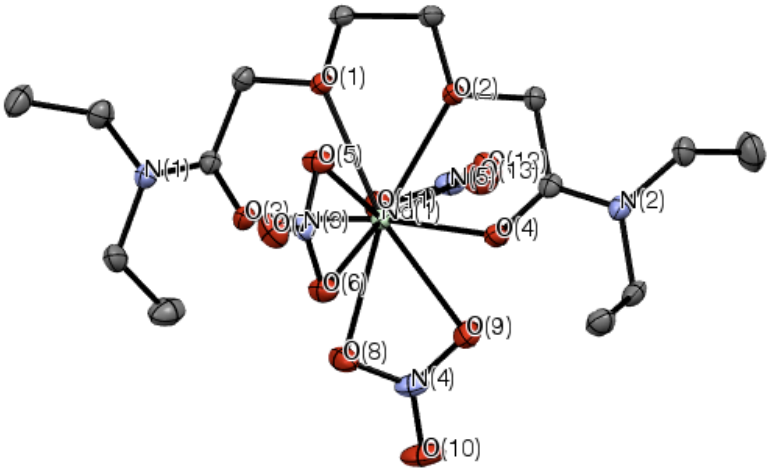

Figure 7-9 ORTEP representation of [Nd(DOODAC2)(NO_3)$_3$] complex.E llipsoids are displayed at 30% probability. Hydrogen atoms and solvent molecule are omitted for clarity.

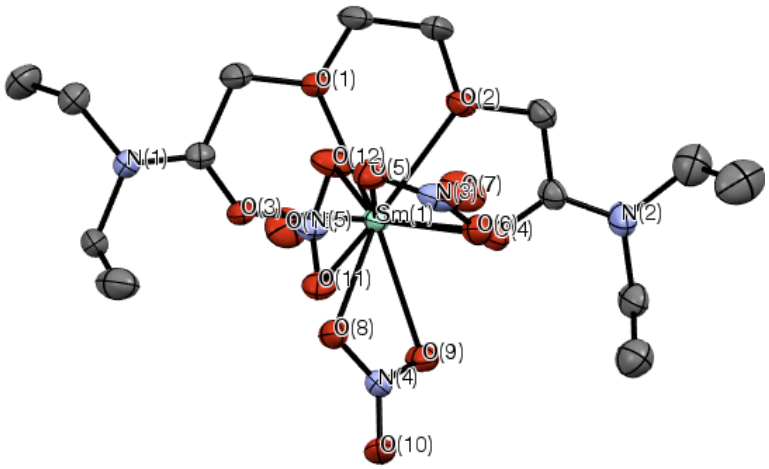

Figure 7-10 ORTEP representation of [Sm(DOODAC2)(NO_3)$_3$] complex. Ellipsoids are displayed at 30% probability. Hydrogen atoms and solvent molecule are omitted for clarity.

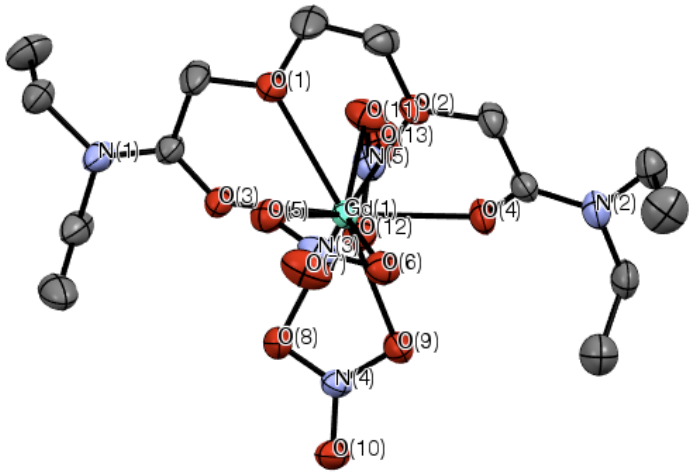

Figure 7-11 ORTEP representation of [Gd(DOODAC2)(NO_3)$_3$] complex. Ellipsoids are displayed at 30% probability. Hydrogen atoms and solvent molecule are omitted for clarity.

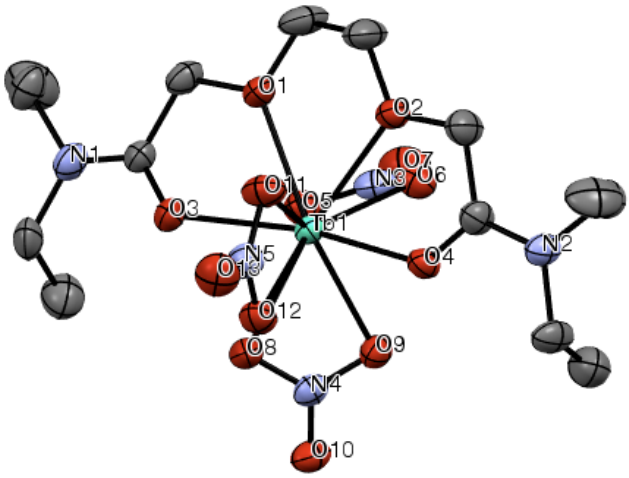

Figure 7-12 ORTEP representation of [Tb(DOODAC2)$(NO_3)_3$]. Ellipsoids are displayed at 30% probability. Hydrogen atoms and solvent molecule are omitted for clarity.

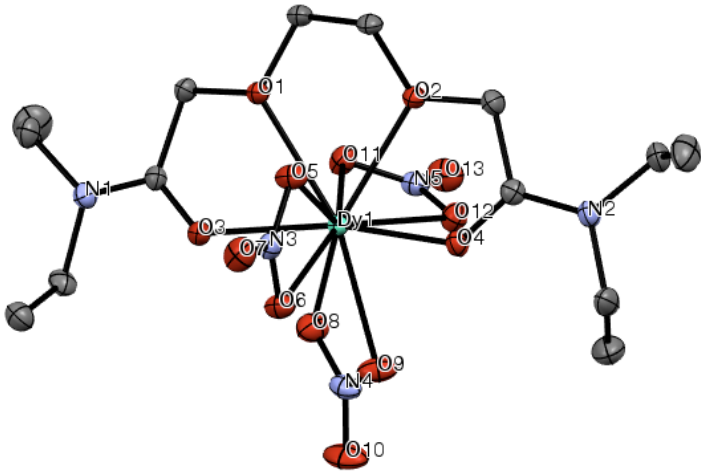

Figure 7-13 ORTEP representation of [Dy(DOODAC2)$(NO_3)_3$] complex. Ellipsoids are displayed at 30% probability. Hydrogen atoms and solvent molecule are omitted for clarity.

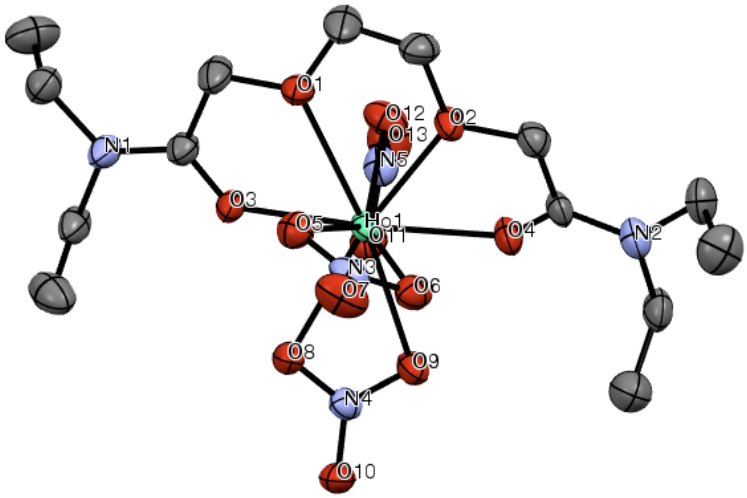

Figure 7-14 ORTEP representation of [Ho(DOODAC2)$(NO_3)_3$] complex. Ellipsoids are displayed at 30% probability. Hydrogen atoms and solvent molecule are omitted for clarity.

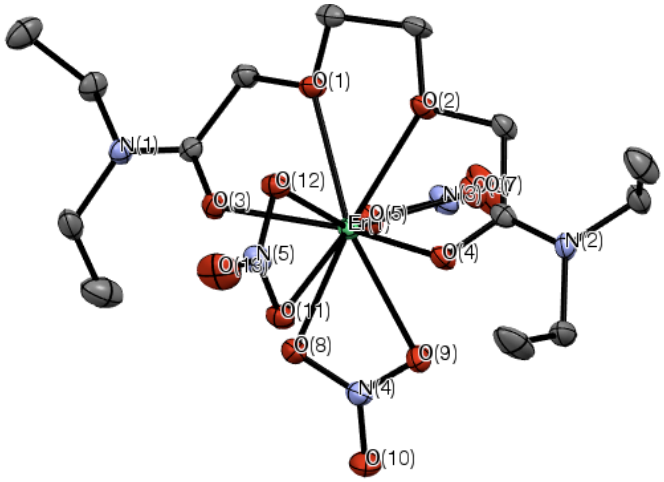

Figure 7-15 ORTEP representation of [Er(DOODAC2)$(NO_3)_3$] complex. Ellipsoids are displayed at 30% probability. Hydrogen atoms and solvent molecule are omitted for clarity.

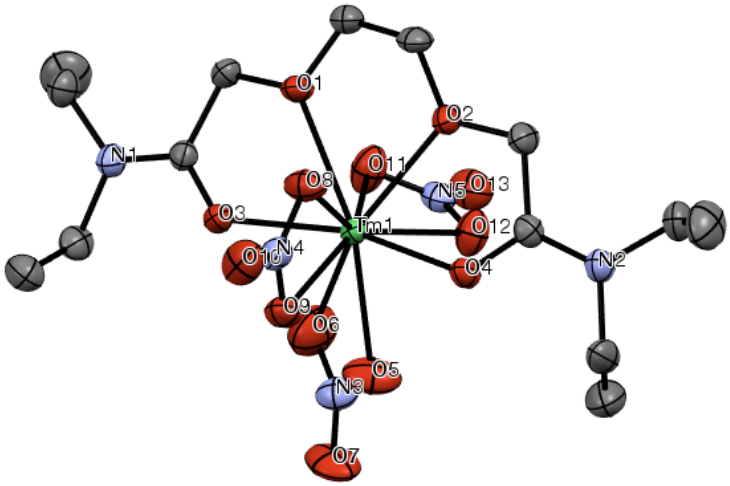

Figure 7-16 ORTEP representation of [Tm(DOODAC2)$(NO_3)_3$] complex. Ellipsoids are displayed at 30% probability. Hydrogen atoms and solvent molecule are omitted for clarity.

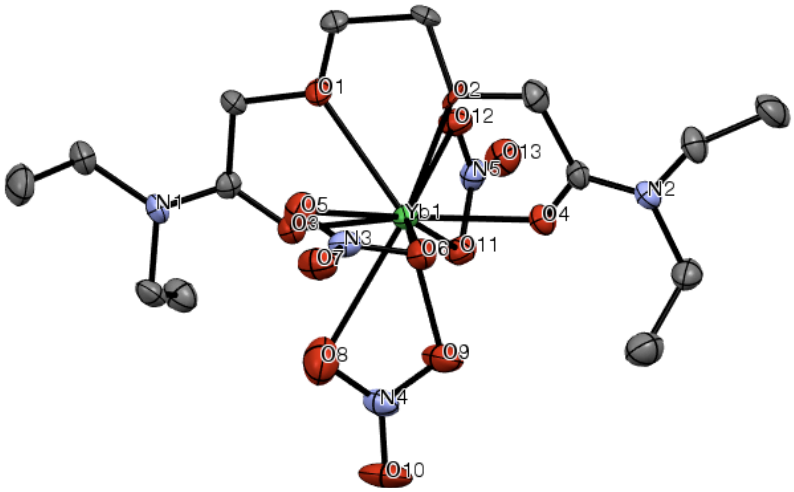

Figure 7-17 ORTEP representation of [Yb(DOODAC2)$(NO_3)_3$] complex. Ellipsoids are displayed at 30% probability. Hydrogen atoms and solvent molecule are omitted for clarity.

Appendix C NMR Spectra of [Ln]:[DOODAC2]=1:1 complexes

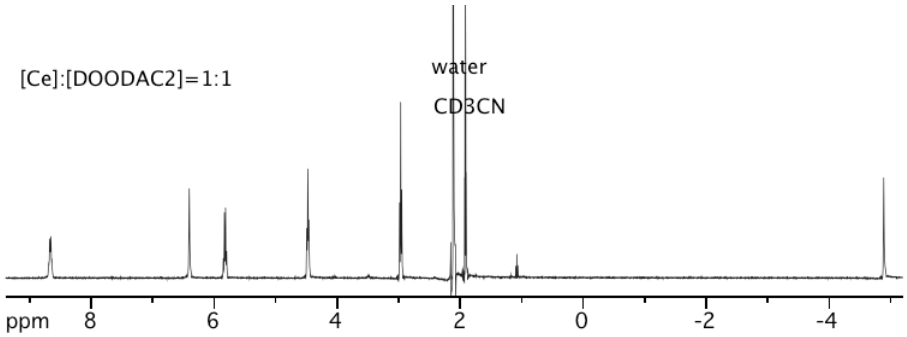

Figure 7-18 ^{1}H NMR spectrum of [Ce]:[DOODAC2]=1:1 acetonitrile-d_3 solution measured at 298 K.

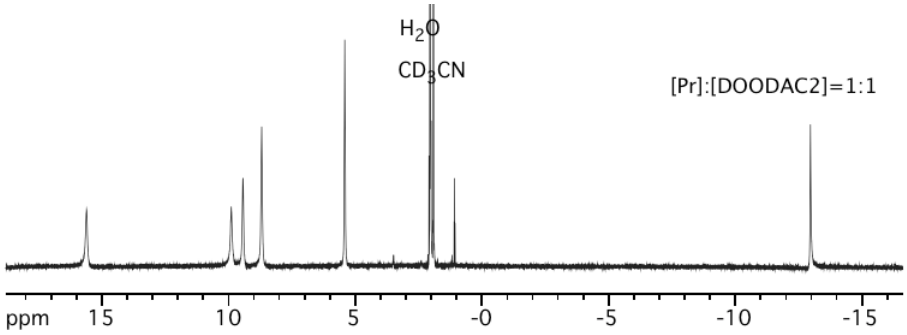

Figure 7-19 ^{1}H NMR spectrum of [Pr]:[DOODAC2]=1:1 acetonitrile-d_3 solution measured at 298 K.

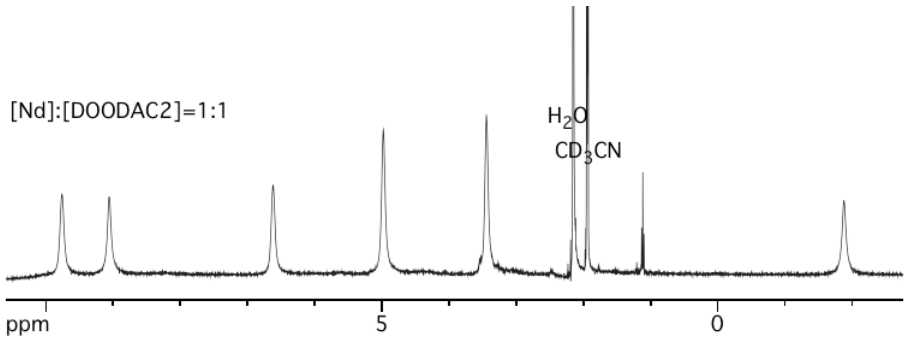

Figure 7-20 ^{1}H NMR spectrum of [Nd]:[DOODAC2]=1:1 acetonitrile-d_3 solution measured at 298 K.

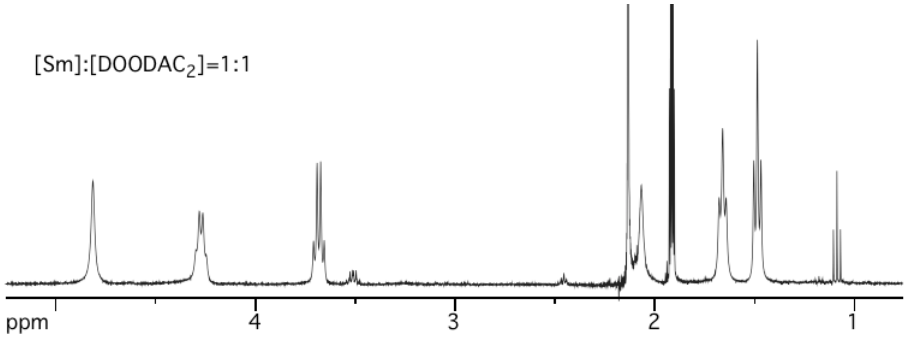

Figure 7-21 ^{1}H NMR spectrum of [Sm]:[DOODAC2]=1:1 acetonitrile-d_3 solution measured at 298 K.

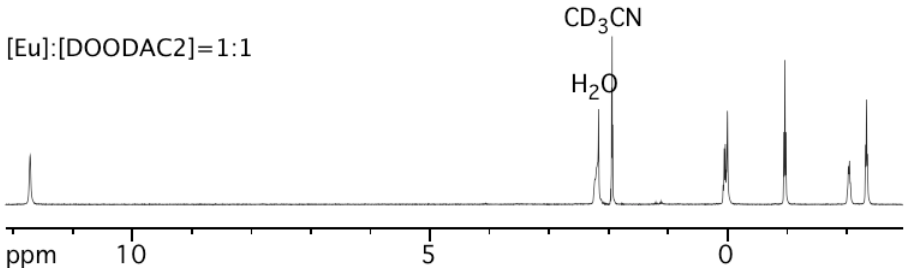

Figure 7-22 ^{1}H NMR spectrum of [Eu]:[DOODAC2]=1:1 acetonitrile-d_3 solution measured at 298 K.

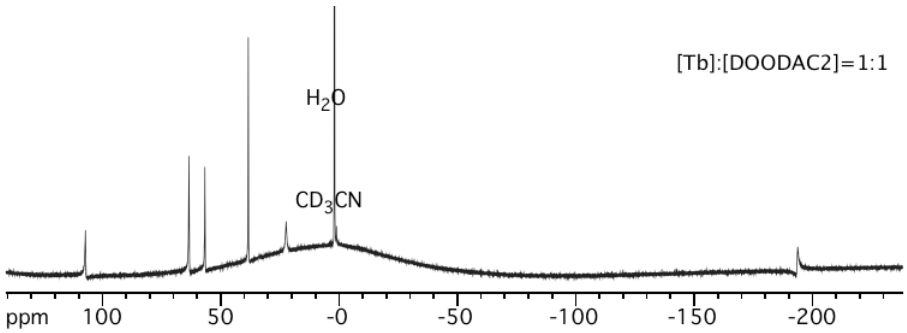

Figure 7-23 ^{1}H NMR spectrum of [Tb]:[DOODAC2]=1:1 acetonitrile-d_3 solution measured at 298 K.

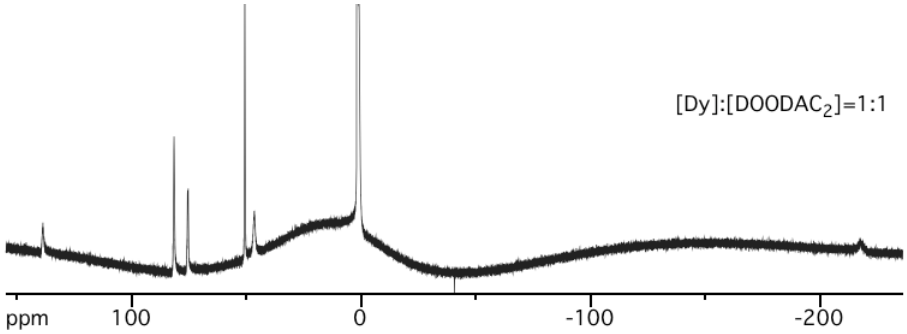

Figure 7-24 ^{1}H NMR spectrum of [Dy]:[DOODAC2]=1:1 acetonitrile-d_3 solution measured at 298 K.

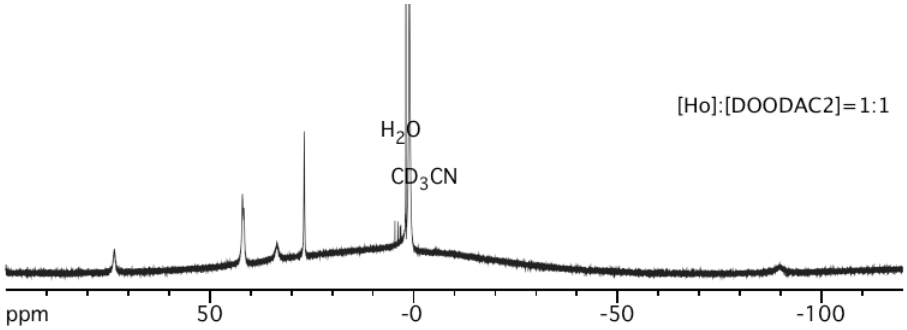

Figure 7-25 ^{1}H NMR spectrum of [Ho]:[DOODAC2]=1:1 acetonitrile-d_3 solution measured at 298 K.

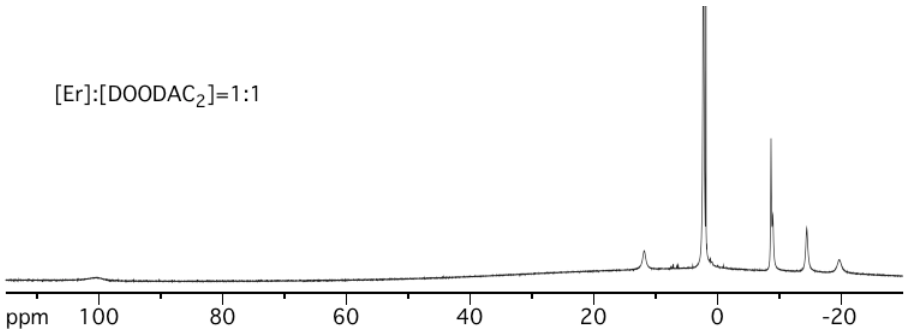

Figure 7-26 ^{1}H NMR spectrum of [Er]:[DOODAC2]=1:1 acetonitrile-d_3 solution measured at 298 K.

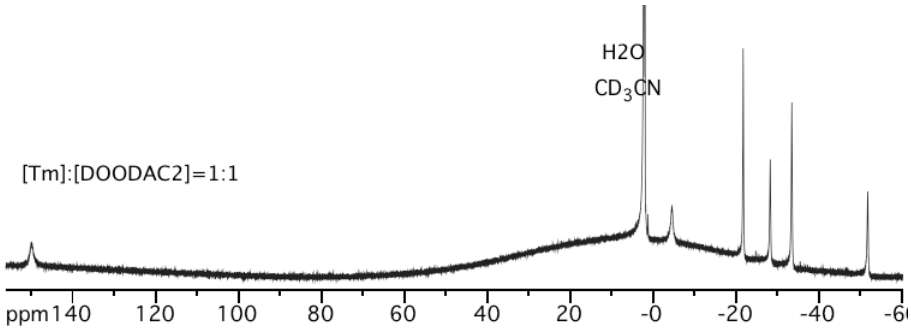

Figure 7-27 ^{1}H NMR spectrum of [Tm]:[DOODAC2]=1:1 acetonitrile-d_3 solution measured at 298 K.

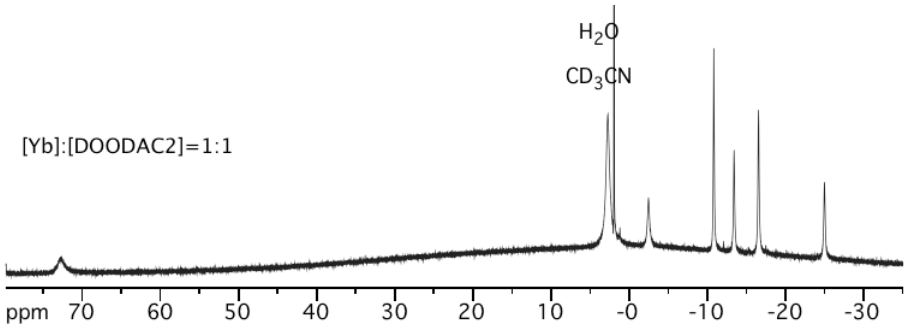

Figure 7-28 ^{1}H NMR spectrum of [Yb]:[DOODAC2]=1:1 acetonitrile-d_3 solution measured at 298 K.

Appendix D Crystallographic parameters of ^{15}N enriched Ln(III) nitrate complexes with TEDGA

Table 7-3 Crystallographic parameters of La and Lu of ^{15}N enriched nitrate complexes with TEDGA

	$[La(TEDGA)_3][La(^{15}NO_3)_6]$	$[Lu(TEDGA)_3](^{15}NO_3)_3\,4H_2O$
Empirical Formula	$C_{36}H_{72}N_{12}O_{27}La_2$	$C_{36}H_{80}N_9O_{22}Lu$
Formula Weight	1382.84	1166.06
Crystal Color, Habit	colorless, block	colorless, block
Crystal System	triclinic	monoclinic
Space Group	P-1 (#2)	Pn (#7)
Lattice Parameters	a = 12.3123(3) Å b = 14.1643(3) Å c = 17.2608(4) Å α = 84.5024(7) ° β = 86.3477(8) ° γ = 75.6231(8) °	a = 11.7719(3) Å b = 12.3563(4) Å c = 18.5414(5) Å β = 94.2462(7) °
Z	2	2
D_{calc} /g cm^{-3}	1.583	1.299
F000	1404	1084
m(MoKa) /mm^{-1}	1.54	1.90
Reflections collected	26098	24449
Independent reflections	12963 (Rint = 0.0229)	11531 (R_{int} = 0.0294)
R1	0.0363	0.0385
wR2 (all data)	0.0971	0.0891
GOF	1.087	1.045
$\Delta\varrho$	2.34 / -1.23	0.98 / -0.74

Acknowledgement

First of all, I would like to thank Professor Yasuhisa Ikeda and Assistant Professor Masayuki Harada at Tokyo Institute of Technology for their constant guidance and discussion throughout the duration of this work.

I am deeply grateful to Professor Emeritus Ingmar Grenthe at Royal Institute of Technology (KTH) for providing an invaluable opportunity to study at KTH, welcoming me, and continuous encouragement. I appreciate his knowledge, sincere attitude towards chemistry and sense of humor.

I wish to express special thanks to Associate Professor Zoltán Szabó at Royal Institute of Technology (KTH) for teaching of NMR spectroscopic techniques, insightful suggestions and helpful supports during my stay at KTH. This study could never have been completed without Professor Grenthe and Professor Szabó's supports and collaborations.

I would like to deeply thank to Dr. Mototetsu Kimura at Tsukahara Laboratory for his advice and valuable comments for my manuscripts, and hearty encouragement.

I wish to express my grateful appreciation to Associate Professor Takehiko Tsukahara for stimulating discussion and helpful supports for NMR measurements in theoretically and experimentally.

I deeply thank to Dr. Takeshi Kawasaki for his kind assistance and collaboration. The single crystal X-ray diffraction studies could never have been done without his guidance of measurement and crystal structure analyses.

I would like to thank to Professor Yasuhiro Yamada at Tokyo University of Science for sincere advice on my career when I proceeded to the graduate school of Tokyo Institute of Technology.

I would like to acknowledge to Professor Osamu Tsutsumi at Ritsumeikan University for supporting organic synthesis, experimental techniques.

I greatly acknowledge to Associate Professor Hirotoshi Mori at Ochanomizu University for teaching DFT calculations.

I would like to thank to Dr. Thomas Bell for his support to improve my English skill. His words made me "stay positive".

I would like to express thank to Dr. Ruxandra Toma for her friendship. Her positive attitude and personality brightened the atmosphere of our laboratory during her stay in Japan.

Special thanks to all previous and present colleagues in Ikeda and Tsukahara Laboratory for their kind assistance and cooperation. Mr. Dongki Hwang always cheered me up and I wish him all the best for his future career.

I thank to all of my friends especially for Mr. Masayuki Barada, Ms. Kumiko Nakano and Ms. Mio Fujioka for their friendship and encouragement.

Finally, I sincerely express my appreciation to my family, my mother and Mr. Takaaki Hagiwara for their love and support during my study.

This study was carried out at Ikeda Laboratory at Tokyo Institute of Technology from April 2010 to September 2014, and Royal Institute of Technology (KTH) from March 2012 to May 2012.

September 2014
Shin OKUMURA